LOCA Mass and Energy Release Analysis

Code Applicability Report for US-APWR

Non-Proprietary Version

June 2009

May 06, 2009

Mr. Yoshiki Ogata, General Manager
APWR Promoting Department
Mitsubishi Heavy Industries, Ltd.
16-5, Konan 2-Chome, Minato-Ku
Tokyo, 108-8215 Japan

SUBJECT: FINAL SAFETY EVALUATION FOR TOPICAL REPORT MUAP-07012-P AND MUAP-07012-NP, REVISION 2 “LOCA MASS AND ENERGY RELEASE ANALYSIS CODE APPLICABILITY REPORT FOR US-APWR”

Dear Mr. Ogata:

On July 20, 2007, Mitsubishi Heavy Industries, Ltd. (MHI) submitted Topical Report MUAP-07012-P and MUAP-07012-NP, Revision 0, “LOCA Mass and Energy Release Analysis Code Applicability Report for US-APWR” to the staff for review. On January 26, 2009, a U.S. Nuclear Regulatory Commission (NRC) draft safety evaluation (SE), regarding our approval of MUAP-07012, was provided for your review and comments. By letter dated March 3, 2009, (MHI REF: UAP-HF-09069) MHI provided four comments on the draft SE.

The NRC staff has reviewed Topical Report MUAP-07012, Revision 2 and has found that this report is acceptable for use by MHI for United States-Advanced Pressurized Water Reactor design certification activities to the extent specified and under the limitations delineated in the topical report and in the enclosed SE. The SE defines the basis for acceptance of the topical report. Our acceptance applies only to the material provided in the subject topical report. We do not intend to repeat our review of the acceptable material described in the topical report.

We request that MHI publish an accepted version of this topical report. The accepted version of this topical report shall incorporate this letter and the enclosed SE after the title page. Also, the accepted version must include NRC requests for additional information and your responses.

The accepted version shall include an "-A-" (designating accepted) following the topical report identification symbol. If future changes to the NRC's regulatory requirements affect the acceptability of this topical report, MHI will be expected to revise the topical report appropriately, or justify its continued use.

Sincerely,

/RA/

Carey Bickett, Acting Chief
US-APWR Projects Branch
Division of New Reactor Licensing
Office of New Reactors

Docket No. 52-021

Enclosure:
As stated

The accepted version shall include an "-A-" (designating accepted) following the topical report identification symbol. If future changes to the NRC's regulatory requirements affect the acceptability of this topical report, MHI will be expected to revise the topical report appropriately, or justify its continued use.

Sincerely,

/RA/

Carey Bickett, Acting Chief
US-APWR Projects Branch
Division of New Reactor Licensing
Office of New Reactors

Docket No. 52-021

Enclosure:
As stated

DISTRIBUTION:

PUBLIC	RidsNroDnrlNmip	RidsNroDsraSpcv
JCiocco, NRO	WJensen, NRO	RReyes, NRO
RidsNroLACSmith	NMIP R/F	RidsOgcMailCenter
D081	RidsAcrsAcnMailCenter	*via email (attached)

ACCESSION NUMBER: ML090750646 **NRO-002**

OFFICE	DNRL/NMIP: PM	DNRL/NMIP: PM	DNRL/NMIP: LA	DSRA/SPCV: BC	DNRL/NMIP: BC
NAME	RReyes	JCiocco	CSmith*	CJackson	CBickett
DATE	05/06/2009	04/06/2009	05/06/2009	04/10/2009	05/06/2009

OFFICIAL RECORD COPY

FINAL SAFETY EVALUATION BY THE OFFICE OF NEW REACTORS

TOPICAL REPORT MUAP-07012-P R2

"LOCA MASS AND ENERGY RELEASE ANALYSIS CODE APPLICABILITY REPORT FOR US-APWR"

MITSUBISHI HEAVY INDUSTRIES, LTD.

DOCKET NO. 50-021

1.0 INTRODUCTION

Topical Report MUAP-07012 (Reference 1) describes a portion of the methodology which Mitsubishi Heavy Industries (MHI) uses in the evaluation of the ability of the United States-Advanced Power Water Reactor (US-APWR) containment building to withstand the over-pressure and temperature that would be produced following a large loss of coolant accident (LOCA). Specifically the topical report presents methodology for calculating the steam, water and nitrogen releases from postulated reactor coolant piping breaks. These releases are then utilized in the model of the containment building to evaluate the increase in internal pressure and temperature. The containment building model is not part of the MUAP-07012 review. During the review, the U.S. Nuclear Regulatory Commission (NRC) staff issued a number of requests for additional information (RAIs). MHI's responses to these RAIs are included in Reference 1.

The methodology in MUAP-07012 is based on that which has been previously approved by the NRC staff. In particular, for the initial periods of discharge from the reactor, computer codes developed by Westinghouse (Reference 2), which have previously been approved by the staff, are utilized. For the final period of the discharge, MHI methodology uses the GOTHIC computer code which was developed by the Electric Power Research Institute and has also been utilized in approved containment evaluations (Reference 3). Revisions to the approved methodology were necessary because of special features of the US-APWR. The special features which would impact the discharge to the containment building during a LOCA include the advanced accumulators, the heavy neutron reflector within the reactor vessel and the in-containment refueling water storage pit (RWSP).

2.0 REGULATORY EVALUATION

General Design Criterion (GCD) 50 of the NRC's regulations requires that the containment structure and the containment heat removal systems be designed so that the containment structure can accommodate, without exceeding the design leakage rate and with sufficient margin, the calculated pressure and temperature conditions resulting from LOCA.

The mass flow rate of fluid from a postulated primary system piping break and the energy contained within that fluid are key factors which must be included in the evaluation of the adequacy of the containment structure. In reviewing MUAP-07012, the staff utilized the guidance within Standard Review Plan (SRP) 6.2.1.3, "Mass and Energy Release Analysis for Postulated Loss-of-Coolant Accidents (LOCAs)." Adherence to the guidance of SRP 6.2.1.3 ensures that the requirements of GDC 50 will be met for this area of the review.

3.0 TECHNICAL EVALUATION

Following a LOCA caused by a large piping rupture of reactor system piping, the sequence of events including the recovery of reactor core cooling has been divided into four phases namely:

1. The blowdown period: During this period coolant is rapidly ejected from the reactor system into the containment building and the reactor core temperature increases because of the lack of cooling.

2. The refill period: During this period the reactor vessel lower plenum is refilled with emergency coolant to the bottom of the core. Little additional mass or energy release to the containment will occur and the core temperature will continue to increase.

3. The reflood period: During this period the core is recovered with water and cooled below the initial temperature that occurred before the start of the accident. As the heated fuel comes in contact with the rising water level, experiments of simulated core reflooding have shown that a large fraction of the emergency coolant which reenters the bottom of the core will be carried out of the top of the core along with the exiting steam as water droplets. Depending on the break location, these droplets will be heated by the primary system piping and the stored energy within the steam generators to be turned into steam before flowing into the containment building.

4. The post-reflood or long-term cooling period: Evaluations for this period should consider the core decay heat and the removal of the remaining sensible heat from the reactor system and steam generators. During the early portion of this period, the core will still be boiling at a rapid rate. Void fraction evaluations have shown that a two-phase mixture will extend above the core so that additional liquid will enter the steam generator tubes. The flow of a two-phase mixture through the reactor system will remove the remaining sensible heat and will provide for additional steam formation to be added to the containment building.

As discussed in Reference 2, the SATAN-VI computer code is used to determine the mass and energy addition rates to the containment during the blowdown phase of the accident. To obtain a conservatively high energy release from the core during the blowdown period, a core average channel is modeled assuming nucleate boiling for an extended period to maximize the energy release. By this means, a major portion of the available energy is removed from the core during the blowdown. With these assumptions, the core transfers more heat to the containment than would be predicted by a calculation suitable for emergency core cooling performance evaluation. This additional energy release from the core will increase the calculated containment pressure and therefore provides a margin of conservatism in the analyses.

MHI will assume a refill period of zero duration. This is the assumption which is recommended in SRP 6.2.1.3. The assumption is conservative since steaming to the containment would be reduced as the lower plenum filled. It is, therefore, conservative for containment analysis to assume that the lower plenum is filled at the end of the blowdown.

The analysis of the reflood phase of the accident is important with regard to pipe ruptures of the reactor coolant system cold legs, since the steam and entrained liquid carried out from the core for these break locations will pass through the steam generators. The entrained water leaving the core and passing through the steam generators will be evaporated.

MHI will utilize the WREFLOOD code, as described in Reference 2, to calculate mass and energy release to the containment during the reflood period. The WREFLOOD code utilizes a reactor coolant system hydraulic resistance model and an energy balance model. The hydraulic model determines the core flooding rate, whereas the energy balance model determines the core exit conditions and the energy addition from the steam generators. The rate of energy release to the containment during the reflood period will be proportional to the core flooding rate.

The effluent fraction of the core inlet flow rate is calculated from a correlation based on the results of the FLECHT experiments. The results of the FLECHT experiments show that liquid entrainment continues until the fuel is recovered with water to an elevation of approximately four feet from the top. For conservatism plants, using the methodology of Reference 2 have assumed that quenching of the core occurs at an elevation of two feet from the top. This is the assumption recommended by SRP 6.2.1.3 and is the assumption used by MHI. All the available sensible heat in the core and in the neutron shield is added to the containment during the reflood period. The metal of the reactor system primary system piping is lumped with the metal in the steam generators. Heat transfer assumptions are made, which maximize the flow of sensible heat into the reactor system fluid.

For the blowdown and reflood period, modifications were required to both the SATAN-VI and the WREFLOOD computer codes to account for the advanced accumulators of US-APWR. The advanced accumulators are designed to supply emergency coolant at a rapid rate at the start of the accident and then to supply emergency coolant at a slower rate, but for longer time during the core reflood. The modeling of these injection characteristics required programming changes to both SATAN-VI and WREFLOOD.

Essentially, the same advanced accumulator model which has been programmed into SATAN-VI and WREFLOOD has also been programmed into the WCOBRA/TRAC computer code. This code is being utilized by MHI to evaluate compliance with Title 10 of the *Code of Federal Regulations* (10 CFR), Part 50.46 following a large break LOCA (Reference 4). The staff is performing a detailed review of this model as part of the 10 CFR 50.46 compliance review. Provided that the advanced accumulator model is found to be acceptable for the 10 CFR 50.46 compliance review, the staff concludes that the model is also acceptable for containment analysis. MHI performed a sensitivity study to determine the initial accumulator conditions and injection line resistance which produce conservative results for containment analyses. These conservative inputs are used for US-APWR safety analysis.

Following a large cold leg break, once the core has been reflooded and a static pressure balance has been reached between the water in the downcomer and the water in the core and upper plenum, additional emergency coolant added to the downcomer or to the cold legs will spill out of the break. With no additional flow into the core from the bottom, the core will soon begin to boil. Once boiling has begun, additional coolant will flow into the core from the downcomer to replenish that which is boiled away. As a result of boiling, the void fraction in the core will become higher than that in the downcomer. A two-phase level will therefore rise above the core so that a pressure balance is maintained. Reference 2 describes the Westinghouse FROTH methodology which calculates the two-phase level and the additional steaming which will occur if the two phase level reaches the steam generators. By this process, the remainder of the available steam generator energy is removed to be added to the containment building.

Instead of using the approved Westinghouse FROTH methodology described in Reference 2, MHI developed a reactor system model utilizing the GOTHIC computer code (Reference 5). The same void fraction model will be utilized by MHI in the GOTHIC reactor system model, as was approved by the NRC staff for the Westinghouse FROTH model. At the request of the NRC staff, MHI provided additional details of the GOTHIC reactor system model. Within GOTHIC, the reactor system is divided into sufficient detail using a multi-node approach such that the two-phase mixture from the core reaches the steam generators where it is all turned to steam and flows into the containment through one side of the assumed double-ended break in a cold leg. Excess emergency core cooling system (ECCS) water is spilled out of the other side of the break. The spilled ECCS water is assumed not to mix with the steam from the core and steam generators which is conservative. Heat transfer is evaluated from the steam generators and reactor system metal until all available sensible heat is removed and added to the containment. The advanced accumulators will still be injecting into the reactor system at the beginning of the post-reflood period. GOTHIC uses a simplified model of the advanced accumulators which holds the accumulator flow resistance essentially constant until they have emptied. The simplified modeling was determined to be appropriate, based on a more detailed analysis. The advanced accumulators will be emptied before peak containment pressure is reached for the limiting large break LOCA.

Release of the accumulator cover gas will occur after the water in the accumulators has depleted. The nitrogen gas release is conservatively assumed to occur at the end of reflood phase, which is before the time of peak containment pressure for the limiting case. This assumption is conservative, since the nitrogen gas affects the peak pressure magnitude. Although the nitrogen gas temperature will decrease with expansion as accumulator water is discharged, the temperature of the released gas is conservatively assumed constant at the initial value, which is the maximum operating temperature.

MHI will calculate the containment pressure and temperature for the functional design evaluation using the GOTHIC code. Reference 1 contains a brief description of the GOTHIC model. The details of the model have been submitted with the Design Control Document (DCD) for the US-APWR (MUAP-DC006). The staff will defer the review of the GOTHIC containment model to the DCD review.

During the blowdown period, the flow from the postulated reactor system piping rupture to the containment will be at sonic velocities. For this condition, the containment pressure will have little influence on the mass flow rate from the break. Flow from the ECCS pumps, which take suction from the in-containment RWSP, is not assumed during the blowdown period which is conservative for containment analysis. Changes in RWSP temperature, as well as containment pressure, will affect the steaming rate to the containment during core reflood. For this reason, MHI links the GOTHIC containment simulation with the reactor system simulation in WREFLOOD. Similarly, during the post reflood period, the multi-node reactor system model in GOTHIC is solved simultaneously with the GOTHIC containment model. Using a single computer run for both the containment and the reactor system analysis avoids the need for iteration between computer codes, improves accuracy, and is acceptable to the staff.

In the US-APWR design, water from the accumulators is injected into the cold legs, whereas water from the safety injection pumps is injected directly into the downcomer. The safety injection pumps take suction from the RWSP. In the WREFLOOD and GOTHIC reactor system models, MHI takes credit for mixing of the injected accumulator fluid with steam contained within the cold-leg piping. The mixing of steam and accumulator water reduces the amount of steam released to the containment and results in a lower calculated containment pressure. Experimental steam-water mixing studies were performed by EPRI (Reference 6) for water streams injected into steam filled piping test sections. The results of these tests showed that complete mixing occurred immediately, so that thermal equilibrium was obtained at a very short distance from the injection nozzle. Based on these tests, the staff accepted the assumption of complete steam-water mixing in the cold legs for the Westinghouse methodology in Reference 2 and finds this assumption also acceptable for MHI.

The EPRI steam-water mixing data is not applicable to the condition of the safety injection water which is pumped directly into the reactor vessel downcomer. This water may enter the reactor system below the downcomer water level and will not be susceptible to steam-water mixing. MHI will therefore not take credit for steam-water mixing in the downcomer or on any ECCS water stream that spills from the break. Since the accumulators will be emptied early during the course of the accident, steam-water mixing with injected ECCS water will not be credited during the long-term cooling phase of the accident.

The staff noted that the post-reflood steam release to the containment, as calculated by the GOTHIC reactor system simulation, is oscillatory as compared with the previously approved FROTH code methodology in WCAP-10325 which MHI references. In addition, after approximately 30,000 seconds, the steam release to the containment was less than that which would be expected from continued core boil-off. The staff was concerned that the oscillations may be an artifact of the GOTHIC reactor system model, which might cause unrealistic steam condensation to be calculated within the core and lower plenum of the reactor vessel. The staff did not understand why the long-term steam release rate predicted by GOTHIC would be less than that resulting from decay heat boiling, since the applicant’s assumptions for downcomer condensation are designed to conservatively eliminate steam condensation after accumulator injection. The staff notes that SRP 6.2.1.3 recommends the following: “Steam from decay heat boiling in the core should be assumed to flow to the containment by the path which produces the minimum amount of mixing with ECCS injection water.” For a postulated break at the reactor system pump suction, compliance with this recommendation for US-APWR would mean that all steam from the core would be assumed to flow directly to the containment without passing any of the ECCS injection locations.

In response to staff questions, MHI revised the mass and energy release model for the post-reflood period. The revised model will eliminate core oscillations by the use of a lag controller in the GOTHIC reactor system model and improvement in the model initialization which begins at the end of the reflood period. Late in the analysis, after the time when essentially all available sensible heat is removed from the reactor system and steam generators, MHI will calculate steam release to the containment using a boil-off calculation for the core decay heat which will pass all the available steam release directly to the containment. The staff concludes that the revised mass and energy model is in conformance with SRP 6.2.1.3 and is, therefore, acceptable. The revised mass and energy release model is predicted to result in a slightly higher peak containment pressure and slightly higher containment pressures during the long term cooling period. MHI believes that the resulting peak containment pressures will still be well below the US-APWR design pressure and that the long-term pressure response will be less than 50 percent of the peak containment pressure after 24 hours as recommended by SRP 6.2.1.1.A.

4.0 CONCLUSION

The NRC staff has reviewed MUAP-07012 "LOCA Mass and Energy Release Analysis Code Applicability Report for US-APWR." The staff concludes that the applicant's proposed methodology follows the guidance given in SRP 6.2.1.3 and is, therefore, in conformance with the NRC's regulations, and is acceptable for referencing provided that the following conditions are met:

- The staff did not review the models for the advanced accumulator that the applicant added to SATAN VI and WREFLOOD for the mass and energy release calculations. These models are essentially the same as programmed into WCOBRA-TRAC for the ECCS evaluation (Reference 4) which is also under review, by the staff. In the WCOBRA-TRAC review, the advanced accumulator model is being reviewed in detail. The staff will consider the advanced accumulator (Reference 7) to be acceptable for the mass and energy calculations when it is approved for the ECCS evaluation.

- The staff reviewed the methodology in MUAP-07012 for application to the US-APWR mass and energy release determination for containment functional design evaluation. Other safety analysis applications will require additional justification and staff review.

- The staff's acceptance of the methodology in MUAP-07012 is for the revised methodology for which a lag constant has been applied during the post-reflood period to dampen the core inlet oscillations predicted by the GOTHIC reactor system model. This methodology utilizes the direct steaming model after the time when essentially all available sensible heat is removed from the reactor system and steam generators.

The GOTHIC containment model for US-APWR is briefly described in MUAP-07012. The staff did not review the details of that model as part of the MUAP-07012 review. The containment modeling for US-APWR will be reviewed with Chapter 6.2 of the DCD.

5.0 REFERENCES

- "LOCA Mass and Energy Release Analysis Code Applicability Report for US-APWR," MUAP-07012-NP, Revision 2, ADAMS Accession No., ML081610448, May 2008.

- "Westinghouse LOCA Mass and Energy Release Model for Containment Design March 1979 Version," WCAP-10325-P-A, May 1983.

- Letter from Gerald T. Bischof (Virginia Electric and Power Company) to United States Nuclear Regulatory Commission dated November 6, 2006, Transmittal of Approved Topical Report DOM-NAF-3 NP-A, "GOTHIC Methodology for Analyzing the Response to Postulated Pipe Ruptures inside Containment." ADAMS Accession No., ML063190467, November 2006.

- 7 -

- "Large Break LOCA Applicability Report for US-APWR," MUAP-07011-NP, Revision 0, ADAMS Accession No., ML072140123, July 2007.

- "GOTHIC Containment Analysis Package Technical Manual, Version 7.2a (QA)," NAI 8907-06 Rev 16, January 2006.

- Lilly, G.P. and L.E. Hochreiter, "Mixing of Emergency Core Cooling Water with Steam: 1/3 Scale Test and Summary," EPRI 294-2, Electric Power Research Institute, June 1975.

- "The Advanced Accumulator," MUAP-07001-NP, Revision 1, ADAMS Accession No., ML070740602, February 2007.

DC Mitsubishi - US APWR Mailing List (Revised 04/01/2009)

cc:

Mr. Glenn H. Archinoff
AECL Technologies
481 North Frederick Avenue
Suite 405
Gaithersburg, MD 20877

Ms. Michele Boyd
Legislative Director
Energy Program
Public Citizens Critical Mass Energy
and Environmental Program
215 Pennsylvania Avenue, SE
Washington, DC 20003

Atsushi Kumaki
Mitsubishi Heavy Industries, Ltd.
APWR Promoting Department
Wadasaki-cho- 1-1-1, Hyogo-ku
Kobe 652-8585 JAPAN

Dr. Masanori Onozuka
Mitsubishi Nuclear Energy Systems, Inc.
2300 Wilson Blvd.
Suite 300
Arlington, VA 22201-5426

Dr. C. Keith Paulson
Mitsubishi Nuclear Energy Systems, Inc.
300 Oxford Drive, Suite 301
Monroeville, PA 15146

Mr. Tom Sliva
7207 IBM Drive
Charlotte, NC 28262

Mr. Robert E. Sweeney
IBEX ESI
4641 Montgomery Avenue
Suite 350
Bethesda, MD 20814

Mr. Ed Wallace
General Manager - Projects
PBMR Pty LTD
P. O. Box 9396
Centurion 0046
Republic of South Africa

Mr. Gary Wright, Director
Division of Nuclear Facility Safety
Illinois Emergency Management Agency
1035 Outer Park Drive
Springfield, IL 62704

DC Mitsubishi - US APWR Mailing List

Email

APH@NEI.org (Adrian Heymer)
atsushi_kumaki@mhi.co.jp (Atsushi Kumaki)
awc@nei.org (Anne W. Cottingham)
BrinkmCB@westinghouse.com (Charles Brinkman)
chris.maslak@ge.com (Chris Maslak)
ck_paulson@mnes-us.com (C Keith Paulson)
ckpaulson@aol.com (C.K. Paulson)
CumminWE@Westinghouse.com (Edward W. Cummins)
cwaltman@roe.com (C. Waltman)
david.hinds@ge.com (David Hinds)
david.lewis@pillsburylaw.com (David Lewis)
DeLaBarreR@state.gov (R. DeLaBarre)
donald.woodlan@luminant.com (Donald Woodlan)
erg-xl@cox.net (Eddie R. Grant)
gcesare@enercon.com (Guy Cesare)
greshaja@westinghouse.com (James Gresham)
james.beard@gene.ge.com (James Beard)
jerald.head@ge.com (Jerald G. Head)
jgutierrez@morganlewis.com (Jay M. Gutierrez)
jim.riccio@wdc.greenpeace.org (James Riccio)
jin_chung@mnes-us.com
JJNesrsta@cpsenergy.com (James J. Nesrsta)
John.O'Neill@pillsburylaw.com (John O'Neill)
Joseph_Hegner@dom.com (Joseph Hegner)
kcrogers@aol.com (K. C. Rogers)
KSutton@morganlewis.com (Kathryn M. Sutton)
kwaugh@impact-net.org (Kenneth O. Waugh)
lchandler@morganlewis.com (Lawrence J. Chandler)
lon.burnam@house.state.tx.us (Lon Burnam)
Marc.Brooks@dhs.gov (Marc Brooks)
maria.webb@pillsburylaw.com (Maria Webb)
mark.beaumont@wsms.com (Mark Beaumont)
masahiko_kaneda@mhi.co.jp (Masahiko Kaneda)
masanori_onozuka@mnes-us.com (Masanori Onozuka)
masayuki_kambara@mhi.co.jp (Masayuki Kambara)
matias.travieso-diaz@pillsburylaw.com (Matias Travieso-Diaz)
mayorsouthern@granbury.org (Mayor David Southern)
media@nei.org (Scott Peterson)
mike_moran@fpl.com (Mike Moran)
MSF@nei.org (Marvin Fertel)
mutsumi_ishida@mnes-us.com (Mutsumi Ishida)
mwetterhahn@winston.com (M. Wetterhahn)
nan_sirirat@mnes-us.com (Sirirat Mongkolkam)
nirsnet@nirs.org (Michael Mariotte)

DC Mitsubishi - US APWR Mailing List

patriciaL.campbell@ge.com (Patricia L. Campbell)
paul.gaukler@pillsburylaw.com (Paul Gaukler)
Paul@beyondnuclear.org (Paul Gunter)
plarimore@talisman-intl.com (Patty Larimore)
pshastings@duke-energy.com (Peter Hastings)
RJB@NEI.org (Russell Bell)
RKTemple@cpsenergy.com (R.K. Temple)
Russell.Wells@Areva.com (Russell Wells)
sabinski@suddenlink.net (Steve A. Bennett)
sandra.sloan@areva.com (Sandra Sloan)
satoshi_hanada@mnes-us.com (Satoshi Hanada)
satoshi_watanabe@mnes-us.com (Satoshi Watanabe)
sfrantz@morganlewis.com (Stephen P. Frantz)
shinji_kawanago@mnes-us.com (Shinji Kawanago)
stephan.moen@ge.com (Stephan Moen)
steven.hucik@ge.com (Steven Hucik)
Tansel.Selekler@nuclear.energy.gov (Tansel Selekler)
tgilder1@luminant.com (Tim Gilder)
tmatthews@morganlewis.com (T. Matthews)
tom.miller@hq.doe.gov (Tom Miller)
trsmith@winston.com (Tyson Smith)
Vanessa.quinn@dhs.gov (Vanessa Quinn)
VictorB@bv.com (Bill Victor)
vijukrp@westinghouse.com (Ronald P. Vijuk)
Wanda.K.Marshall@dom.com (Wanda K. Marshall)
whorin@winston.com (W. Horin)
yoshiki_ogata@mhi.co.jp (Yoshiki Ogata)

Revision History

Revision	Page	Description
0	All	Original issue
1		This revision is primarily intended to replace a sample analysis in this report with the limiting case of the containment analyses for the loss-of-coolant accident described in the US-APWR design control document. Some validation studies based on the sample analysis are also revised for consistency, although the results remain unchanged. The replaced objects are as follows:
	2-16	- The figure of Steam Generator (Figure 2-5)
	3-32	- The peak pressure and vapor temperature in the sample analysis
	3-44	- The verification of advanced accumulator model built into SATAN-VI and WREFLOOD code (Table 3-3)
	3-54	- The main input description for sample analysis of mass and energy release (Table 3-12)
	3-101, 3-102	- The sensitivity analysis results on the steam/water mixing model at DVI (Figure 3-7 and Figure 3-8)
	3-112 to 3-119	- The sample analysis results (Figure 3-18 to Figure 3-25)
	C-4 to C-7	- The validation of the NR Model (Figure C-2 to Figure C-8)
2		This revision is intended to incorporate the responses to RAIs from the NRC. The evaluation model to resolve the flow oscillation issue raised with the additional NRC questions on March 7, 2008 and March 12, 2008 is also described in this revision.
	3-2	- Description of SATAN-VI nodalization for accumulators and pumped injection system (for RAI 9)
	3-5 to 3-6	- Difference of advanced accumulator model between SATAN, WREFLOOD and WCOBRA/TRAC(M1.0) (for RAI 1a) - Discussion on the effect of inertia for injection line (for RAI 1b)
	3-7	- Description of treatment for steam condensation in the downcomer during reflood phase (for RAI 6 and 15)
	3-8	- Parameter exchange between WREFLOOD and GOTHIC (for RAI 6)
	3-9, 3-10	- NR modeling in the blowdown phase (for RAI 6)
	3-10	- Addition of subsection 3.2.3.5 related to fuel rod number for Reflood (for RAI 6)
	3-11, 3-12	- Discussion on the core quench for 14-ft fuel (for RAI 18)
	3-18	- Description for the GOTHIC version (for RAI 11i)

Revision	Page	Description
2	3-19	- Fuel modeling as a conductor in post-reflood phase (for RAI 11c)
	3-20	- Decay heat calculation for US-APWR (for RAI 11e)
	3-20, 3-21	- Treatment of the RV metal in post-reflood phase (for RAI 11f)
	3-21, 3-22	- Treatment of the primary loop metal in post-reflood phase (for RAI 11g, 11h)
	3-22 to 3-25	- Description of the GOTHIC film heat transfer option (for RAI 11d)
	3-25 to 3-26	- Description of the vessel froth model in post-reflood phase (for RAI 11j)
	3-26 to 3-27	- Treatment of advanced accumulator in GOTHIC (for RAI 2)
	3-27	- Treatment of accumulator gas (for RAI 21)
	3-27 to 3-30	- Applied options of GOTHIC (for RAI 11b)
	3-31	- Change of subsection title for US-APWR plant analyses
	3-31, 3-32	- The descriptions of the transition between SATAN-VI and WREFLOOD (for RAI 4)
	3-31	- Description of modeling options for SATAN-VI and WREFLOOD (for RAI 7)
	3-31, 3-32	- Description of model conservatisms involving code inputs (RAI 12)
	3-32	- Table including the results of the base case is referred to.
	3-32	- Additional plots in post-reflood phase are provided. (for RAI 11j)
	3-32	- Mass and energy related parameters at the time of transition from the end of blowdown to the beginning of reflood for the base case are provided. (for RAI 6)
	3-32	- Mass and energy balance tables are provided. (for RAI 13)
	3-32	- Mass and energy release tables are provided. (for RAI 14)
	3-32	- Subsection 3.4.2 for sensitivity studies is added.
	3-32, 3-33	- Subsection for the sensitivity study on ECCS conditions are added. (for RAI 3)
	3-33, 3-34	- Subsection for the sensitivity study on loop pipe resistance is added. (for RAI 8, RAI 11a)
	3-34, 3-35	- Subsection for the sensitivity study on loop seal formation is added. (for RAI 11k)
	3-35	- Subsection for treatment of spilled accumulator Water is added. (for RAI 16, 17)

Revision	Page	Description
2	3-35 to 3-37	- Subsection on the Effects of Flow Oscillation is added. (for RAI 20)
	3-37 to 3-41	- Subsection 3.4.3 “Proposed Evaluation Model for Post-reflood Long-term Period” is added. (for RAI 20)
	3-46	- Table 3-5 related to the accumulator model in GOTHIC is provided. (for RAI 2)
	3-47 to 3-48	- Table 3-6 related to applied options of GOTHIC is provided.(for RAI 11b)
	3-49 to 3-51	- Table 3-7 for comparison of GOTHIC US-APWR model with FROTH is provided. (for RAI 11j)
	3-52, 3-53	- Tables related to modeling options for SATAN-VI and WREFLOOD are provided. (for RAI 7)
	3-55	- Table 3-13 related to model conservatisms involving code inputs is provided. (for RAI 12)
	3-56	- Table 3-14 for sensitivity of ECCS conditions is provided. (for RAI 3)
	3-57	- Table 3-15 for water mass and RCS temperature transient is provided. (for RAI 4)
	3-58, 3-59	- Tables for mass and energy distribution transient are provided. (for RAI 13)
	3-60 to 3-94	- Table 3-18 to Table 3-21 for break mass and energy flow rate are provided. (for RAI 14)
	3-96	- Noding diagram of SATAN-VI is revised. (for RAI 9)
	3-98, 3-99	- Figures related to the discussion on the effect of inertia for injection line are provided. (for RAI 1b)
	3-108	- Core decay heat curve is provided. (for RAI 11e)
	3-109	- Heat transfer selection logic is provided. (for RAI 11d)
	3-110	- Figure 3-16 showing the concept of vessel two-phase level by GOTHIC is provided. (for RAI 11j)
	3-111	- Noding diagram of US-APWR referenced by Table 3-6 is provided. (for RAI 11b)
	3-120	- Figure 3-26 for RWSP water temperature of the base case is provided.
	3-121 to 3-125	- Figures related to the vessel froth model in post-reflood phase are provided. (for RAI 11j)
	3-126 to 3-134	- Figures related to the sensitivity study on ECCS conditions are provided. (for RAI 3)
	3-135 to 3-139	- Figures related to the sensitivity study on loop pipe resistance are provided. (for RAI 8, RAI 11a)

Revision	Page	Description
2	3-140 to 3-146	- Figures related to the sensitivity study on loop seal formation are provided. (for RAI 11k)
	3-147	- Figure 3-53 related to the Effects of Flow Oscillation is added. (for RAI 20)
	3-148 to 3-158	- Figures related to the proposed model that eliminates flow oscillation effects are provided. (for RAI 20)
	4-1	- Editorial revision
	5-2	- References 18 to 21 are added.
	D-1 to D-14	- Appendix D is added for the sensitivity study related to the treatment of spilled accumulator water. (for RAI 16, 17)
	E-1 to E-6	- Appendix E is added for the sensitivity study related to the Effects of Flow Oscillation. (for RAI 20)
	F-1 to F-121	- Appendix F is added to attach all of the responses to RAIs.

Mitsubishi Heavy Industries, Ltd.
16-5, Konan 2-chome, Minato-ku
Tokyo 108-8215 Japan

ABSTRACT

The Standard Review Plan (Reference 1) states that LOCA mass and energy release evaluation analyses performed with the Appendix K ECCS computer codes which were developed to comply with the ECCS Acceptance Criteria presented in 10CFR50.46 and 10CFR50 Appendix K shall be acceptable. “Westinghouse LOCA Mass and Energy Release Model for Containment Design March 1979 Version (Reference 2)” conforms to the standard and is approved by the NRC.

In order to meet this standard while incorporating modified analytical models reflecting US-APWR new features, MHI has developed a modified mass and energy release model which is based on the ECCS Appendix K codes (SATAN-VI and WRFLOOD). Where applicable and appropriate, conservative models for mass and energy release calculations have been added into the codes.

A sample mass and energy release calculation, in which a double ended guillotine break at pump suction was assumed as postulated LOCA condition was performed by using the analytical models described above.

The methodology as presented will be used when determining maximum containment pressure and temperature following a loss-of-coolant accident for the US-APWR.

Table of Contents

List of Tables

Rev. 2

Rev. 2

List of Figures

Rev. 2

Rev. 2

Rev. 2

List of Acronyms

ACC	Accumulator
APWR	Advanced Pressurized Water Reactor
CS	Containment Spray
CSS	Containment Spray System
CVCS	Chemical and Volume Control System
DNB	Departure from Nucleate Boiling
DVI	Direct Vessel Injection
ECCS	Emergency Core Cooling System
EPRI	Electric Power Research Institute
EPS	Emergency Power Source
ESF	Engineered Safety Feature
FA	Fuel Assembly
Fout	Core carryover rate fraction in the reflooding phase
HHSI	High Head Injection System
ICIS	In-Core Instrumentation System
LOCA	Loss Of Coolant Accident
LP	Lower Plenum of reactor vessel
M&E	Mass and Energy
MSLB	Main Steam Line Break
NPSH	Net Positive Suction Head
NR	Neutron Reflector
PWR	Pressurized Water Reactor
PZR	Pressurizer
RCCA	Rod Cluster Control Assemblies
RCP	Reactor Coolant Pump
RCS	Reactor Coolant System
RHR	Residual Heat Removal
RV	Reactor Vessel
RVH	Reactor Vessel Head
RVI	Reactor Vessel Internal
RWSP	Refueling Water Storage Pit
SDV	Safety Depressurization Valve
SG	Steam Generator
SRP	Standard Review Plan
SRV	Safety Relief Valve
Tinlet	Primary coolant temperature at reactor vessel inlet nozzle
TDF	Thermal Design Flow
UP	Upper Plenum of reactor vessel
Vin	Core flooding rate in the reflooding phase

Rev. 2

1.0 INTRODUCTION

This report documents the acceptability of use of analysis codes and methodologies approved for the existing Pressurized Water Reactor (PWR) in their application to the US-APWR. The US-APWR is an advanced PWR with improved design to enhance reliability while retaining many basic features of the existing four-loop PWR. Therefore the methodologies for the existing PWRs are applicable to the US-APWR with minor modifications for the improved features.

This report demonstrates the applicability of the PWR analysis codes and methodologies used for calculation of mass and energy release to the containment following a design basis loss-of-coolant accident (LOCA) to the US-APWR. The method as presented are intended for use when determining maximum containment pressure and temperature following a loss-of-coolant accident.

Chapter 2 presents an overview of the US-APWR plant design features related to the LOCA analyses to assist in understanding applicability of the approved methodologies for current PWRs to the US-APWR.

Chapter 3 addresses the codes and methodology used for the mass and energy release analysis. In Section 3.2, the mass and energy release model with minor modifications reflecting the improved features of the US-APWR for the blowdown and reflood phases are described. And in Section3.3, the mass and energy release model for the post-reflood phases are described.

Also, Section 3.4 presents a sample mass and energy release calculation result performed by using the analytical models described above and its containment response.

Chapter 4 summarizes the version of the mass and energy release evaluation model with minor modifications, which is based on the approved methodology and discusses the conclusions.

2.0 US-APWR PLANT DESIGN AND FEATURES

This section describes certain aspects of the US-APWR design in order to assist in the understanding the applicability of the approved methodologies for current PWRs to the US-APWR. The US-APWR features highly reliable prevention functions, well-established mitigation systems with active safety functions, and passive safety functions. The primary system design, loop configuration, and main components are similar to those of currently operating PWRs.

2.1 Main Specifications

The US-APWR is an advanced PWR of improved design to enhance reliability while retaining the basic features of existing 4-loop PWRs. The main specifications of the US-APWR in comparison with existing 4-loop PWRs in the U.S. are shown in Table 2-1.

2.2 Reactor and Core

2.2.1 General Features

The reactor configuration of the US-APWR is shown in Figure 2-1. Comparisons of core parameters between the US-APWR and US current 4-loop PWRs are shown in Table 2-2. The fuel assemblies, rod cluster control assemblies, reactor vessel internals and thermal hydraulic design are described below.

2.2.2 Fuel Assemblies

The fuel assembly consists of the 264 fuel rods arranged in a square 17x17 array, together with 24 control rod guide thimbles, an in-core instrumentation guide tube, 11 grid spacers, and top and bottom nozzles. This design maintains the same grid spacing (approximately 18 inches) as the 17x17 fuel assembly design in current plants. This relatively shorter grid spacing provides greater margin to grid fretting and improves DNB performance in comparison with the widely used standard design of about 14 ft heated length and 10 grid design. Fuel assembly characteristics are shown in Table 2-3.

2.2.3 Reactor Vessel Internals

The arrangement of the reactor vessel internals (RVI) of the US-APWR is shown in Figure 2-1. The increased fuel element length in the US-APWR is enabled by the integration of the lower core plate and lower core support plate.

The coolant flows from the RV inlet nozzles down the annulus between the core barrel and the RV and then into a plenum at the bottom of the RV. The flow then turns and passes through the lower core support plate and into the core. After passing through the core, the coolant enters the upper plenum and then flows radially to the core barrel outlet nozzles. A small amount of coolant flows into the vessel head plenum from the annulus to cool the vessel head area.

A neutron reflector (NR) is used in the US-APWR to improve neutron utilization and thus the fuel cycle cost, to reduce neutron irradiation of the RV, and to increase structural reliability by eliminating bolts in the high neutron flux region. The NR assembly is shown in Figure 2-2.

The NR is located between the core barrel and core, and lines the core cavity. The NR consists of ten thick stainless steel blocks. These blocks are aligned by alignment pins and fixed to the lower core support plate by tie rods and bolts. The top and bottom are supported and aligned by alignment pins that are welded to the core barrel.

The NR is cooled by up-flow through cooling holes in the blocks. The flow is sufficient to avoid coolant boiling and prevent excessive stress and thermal deflections of the blocks due to the gamma heating. The total core bypass flow is approximately 7.5% of total reactor coolant system (RCS) flow rate. It is relatively larger than the flow rate at a existing PWR plant so as to allow enough cooling for the NR and to keep the Reactor Vessel Head (RVH) coolant temperature at Tinlet.

2.3 Reactor Coolant System

2.3.1 General Features

The RCS consists of the RV, the steam generators (SGs), the reactor coolant pumps (RCPs), the pressurizer (PZR) and the reactor coolant pipes and valves. The flow schematic for the RCS is shown in Figure 2-3.

The reactor coolant flows through the hot leg pipes to the SGs and returns to the RV via the cold leg pipes and the RCPs. The PZR is connected to one hot leg via the surge line and to two cold legs via the spray lines.

The reactor coolant system, including connections to related auxiliary systems, constitutes the reactor coolant pressure boundary.

The reactor coolant system performs the following functions.

- Circulates the reactor coolant through the reactor core and transfers heat to the secondary system via the steam generators.
- Cools the core sufficiently to prevent core damage during reactor operation.
- Forms the reactor coolant pressure boundary, which functions as a barrier to prevent radioactive materials in the reactor coolant from being released to the environment.
- Functions as a neutron moderator and reflector and as a solvent for boron.
- Controls the reactor coolant pressure.

The RV, SGs, RCPs, and PZR are individually described below.

2.3.2 Reactor Vessel

The reactor vessel (RV), shown in Figure 2-4, is a vertical cylindrical vessel with hemispherical top and bottom heads. The top head is a removable flanged closure head connected to the RV upper shell flange by stud bolts. Pads on the RV nozzles support the vessel.

The RV has four inlet nozzles, four outlet nozzles and four Direct Vessel Injection (DVI) nozzles, which are located between the upper reactor vessel flange and the top of the core, so as to maintain coolant in the reactor vessel in the case of leakage in the reactor coolant loop.

2.3.3 Steam Generators

The SGs, shown in Figure 2-5, are vertical shell U-tube evaporators with integral moisture separating equipments.

The design of the SGs for the US-APWR has been improved to attain high efficiency and reliability by adopting 3/4 inch (19.05 mm) outer diameter tubes made of alloy 690 thermal treated, which are arranged triangularly in 1 inch (25.4mm) pitch.

The reactor coolant enters the tube inlet plenum via the hot side primary coolant nozzle, flows through the inverted U-tubes, transferring heat from the primary side to the secondary side, and leaves from the SG lower head via the cold side primary coolant nozzle. The lower head is divided into inlet and outlet chambers by a vertical partition plate extending from the apex of the lower head to the tube sheet.

Steam generated on the shell side (secondary side) flows upward and exits through the outlet nozzle at the top of the vessel. Feedwater enters the steam generator at an elevation above the top of the U-tubes through a feedwater nozzle. The feedwater enters a feedring and is distributed through nozzles attached to the top of the feedring.

2.3.4 Reactor Coolant Pumps

The reactor coolant pumps (RCPs) for the US-APWR are upsized versions of the Type 93A pumps used in existing Westinghouse's design PWRs. Their design is similar to that of the Type 93A RCPs.

The RCPs of US-APWR, shown in Figure 2-6, are vertical, single-stage, centrifugal, shaft seal units, driven by three-phase induction motors. The shaft is vertical with the motor mounted above the pump. A flywheel on the shaft above the motor provides additional inertia to extend pump coastdown. The pump suction is at the bottom, and the discharge is located on the side.

The reactor coolant that enters from the bottom of the casing is accelerated by the impeller and causes a pressure increase across the diffuser. The diffuser is located at the center of the casing in order to attain high hydraulic efficiency.

The US-APWR reactor coolant pump has achieved larger capacity and higher efficiency than those of Type 93A pump by improving of the impeller and diffuser configuration.

2.3.5 Pressurizer

The pressurizer (PZR), shown in Figure 2-7, is a vertical, cylindrical vessel with hemispherical top and bottom heads. The PZR is connected to one hot leg of the reactor coolant loops via the surge line and to two cold legs via the spray lines.

Electrical immersion heaters in the bottom head and the spray nozzle located in the top head control the primary system pressure.

The relief and safety valves at the top head provide overpressure protection of the RCS. The overpressure protection function of the US-APWR is performed as follows.

- Spring-loaded safety relief valves (SRVs) are installed on separate relief lines at the top of the pressurizer.
- An additional relief line has motor-operated relief valves for safety depressurization valves (SDVs). The valves are arranged in parallel and are driven by motor operators. A remotely controlled, motor-operated isolation valve is installed upstream of each the SDVs to allow isolation in the event of a leak.
- The relief lines discharge through spargers in the refueling water storage pit (RWSP) inside the containment.
- Safety relief valves are installed in the each residual heat removal system to provide overpressurization protection for unacceptable combinations of high reactor coolant system pressure and low reactor coolant system temperature.

2.4 Engineered Safety Features

2.4.1 General Features

The engineered safety features (ESFs) serve to mitigate the consequences of a design basis accident in which radioactive fission products are released from the reactor coolant system. The ESFs consist of the emergency core cooling system (ECCS), containment spray system (CSS), containment system, annulus air cleanup system and main control room heat, ventilation and air conditioning system.

The simplified configuration of the ECCS and CSS is shown in Figure 2-8.

The US-APWR employs the following advanced technologies for the ECCS and CSS to enhance its simplification.

a. Four-train, Direct Vessel Injection for High Head Injection System

The US-APWR employs a 4-train direct vessel injection (DVI) system. This system configuration increases redundancy and independence, and enhances safety and reliability. The capacity of each train is 50% of the capacity of a single train of a conventional two train system. Inter-connecting piping between each train is also eliminated.

The support system and the emergency AC power supply system also adopt a 4-train configuration to enhance the reliability of the system.

b. Emergency Water Storage inside the Containment

The US-APWR eliminates potentially high risk operator actions to realign the suction in an emergency such as a Loss of Coolant Accident (LOCA) by installing the Refueling Water Storage Pit (RWSP) inside the containment. The RWSP is formed with a lined concrete structure and works as the emergency water source. This design significantly contributes to lowering the estimated core damage frequency.

c. Passive Low Head Injection

The safety system of the US-APWR consists of an optimized combination of active and passive components. The advanced accumulator is a passive component employed to enhance safety by improving flow injection characteristics and eliminating the need of the low head injection system. By adopting the vortex damper mechanism, the advanced accumulator supplies water with a large flow rate at the early stage of LOCA, and lower flow rate at the later stages.

The ECCS, CSS and containment system are described below.

2.4.2 Emergency Core Cooling System

The ECCS, shown in Figure 2-9, includes the accumulator system, high head injection system and emergency letdown system. The ECCS injects borated water into the reactor coolant system following a postulated accident and performs the following functions;

- Following a loss-of-coolant accident, the ECCS cools the reactor core, prevents serious damage to the fuel and fuel cladding, and limits the zirconium-water reaction in the fuel cladding to a very small amount.
- Following a main steam line break (MSLB), the ECCS provides negative reactivity to shut down the reactor.
- In the event that the normal CVCS letdown and boration capability are lost, the ECCS provides emergency letdown and boration of the RCS to orderly shutdown the reactor.

Compliance of the US-APWR ECCS with the 10 CFR 50.46 acceptance criteria is evaluated by ECCS Performance Analysis.

The ECCS design is intended to accomplish the following functions;

- In combination with control rod insertion, the ECCS is designed to shut down and cool the reactor during the following accidents;
    - Small break loss-of-coolant accidents
    - Control rod ejection
    - Main steam line break
    - Steam generator tube rupture
- The ECCS is designed with sufficient redundancy (four trains) to accomplish the specified safety functions assuming a single failure of an active component in the short term following an accident with one train out of service for maintenance, or a single failure of an active component or passive component for the long term following an accident with one train out of service.
- The emergency power source supply electrical power to the essential components of the ECCS, so the design functions are maintained during a loss of offsite power.

- The ECCS is automatically activated by a safety injection signal.
- The ECCS design permits periodical tests and inspections to verify integrity and operability.

2.4.2.1 Accumulator System

The accumulator system stores borated water under pressure and automatically injects it if the reactor coolant pressure decreases significantly. The accumulator system consists of four accumulators and the associated valves and piping, one for each RCS loop. The system is connected to the cold legs of the reactor coolant piping and injects borated water when the RCS pressure falls below the accumulator operating pressure. The system is passive. Pressurized nitrogen gas forces borated water from the tanks into the RCS.

As shown in Figure 2-10 accumulators incorporate internal passive flow dampers and a stand pipe which function to inject a large flow to refill the reactor vessel in the first stage of injection, and then reduce the flow as the water level in the accumulator drops. When the water level is above the top of the standpipe, water enters the flow damper through both inlets at the top of the standpipe and at the side of the flow damper such that water is injected at a large flow rate. When the water level drops below the top of the standpipe, water enters the flow damper only through the side inlet, so that accumulator injects water at a relatively low flow rate.

The accumulators provide large flow injection to refill the reactor vessel and continue with small flow injection during core reflooding in conjunction with the safety injection pumps. The combined performance of the accumulator system and the high head injection system eliminate the need for a conventional low head injection system. The accumulator system's performance for the US-APWR is shown in Figure 2-10.

2.4.2.2 High Head Injection System

The direct vessel injection (DVI) is employed for the high head injection system. The high head injection system consists of four independent trains, each containing a safety injection pump and the associated valves and piping. The safety injection pumps start automatically upon receipt of the safety injection signal. One of four independent safety electrical buses is available to each safety injection pump.

The safety injection pumps are aligned to take suction from the refueling water storage pit and to deliver borated water to the DVI nozzles on the reactor vessel. Two safety injection trains are capable of meeting the design cooling function for a Large Break LOCA, assuming a single failure in one train and another train out of service for maintenance. In the existing PWRs, the requirement for a Large Break LOCA is met through a low head injection pump that generally serves also as an RHR pump. Therefore, the capacity of the US-APWR high head injection pump is larger than the conventional high head pump in order to provide sufficient flow during the large break LOCA.

The refueling water storage pit in the containment provides a continuous borated water source for the safety injection pumps, thus eliminating the need for realignment from the refueling water storage pit to the containment sump.

2.4.3 Containment Spray System

The containment spray system (CSS), shown in Figure 2-11, consists of four independent trains, each containing a containment spray/residual heat removal (CS/RHR) heat exchanger, a CS/RHR pump, spray nozzles, piping and valves. The CS/RHR heat exchangers and the CS/RHR pumps are used for both CSS and RHRs function. The CSS sprays borated water into the containment vessel in the event of a loss-of-coolant accident.

The containment spray system functions to maintain the containment vessel internal peak pressure below the design pressure and reduce it to approximately atmospheric pressure in the event of a loss of coolant accident or a main steam line break.

The CSS is designed based on the following.

- Its safety functions can be accomplished if there is a single failure of an active component for a short term following an accident with one train out of service for maintenance, or a single failure of an active component or a single failure of a passive component for a long term following an accident with one train out of service for maintenance.
- The emergency power source can supply electrical power to the essential equipment of the CSS, so that safety functions can be maintained during a loss of offsite power.
- The CSS is automatically initiated by a containment spray signal.
- The CSS design permits periodic tests and inspections to verify integrity and operability.
- The CSS is capable of reducing the containment pressure to less than 50% of the peak calculated pressure for the design basis loss-of-coolant accident within 24 hours after the postulated accident.

The CSS is automatically actuated on receipt of a containment spray signal. When the signal is received, the CS/RHR heat exchanger outlet valves open and the CS/RHR pumps start. The CS/RHR pump motor is connected to a safety bus, so the emergency power source can supply electrical power in case of a loss of offsite power. The CS/RHR pumps take suction from the refueling water storage pit, and the stop valve on the inlet line is always open during reactor operation. The spray water is cooled by the CS/RHR heat exchangers and is delivered to the spray headers located in the top of the containment vessel.

The refueling water storage pit (RWSP) in the containment provides a continuous suction source for the CS/RHR pumps, thus eliminating the need for realignment from the refueling water storage pit to the containment sump.

The safety system pumps (CS/RHR pumps and safety injection pumps), which require sufficient net positive suction head (NPSH) to draw water from the recirculation sumps inside the containment, are located at the lowest level of the reactor building to secure the required NPSH. Also, they are located adjacent to the containment to minimize pipe lengths.

2.4.4 Containment System

The containment system includes the containment vessel, the annulus enclosing the containment penetration area, and the containment isolation function performed by the isolation valves, airlocks and equipment hatch.

The containment system provides an effective leak-tight barrier and environmental radiation protection under all postulated conditions, including a loss-of-coolant accident.

2.4.4.1 Containment Vessel

The containment vessel is designed to completely enclose the reactor and reactor coolant system and to ensure that essentially no leakage of radioactive materials to the environment would result even if a major failure of the reactor coolant system were to occur. The configuration of containment vessel is shown in Figure 2-12.

The containment vessel consists of a prestressed, post-tensioned concrete structure with a cylindrical wall, a hemispherical dome, and a flat reinforced concrete foundation slab. The inside surface of the structure is lined with carbon steel.

The design pressure and temperature of the containment vessel are defined by the following postulated accidents.

- Loss- of-coolant accident (LOCA)
- Main steam line break (MSLB)

The containment vessel is designed to contain the energy and radioactive materials that result from a postulated loss-of-coolant accident, and for an 68 psig internal pressure to ensure a high degree of leak tightness during normal operation and under accident conditions.

An internal polar crane is supported by the containment vessel. A continuous crane girder transfers the polar crane loads to the containment vessel wall.

Hydrogen igniters are provided for protection against possible detonation following a core damage accident.

2.4.4.2 Refueling Water Storage Pit

The refueling water storage pit (RWSP) is located in the lowest part of the containment vessel. The RWSP provides a continuous suction source for both the safety injection pumps and the CS/RHR pumps. The wall and the floor of the RWSP are lined with stainless steel liner plates. The RWSP has four recirculation sumps on the floor; these sumps are provided with recirculation screens.

Table 2-1 Comparison of Principal Parameters

Parameter	US-APWR	US Current 4-loop PWR	Ratio
Core Thermal Output (MWt)	4,451	3,565 (3853)	1.25
Operation Pressure (psia)	2,250	2,250 (2250)	-
Hot Leg Temperature (deg. F)	617	620 (626)	-
Cold Leg Temperature (deg. F)	551	557 (559)	-
Thermal Design Flow (gpm/loop)	112,000	93,600	1.20
Number of Fuel Assembly	257	193 (193)	1.33
Fuel Assembly Lattice	17x17	17x17	-
Effective Fuel Length (ft)	14	12 (14)	-
Number of Fuel Rods per FA	264	264	-
Average Linear Heat Rate (kW/ft)	4.6	5.7 (5.2)	0.8
Number of RCCAs	69	53 (57)	1.30
Number of Control Rods per RCCA	24	24 (24)	-
SG Heat Transfer Area (ft^2)	91,500	55,000	1.66
PZR Volume (ft^3)	2,900	1,800	1.6
PZR Volume to Thermal Power (ft^3/MWt)	0.65	0.50	1.3
Containment Design Pressure (psig)	68	52 (56.5)	-

Vogtle Unit #1 are referred to as a US current 4-loop PWR.
Data in parentheses are those of South Texas Project Unit 1 and 2, current 4-loop PWR using 14-ft fuel. They are in the database of International Nuclear Safety Center and last updated on 01/97.

Table 2-2 Key Parameters of Core Design

Parameter	US-APWR	US Current 4-loop PWR
Core Thermal Output	4,451 MWt	3,565MWt
Heat Generated in Fuel	97.4 %	97.4 %
Number of Fuel Assemblies	257	193
Fuel Assembly Lattice	17x17	17x17
Effective Fuel Length	14 ft	12 ft
Average Linear Heat Rate	4.6 kW/ft	5.7 kW/ft
Primary System Pressure	2,250 psia	2,250 psia
Thermal Design Flow (TDF)	448,000 gpm	374,400 gpm
Coolant Temperature		
Hot Leg	617 °F*	620 °F*
RV Average	584 °F*	588 °F*
Cold Leg	551 °F*	557 °F*
Core Bypass Flow	7.5 %**	6.3 %

* Given as approximate figures
** Nominal value for DNBR analysis

Table 2-3 Fuel Assembly Specification

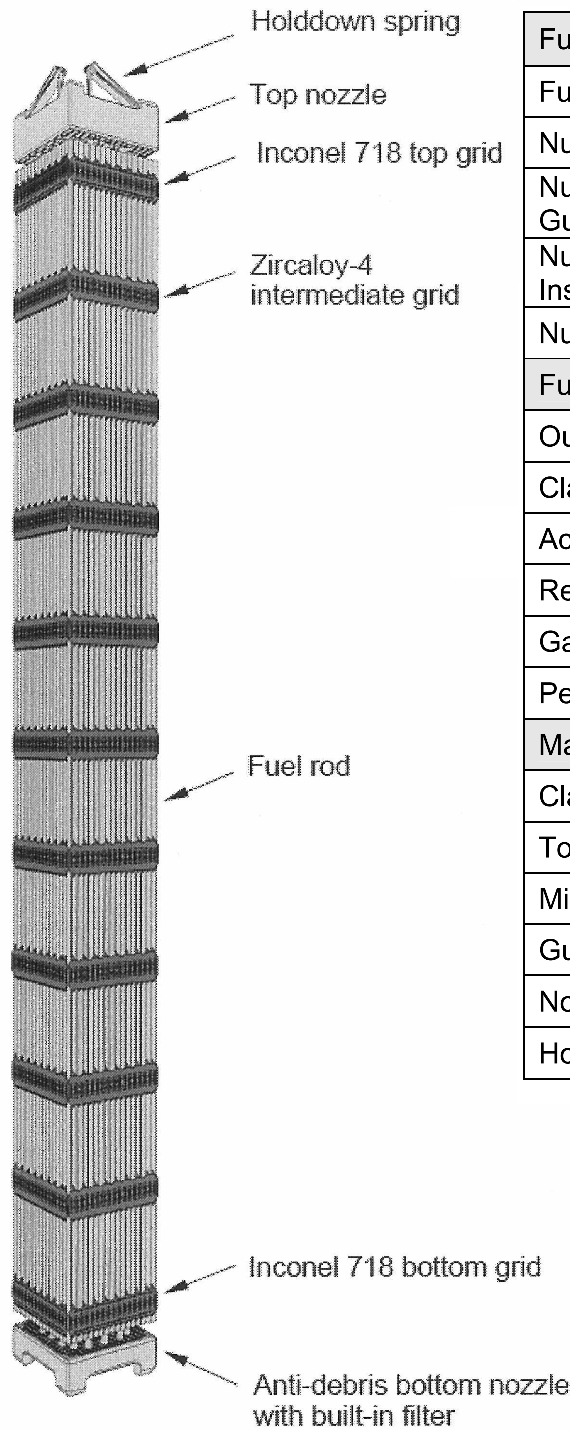

Fuel Assemblies	
Fuel Rods Array	17 x 17
Number of Fuel Rods	264
Number of Control Rod Guide Thimbles	24
Number of In-core Instrumentation Guide Tube	1
Number of Grid Spacers	11
Fuel Rods	
Outside Diameter	0.374 in. (9.50mm)
Cladding Thickness	0.022 in. (0.57mm)
Active Fuel Length	165.4" (4,200mm)
Reload Fuel Enrichment	Max. 5 wt%
Gadolinia Content	Max. 10 wt%
Pellet Density	97 %TD
Materials	
Cladding	ZIRLO™
Top & Bottom Grids	Inconel 718
Middle Grids	Zircaloy-4
Guide Thimbles	Zircaloy-4
Nozzles	Stainless Steel
Holddown Springs	Inconel 718

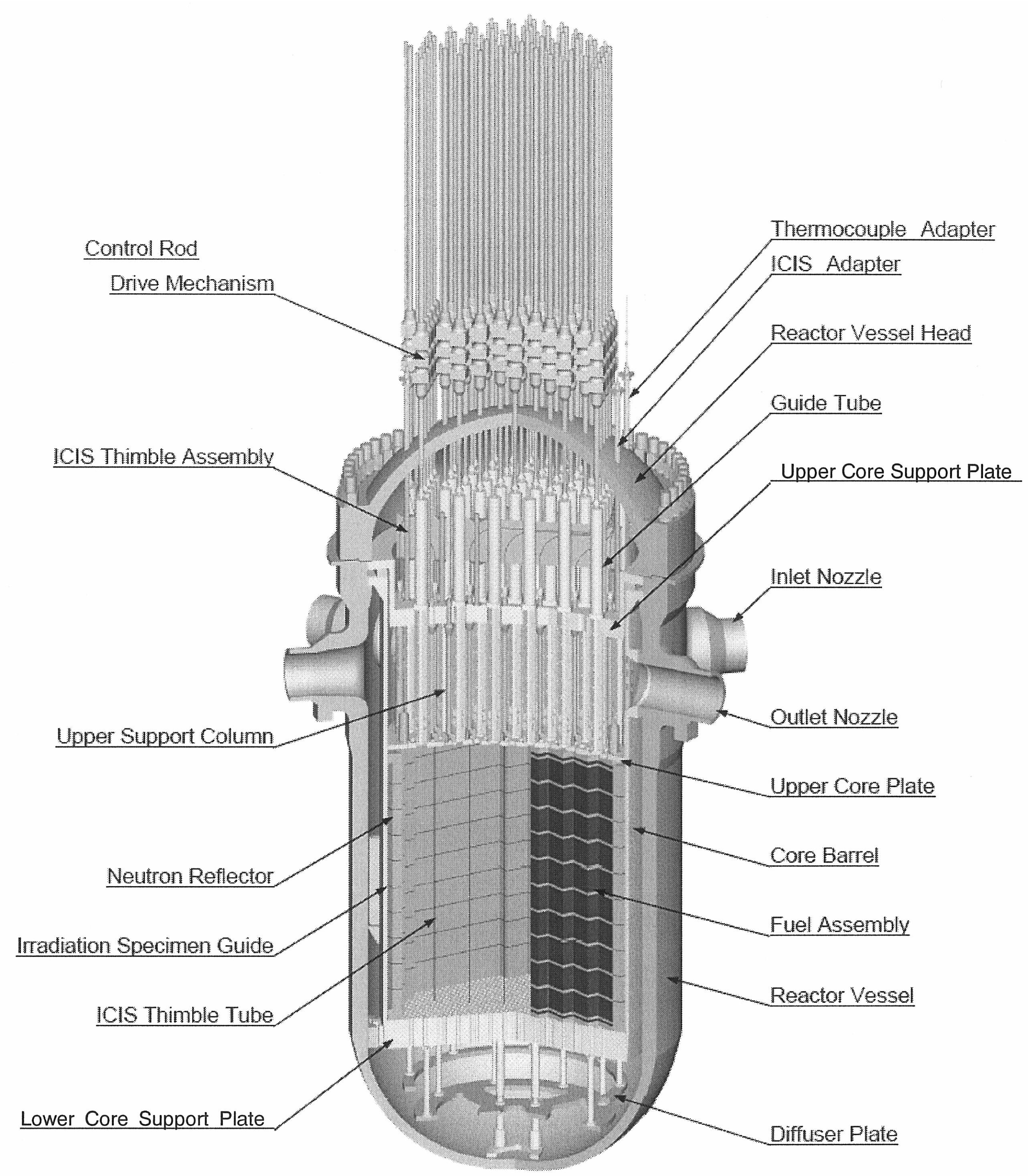

Figure 2-1 Reactor General Assembly

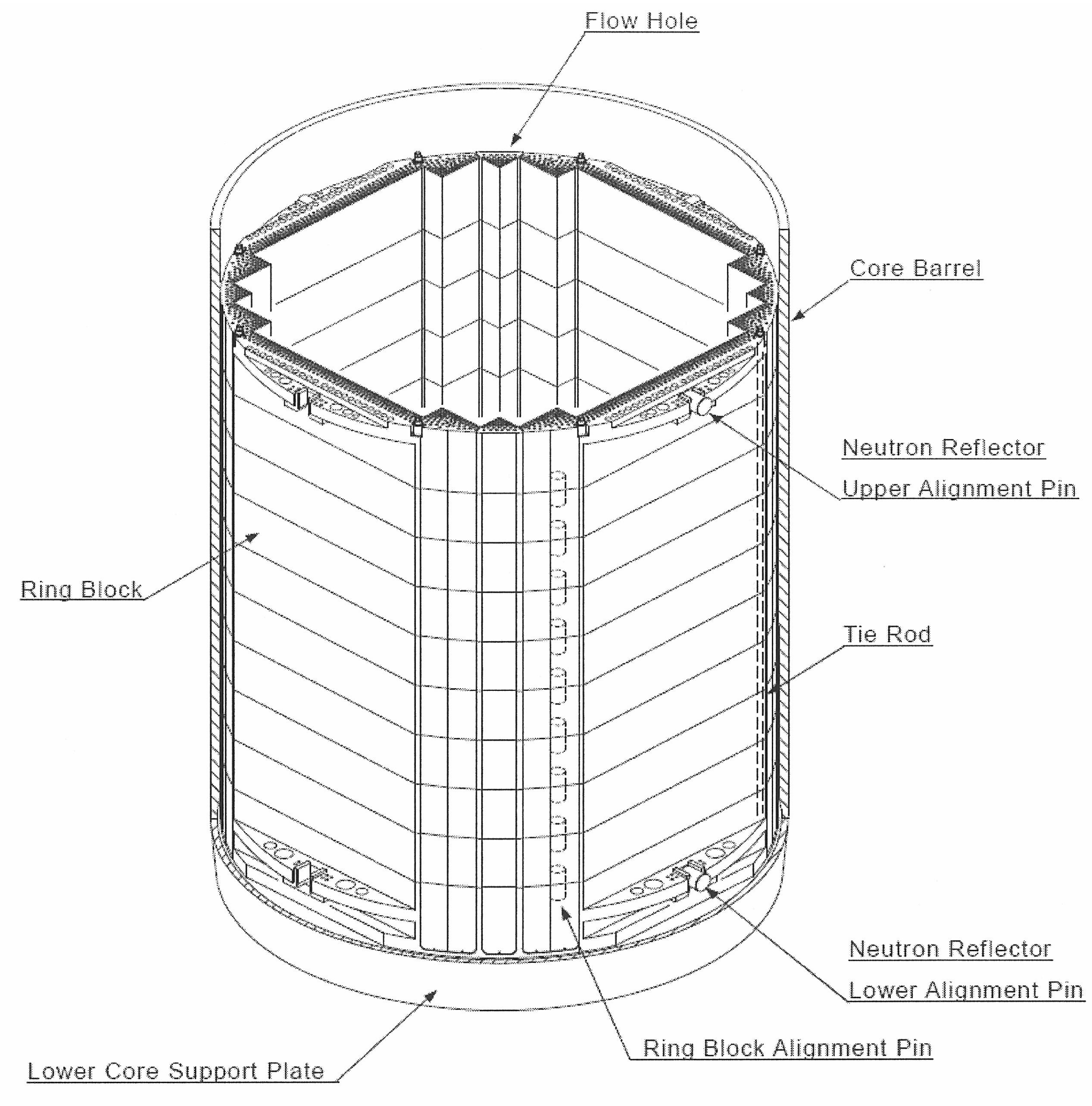

Figure 2-2 Neutron Reflector Assembly

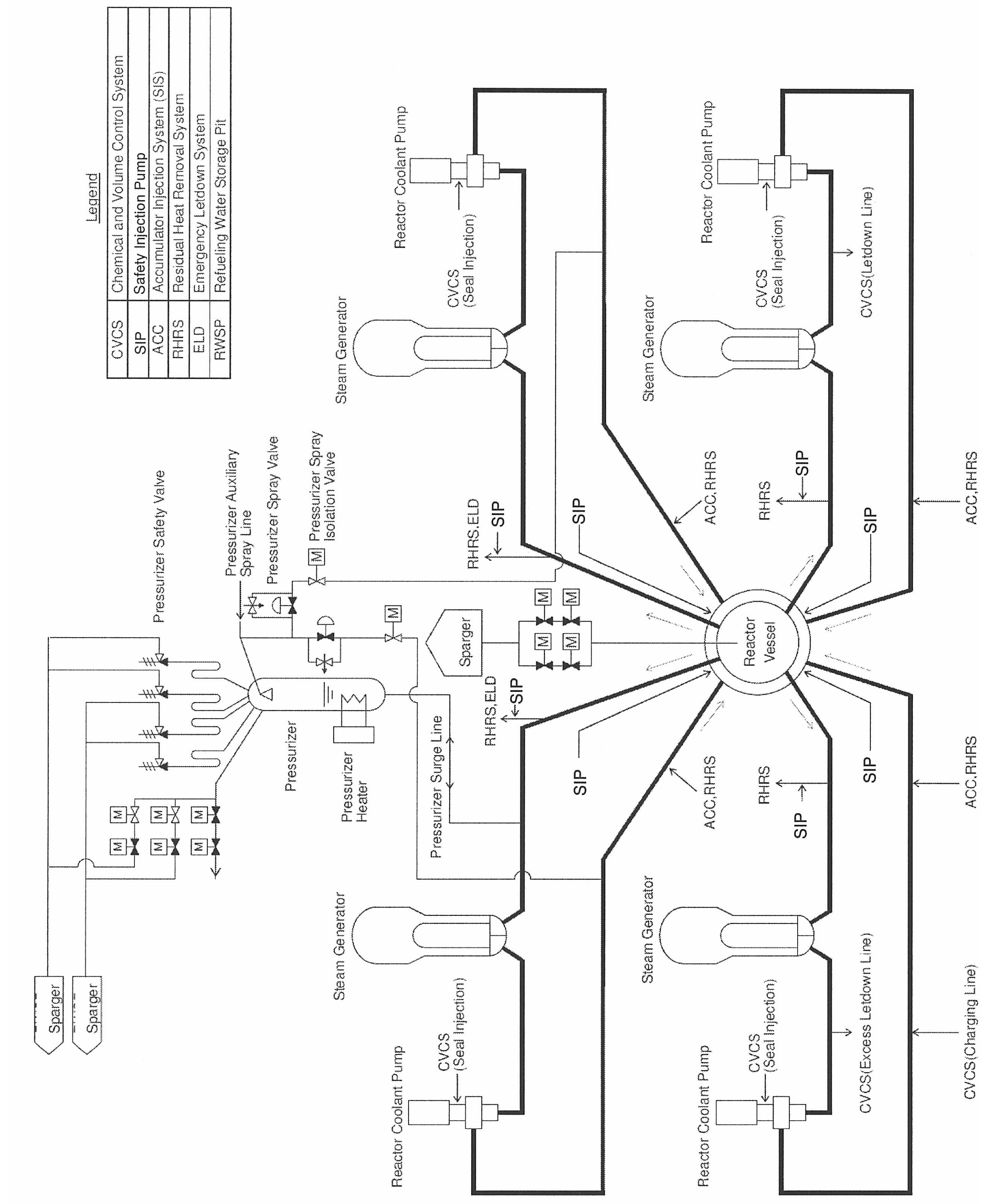

Figure 2-3 Reactor Coolant System

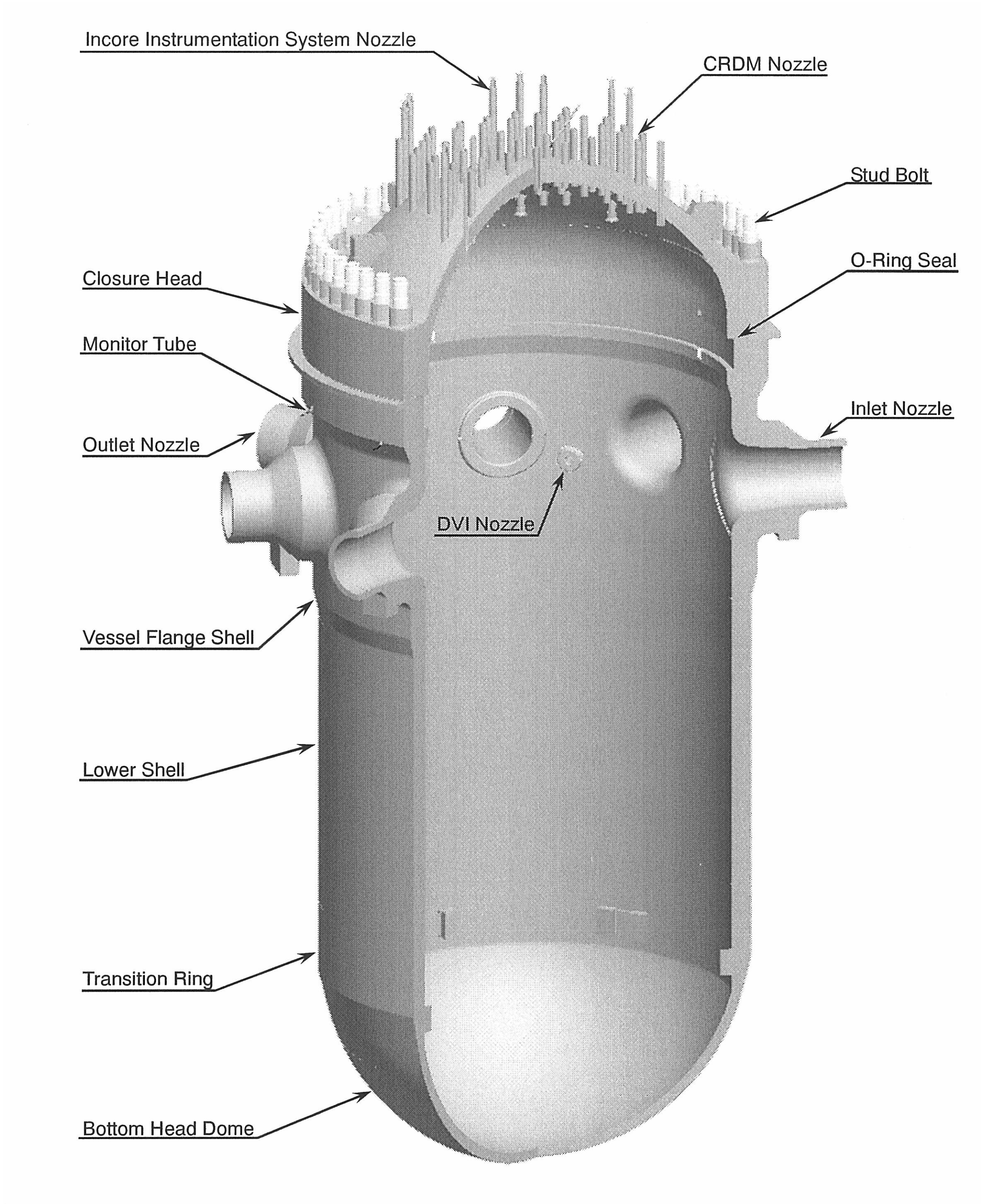

Figure 2-4 Reactor Vessel

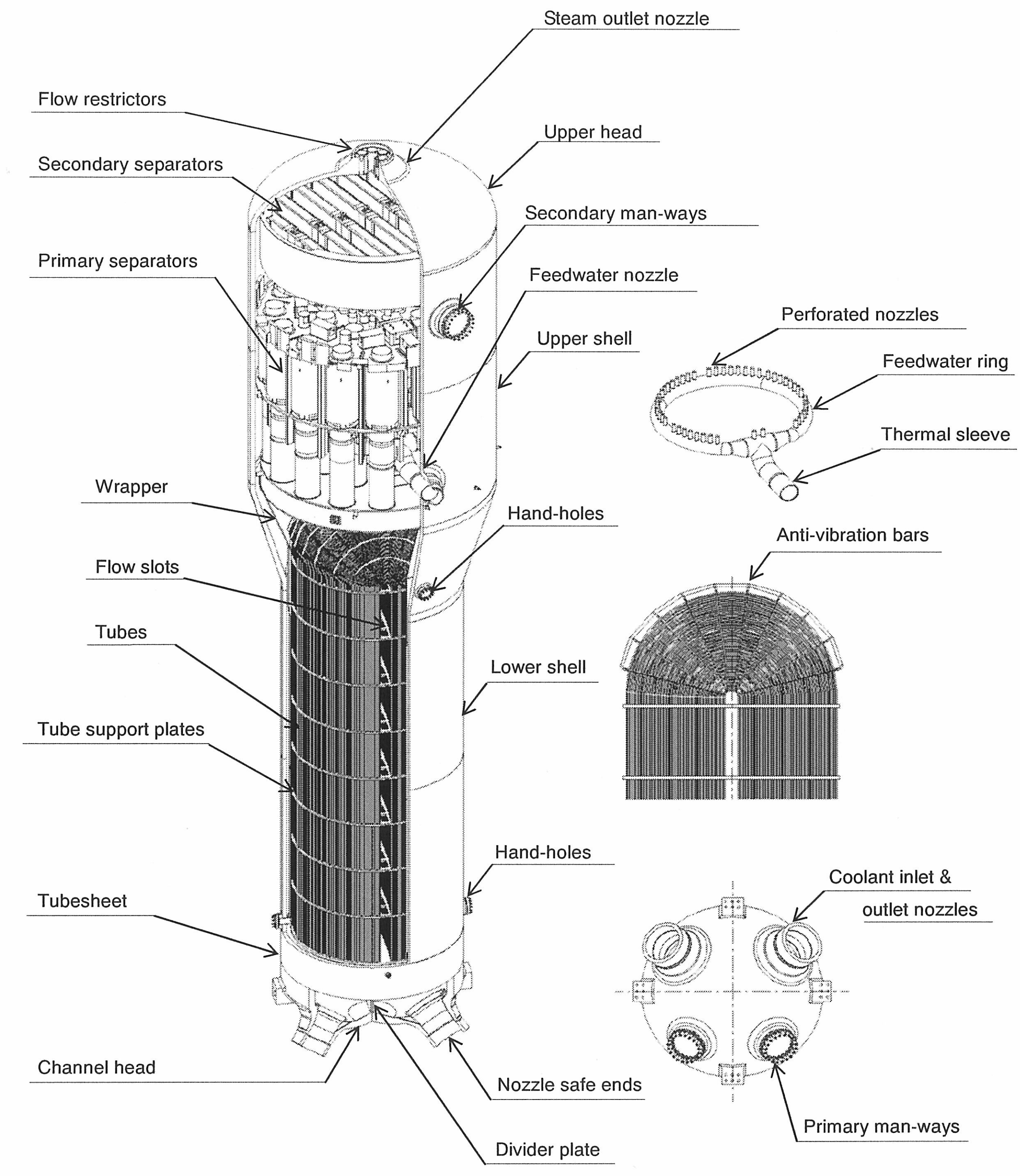

Rev. 1

Figure 2-5 Steam Generator

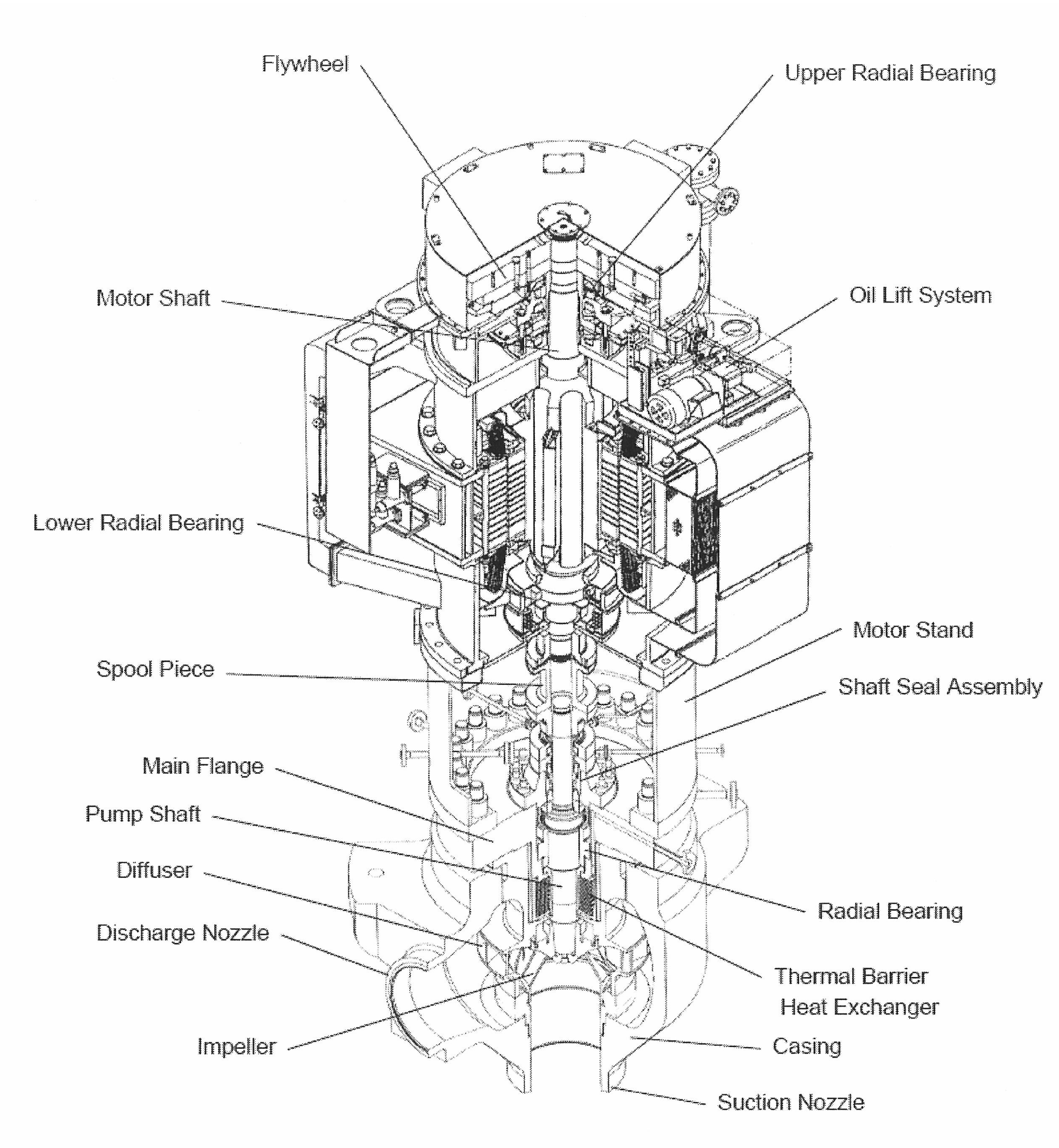

Figure 2-6 Reactor Coolant Pump

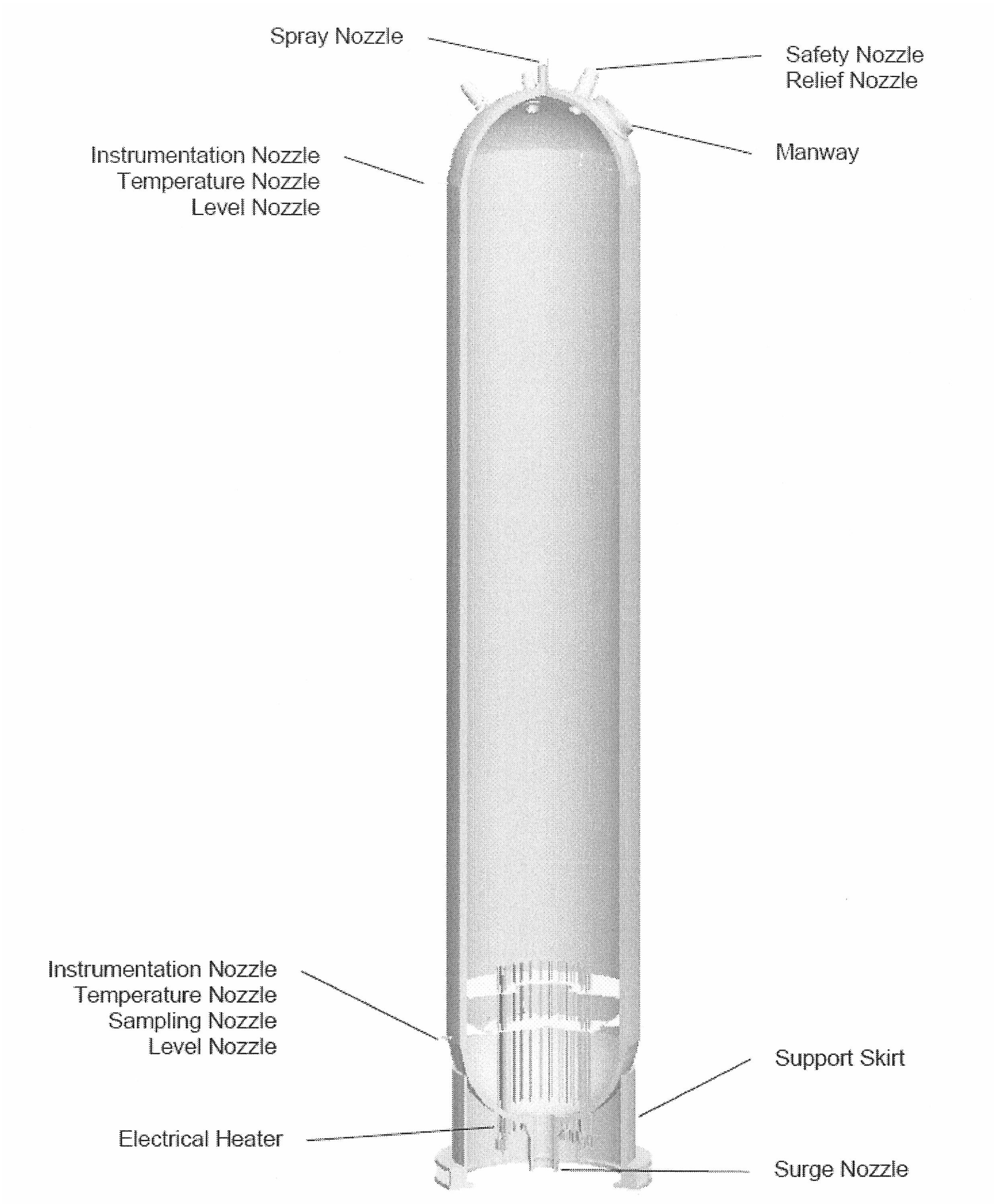

Figure 2-7 Pressurizer

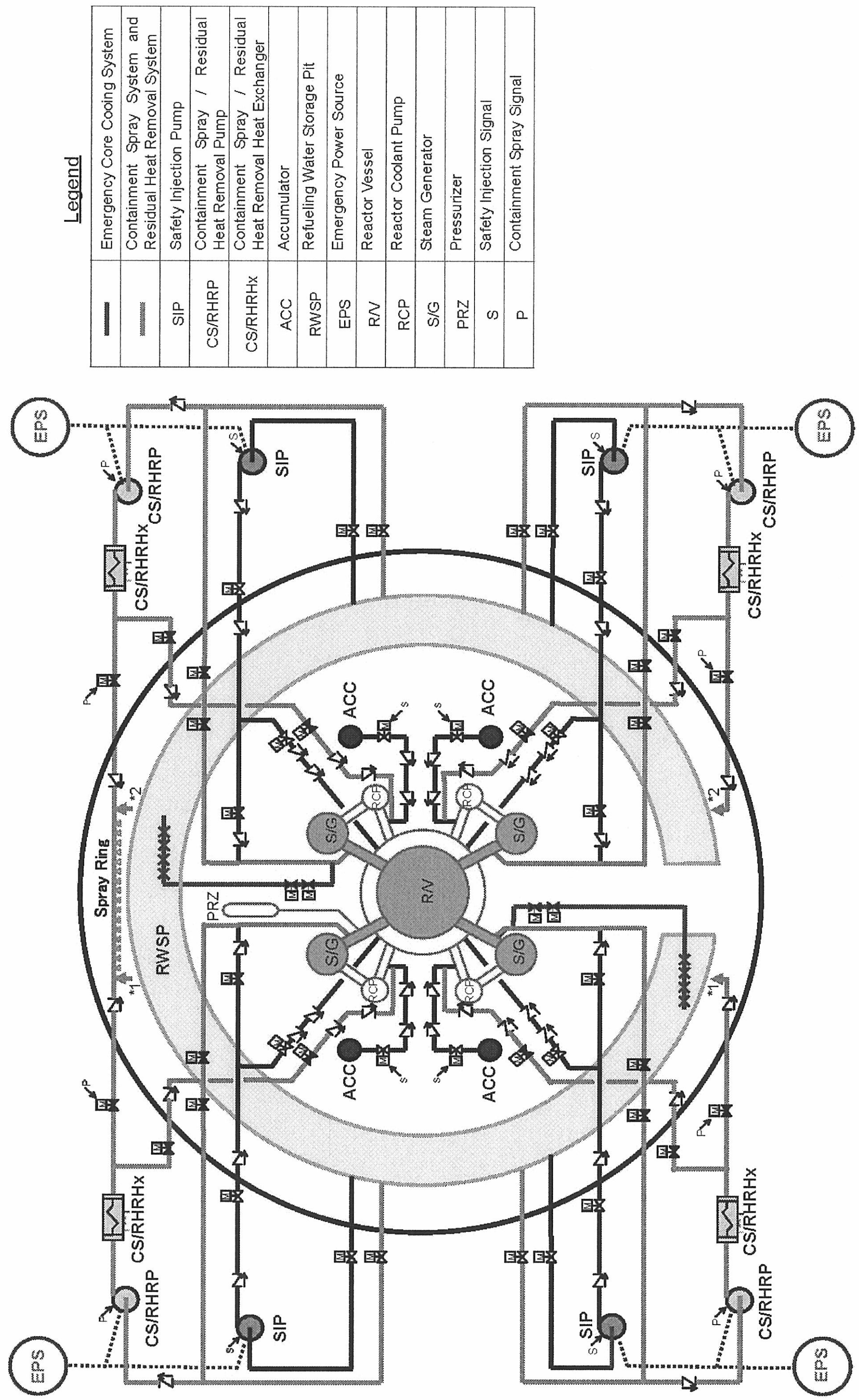

Figure 2-8 Simplified Configuration of ECCS and CSS

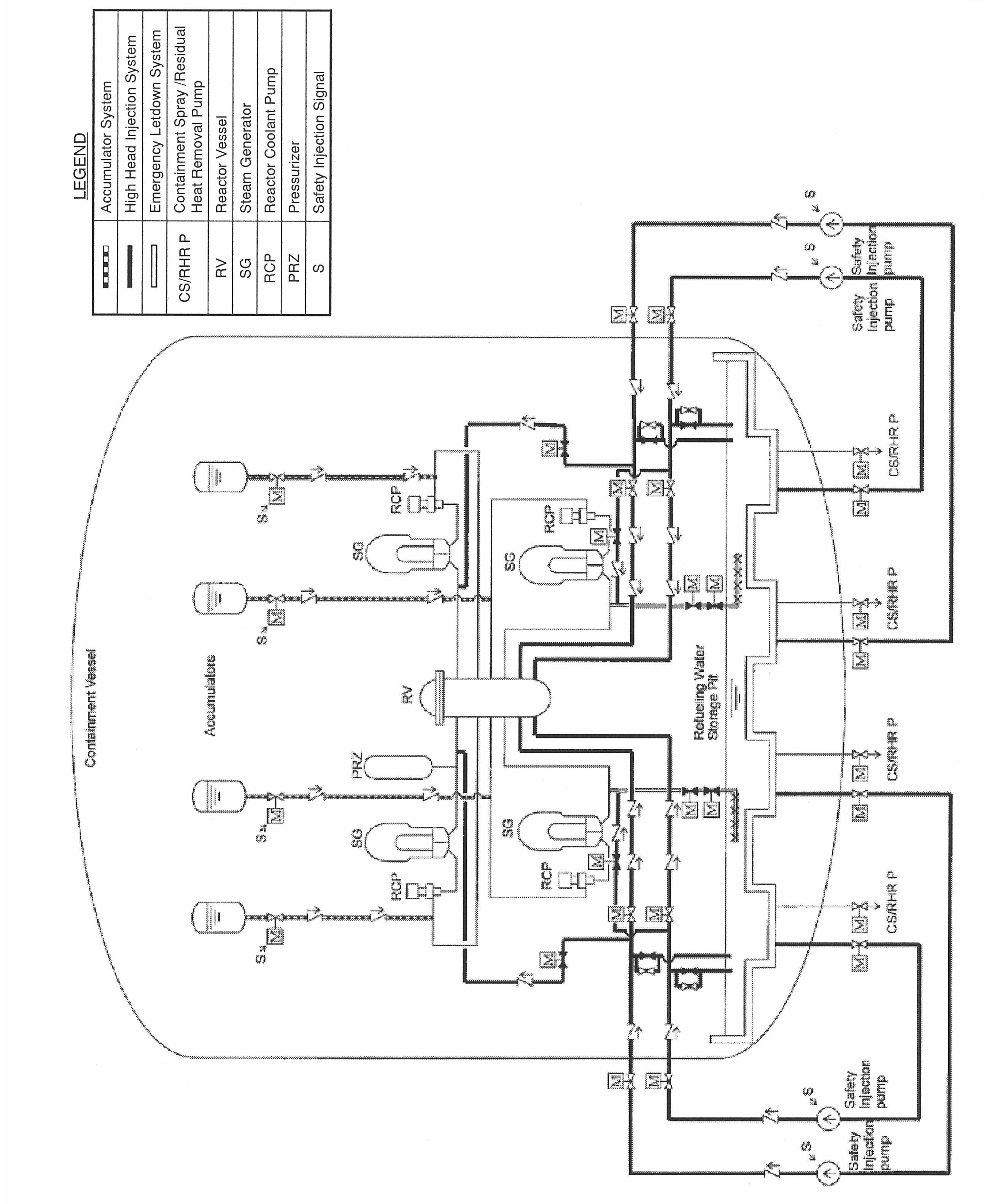

Figure 2-9 Emergency Core Cooling System

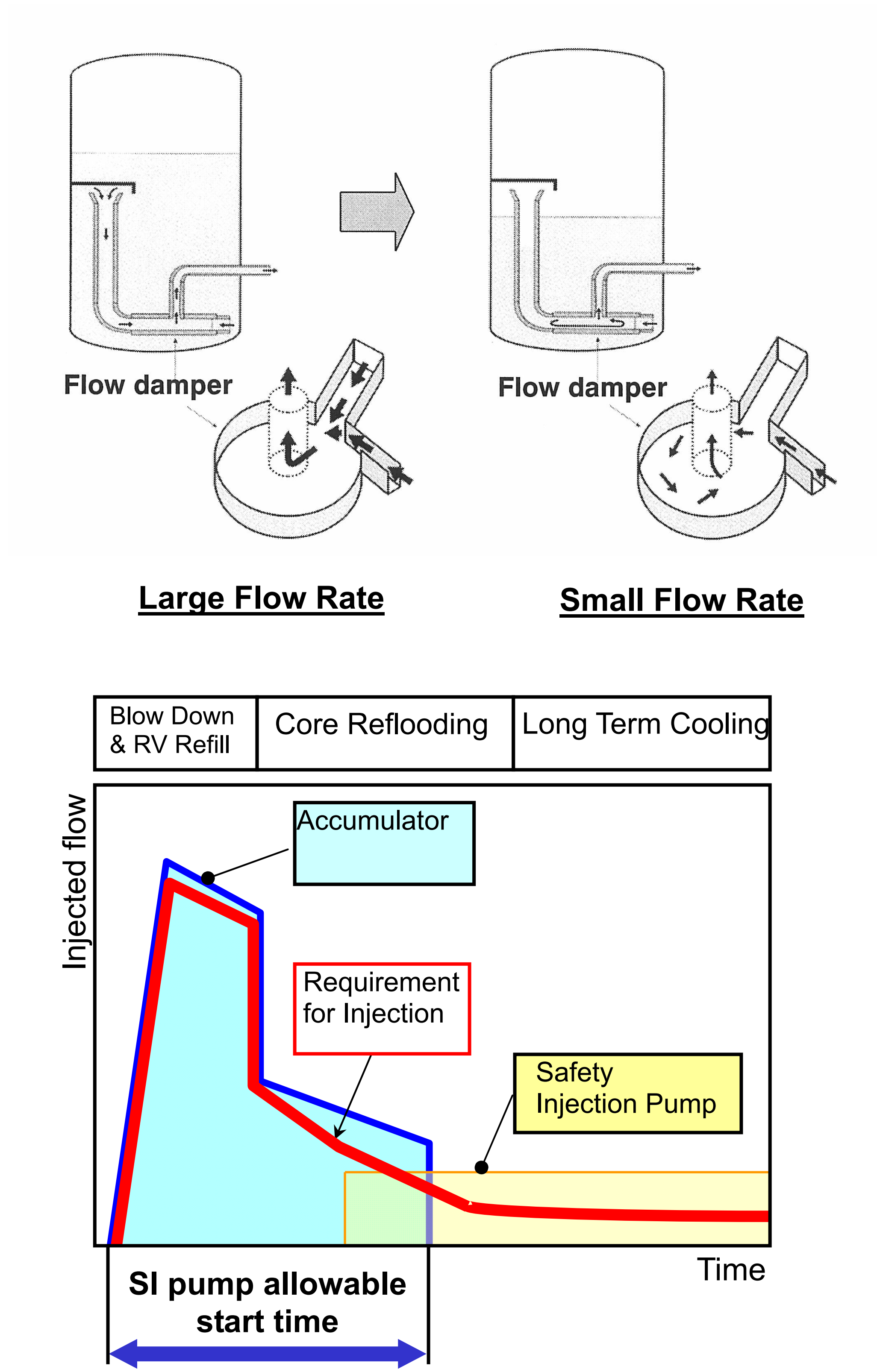

Figure 2-10 Safety System Performance for US-APWR

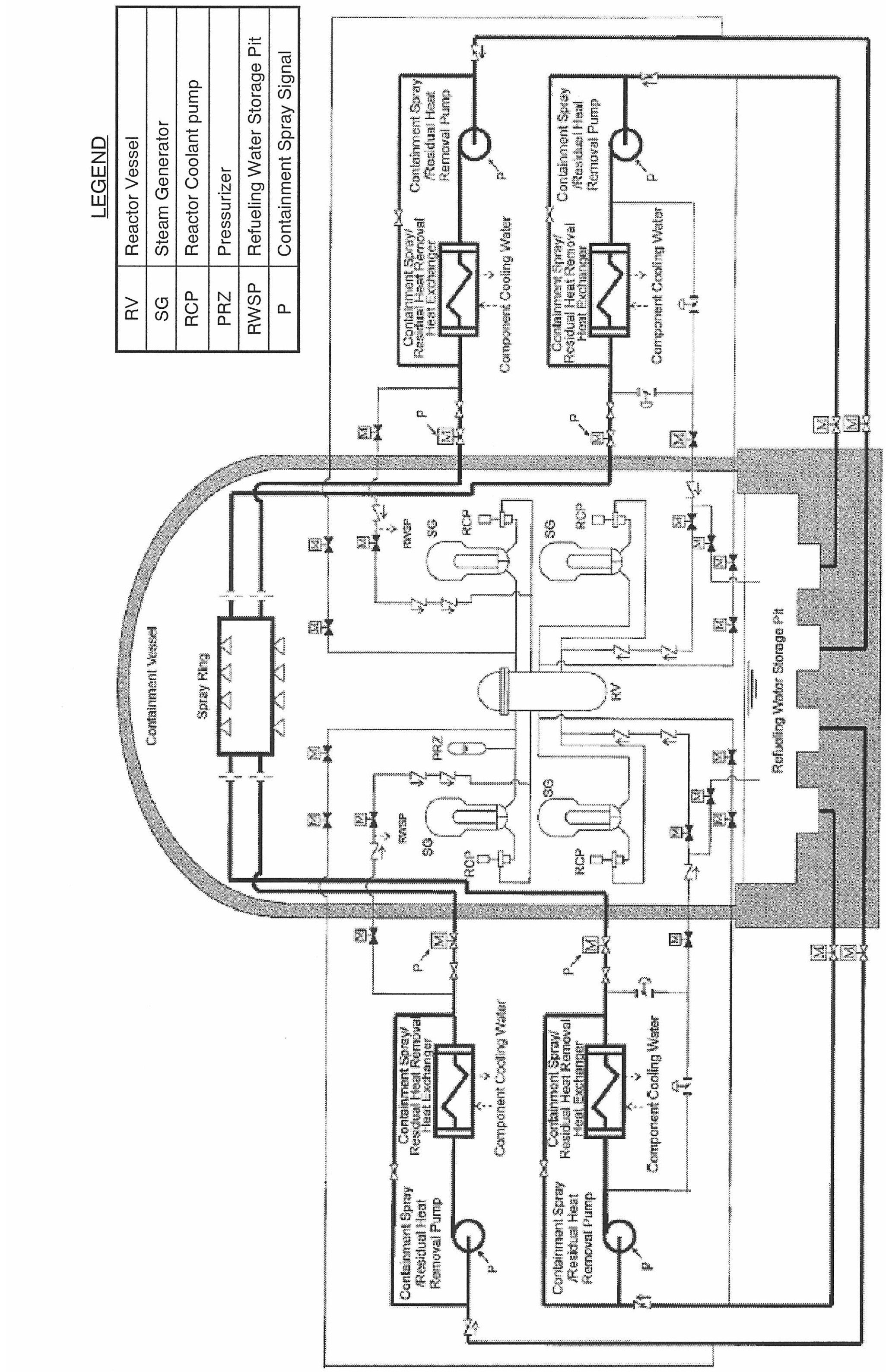

Figure 2-11 Containment Spray System

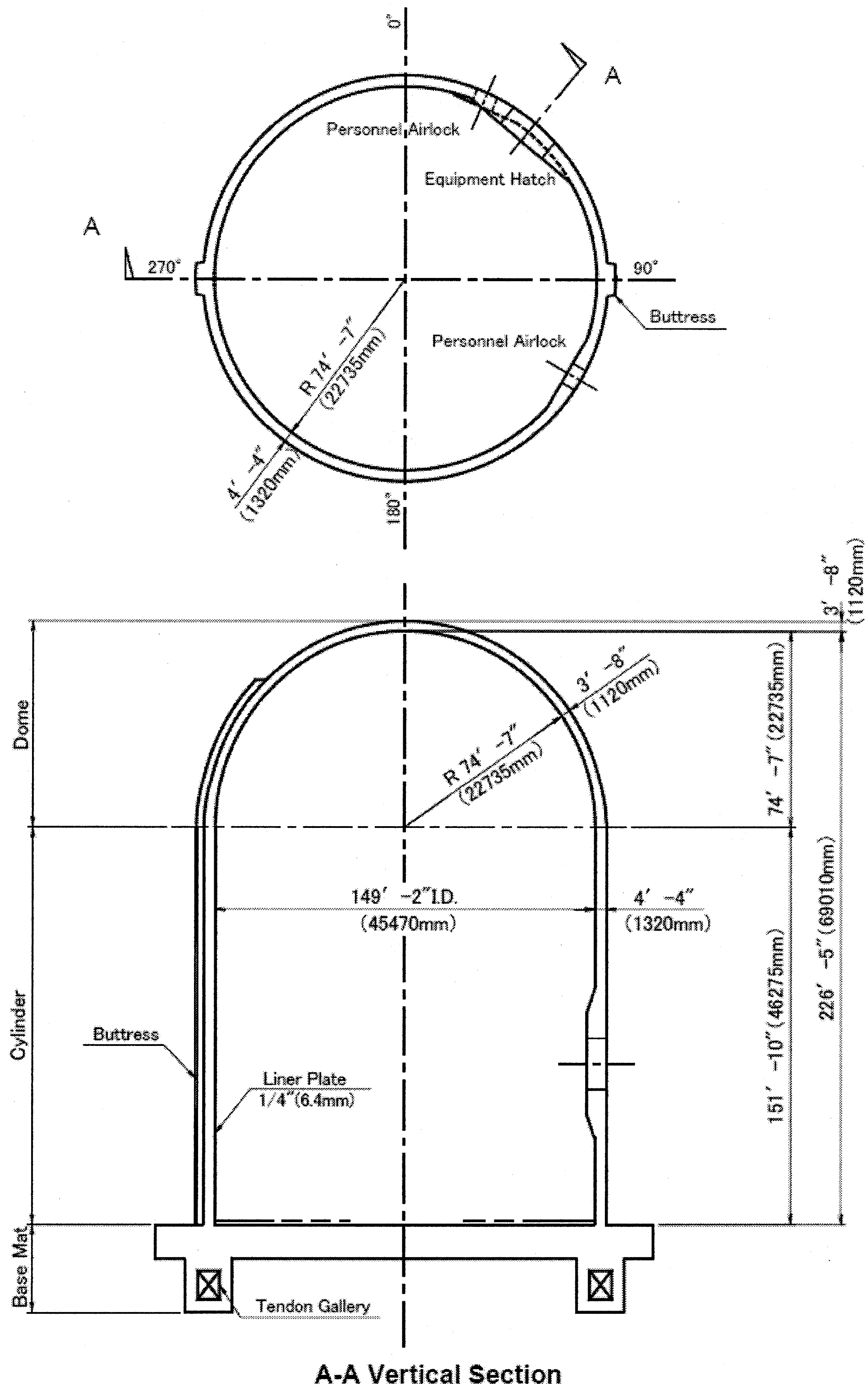

Figure 2-12 Configuration of Containment Vessel

3.0 LOCA MASS AND ENERGY RELEASE EVALUATION CODE AND METHODOLOGY

3.1 Introduction

The Standard Review Plan (Reference 1) states that LOCA mass and energy release evaluation analyses performed with the Appendix K ECCS computer codes which were developed to comply with the ECCS Acceptance Criteria presented in 10CFR50.46 and 10CFR50 Appendix K shall be acceptable. “Westinghouse LOCA Mass and Energy Release Model for Containment Design March 1979 Version (Reference 2)” conforms to the standard and is approved by the NRC.

In order to meet this standard while incorporating modified analytical models reflecting US-APWR new features, MHI has developed a modified mass and energy release model which is based on the ECCS Appendix K codes (SATAN-VI and WRFLOOD). Where applicable and appropriate, conservative models for mass and energy release calculations have been added into the codes.

The methodology for the transient mass and energy release is shown conceptually in Figure 3-1. The development of the mass and energy release calculations proceeds as follows:

1. As described in Section 3.2, the mass and energy release for the blowdown and reflood phases are calculated with SATAN-VI(M1.0) modified based on the SATAN-VI code and WREFLOOD(M1.0) modified based on the WREFLOOD code. The outputs from those codes are inputs to the GOTHIC code, which provides the transient RWSP temperature and containment back pressure in response to the calculated mass and energy release from SATAN-VI(M1.0) and WREFLOOD(M1.0).
2. The full short and long term containment response is calculated with a single GOTHIC run. The GOTHIC model includes a simplified primary/secondary system model for calculating the post-reflood mass and energy release as described in Section 3.3. During the blowdown and reflood phases, the GOTHIC primary/secondary system model is isolated and the mass and energy release from item 1 is supplied as a boundary condition for the containment. At the end of reflood, the GOTHIC primary/secondary system model is opened at the break location and the mass and energy release for the remainder of the transient is calculated by GOTHIC.

A sample containment pressure transient based on this mass and energy release model is shown in Section 3.4. A great deal of conservatism is incorporated into the MHI model, as shown in Reference 2, which specifies and quantifies the major conservatisms.

3.2 Blowdown and Reflood Phases Mass and Energy Release Evaluation Methodology

This section describes modifications to the approved Westinghouse Mass and Energy Release Model for containment design that is documented in Reference 2, and the applicability to US-APWR of these modifications for the LOCA Mass and Energy Release code and Methodology. The containment analysis code system for the blowdown and reflood phase is shown in Figure 3-1.

3.2.1 Approved Methodology

The March 1979 version of the model (Reference 2) is based on the computer codes which were developed to comply with the ECCS Acceptance Criteria presented in 10CFR50.46 and 10CFR50 Appendix K.

The following computer codes are utilized for the mass and energy release analysis during Blowdown and Reflood phases.

Blowdown	SATAN-VI	(Reference 3)
Reflood	WREFLOOD	(Reference 4)

The use of ECCS computer codes for containment mass and energy release is recognized as a valid approach by the NRC in Standard Review Plan 6.2.1.3 (Reference 1). The MHI modifications to the Westinghouse Mass and Energy Release Model are consistent with this NRC position.

The system noding scheme used for mass and energy release evaluation is the 68 node model for the SATAN-VI(M1.0) shown in Figure 3-2 and Table 3-1, which is the same as that used in the approved mass and energy release model for standard Westinghouse 2/3/4-loop plant. [ ] The high head injection is conservatively assumed unavailable during blowdown phase along with the assumption of loss of offsite power. Rev. 2

A 19 element model is used to describe the system for the WREFLOOD(M1.0) code. This modeling is unchanged from that used in the approved mass and energy release model. The nodalization for the WREFLOOD(M1.0) model is shown in Figure 3-3 and Table 3-2.

3.2.2 Evaluation Approach

The US-APWR is a four-loop, pressurized-water reactor with a thermal output of 4,451 MW. Each of the four loops consists of a steam generator, reactor coolant pump, associated piping, and emergency core cooling system with the following US-APWR design features.

- Advanced Accumulator
- Direct Vessel Injection for Safety Injection Pump
- In-containment Refueling Water Storage Pit (RWSP)
- Neutron Reflector

Code modifications have been implemented to model the US-APWR design features. Also applicable range of the model for the principal parameters changed from current Westinghouse 4-loop plants has been investigated.

Section 3.2.3 provides a description and justification for the model modified during each phase of the LOCA transient (blowdown, refill and reflood, except post reflood). It is described that the differences with the approved mass and energy release evaluation model presented in Reference 2. The use of options in the computer code input will be described along with the significant changes to the reference methodology input.

Evaluations for the modifications were made by means of comparisons with test results and/or sensitivity studies, which were selected to evaluate specific modeling modifications.

3.2.3 Code Applicability for US-APWR Features

The calculation model for LOCA analysis is divided into four phases: 1) Blowdown, which includes the period from the time of the accident inception, at steady state full power operation, to the time that the Reactor Coolant System has depressurized to the containment pressure, 2) Refill, which is the period from the end of blowdown to the time that the vessel lower plenum has been refilled by the ECCS, 3) Reflood, which begins when water enters the active core to the time that the reactor core is quenched, and 4) Post-reflood, which begins when the core is quenched and continues until the containment pressure has decreased sufficiently.

3.2.3.1 Advanced Accumulator for Blowdown, Refill and Reflood

The advanced accumulator operation has two injection modes (Reference 14). The first injection mode is basically the same as that of conventional accumulators, in which a relatively large flow is supplied. This injection mode begins during blowdown phase and continues to the early reflood phase. After the first injection mode, the second injection mode begins with a smaller injection flow rate which corresponds to injection by a conventional low head SI pump. The injection flow rate is changed by flow damper resistance, which mainly depends on the accumulator water level.

The accumulator performance model built into SATAN-VI and WREFLOOD is described below to account for its injection flow characteristics.

$$P_{gas} - P_{inj} = K_{ACC} \cdot \rho \frac{V_D^2}{2} - \rho g\left(H_t - H_p\right)$$

$$P_{gas} = \left(\frac{V_{gas0}}{V_{gas}}\right)^{\kappa} \cdot P_{gas0}$$

$$\frac{dV_{gas}}{dt} = A \cdot V_D$$

P_{gas} : Gas pressure in accumulator
P_{gas0} : Initial gas pressure in accumulator
V_{gas} : Gas volume in accumulator
V_{gas0} : Initial gas volume in accumulator
P_{inj} : Pressure at the injection point (RCS pressure)
K_{ACC} : Total resistance coefficient of the flow damper and injection piping
H_t : Difference in height between accumulator water level and vortex chamber
H_p : Difference in height between injection point and vortex chamber
V_D : Fluid velocity of the injection piping
A : Cross sectional area of the injection pipe inside
g : Acceleration of gravity
t : Time
ρ : Density of water
κ : Adiabatic exponent

In the above:
K_{ACC} has two values : $K_{ACC}=K1$ before switching of injection flow rate by flow damper.
$K_{ACC}=K2$, after switching of injection flow rate by flow damper.

The total resistance coefficient, K_{ACC}, is determined from the ACC flow rate coefficient, C_v and the resistance coefficient of the injection piping. The flow rate coefficient is a function of the cavitation factor, σ_v, and the water level in the ACC. The total resistance coefficient is calculated each time step as follows:

1) σ_v is calculated from the flow condition at flow damper

$$\sigma_v = \frac{P_D + P_{at} - P_v}{\left(P_{gas} + \rho g H_t\right) - \left(P_D + \frac{\rho V_D^2}{2} + \rho g H_D\right)}$$

σ_v : Cavitation factor
P_{at} : Atmospheric pressure
P_D : Flow damper outlet pressure (gage)
P_{gas} : Gas pressure in accumulator (gage)
P_v : Saturated vapor pressure
V_D : Fluid velocity of the injection piping
ρ : Density of water
g : Acceleration of gravity
H_t : Difference in height between accumulator water level and vortex chamber
H_D : Difference in height between flow damper outlet piping and vortex chamber

2) The flow rate coefficient C_v is calculated using the following correlations obtained from test data which cover the range of applicability for the US-APWR design

For large flow rate: $C_v = 0.7787 - 0.6889\exp(-0.5238\sigma_v)$

For small flow rate: $C_v = 0.07197 - 0.01904\exp(-6.818\sigma_v)$

3) C_v is converted to the resistance coefficient of flow damper K_D

$$K_D = 1/C_v^2$$

4) Total resistance coefficient is calculated by ;

$$K_{ACC} = K_D + K_{pipe}$$

K_{ACC} : Total resistance coefficient of the flow damper and injection piping
K_{pipe} : Total resistance coefficient of the injection piping

Appendix A and B describes above process in detail for SATAN-VI (M1.0) and WREFLOOD (M1.0), respectively. The equations used to calculate the accumulator performance are identical to those for the large-break LOCA code WCOBRA/TRAC (M1.0) (Reference 21) and there are no significant differences that affect the calculated accumulator flow rate. The main difference in modeling of the accumulator from WCOBRA/TRAC (M1.0) is that the accumulator injection line is treated as a path in the model for SATAN-VI (M1.0) and WREFLOOD (M1.0) while it is explicitly modeled as a control volume with multiple cells for WCOBRA/TRAC. Therefore, the flow damper outlet pressure, P_D, used in the following equation for the cavitation factor has to be calculated with an iterative scheme in the SATAN-VI and WREFLOOD as described in Appendix A and B, while P_D is obtained from the Rev. 2

pressure of the cell next to the accumulator tank in the WCOBRA/TRAC calculation.

In calculating P_D with the iterative scheme, accumulator flow is assumed to be quasi-steady so as not to account for fluid inertia in the injection path. The following paragraphs provide a discussion on the effect of not including fluid inertia in calculating P_D while it is accounted for in the momentum equation.

Fluid inertia effects are potentially significant only when the rate of change of the flow rate is large. So the discussion here is focused on the blowdown phase. Rev. 2

Fluid inertia affects the cavitation factor, σ_v, through the damper exit pressure, P_D. Figure 3-4 shows the relation between σ_v and flow rate coefficient, C_v. The resistance of the flow damper, K, is related to C_v by K=1.0/ $C_v{}^2$. The upper curve gives the relation between σ_v and C_v for the large-flow phase, which covers the blowdown phase. This curve indicates that C_v is essentially unaffected by changes in σ_v when σ_v is larger than around 5.

Figure 3-5 shows the transient of σ_v of the intact-loop accumulator during the blowdown phase, which indicates that σ_v is large enough not to affect C_v especially in the early blowdown phase when the effect of fluid inertia is large. This demonstrates that even if P_D is changed by fluid inertia, in turn leading to a change of σ_v, C_v is not affected.

The verification of the advanced accumulator model built into the SATAN-VI and WREFLOOD codes was performed by comparing code results with hand calculations. The condition parameters of the primary loop and accumulators at various time points during accumulator operation were taken from the code output files. The code-calculated accumulator injection flow rate was compared with hand calculations by using the above equations. The result of verification is shown in Table 3-3. The flow rate obtained by the code calculation agreed with the hand calculation results.

It was therefore confirmed that the modification for SATAN-VI and WREFLOOD code was correct and that the advanced accumulator model works as expected.

The treatment of uncertainties in the accumulator initial conditions (pressure, water mass) and the injection pipe resistance will be established by sensitivity studies. For the sample analysis which is described in section 3.4, the minimum pressure, minimum water mass and maximum resistance coefficient for injection pipe were used.

3.2.3.2 Direct Vessel Injection for Reflood

The WREFLOOD code includes a steam/water mixing model which accounts for the interaction of loop steam with ECC injection water. For the ACC injection at the cold leg, a complete steam/water mixing and thermal equilibrium are assumed as in prior applications of

WREFLOOD for existing PWRs.

For the pumped safety injection, there is a potential for the incomplete interaction between loop steam and safety injection flow through the DVI nozzle located at the downcomer. The degree of condensation depends on the downcomer water level and DVI nozzle location. It is conservatively assumed that there is no mixing of steam and safety injection water through the DVI nozzles to maximize the energy release to the containment. This is conceptually shown in Figure 3-6. This assumption is actually implemented in WREFLOOD (M1.0) by a revision of the mass and energy balance for the downcomer. Complete mixing of DVI flow and water flow from the intact loop is assumed for calculating the enthalpy of the water entering the downcomer. All flow from DVI and the intact loop is added to the downcomer water when the downcomer is not full. When the downcomer is full, the combined DVI and intact loop flow that is in excess of the core inlet flow is spilled to the containment. The enthalpy of this spillage is the mixture enthalpy of the combined DVI and intact loop water flow. Steam flow from the intact loop passes the downcomer with no interaction with DVI flow. Condensation due to direct contact of DVI water flow with steam flow from the intact loop in the downcomer is disregarded. Rev. 2

To verify the assumption for condensation on the pumped safety injection flow, sensitivity studies were performed to evaluate the impact of the mixing assumption for the DVI in the US-APWR containment mass and energy release analyses. Both cases are calculated until end of reflood phase.

Case 1 : No steam/water mixing at DVI point
Case 2 : complete steam/water mixing at DVI point
(note: Complete steam/water mixing at ACC injection point was assumed in both cases. Other assumptions, initial conditions, etc. are identical for the two cases.)

The results of the sensitivity studies are shown in Figure 3-7 and Figure 3-8 with results from both cases. Figure 3-7 shows that the integral of energy flow rate from the break for case 1 (No steam/water mixing at DVI point) rises faster than that of case 2 (complete steam/water mixing at DVI point). The containment internal pressure for case 1 is slightly higher than that of case 2 (Figure 3-8). Therefore case 1 is assumed in the mass and energy release analysis to provide conservative results for containment integrity evaluation.

3.2.3.3 Refueling Water Storage Pit (RWSP) for Reflood

In the US-APWR design, the RWSP is located at the bottom periphery of the containment and connected to the containment atmosphere with pipes. Hence liquid and steam released from the RCS flow into the RWSP and the RWSP water temperature changes during LOCA transients. As the RWSP temperature changes, the safety injection water temperature will also change continuously. The containment back pressure as RWSP back pressure also will change as the transient progresses. The reflood and flow rate of safety injection is affected by containment back pressure.

For the currently approved mass and energy release evaluation methodology, the safety injection water temperature was constant because the RWSP is outside the containment. Also high containment back pressure (design pressure) was assumed. For the US-APWR design the RWSP is located within the containment. Therefore, it is necessary to couple mass and energy release calculation to containment response to model the changing RWSP water temperature and containment back pressure.

To achieve the above modeling, the WREFLOOD(M1.0) code was synchronized with the containment response analysis code (GOTHIC) to compute RWSP water enthalpy and containment back pressure at each time step. A modification to allow this code coupling was needed only for the WREFLOOD code. The original GOTHIC code has built-in capabilities (referred to as Inter Process Communications) to send or receive data with external codes, so there was no modification of necessity for GOTHIC. WREFLOOD is modified by the addition of two subroutines to communicate with GOTHIC and code logic to set the current containment pressure and RWSP water temperature in WREFLOOD to match the current GOTHIC calculated values.
Data transferred from WREFLOOD to GOTHIC are as follows:

WREFLOOD time
Break mass flow rate (SG side)
Break flow enthalpy (SG side)
Break mass flow rate (RCP side)
Break flow enthalpy (RCP side)
DVI mass flow rate
Spilt mass flow rate
Spilt flow enthalpy

Rev. 2

Data transferred from GOTHIC to WREFLOOD are as follows:
GOTHIC time
Containment pressure
RWSP water enthalpy

Validation of this function is confirmed by comparing transferred data in both sender and receiver sides.

These modifications for the WREFLOOD code affect only the input data handling and do not change the analytical method.

3.2.3.4 Neutron Reflector for Blowdown and Reflood

Rev. 2

Figure 3-9 shows the NR. The NR consists of ten thick stainless steel blocks and is heated by gamma irradiation during normal operation. The NR is designed to be cooled by up flow through the cooling holes in the blocks to prevent excessive stress and thermal deflections of the blocks due to the gamma heating. As a result of the cooling that is provided, the temperature of the neutron reflector is kept around average fluid temperature during normal operation.

In a postulated loss-of-coolant accident (LOCA), the NR works as a heat source to the containment similar to other metal in the primary system. During the blowdown phase a small part of the stored energy is released as the fluid temperature decreases. During the reflood phase the NR has experiences quenching like does the core due to the NR's large mass and the large heat transfer area.

The steam generation due to cooling of the NR increases the energy release rate to the containment. Similarly, entrainment of liquid from the NR into the upper plenum and the steam generator increases the heat release rate from the secondary side of the steam generator to the containment. These two effects would also reduce the flooding rate. Therefore the NR is expected to cause longer reflood period with a little larger energy release rate, which results in small increase of the containment pressure. The effect, however, is considered to be quantitatively small because the stored energy of the NR is only about [ ] % of the energy released from the core during reflood period.

The NR is modeled using metal model in SATAN-VI. In the normal power operation, the neutron reflector metal temperature is higher than the coolant temperature due to the heat generated by gamma ray absorption. SATAN-VI is modified to allow different initial temperatures for the metal and fluid.

Rev. 2

Rev. 2

Validity of the above modeling approach for a conservative analysis was confirmed by the simulation of phenomena related to the NR during the reflood phase with the best-estimate code, WCOBRA/TRAC. The results of the study are described in Appendix C.

3.2.3.5 Core Fuel Rod Number for Reflood

Rev. 2

3.2.3.6 Parameter Range

Since the US-APWR has design, geometric, functional, and phenomenological similarities to current Westinghouse 4-loop PWRs, the model approved for them can be basically applied to the US-APWR with modifications concerning its specific features.

This section describes whether applicable range of physical models in the codes covers the range of parameters during LOCA for the US-APWR.

As shown in
Table 2-1 the US-APWR has the following characteristics compared with current 4-loop PWRs.

- Almost same operating fluid conditions
- Lower average linear heat rate by increasing fuel length
- Higher containment design pressure

As to the blowdown analysis, since the constitutive models of the SATAN-VI code are generic and cover wide range of parameters from the normal operation to the end of blowdown when the primary system pressure settles close to the containment pressure, the above two differences will not affect applicable range of the code.

However, the WREFLOOD code used for the reflood phase has the specific correlation for reflooding of the core. That is the correlation for the mass effluent fraction as shown below.

[ ]

Where:

F_{out} = Fraction of inlet water not stored below the quench front and assumed to exit core.
Z_q = Quench front level in core, inch.
$Q'\max$ = Peak heat generation rate, kW/ft. (*1)
P = System pressure, psia.
ΔT_{sub} = Inlet water subcooling, $°F$.
V_{in} = Inlet water flooding rate, inch/sec.

(*1) [ ]

As the reflood water enters the bottom region of the core during the reflood transient and comes into contact with hot fuel rods, boiling occurs in the core. The steam thus formed in the lower region of the core flows up through the core and vented through the reactor coolant loops. As the steam flows up through the core, part of the reflood water in the core is entrained in the steam and carried out of the vessel. To account for the steam flow with entrained water from the core to the loops, above empirical correlation was developed from FLECHT (Reference 16) experimental results.

This equation contains a quench front level term Z_q. Based on FLECHT data, the correlation was found to be valid until the quench front level neared but did not reach the top of the core. At that elevation the core was found to be quenched from the top so that water was no longer carried out the top of the core. The FLECHT data was obtained from a facility simulating a Rev. 2

12-foot reactor core. In modeling the 14-foot fuel of US-APWR with regard to termination of liquid carryout, liquid entrainment is assumed to continue until the water level in the core is 2 feet from the top of the core in conformance with Acceptance Criterion 1.C.iii. of SRP 6.2.1.3. Rev. 2

This correlation was validated as shown in Figure 3-10 and Figure 3-11, which are from Reference 4, and has been used for Westinghouse-type PWRs.

As described before the US-APWR has lower average linear heat rate and higher containment design pressure, which results in higher system pressure during reflood phase, compared with current 4-loop plants.

The peak heat generation rate, $Q'\max$ in the correlation is calculated using average linear heat rate, decay heat fraction at the beginning of the reflood and peaking factor based on FLECHT tests, which is around 0.5kW/ft for a typical current 4-loop plant with 12-ft core.

[ ]

( )

As described above $Q'\max$ of a typical current 4-loop plant is around 0.5kW/ft. However, this is not necessarily within the range of validation, 0.69 through 1.24 kW/ft, as shown in the table on Figure 3-10, where peak heat generation rate is called peak power. In order to confirm performance of the correlation, comparison with the FLECHT SEASET (Reference 17) data with lower peak heat generation rate was performed.

FLECHT SEASET program was conducted using rod bundle simulating 17x17 type fuel assembly to provide data and analysis that would improve understanding of the complex two-phase flow phenomena that occurs during a postulated PWR loss-of-coolant accident.

The following test data, which show effects of peak power, were selected from Unblocked Bundle Reflood Task series, the initial phase in the comprehensive tasks of the FLECHT SEASET program. Other conditions of the tests except peak power are within the range of Fout correlation.

Run number	31203	31021	34524
Pressure	40 psia	40 psia	40 psia
Peak power	0.7 kW/ft	0.4kW/ft	1.0kW/ft
Flooding rate	1.51 inch/sec	1.52 inch/sec	1.57inch/sec
Subcooling	141 F	141F	142F

Figure 3-12 compares carryout fraction by the correlation with test data. The calculation was performed by spreadsheet software. The carryout fraction is defined as the next expression.

$$Carryout\ Fraction = \frac{Mass\ \ out(lbm)}{Mass\ \ in(lbm)}$$

Excellent agreement with data is noted in the low power region, which proves that the correlation is applicable to 17x17 type fuels with lower linear power.

3.3 Post-reflood Mass and Energy Release Evaluation Methodology

The post-reflood mass and energy release analysis is performed with the GOTHIC computer code (Reference 5). The MHI's approach allows the mass and energy release from the primary system to be coupled with the containment response calculation because both are included in the same model. The US-APWR mass and energy release model is similar to the model used by Dominion in their containment analysis methodology, which was previously approved by the NRC (Reference 8) for Surry. In the Surry application (Reference 2), it was shown that the methodology described here gave a post-reflood mass and energy release rate that closely matched the previously approved Westinghouse methodology (Reference 8).

The details of the post-reflood mass and energy release along with an overview of the GOTHIC code are provided below.

3.3.1 GOTHIC Computer Code Overview

GOTHIC is a general purpose thermal-hydraulics code for performing design, licensing, safety and operating analysis of nuclear power plant containments and other confinement buildings. GOTHIC was developed for the Electric Power Research Institute (EPRI) by Numerical Applications, Inc. (NAI) (Reference 5). A summary description of GOTHIC capabilities is given below. More detailed descriptions of the code user options, models and qualification are documented in References (5,6,7).

GOTHIC solves the conservation equations for mass, momentum and energy for multicomponent, multi-phase flow in lumped parameter and/or multi-dimensional geometries. The phase balance equations are coupled by mechanistic models for interface mass, energy and momentum transfer that cover the entire flow regime from bubbly flow to film/drop flow, as well as single phase flows. The interface models allow for the possibility of thermal non equilibrium between phases and unequal phase velocities, including countercurrent flow. GOTHIC includes full treatment of the momentum transport terms in multi-dimensional models, with optional models for turbulent shear and turbulent mass and energy diffusion. Other phenomena include models for commonly available safety equipment, heat transfer to structures, hydrogen burn and isotope transport.

Conservation equations are solved for up to three primary fields and three secondary fields. The primary fields are steam/gas mixture, continuous liquid and liquid droplet; the secondary fields are mist, ice, and liquid components. For the primary fields, GOTHIC calculates the relative velocities between the separate but interacting fluid fields, including the effects of two-phase slip on pressure drop. GOTHIC also calculates heat transfer between phases, and between surfaces and the fluid. Reduced equation sets are solved for the secondary fields by the application of appropriate assumptions as described in the reference documents.

The three primary fluid fields may be in thermal non equilibrium in the same computational cell. For example, saturated steam may exist in the presence of a superheated pool and subcooled drops. The solver can model a wide range of fluid conditions that encompass the expected containment and primary/secondary system conditions for the US-APWR LOCA analysis.

The steam/gas mixture is referred to as the vapor phase and is comprised of steam and, optionally, up to eight different noncondensing gases. The noncondensing gases available in the model are defined by the user. Mass balances are solved for each component of the steam/gas mixture, thereby providing the volume fraction of each type of gas in the mixture.

The mist field is included to track very small water droplets that form when the containment atmosphere becomes super saturated with steam. The liquid component field allows particles or liquid globules to be tracked in the liquid phase. The ice field models melting, freezing, and sublimation and is used for ice condenser containment modeling.

The principal element of the model is a control volume, which is used to model the space within a building or subsystem that is occupied by fluid. The fluid may include noncondensing gases, steam, drops or liquid water. GOTHIC features a flexible noding scheme that allows computational volumes to be treated as lumped parameter (single node) or one-, two- or three-dimensional, or any combination of these within a single model.

Solid structures are referred to in GOTHIC as thermal conductors. Thermal conductors are modeled as one-dimensional slabs for which heat transfer occurs between the fluid and the conductor surfaces and, within a conductor, perpendicular to the surfaces. The one-dimensional thermal conductors can be combined into a conductor assembly to model two-dimensional conduction.

GOTHIC includes a general model for heat transfer between thermal conductors and the steam/gas mixture or the liquid. There is no direct heat transfer between thermal conductors and liquid droplets. Thermal conductors can exchange heat by thermal radiation. Any number of conductors can be assigned to a volume.

Fluid boundary conditions allow the user to specify mass sources and sinks and energy sources and sinks for control volumes. Thermal boundary conditions applied through a heat transfer option on a thermal conductor surface can be used as energy sources and sinks for solid structures.

There are four features in GOTHIC for modeling hydraulic connections. These are flow paths, network models, cell interface connections in subdivided volumes, and 3D connectors for subdivided volumes. Flow paths model hydraulic connections between any two computational cells, which includes lumped parameter volumes and cells in subdivided volumes. Flow paths are also used to connect boundary conditions to computational cells where mass, momentum and energy can be added or removed. A separate set of momentum equations is solved for flow paths.

Network nodes and links are available specifically for modeling building ventilation or piping systems. These types of hydraulic connections can include multiple branches between connected volumes. Network nodes are assigned to the branch points.

Adjacent cells within a subdivided volume communicate across the cell interface, based on the characteristics of the hydraulic connection. 3D flow connectors define the hydraulic connection across cell interfaces that are common to two subdivided volumes.

GOTHIC includes an extensive set of models for operating equipment. These items include pumps and fans, valves and doors, heat exchangers and fan coolers, vacuum breakers, spray nozzles, coolers and heaters, volumetric fans, hydrogen recombiners, ignitors, pressure relief valves.

Initial conditions allow the user to specify the state of the fluid and solid structures within the modeled region at the start of a transient. These include the initial temperature and composition of the containment atmosphere, the location and temperature of liquid pools, the location and amount of liquid components, and the temperatures of solid structures within the building.

Additional resources available to expand the realm of situations that can be modeled by GOTHIC include functions, control variables, trips and material properties.

3.3.2 Modeling Approach

The approach for the post-reflood mass and energy release analysis utilizes an integrated GOTHIC model that calculates both the primary system post reflood behavior following a LOCA and the corresponding containment response. During a LOCA event, most of the vessel water will be displaced by the steam generated by flashing. The vessel is then refilled by the advanced accumulators and high head injection systems. GOTHIC is not suitable for modeling the reflood period because it involves quenching of the fuel rods where film boiling conditions may exist. Current versions of GOTHIC do not have models for quenching and film boiling. For the period from LOCA initiation through the end of reflood, the mass and energy release rates are obtained from the SATAN-VI(M1.0) and WREFLOOD(M1.0) codes, as described in the Section 3.2, and supplied to the GOTHIC containment model through boundary conditions.

GOTHIC can model the primary system mass and energy release after the core has been recovered. Beyond this time, injection systems continue to supply water to the vessel. Residual stored energy and decay heat comes from the fuel rods. Stored energy in the vessel and primary system metal are also gradually released to the injection water which eventually spills out the break and into the containment.

Buoyancy driven circulation through the intact steam generator loops will remove stored energy from the steam generator metal and the water on the secondary side. Depending on the location of the break, the water injected into the primary system may pass through the steam generator on the broken loop and pick up heat from the stored energy in the secondary system.

The post-reflood mass and energy release must account for the transfer of decay heat and the stored energy in the primary and secondary systems to the containment. The following paragraphs describe the methodology used to analyze these phenomena in GOTHIC. Key elements of the containment model are summarized first, followed by a description of the primary system model.

3.3.2.1 GOTHIC Containment Model

Since the GOTHIC containment model is an integral part of the mass and energy release calculation through its coupling with SATAN-VI(M1.0) and WREFLOOD(M1.0) and post-reflood mass and energy discussed here, the GOTHIC containment model is briefly described here.

Consistent with approved methods for existing PWR LOCA containment response, the US-APWR containment is modeled[ ]. The RWSP is included as a pool at the bottom of the containment. [

]

The model includes passive heat sinks for the containment shell and interior concrete and metal. The convective and condensation heat transfer is modeled using NRC approved methods.

The break flow is modeled by liquid, drop and steam injection as appropriate for the primary system conditions in a manner that is consistent with previously approved methods.

The containment sprays are modeled using the GOTHIC drop field. The water is taken from the RWSP, passed through the CS heat exchanger and injected at the nozzle manufacturer’s specified nominal drop size. GOTHIC’s interfacial heat and mass transfer models are used to calculate the effectiveness of the containment sprays.

3.3.2.2 GOTHIC Mass and Energy Release Analysis Methodology

GOTHIC is used to model the primary system mass and energy release after the core has been quenched. The modeling approach described below is similar to that used in previous analyses that have been reviewed and approved by the NRC (Reference 8).

(1) GOTHIC version

GOTHIC version 7.2a-patch5, revised from version 7.2a, is used for the US-APWR analyses.

This patch to GOTHIC version 7.2a was created to correct errors in the implementation of the Yeh correlation. The Yeh correlation is used to predict the two-phase mixture level and the vapor volume fraction within subdivided volume cells that are connected to a Flow Path or Network Link. These values are then used to determine the outflow conditions for the connected Flow Path or Network Link.

Two errors were identified in the original implementation: 1) the phase velocities were used to calculate the mixture level rather than the superficial velocities, 2) the Yeh correlation was only applied if the liquid volume fraction in the cell was above 0.5. Item 1 tended to cause the mixture level to be overestimated, while item 2 tended to cause the mixture level to be underestimated. Because of these counteracting effects, it is difficult to predetermine the impact of the problem on a particular model and to determine conservative input adjustments to counteract the errors. The patch was implemented for use in modeling situations that require the Yeh correlation on an interim basis until the next full release of GOTHIC becomes available. The patch is released under NAI's QA program for GOTHIC, which satisfies the requirements of 10CFR50 Appendix B with error reporting in accordance with 10CFR21. Rev. 2

No GOTHIC modification for specific application to the US-APWR is made.

(2) Noding

The GOTHIC noding for US-APWR post-reflood mass and energy release analysis is shown in Figure 3-13 and Table 3-4 describes each node. [ ]

[ ]

In order to calculate the natural circulation through the intact loop and the correct water level in the vessel and downcomer, accurate bottom elevations and heights are specified for all of the primary system volumes.

(3) Conductors Rev. 2

Conductors are included to model the stored energy in the primary system and the steam generators and to model the heat transfer across the steam generator tube surfaces. The initial temperatures for the conductors are set such that the remaining stored energy at the end of reflood, as calculated by WREFLOOD(M1.0) is conserved.

The fuel rods are modeled as a single WALL type conductor. The surface area of the conductor is the total surface area of the fuel rods and the conductor thickness is specified to include the total mass of the fuel. Nominal thermal properties are specified for the fuel and cladding. The following figure of the cross section of the fuel illustrates how a fuel rod, including the cladding, is represented in the GOTHIC model. The slab conductor is defined such that the surface area exposed to the fluid and the mass of each material are preserved. Compared to the cylindrical rod geometry, the slab geometry has a shorter effective conduction length which results in a faster (conservative) release of the stored energy in the fuel.

Since the core has quenched and is covered, the energy to be released is from the decay power generation and a small amount of stored energy as the pressure slowly changes. Therefore, the exact core geometry is less important. Rev. 2

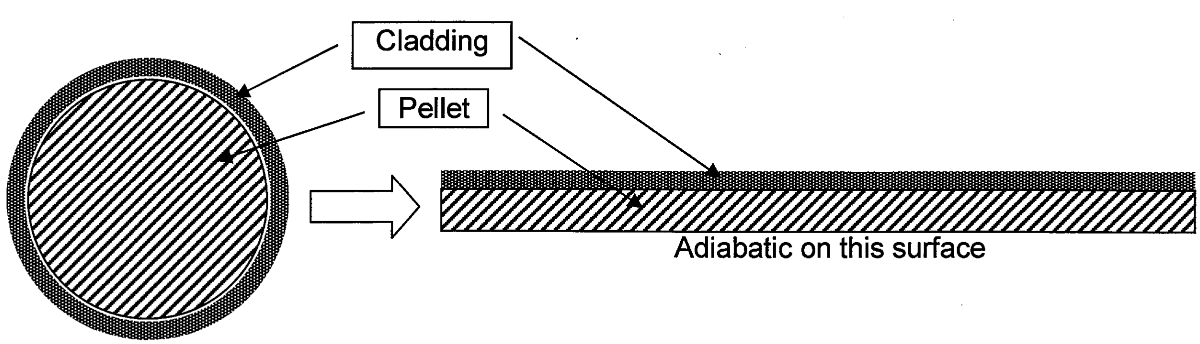

Cylindrical Fuel Rod GOTHIC Slab Conductor

Core decay heat is modeled using a heater component with a time dependent heat rate. The ANS 1979 decay heat curve with two sigma uncertainty (Reference 11,12,13) is modeled . The decay heat is assumed to be based on infinite time at full power. The decay heat curve used in the GOTHIC modeling is consistent with the reflood phase analysis.

A decay heat curve based on ANSI/ANS-5.1-1979 (ANS-1979) model, which had been incorporated into the original SATAN and WREFLOOD codes, is used for the containment analyses for the US-APWR. The decay heat curve is shown in Figure 3-14 and the assumptions for input selection for this decay heat curve are described in the Reference 2 as follows:

1.	Actinide contribution	: ^{239}U and ^{239}Np
2.	Actinide production (R-factor)	: 0.70
3.	Neutron capture effect	: Gmax
4.	Power history	: 10^{8} seconds
5.	Fissile element	: 92% ^{235}U, 8%^{238}U

These assumptions are considered applicable for the US-APWR since:

1. Actinide decay heat: the contribution of both ^{239}U and ^{239}Np decay heat was included considering an infinite operating time. Explicit analysis of the US-APWR core show that the most limiting R-factor is about [ ]. Rev. 2
2. Fission products (FPs) decay heat: the decay heat multiplier to account for the effect for neutron capture (G-factor) is assumed to be the maximum table value (G-max). The length of full power operation of 10^{8} seconds before shutdown covers up to US-APWR 24-month operation conditions. Finally, the assumption that fission products are attributed to an 8% of ^{238}U and 92% ^{235}U with the conservative assumption that the fission energy release is 200MeV/fission covers US-APWR core conditions.

Therefore, the decay heat originally incorporated into SATAN and WREFLOOD code, which input selection assumptions are described in the Reference 2 for generic use, can be apply for the US-APWR mass and energy analysis.

[ ] Rev. 2

Rev. 2

Rev. 2

Rev. 2

(4) Film Heat Transfer Model

The FILM option is used for heat transfer for all conductors in the primary and secondary systems. This option includes convective and boiling heat transfer modes to the vapor and liquid. The heat transfer will be to the liquid phase unless there is insufficient water to support a liquid film on the surfaces. Convective heat transfer is the maximum of standard correlations for natural and forced convection. For boiling heat transfer, both nucleate and bulk boiling correlations are included. Film boiling is conservatively not considered.

The correlations are all based on best estimates. However, the following modeling conservatisms assure that the overall heat transfer rate is conservatively high: Rev. 2

1. All the vessel metal conductors are assigned to the core region to assure that they are in contact with the liquid to maximize the heat release.
2. The lumped modeling approach for the uphill SG tubes and the SG secondary side assures that both sides of the tubes are fully in contact with the water to maximize the heat transfer rate and the heat release from the steam generators.
3. For the downhill SG tubes, the outside of the tubes are in full contact with the SG water to maximize the heat transfer to the steam. The heat transfer to the steam on the inside of the tubes is the maximum of forced and natural convection.

4. All of the metal on the secondary side of the SG is in full contact with the liquid to maximize the heat release rate.

Using the FILM option, the logic for selecting the heat transfer coefficients for heat transfer between the conductor surface and the fluid is shown in Figure 3-15.
Heat transfer coefficients are calculated for both the liquid and vapor phases, even though all heat transfer is generally to only one phase as determined by the logic shown in Figure 3-15. The phase heat transfer coefficients are multiplied by ramp functions that force the heat transfer to zero as the phase is depleted. The ramp functions are

and

Rev. 2

The ramp functions are applied as modifiers on the heat transfer coefficients, described below.

Single Phase Vapor

The single-phase vapor heat transfer coefficient (Hspv) is given by

$$H_{spv} = Max\begin{bmatrix} \dfrac{8k_v}{D_h} \\ \dfrac{k_v}{D_h}0.023Re_v^{0.8}Pr_v^{0.4} \\ \dfrac{k_v}{D_h}Max\left(0.13\left[Gr_vPr_v\right]^{1/3}, 0.59\left[Gr_vPr_v\right]^{0.25}\right) \end{bmatrix}$$

The first formula is a minimum value based on conduction through the vapor. The second formula is the Dittus-Boelter correlation for turbulent forced convection (Reference 18). The third formula is for turbulent natural convection. The temperature difference in the Grashof number is given by

$$\Delta T = T_v - Max[T_w, T_{sat}(P_{vs})]$$

The wall source term for single-phase vapor heat transfer is

$$Q_{w_v} = \lambda_{w_v} H_{spv} A_{cn}(T_w - T_v)$$

Single-Phase Liquid

The single-phase liquid heat transfer coefficient is given by

$$H_{spl} = Max\begin{bmatrix} \dfrac{2k_l}{\delta} \\ \dfrac{k_l}{D_h} 0.023 Re_l^{0.8} Pr_l^{0.4} \\ \dfrac{k_l}{D_h} Max\left(0.13\left[Gr_l Pr_l\right]^{1/3}, 0.59\left[Gr_l Pr_l\right]^{0.25}\right) \end{bmatrix}$$

These formulas are essentially identical to those used for single phase vapor. The primary difference is that the formulas are based on liquid properties. The first formula gives the heat transfer coefficient for conduction through a liquid film of thickness Rev. 2

[ ]

where the parameter f_{wa} is an adjustment factor for wetted areas. If there is sufficient liquid in the volume to cover all the wettable walls with a film that is at least 0.0001 ft thick, then all the wettable walls will be wet. If there is insufficient liquid to cover all the wettable walls, then a fraction of each wettable wall will be dry. A wall is wettable if the surface temperature is below the saturation temperature at the total fluid pressure.

The third formula is for turbulent natural convection. The temperature difference in the Grashof number is given by

$$\Delta T = T_l - Min[T_w, T_{sat}]$$

The wall source term for single-phase liquid heat transfer is

$$Q_{w_l} = \lambda_{w_l} H_{spl} A_{cn}(T_w - T_l)$$

Boiling

If the wall temperature is greater than the saturation temperature at the total pressure, then the liquid is in a boiling heat transfer regime. In the nucleate boiling regime, the Chen (Reference 19) correlation is used. If the liquid is subcooled, subcooled boiling occurs that allows the generation of steam without bringing the bulk liquid temperature up to the saturation temperature. The Chen correlation is extended to cover subcooled nucleate boiling.

Condensation Rev. 2

Although condensation heat transfer correlations are incorporated into GOTHIC, they do not come into play for the reactor coolant system model.

(5) Vessel Froth Level Rev. 2

During the early part of the post-reflood phase, there is substantial boiling in the vessel due to the decay heat and the release of stored energy in the fuel, vessel and internals. The boiling raises the surface level of the water in the vessel. The surface level affects the amount of water that is carried into the steam generators with the steam produced in the vessel and, consequently, the rate of energy removal from the steam generators. The stored energy in the steam generators will be released more quickly if there is significant water carried into the steam generators.

Rev. 2

Rev. 2

(6) Steam Condensation in Cold Leg and Downcomer Volumes

Rev. 2

In the US-APWR design, cold water from the accumulators is injected into the cold leg, while safety injection water from the RWSP is introduced directly into the downcomer. The mixing of the cold injected water with steam from the steam generators influences the condensation rate, the flow rate through the steam generators and the steam flow to the containment.

Experimental evidence (Reference 10) indicates that during safety injection in the post-reflood phase, the cold leg condensation rate is maximized. These tests were for a 1/3 scale (10" diameter) cold leg. [ ] thus maximizing the liquid surface area that is in contact with the steam. This approach is consistent with the experimental evidence and with previously accepted methods for treating the cold leg injection (Reference 8).

In the downcomer volume, the model liquid/vapor interface area is set to zero. Therefore the condensation in the downcomer due to the direct vessel injection is not considered. This is the conservative assumption to obtain higher containment pressure and temperature.

(7) Advanced Accumulators

GOTHIC has not been modified to include a model of the advanced accumulator because during the post-reflood phase the accumulator operates in the low flow mode, in which the flow resistance is nearly constant. The accumulator is modeled using basic GOTHIC modeling elements. The model includes the accumulator tank with the end of reflood water inventory and gas pressure specified. The flow from the accumulator is calculated by GOTHIC for the flow path connecting the accumulator to the cold leg with an constant resistance factor, whose Rev. 2

value is calculated at the end of reflood in WREFLOOD (M1.0). Uncertainty of the flow resistance is included in the sensitivity studies for accumulator parameters.

Table 3-5 shows the result of the hand calculation using characteristics of the accumulator flow damper in order to confirm that the resistance factor at the end of reflood is appropriate on the accumulator conditions during long-term cooling period. The hand calculation was performed with the method described in Appendix B . This result indicates that the flow resistance inputted in GOTHIC is consistent with the calculated value using accumulator conditions during long-term period.

For the US-APWR large-break LOCA, N2 gas of the accumulator is released to the containment via reactor coolant loops after the low flow injection mode is terminated after the end of core reflood. The release of the N2 gas is accounted in the GOTHIC evaluation model using boundary conditions that inject the N2 gas directly into the containment. Parameters related to the gas injection are given conservatively as follows:

Rev. 2

(8) Model Options

The GOTHIC model for the long term mass and energy release is based on the approach used for the Surry Nuclear Plant (Reference 8). In the Surry analysis, it was shown that the methodology gave a mass and energy release rate that was very close to that calculated using the Westinghouse methodology (Reference 2) which is conservative.

The peak containment pressure is determined mainly by the rate of energy release from the secondary side of the steam generators. From the FLECHT SEASET Steam Generator Separate Effects Tests (Reference 20), it is apparent that the heat release rate from the steam generators is dominated by the rate of water delivery to the SG primary side. As long as the SGs are hotter than the primary system, the heat from the secondary side is enough to boil all of the water that enters the SG tubes. Heat transfer to the generated steam is relatively small.

Therefore, the mass and energy release is primarily a function of the buoyancy driven water flow through the intact and broken loops and the amount of water that is carried from the core and into the SG tubes. Based on these observations, the predicted mass and energy release may be influenced by

- Noding of the SG primary side
- Noding of the SG secondary side
- Noding of the hot legs
- Noding of the SG inlet riser and inlet plenum
- Core and Upper Plenum noding
- Hydraulic diameter for the core and upper plenum nodes
- Loop resistance factors
- Flow Path stratified flow option
- Flow Path momentum transport option
- Flow Path compressibility option
- Liquid/Vapor Interface Area

Rev. 2

Rev. 2

Based on the above models, the long term mass and energy will be conservatively predicted by GOTHIC. The following options relevant to mass and energy release calculations are identified for each node and junction in Table 3-6.

For Volumes, see Table 3-6 (1/2):

For Flow Paths, see Table 3-6 (2/2):

Various GOTHIC models for the US-APWR post-reflood analysis affecting mass and energy release are compared to the Reference 2 in Table 3-7. Rev. 2

3.4 Analyses for US-APWR

Rev. 2

3.4.1 Base Case Analysis

A sample analysis for US-APWR was performed by using the codes described above; SATAN-VI(M1.0), WREFLOOD(M1.0) and GOTHIC.

The blowdown period is defined as the time from the accident inception, at steady state 102 % power operation, to the time that the Reactor Coolant System has depressurized to the containment pressure. The refill period is defined as the period from the end of blowdown to the time that the vessel lower plenum has been refilled by the ECCS. The reflood period is defined to the period from the time when water enters the active core to the time that the reactor core is quenched.

The SATAN-VI computer code has a model for calculating counterflow conditions in vertical flow paths by utilizing a drift flux approach. The most significant use of this model is in the calculation of sustained downflow of the accumulator water in the downcomer (called end of bypass). It is used to more accurately calculate the water inventory in the vessel at end of blowdown. This model is incorporated to comply with the requirements of 10 CFR 50.46 and does not affect the mass and energy release results significantly since the reactor vessel lower plenum is conservatively assumed to be full at the end of blowdown. That is, the refill period is conservatively assumed to be 0 seconds. This assumption is in conformance with Acceptance Criterion 1.C.iii. of SRP 6.2.1.3. Rev. 2

WREFLOOD reads temperatures and mass inventory at the end of blowdown period from SATAN-VI (1.0). Then the code calculates the transient for the refill period during which the water level in the reactor vessel increases due to the ECCS injection, until it reaches the bottom of the fuel rods. With this calculation, the vessel inventory and the parameters related to the ECCS are updated. The problem time, however, is retained at the end of blowdown. Then calculation for reflood period starts.

Comparisons of the options in the tables (Table 3-8 through Table 3-11) to those selected for analysis of US-APWR are provided below. They show that, except for Table 3-11, standard model options are used for the US-APWR. In Table 3-11, PREF and HINJ are supplied from GOTHIC calculated values, since they are available through the simultaneous calculation with GOTHIC. The GOTHIC model is constructed to give conservatively high values for the containment pressure and RWSP enthalpy.

The main parameters used in mass and energy release and containment response analysis are shown in Table 3-12. A double ended guillotine break at pump suction was assumed as postulated LOCA condition. The assumptions for the US-APWR analysis are compared with those of Section 5.1 of Reference 2 in Table 3-13. The comparison shows that the Rev. 2

assumptions are essentially the same except for the SG secondary side mass and the post-reflood model, which is based on the GOTHIC code in the US-APWR compared to the FROTH code in WCAP-10325-P-A. In the FROTH analysis for post-reflood period, the steam exiting from the SG is artificially assumed to be saturated. In the GOTHIC analysis, the steam exit condition depends on the calculated heat transfer across the SG tubes and the steam may exit in a superheated condition. This is consistent with the observations from the FLECHT-SEASET Steam Generator Separate Effects tests. The influence of the steam condition on the containment peak pressure is slight. Rev. 2

The mass and energy release results of each phase are shown Figure 3-18 to Figure 3-23, and containment pressure and vapor temperature are shown in Figure 3-24 and Figure 3-25. The peak pressure is 57.5 psig which appears at 1964 sec. The peak temperature of the vapor is 282 deg F at 1797 sec. Table 3-14, prepared for Subsection 3.4.2.1, includes the results for the base case, listing the figures for the containment pressure, average containment atmospheric temperature, and average RWSP water temperature. Rev. 1

Plots of the void fractions and integrated mass flow rates of the fluid leaving the core and entering the steam generators as a function of time are provided with Figure 3-27 through Figure 3-31.

The reactor system water mass and temperature, temperature of the fuel in the core, the neutron reflector, reactor vessel heavy metal, steam generator heavy metal and steam generator water mass and temperature at the time of transition from the end of blowdown to the beginning of reflood for the base case are provided in Table 3-15. Mass and energy balance tables for the base case are provided as Table 3-16 and Table 3-17. Rev. 2

Table 3-18 through Table 3-21 show tabulations of the mass and energy release for the base case. Table 3-20, the post-reflood mass and energy table, lists the mass and energy release rates for the reactor vessel side and the steam generator side of the break. Since steam and water are treated separately using non-equilibrium features in the GOTHIC, each enthalpy value in Table 3-20 is obtained by averaging the conditions for saturated or superheated steam and those for subcooled water using GOTHIC output. Each set of time dependent mass and energy data in Table 3-20 is picked up from plotting data at regular intervals. The data in Table 3-20 are the same as Table 6.2.1-21 in the US-APWR DCD revision 0. Table 3-21 also gives the post-reflood mass and energy for the same case with steam and liquid separated. Since mass and energy data in Table 3-21 are calculated ones so as to conserve integral values, they are not necessarily identical to values at the same time in Table 3-20.

3.4.2 Sensitivity Studies for Establishment of Evaluation model

3.4.2.1 Sensitivity Studies on ECCS Conditions

Rev. 2

The conservatisms in the assumptions made in the LOCA analyses regarding ECCS operability are as follows:

- For the high head injection systems (HHIS), it is assumed that one train is out of service and another train is lost based on the postulated single failure. This results in the loss of two-out-of-four trains. Uncertainty of the SI system is conservatively accounted for in the SI characteristics.
- Minimum accumulator water volume and pressure, and maximum injection resistance are assumed to minimize steam condensation by the injected water.

Sensitivity studies to confirm the analytical conditions for HHSI and accumulator that result in maximum accident pressure and temperature are prepared for the limiting break condition. Table 3-14 shows the results for the sensitivity studies, listing the figures for the containment pressure, average containment atmospheric temperature, and average RWSP water temperature for each case analyzed. These results demonstrate the following:

- The minimum ECCS flow conditions result in maximum accident pressure and temperature.
- The accumulator water volume, pressure, and injection resistance assumed for the limiting case to minimize steam condensation, as described above, give the most severe results. These parameters, however, do not have large effect on the peak containment pressure and temperature because the peak pressure appears in the long term cooling phase, when steam condensation resulting from the accumulator water injection is relatively small compared to that in the reflood phase. Rev. 2

3.4.2.2 Sensitivity Study on Loop Pipe Resistance

WREFLOOD analysis and GOTHIC analysis use best estimate design value of primary loop piping resistance. A sensitivity analysis was performed to confirm quantitative effect of piping resistance error on the containment pressure. The sensitivity study used 20% lower piping resistance. In the sensitivity study GOTHIC loop resistance is also reduced 20% and analysis results show the effect of the reduced loop resistance both in reflood and post-reflood phases.

The following parameters from the sensitivity study are shown in Figure 3-41 to Figure 3-45 in comparison to the base case.

Integral of broken loop SG side break flow from WREFLOOD (Figure 3-41)
Integral of broken loop RCP side break flow from WREFLOOD (Figure 3-42)
Integral of broken loop SG side steam flow from GOTHIC (Figure 3-43)
Integral of broken loop RCP side steam flow from GOTHIC (Figure 3-44)
Containment pressure (Figure 3-45)

Results of the sensitivity study show slightly larger steam flow to the containment than the base case as shown in Figure 3-41 to Figure 3-44. The peak containment pressure is about 72.5 psia and is 0.3 psi higher than the base case as shown in Figure 3-45. The peak pressure is substantially lower than the design pressure. The effect of 20% lower loop resistance on the peak containment pressure is small, because most of the loop resistance is due to the RCP and piping resistance is relatively small.

This increase in the peak containment pressure due to lower primary loop resistance is small relative to the identified conservative margin in peak pressure, [ ], as described in Appendix D.

3.4.2.3 Sensitivity Study on Loop Seal Formation

A sensitivity study was performed to address the concern raised by the NRC that the loop seal formation in the intact loop pump suction leg during post-reflood phase may occur and will block steam flow to the injection point of the intact loop cold leg with no steam condensation. This causes steam flow to increase in the broken loop and may raise containment pressure.

In the sensitivity study, steam flow to the intact loop cold leg is completely blocked by removing flow path from the pump suction leg to the cold leg as shown in Figure 3-46 to simulate the loop seal formation in the intact loop pump suction leg. Rev. 2

The following parameters from calculated results are shown in Figure 3-47 to Figure 3-52 in comparison to the base case.

Break steam flow from broken loop SG side (Figure 3-47)
Break steam flow from broken loop RCP side (Figure 3-48)
Integral of total steam flow to the containment (Figure 3-49)
Broken loop SG secondary side temperature (Figure 3-50)
Intact loop SG secondary side temperature (Figure 3-51)
Containment pressure (Figure 3-52)

For the sensitivity case, almost all steam generated in the core flows into the broken loop and the net steam release from the RCP side break is almost zero, as shown in Figure 3-47 and Figure 3-48. On the other hand, the steam release from the RCP side for the base case is quite large because of the generated steam in the intact-loop SG tubes, as described below. As a result, total steam flow to the containment for the sensitivity case is much smaller than the base case as shown in Figure 3-49.

The secondary side temperature of the broken loop SG and intact loop SG are shown in Figure 3-50 and Figure 3-51, respectively. Cooldown of the broken loop SG secondary side is faster than the base case, but the intact loop SG secondary side, which has much more energy than broken loop SG, is only slightly cooled due to the oscillatory flow through the intact hot leg. The net result is much slower energy release to the containment and the containment pressure during post-reflood phase is much lower than the base case as shown in Figure 3-52.

3.4.2.4 Treatment of Spilled Accumulator Water

For the limiting pump suction break, accumulator water injected into the pump-discharge side does not spill directly from the break. In case of a break at the pump discharge side, which is called cold-leg break hereafter, spillage of the broken loop accumulator is possible. The cold-leg break is much less limiting in terms of the overall containment peak pressure than the pump suction break and is not evaluated for peak containment pressure analysis.

The relation between the pump-suction break and the cold-leg break for the blowdown and reflood phases has been demonstrated for current 4-loop plants with the approved methodology described in WCAP-10325-P-A. This relation should be the same for the US-APWR due to almost the same plant configuration and the analytical methodology.

Rev. 2

Therefore, in order to demonstrate the conservativeness of the GOTHIC model and the actual relation between both break cases, calculations for both break cases have been performed using a more realistic GOTHIC model within the expected parameter ranges. The results of the study are described in Appendix D.

3.4.2.5 Effects of Flow Oscillation in GOTHIC Analysis

Standard Review Plan 6.2.1.3 recommends the following:
“Steam from decay heat boiling in the core should be assumed to flow to the containment by the path which produces the minimum amount of mixing with the ECCS injection water.”

The post-reflood steam release to the containment as calculated by the GOTHIC primary system simulation is oscillatory as compared with the previously approved methodology in WCAP-10325. To maintain quasi-steady flow into the lower plenum, the flow rate must closely match the boiling rate in the core. The lower plenum flow rate is determined by the driving pressure differential which depends on the water head in the downcomer, the flow resistance on the water flow through the downcomer, lower plenum and into the core, the gravitational head in the core and the flow resistance on the steam flow through the core, upper internals and the Steam Generator loops. Assuming that the downcomer remains full, a balanced system depends on having just the right amount of water in the vessel to balance the pressures around the loop. Starting from a balanced state, a reduction in the core power leads to a reduction in boiling and reduced pressure drop between the core and the containment through the steam generators. The lower pressure in the core allows an increase in the flow into the core. Since the water in the lower plenum is subcooled, this leads to further reduction in boiling. This positive feedback effect allows the vessel water inventory to rise to a level that overshoots the new balanced operating point. In order to reach the new balance operating point, the water inventory in the vessel must be reduced. This is accomplished by reducing the inflow to zero, or less, and reestablishing the boiling rate. As the boiling rate increases, the flow resistance through the steam generators increases and water is forced back into the lower plenumand downcomer. This results in the oscillating flow predicted by GOTHIC.

Based on extensive modeling sensitivity studies, it is believed that these oscillations are real and inherent in the physical systems. Nevertheless, it is recognized that the oscillations may cause steam condensation to be calculated within the core and lower plenum of the reactor vessel and reduce the steaming rate to the containment. Therefore, a revised model is proposed that eliminates the oscillations and maximizes the steam flow to the containment by decoupling the downcomer and lower plenum during the long term decay heat phase of the mass and energy release to comply with the requirements of SRP 6.2.1.3. Rev. 2

Figure 3-53 compares the integral of the steam release rate calculated using the original GOTHIC methodology that includes the oscillatory flow with the steaming rate due to decay heat calculated using the following expression.

In order to evaluate the effects of oscillation, a sensitivity study has been performed on the limiting case of the US-APWR containment analyses as described in Appendix E.

3.4.3 Proposed Evaluation Model for Post-reflood Long-term Period

Sensitivity studies shown in Subsection 3.4.2 demonstrates that the base case analysis is appropriate or has sufficient conservatism except for the calculated flow oscillation. This subsection describes a proposed post-reflood mass and energy release model which eliminates the effects of the flow oscillation without significant change in the evaluation model described in Section 3.3.

3.4.3.1 Model to Eliminate Effects of Flow Oscillation

Rev. 2

3.4.3.2 Initial Conditions

Rev.2

Initial conditions for the post-reflood phase are also slightly changed to eliminate factors that affect stability of the calculated flow rate.

Rev.2

3.4.3.3 Sensitivity Analyses with Revised Model that Eliminates Oscillation Effects

Rev.2

(3) Results from the Proposed Model that Eliminates Oscillation Effects

Rev.2

The containment pressure for the proposed-model case is still below the design criteria of the US-APWR with substantial margin. Figure 3-61 through Figure 3-64 compare major parameters versus time for the both cases.

3.4.3.4 Conclusion

Table 3-1 SATAN-VI Code Noding for Blowdown Phase Mass & Energy Release Analysis

Table 3-2 WREFLOOD Code Noding for Reflood Phase Mass and Energy Release Analysis

Node	Physical description
Loop 1 (broken loop)	
1	Outlet nozzle of reactor vessel
2	Hot leg
3	SG inlet plenum
4	SG tubes
5	SG outlet plenum
6	Pump suction leg
Loop 2 (Intact loop)	
1	Outlet nozzle of reactor vessel
2	Hot leg
3	SG inlet plenum
4	SG tubes
5	SG outlet plenum
6	Pump suction leg
7	Reactor coolant pump
8	Cold leg
9	Inlet nozzle of reactor vessel
10	Downcomer
11	Inlet nozzle of reactor vessel
12	Cold leg
13	Reactor coolant pump

Table 3-3 Verification of Advanced Accumulator Model Built into SATAN-VI and WREFLOOD Code

Rev. 1

Table 3-4 GOTHIC Code Noding for Post-reflood Mass and Energy Release Analysis

Table 3-5 Hand Calculation of Accumulator Resistance Coefficient

Rev. 2

Table 3-6 GOTHIC Options Used for US-APWR Mass and Energy Release Evaluation, Long Term of Loss-of-Coolant Accident (Sheet 1 of 2)

Rev. 2

Table 3-6 GOTHIC Options Used for US-APWR Mass and Energy Release Evaluation, Long Term of Loss-of-Coolant Accident (Sheet 2 of 2)

Rev. 2

Table 3-7 Comparison of GOTHIC US-APWR model with FROTH (Sheet 1 of 3)

Item	FROTH	GOTHIC	Comment
1. Steam generation rate in core	FROTH calculates steam generation rate in core accounting for decay heat and heat from metal. Water is assumed always saturated.	GOTHIC calculates steam generation rate by energy balance in core accounting for inlet flow, outlet flow, decay heat and heat from metal. Inlet flow and outlet flow are calculated by momentum equation. Subcooled inlet water is allowable.	FROTH calculation model is too conservative. GOTHIC is realistic.
2. Core void fraction	Calculated by Yeh correlation with steam velocity of half of total core generated steam flow. The calculated void fraction is corresponding to core average.	All steam generated in the core is used for void fraction calculation. Ishii's drag coefficient is applied for interfacial force calculation. Calculated void fraction is corresponding to core exit void fraction.	Generally GOTHIC gives higher void fraction in the core because of higher steam velocity. Higher void fraction gives smaller water head in core and results in larger available water head for SG froth and larger available pressure drop for steam flow in loop. These result in conservative result.
3. Downcomer level	Assumed always full	GOTHIC calculates water level with mass and energy balance considering water flow from intact loop, injected water flow, water flow to core and spilt water flow.	No artificial modeling is applied in GOTHIC.GOTHIC model is realistic.
4. Flow split of steam flow from core		Loop momentum balance decides flow split internally.	GOTHIC calculates more flow to intact loop than FROTH. This results in more rapid heat release from intact loop SG secondary side than FROTH.

Rev. 2

Table 3-7 Comparison of GOTHIC US-APWR model with FROTH (Sheet 2 of 3)

Item	FROTH	GOTHIC	Comment
5. Steam generator inlet water flow calculation		GOTHIC calculates droplet and water flow into SG U-tube from dynamic momentum equation for each phase. Water head and pressure drop due to flow are considered in momentum equation. If water enters hot side, entire heat transfer area in U-tube hot side is available for steam generation.	Global primary system momentum balance in GOTHIC is almost the same as in FROTH.

Rev. 2

Table 3-7 Comparison of GOTHIC US-APWR model with FROTH (Sheet 3 of 3)

Item	FROTH	GOTHIC	Comment
6. Steam-water mixing	Assumed complete mixing in both intact loop and broken loop cold legs	Assumed almost complete mixing in only intact cold leg	GOTHIC model is conservative.
7. SG heat transfer model	McAdams correlation for secondary side is applied. Heat transfer resistance of tube and primary side is neglected.	GOTHIC FILM option heat transfer model is applied to both secondary side and primary side of U-tubes. Tubes are modeled by conductors. Heat transfer correlation of SG U-tube secondary side is by McAdams.	No substantial difference between FROTH and GOTHIC.
8. The steam condition at the outlet of steam generator	Saturated steam is assumed.	Steam condition is calculated by heat transfer model in SG tubes.	No artificial assumption is applied to GOTHIC. Actually no substantial effects on containment pressure.
9. The containment back pressure	The containment design pressure is used and constant during transient. This pressure is equal to primary system pressure in FROTH.	GOTHIC calculates both the primary system and the containment transients simultaneously. Transient containment pressure is used. GOTHIC treatment is realistic.	In US-APWR the advanced accumulator still works during post-reflood phase. Realistic primary system pressure transient is desirable for the advanced accumulator flow calculation.

Rev. 2

Table 3-8 Model Differences between SATAN V , SATAN VI and SATAN VI (M1.0)

	SATAN V	**SATAN VI**	**SATAN VI (M1.0)**
Drift Flux Model	No	Yes	Yes
Momentum Flux	No	Yes	Yes
Two Phase Pump Model	Simplified Model	Dynamic 2 ϕ Pump Model	Dynamic 2 ϕ Pump Model
Core Heat Release Model	Externally Calculated	Internally Calculated	Internally Calculated
Wall Heat Transfer Correlation (Nucleate Boiling)	Jens-Lottes	Thom	Thom
Thin Metal Heat Release Model	Externally Calculated	Internally Calculated	Internally Calculated
Film Boiling Heat Transfer Correlation	Dougall-Rohsenow	Westinghouse Transition Boiling	Westinghouse Transition Boiling

Rev. 2

Table 3-9 SATAN VI and SATAN VI (M1.0) Comparisons of Significant Standard Inputs for ECCS & Mass/Energy Release Analysis

Input	**Appendix K ECCS Analysis**	**Mass & Energy Release Analysis SATAN VI**	**Mass & Energy Release Analysis SATAN VI (M1.0)**
IMAX	49	71	71
IUCP	0	1	1
IDNB	3	2	2
NCORE	8	2	2
NCHAN	2	1	1
NHOT(1)	6	1	1
PCONT	Minimum Value	Maximum Value	Maximum Value
VWABG1	Intact Loop	Broken Loop	Broken Loop
VWABG2	Broken Loop	Intact Loop	Intact Loop
DNBR	1	0.7	0.7
CON(1)	1	0	0
CON(2)	1	0	0
CON(7)	1	0	0
CON(8)	0	1	1
CON(13)	Minimum Value	Maximum Value	Maximum Value

Rev. 2

Table 3-10 Model Difference between versions of WREFLOOD

	WREFLOOD(IAC)	WREFLOOD(FAC)	WREFLOOD(M1.0)
Injection Section Pressure Drop	No	Yes – Not Used for M & E Analyses	Yes – Not Used for M & E Analyses
Injection section Steam/Water Mixing	No	Yes	Yes – for Accumulator Injection No – for HHIS (DVI Injection)
Two Phase Pressure Drop Multiplier	No	Yes	Yes

Rev. 2

Table 3-11 Comparisons of Significant Standard REFLOOD Inputs for ECCS and Mass & Energy Release Analysis

Input	ECCS value	M & E Value (WREFLOOD)	M & E Value (WREFLOOD (M1.0))	Comment
ITSAT	3	4	4	This input when set to a value of 4 defines the case as a mass & energy release analysis.
IPMP	0	1	1	Reactor Coolant Pumps homologous curves are used for M & E analyses.
PREF	Calculated Containment Pressure	Containment Design Pressure	Calculated Containment Pressure	Calculated containment pressure is conservatively high.
HINJ	Minimum RWSP Water Enthalpy	Maximum RWSP Water Enthalpy	Calculated RWSP Water Enthalpy	Maximum initial RWSP water enthalpy is used.

Rev. 2

Table 3-12 Main Input Description for Sample Analysis of Mass and Energy Release

General		
Core Power	MWt	4451 x 1.02
Coolant Pressure	psia	2250 + 30
Nominal Inlet Temperature	deg F	551 + 4
Nominal Outlet Temperature	deg F	617 + 4
Core		
Fuel Rod Lattice	-	17 x 17
Number of Fuel Assembly	-	257
Active Fuel Length	ft	14
Advanced Accumulator		
Number of Accumulator Operating	-	4/4
Accumulator Liquid Volume	ft^3/unit	[ ]
Accumulator Temperature	deg F	120
Assumed Condition		
Maintenance Outage	-	1 Emergency Power Source
Single Failure	-	1 Emergency Power Source
Containment Spray System		
Number of Spray Pump Operating	-	2/4
Spray Flowrate	GPM/unit	2645
Spray Initiation Time	sec	246
Containment System		
Containment Design Pressure	psig	68
Net Free Volume	ft^3	2.74×10^6
Initial Pressure	psig	2.0
Initial Temperature	deg F	120
Initial Humidity	%	0

Rev. 1

Table 3-13 A comparison of the assumptions to be made for analysis of US-APWR with those of Section 5.1 of WCAP-10325-P-A

	WCAP-10325-P-A Section 5.1	US-APWR
Initial system conditions		
Power level	102 %	same
Fluid temperature	+4 F	same
System volume	+3 %	same
Steam generator parameter, Secondary mass	Based on 100% power, +10%	Based on 100 % power, B.E. + 3 % (consistent with primary system mass.)
Metal stored energy	maximized	same
Decay heat	maximized	same
Core stored energy	maximized	same
Blowdown modeling		
Break size	A full double ended area	same
Core heat transfer coefficient	Best judgment for maximizing to heat release from the core	same
Reflood modeling		
Carryover fraction correlation	ECCS type application	same
Steam water mixing pressure drop	excluded	same
Exit steam generator fluid conditions	saturated	same
Post-reflood modeling		
Exit steam generator fluid conditions	saturated	GOTHIC calculated value

Rev. 2

Table 3-14 Summary of Sensitivity of ECCS Conditions on the Containment Pressure and Temperature

Case	Limiting Case	HHSI Max Safeguards	Accumulator Max Water	Accumulator Max Flow
Break Location	Pump Suction	Pump Suction	Pump Suction	Pump Suction
Break Size and Type	C_D=1.0 Double Ended Guillotine	C_D=1.0 Double Ended Guillotine	C_D=1.0 Double Ended Guillotine	C_D=1.0 Double Ended Guillotine
Offsite Power	Lost	Lost	Lost	Lost
Assumption for Out of service*	1 Emergency Generator	1 Containment Heat Removal System	1 Emergency Generator	1 Emergency Generator
Single Failure	1 Emergency Generator	1 Containment Heat Removal System	1 Emergency Generator	1 Emergency Generator
Safety Injection	2 Pumps Operation Minimum Safeguard	4 Pumps Operation Maximum Safeguard	2 Pumps Operation Minimum Safeguard	2 Pumps Operation Minimum Safeguard
Accumulator Water Volume	Minimum	Minimum	Maximum	Minimum
Accumulator Pressure	Minimum	Minimum	Minimum	Maximum
Accumulator Line Resistance	Maximum	Maximum	Maximum	Minimum
Peak Pressure, psia (psig)	72.2 (57.5)	67.8 (53.1)	71.9 (57.2)	72.1 (57.4)
Peak Atmospheric Temperature, °F	282	276	282	281
Peak RWSP Water Temperature, °F	251	252	251	251
24 hours Pressure, psia (psig)	23.6 (8.9)	Expected to be sufficiently low	Expected to be sufficiently low	Expected to be sufficiently low
Parameters vs time:				
Containment Pressure	Figure 3-24	Figure 3-32	Figure 3-35	Figure 3-38
Atmospheric Temperature	Figure 3-25	Figure 3-33	Figure 3-36	Figure 3-39
RWSP Water Temperature	Figure 3-26	Figure 3-34	Figure 3-37	Figure 3-40

* Out of service basis for the limiting conditions (maintenance or operation surveillance)

Rev. 2

Table 3-15 Water Mass and RCS Temperature Transient

Rev. 2

Table 3-16 Mass Distribution Transient

Phase		Prior to LOCA	End of Blowdown	End of Core Reflood	At Peak Pressure	1 Day into Recirc.
Time (seconds)		0.00	31.60	265.54	1963.7	86400
Initial Mass	RCS and ACC	1278.06	1278.06	1278.06	1278.06	1278.06
Added Mass	Pumped Injection	0.00	0.00	49.70	613.90	28362.65
	Total Added	0.00	0.00	49.70	613.90	28362.65
Total Available (Initial Mass +Total added)		**1278.06**	**1278.06**	**1327.76**	**1891.96**	**29640.71**
RCS Mass Distribution	Reactor Coolant	752.18	68.17	207.23	189.83	206.26
	Accumulator	525.89	460.87	92.06	9.21	0.00
	RCS Total Contents	1278.06	529.05	299.28	199.04	206.26
Effluent	Break Flow	0.00	748.99	1028.49	1698.94	29439.66
	ECCS Spill	0.00	0.00	0.00	0.00	0.00
	Total Effluent	0.00	748.99	1028.49	1698.94	29439.66
Total Accountable		**1278.06**	**1278.04**	**1327.77**	**1897.98**	**29645.92**

Unit: Thousand lbm

Rev. 2

Table 3-17 Energy Distribution Transient

Phase		Prior to LOCA	End of Blowdown	End of Core Reflood	At Peak Pressure	1 Day into Recirc.
	Time (seconds)	0.00	31.60	265.54	1963.7	86400
Initial Energy		1287.49	1287.49	1287.49	1287.49	1287.49
Added Energy	Pumped Injection	0.00	0.00	5.67	90.83	5021.69
	Energy Generated during Shutdown from Decay Heat	0.00	15.58	49.83	224.04	3254.97
	Heat from Secondary	0.00	26.04	26.04	26.04	26.04
	Total Added	0.00	41.62	81.54	340.91	8302.70
Total Available	**(Initial Energy + Added)**	**1287.49**	**1329.11**	**1369.03**	**1628.40**	**9590.19**
RCS Energy Distribution	Reactor Coolant Internal Energy	441.38	17.09	58.37	80.46	70.92
	Accumulator Internal Energy	47.09	41.27	8.24	0.81	0.00
	Energy Stored in Core	43.40	23.08	7.58	5.56	3.77
	Energy Stored in RCS Structure	267.87	255.87	183.82	104.11	63.84
	Steam Generator Coolant Internal Energy	349.58	379.25	318.99	197.89	141.91
	Energy Stored in Steam Generator Metal	138.16	136.48	117.14	77.51	65.60
	RCS Total Contents	1287.49	853.03	694.16	466.34	346.04
Effluent	Break Flow	0.00	476.08	652.54	1132.84	9231.34
	ECCS Spill	0.00	0.00	0.00	0.00	0.00
	Total Effluent	0.00	476.08	652.54	1132.84	9231.34
Total Accountable		**1287.49**	**1329.11**	**1346.70**	**1599.18**	**9577.38**

Unit: Million Btu

Reference Temperature: 32 degF

Rev. 2

Table 3-18 Break Mass and Energy Flow for the Blowdown Phase of the DEPSG Break (Sheet 1 of 3)

Time (sec)	Break Flow (Reactor Vessel Side)			Break Flow (Steam Generator Side)		
	Mass (lbm/sec)	Enthalpy (Btu/lbm)	Energy (Thousand Btu/sec)	Mass (lbm/sec)	Enthalpy (Btu/lbm)	Energy (Thousand Btu/sec)
0.0	0.0	0.0	0.0	0.0	0.0	0.0
0.00037	39367.7	551.1	21695.5	47451.3	553.0	26240.6
0.00102	39475.9	548.5	21652.5	101757.9	550.6	56027.9
0.0112	39130.1	548.1	21447.2	42091.4	548.5	23087.1
0.0211	36128.7	547.7	19787.7	41741.5	548.6	22899.4
0.0515	23343.8	545.7	12738.7	41730.0	548.8	22901.4
0.0611	21272.1	546.1	11616.7	41772.5	549.0	22933.1
0.0711	20482.9	546.9	11202.1	49613.7	549.3	27252.8
0.0912	20875.8	547.9	11437.9	49573.9	549.5	27240.9
0.111	21872.9	548.2	11990.7	52298.0	549.9	28758.7
0.161	23599.5	548.5	12944.3	53529.7	550.8	29484.2
0.222	24642.8	548.5	13516.6	53292.9	552.1	29423.0
0.301	25143.0	548.8	13798.5	52771.2	554.1	29240.5
0.351	25174.2	549.0	13820.6	52247.1	555.6	29028.5
0.451	24831.4	549.4	13642.4	51440.1	558.8	28744.7
0.611	23851.7	549.8	13113.7	49667.7	564.7	28047.4
0.701	23376.9	550.0	12857.3	48773.6	568.3	27718.0
0.801	22955.5	550.1	12627.8	47097.0	572.2	26948.9
0.892	22593.8	550.2	12431.1	45168.5	575.4	25990.0
1.00	22156.2	550.2	12190.3	45392.0	579.0	26282.0
1.09	21789.4	550.3	11990.7	45312.7	581.6	26353.9
1.27	21309.6	550.4	11728.8	44761.2	586.5	26252.4
1.75	20552.4	550.6	11316.2	42786.2	600.7	25701.7
2.20	20134.6	550.7	11088.1	40939.5	616.1	25222.8
2.32	20005.2	550.7	11016.9	40291.3	620.9	25016.9
2.61	19758.0	550.8	10882.7	38300.3	634.5	24301.5
2.82	19471.7	550.9	10727.0	36444.7	646.1	23546.9
3.30	18855.6	551.2	10393.2	31566.7	676.2	21345.4
3.37	18744.9	551.2	10332.2	30574.1	680.5	20805.7
3.51	18535.4	551.3	10218.6	27856.7	689.3	19201.6
3.59	18426.4	551.4	10160.3	26605.1	694.5	18477.2
3.78	18178.5	551.6	10027.3	24039.6	705.4	16957.5
3.98	17916.9	551.8	9886.5	21866.8	714.3	15619.5
4.16	17712.0	552.0	9777.0	20321.5	721.2	14655.9
4.32	17550.1	552.2	9691.2	19287.2	726.8	14017.9
4.56	17298.1	552.5	9557.2	18071.0	733.8	13260.5
4.86	17033.0	552.9	9417.5	16955.9	740.8	12560.9

Rev. 2

Table 3-18 Break Mass and Energy Flow for the Blowdown Phase of the DEPSG Break (Sheet 2 of 3)

Time (sec)	Break Flow (Reactor Vessel Side)			Break Flow (Steam Generator Side)		
	Mass (lbm/sec)	Enthalpy (Btu/lbm)	Energy (Thousand Btu/sec)	Mass (lbm/sec)	Enthalpy (Btu/lbm)	Energy (Thousand Btu/sec)
5.12	16808.2	553.3	9300.0	16226.0	745.1	12090.0
5.60	16450.3	554.1	9115.1	15301.9	749.0	11461.1
5.92	16242.6	554.7	9009.8	14891.4	749.1	11155.1
6.14	16098.5	555.1	8936.3	14686.4	748.0	10985.4
6.68	15794.6	556.1	8783.4	14368.9	743.1	10677.5
7.22	15531.3	557.1	8652.5	14258.5	735.7	10490.0
7.62	15350.4	557.9	8564.0	14294.0	729.0	10420.3
7.98	15206.5	558.6	8494.4	14488.9	722.0	10461.0
8.02	15196.1	558.7	8490.1	14723.8	721.5	10623.2
8.26	15128.7	559.1	8458.5	15040.2	716.4	10774.8
8.34	15756.0	559.7	8818.6	15093.6	718.5	10844.8
8.40	16029.0	559.7	8971.4	15026.1	722.8	10860.9
8.52	16090.0	559.8	9007.2	14553.7	739.5	10762.5
8.78	16004.4	560.2	8965.7	12886.7	789.0	10167.6
8.90	15895.1	560.4	8907.6	12425.1	801.9	9963.7
9.08	15710.5	560.6	8807.3	12142.2	807.6	9806.0
9.86	14727.4	561.8	8273.9	11967.7	802.2	9600.5
10.1	14508.6	562.2	8156.7	11851.1	802.3	9508.1
10.5	14119.1	562.5	7942.0	11638.6	804.5	9363.3
11.2	13710.6	562.7	7715.0	11289.3	808.4	9126.3
11.6	13507.9	562.5	7598.2	11339.8	795.6	9021.9
11.9	13352.6	562.3	7508.2	11560.2	778.4	8998.5
12.5	13080.4	562.0	7351.2	12052.3	747.6	9010.3
13.1	12837.1	561.8	7211.9	12244.3	729.1	8927.3
13.6	12635.0	561.6	7095.8	12079.1	722.0	8721.1
14.5	12335.9	561.6	6927.8	11422.7	725.2	8283.7
15.1	12101.4	561.7	6797.4	10849.1	734.6	7969.7
16.1	11666.0	561.9	6555.1	10022.9	753.8	7555.3
16.8	11348.1	562.2	6379.9	9476.6	769.2	7289.4
17.7	10874.8	562.8	6120.3	8789.5	787.7	6923.5
18.4	10529.9	563.4	5932.5	8373.0	794.6	6653.2
19.0	10210.8	564.1	5759.9	8052.5	797.2	6419.5
20.0	9673.4	566.4	5479.0	7519.7	802.2	6032.3
20.6	9374.9	568.2	5326.8	7234.7	804.5	5820.3
21.8	8726.0	573.3	5002.6	6752.6	812.2	5484.5
22.0	8449.6	575.0	4858.5	6591.6	817.4	5388.0
22.1	8455.7	575.8	4868.8	6529.7	820.1	5355.0

Rev. 2

Table 3-18 Break Mass and Energy Flow for the Blowdown Phase of the DEPSG Break (Sheet 3 of 3)

Time (sec)	Break Flow (Reactor Vessel Side)			Break Flow (Steam Generator Side)		
	Mass (lbm/sec)	Enthalpy (Btu/lbm)	Energy (Thousand Btu/sec)	Mass (lbm/sec)	Enthalpy (Btu/lbm)	Energy (Thousand Btu/sec)
22.4	8174.3	575.8	4706.8	6346.2	827.6	5252.1
22.5	8121.9	576.2	4679.8	6197.9	834.7	5173.4
23.2	7506.8	565.4	4244.3	5537.6	857.3	4747.4
23.5	7418.9	546.8	4056.7	5363.3	856.3	4592.6
23.9	7051.1	525.4	3704.6	5304.6	868.6	4607.6
24.1	6856.5	513.9	3523.6	5096.0	903.6	4604.7
24.3	6495.3	498.7	3239.2	4570.4	988.9	4519.7
24.6	6032.6	482.1	2908.3	3837.4	1123.2	4310.2
24.9	5684.8	470.7	2675.8	3371.5	1203.1	4056.3
25.2	5326.6	456.8	2433.2	2966.9	1233.0	3658.2
25.6	4825.7	439.8	2122.3	2576.6	1242.3	3200.9
26.0	4511.2	428.2	1931.7	2360.9	1246.8	2943.6
26.3	4022.2	420.6	1691.7	2222.3	1249.5	2776.8
26.6	3691.6	407.9	1505.8	2051.7	1252.1	2568.9
26.7	3693.4	402.7	1487.3	1970.7	1253.3	2469.9
27.1	3875.1	388.7	1506.3	1753.1	1256.9	2203.5
27.3	3818.1	383.4	1463.9	1620.9	1258.7	2040.2
28.1	3258.2	364.5	1187.6	1223.5	1265.0	1547.7
28.3	3013.6	356.1	1073.1	1089.7	1266.4	1380.0
28.7	2733.2	342.7	936.7	863.0	1268.5	1094.7
29.0	2602.6	334.0	869.3	746.2	1269.7	947.5
29.2	2413.3	327.3	789.9	678.6	1270.3	862.0
29.6	1782.4	315.2	561.8	578.3	1271.8	735.5
29.9	1036.9	308.6	320.0	502.1	1272.6	639.0
30.2	0.0	0.0	0.0	408.8	1273.5	520.6
31.6	0.0	0.0	0.0	0.0	0.0	0.0

Rev. 2

Table 3-19 Break Mass and Energy Flow for the Reflood Phase of the DEPSG Break (Sheet 1 of 3)

Time (sec)	Break Flow (Reactor Vessel Side)			Break Flow (Steam Generator Side)		
	Mass (lbm/sec)	Enthalpy (Btu/lbm)	Energy (Thousand Btu/sec)	Mass (lbm/sec)	Enthalpy (Btu/lbm)	Energy (Thousand Btu/sec)
31.6	0.0	0.0	0.0	0.0	0.0	0.0
32.9	0.0	0.0	0.0	0.0	0.0	0.0
33.0	0.0	0.0	0.0	49.1	1179.3	57.9
33.1	0.0	0.0	0.0	17.1	1179.3	20.2
33.2	0.0	0.0	0.0	2.8	1179.3	3.3
33.4	0.0	0.0	0.0	0.0	0.0	0.0
33.5	0.0	0.0	0.0	21.6	1179.3	25.5
33.6	0.0	0.0	0.0	31.5	1179.3	37.1
33.7	0.0	0.0	0.0	35.3	1179.3	41.6
33.8	0.0	0.0	0.0	46.0	1179.3	54.2
33.9	0.0	0.0	0.0	52.2	1179.3	61.6
35.7	0.0	0.0	0.0	115.4	1179.6	136.1
36.7	0.0	0.0	0.0	140.3	1179.7	165.5
37.7	0.0	0.0	0.0	161.5	1179.9	190.6
38.7	0.0	0.0	0.0	180.2	1180.0	212.6
39.7	0.0	0.0	0.0	197.1	1180.2	232.6
40.7	0.0	0.0	0.0	212.4	1180.3	250.7
41.8	3737.2	158.2	591.2	444.4	1183.5	525.9
42.8	4175.0	166.3	694.3	495.5	1184.7	587.0
43.8	4145.4	167.3	693.5	491.6	1184.7	582.4
44.8	4094.6	167.9	687.5	485.3	1184.5	574.8
45.8	4041.6	168.5	681.0	478.8	1184.4	567.1
46.0	4030.9	168.7	680.0	477.5	1184.3	565.5
46.8	3988.3	169.2	674.8	472.4	1184.2	559.4
47.8	3935.2	169.7	667.8	466.0	1184.1	551.8
48.8	3882.9	170.3	661.3	459.8	1184.0	544.4
49.8	3831.4	170.9	654.8	453.8	1183.8	537.2
50.8	3781.0	171.5	648.4	447.9	1183.7	530.2
51.8	3731.6	172.1	642.2	442.2	1183.6	523.4
52.8	3683.4	172.6	635.8	436.6	1183.4	516.7
53.1	3669.1	172.8	634.0	435.0	1183.4	514.8
53.8	3636.3	173.2	629.8	431.3	1183.3	510.4
54.8	3590.3	173.7	623.6	426.1	1183.2	504.2
55.8	3545.5	174.3	618.0	421.0	1183.1	498.1
56.8	3501.8	174.8	612.1	416.1	1183.0	492.2
57.8	3459.1	175.4	606.7	411.4	1182.9	486.6
58.8	3417.4	175.9	601.1	406.8	1182.7	481.1
59.8	3376.7	176.5	596.0	402.3	1182.6	475.8

Rev. 2

Table 3-19 Break Mass and Energy Flow for the Reflood Phase of the DEPSG Break (Sheet 2 of 3)

Time (sec)	Break Flow (Reactor Vessel Side)			Break Flow (Steam Generator Side)		
	Mass (lbm/sec)	Enthalpy (Btu/lbm)	Energy (Thousand Btu/sec)	Mass (lbm/sec)	Enthalpy (Btu/lbm)	Energy (Thousand Btu/sec)
60.8	3337.0	177.0	590.6	398.0	1182.5	470.6
61.2	3321.4	177.2	588.6	396.2	1182.5	468.5
61.8	3298.2	177.5	585.4	393.7	1182.4	465.5
62.8	3260.4	178.1	580.7	389.6	1182.3	460.6
63.8	3223.3	178.6	575.7	385.7	1182.2	456.0
64.8	3187.2	179.1	570.8	381.8	1182.2	451.4
65.8	3151.8	179.6	566.1	378.0	1182.1	446.8
66.8	3117.2	180.2	561.7	374.4	1182.0	442.5
67.8	3083.3	180.7	557.2	370.8	1181.9	438.2
68.8	3050.2	181.2	552.7	367.3	1181.8	434.1
69.8	3017.7	181.7	548.3	363.9	1181.7	430.0
70.2	3004.9	181.9	546.6	362.6	1181.7	428.5
70.8	2985.9	182.2	544.0	360.6	1181.6	426.1
71.8	2954.8	182.8	540.1	357.4	1181.6	422.3
72.8	2924.3	183.3	536.0	354.3	1181.5	418.6
73.8	2894.3	183.8	532.0	351.2	1181.4	414.9
74.8	2865.0	184.3	528.0	348.2	1181.3	411.3
75.8	2836.2	184.8	524.1	345.3	1181.3	407.9
76.8	2808.0	185.3	520.3	342.4	1181.2	404.4
77.8	2780.2	185.8	516.6	339.6	1181.1	401.1
78.8	2753.0	186.3	512.9	336.9	1181.1	397.9
79.8	2726.3	186.8	509.3	334.2	1181.0	394.7
80.8	2700.0	187.4	506.0	331.6	1180.9	391.6
81.8	2674.2	187.9	502.5	329.0	1180.9	388.5
82.8	2648.8	188.4	499.0	326.5	1180.8	385.5
83.8	2623.9	188.9	495.7	324.1	1180.8	382.7
84.8	182.6	1140.4	208.2	410.6	1182.1	485.4
85.8	191.9	1039.8	199.5	404.4	1182.2	478.1
87.8	190.7	1042.8	198.9	403.0	1182.2	476.4
91.8	188.4	1049.3	197.7	400.2	1182.1	473.1
92.8	187.8	1051.0	197.4	399.5	1182.1	472.2
100.8	183.4	1064.4	195.2	394.2	1182.0	465.9
108.8	179.3	1076.7	193.1	389.2	1181.9	460.0
116.8	175.5	1087.6	190.9	384.2	1181.8	454.0
120.8	173.7	1092.5	189.8	381.6	1181.7	450.9
122.8	257.2	934.6	240.4	481.6	1183.7	570.1
124.8	256.2	936.2	239.9	480.5	1183.7	568.8
128.8	254.4	938.6	238.8	478.4	1183.7	566.3

Rev. 2

Table 3-19 Break Mass and Energy Flow for the Reflood Phase of the DEPSG Break (Sheet 3 of 3)

Time (sec)	Break Flow (Reactor Vessel Side)			Break Flow (Steam Generator Side)		
	Mass (lbm/sec)	Enthalpy (Btu/lbm)	Energy (Thousand Btu/sec)	Mass (lbm/sec)	Enthalpy (Btu/lbm)	Energy (Thousand Btu/sec)
132.8	252.7	940.1	237.6	476.0	1183.7	563.4
136.8	251.3	940.6	236.4	473.6	1183.6	560.6
140.8	249.9	940.2	235.0	471.1	1183.6	557.6
148.8	247.7	937.4	232.2	465.9	1183.5	551.4
150.8	247.2	936.3	231.5	464.6	1183.5	549.9
154.8	246.4	933.7	230.1	461.8	1183.5	546.5
162.8	244.8	927.5	227.1	456.2	1183.4	539.9
170.8	243.3	920.5	224.0	450.5	1183.4	533.1
174.8	242.7	916.9	222.5	447.6	1183.4	529.7
190.8	239.9	902.8	216.6	436.2	1183.3	516.2
198.8	238.3	896.6	213.7	430.6	1183.2	509.5
206.8	236.7	890.9	210.9	425.0	1183.2	502.9
214.8	234.8	886.2	208.1	419.4	1183.2	496.2
222.8	232.8	882.5	205.4	413.9	1183.1	489.7
230.8	230.5	880.0	202.8	408.4	1183.1	483.2
238.8	227.9	878.8	200.3	402.9	1183.1	476.7
246.8	225.2	878.3	197.8	397.4	1183.0	470.1
254.8	223.8	872.3	195.2	392.4	1183.0	464.2
262.8	222.1	867.5	192.7	387.4	1183.0	458.3
265.5	221.5	866.2	191.9	385.7	1182.9	456.2
265.6	92.6	114.1	10.6	119.9	1179.4	141.4

Rev. 2

Table 3-20 Break Mass and Energy Flow for the Long-term Cooling Phase of the DEPSG Break (Sheet 1 of 6)

Time (sec)	Break Flow (Reactor Vessel Side)			Break Flow (Steam Generator Side)		
	Mass (lbm/sec)	Enthalpy (Btu/lbm)	Energy (Thousand Btu/sec)	Mass (lbm/sec)	Enthalpy (Btu/lbm)	Energy (Thousand Btu/sec)
266.0	453.7	663.8	301.2	542.7	1207.8	655.5
270.0	2012.4	333.0	670.1	4548.9	321.9	1464.3
274.0	721.1	733.2	528.7	3042.4	347.9	1058.5
278.0	460.8	935.5	431.1	2599.8	416.8	1083.6
282.0	658.4	649.4	427.6	1056.3	775.8	819.5
286.0	303.0	1019.0	308.8	1014.9	649.0	658.7
290.0	305.0	844.4	257.5	840.9	591.8	497.6
294.0	357.9	666.6	238.6	543.7	705.7	383.7
298.1	414.3	564.2	233.7	258.3	1173.8	303.2
302.1	428.5	520.7	223.1	210.6	1174.2	247.3
306.1	424.4	496.6	210.8	175.1	1179.2	206.5
310.1	417.2	476.5	198.8	223.9	857.1	191.9
314.1	418.1	495.2	207.0	179.4	967.0	173.5
318.1	418.5	512.4	214.4	225.3	853.9	192.4
322.1	418.6	514.0	215.2	248.3	779.9	193.6
326.1	419.3	511.5	214.5	228.0	799.6	182.3
330.1	418.8	509.4	213.3	215.1	803.5	172.8
334.1	415.5	510.0	211.9	202.9	808.4	164.0
338.1	411.7	510.7	210.3	179.7	843.8	151.6
342.1	408.5	511.5	208.9	156.1	892.2	139.3
346.1	405.4	512.2	207.6	136.6	937.2	128.0
350.1	402.6	513.3	206.7	118.1	987.4	116.6
354.1	399.7	514.7	205.7	101.9	1041.7	106.1
358.1	397.4	516.9	205.4	88.7	1075.9	95.4
362.1	394.9	519.9	205.3	78.8	1117.7	88.1
366.1	392.5	522.6	205.1	68.2	1155.3	78.8
370.1	390.2	525.5	205.1	59.9	1184.1	70.9
374.1	388.2	528.6	205.2	53.5	1190.3	63.7
378.1	385.5	531.4	204.9	49.2	1189.8	58.5
382.1	381.7	532.9	203.4	45.4	1189.8	54.0
386.1	371.1	531.3	197.2	41.9	1189.8	49.9
390.1	416.0	577.5	240.2	142.3	985.9	140.3
394.1	355.2	592.8	210.6	252.8	671.2	169.7
398.1	356.1	558.1	198.7	35.3	1187.9	41.9
402.1	399.2	532.9	212.7	60.1	1188.5	71.4
406.1	355.0	619.2	219.8	400.9	545.4	218.7
410.2	316.0	580.3	183.4	9.1	1157.6	10.5

Rev. 2

Table 3-20 Break Mass and Energy Flow for the Long-term Cooling Phase of the DEPSG Break (Sheet 2 of 6)

Time (sec)	Break Flow (Reactor Vessel Side)			Break Flow (Steam Generator Side)		
	Mass (lbm/sec)	Enthalpy (Btu/lbm)	Energy (Thousand Btu/sec)	Mass (lbm/sec)	Enthalpy (Btu/lbm)	Energy (Thousand Btu/sec)
414.2	320.0	537.6	172.0	33.7	1187.6	40.0
418.2	414.1	591.8	245.1	113.9	1186.0	135.1
422.2	366.8	635.0	232.9	177.5	743.4	132.0
426.2	300.8	591.7	178.0	32.7	1175.5	38.4
430.2	324.9	536.2	174.2	24.6	1186.6	29.2
434.2	388.0	627.8	243.6	154.3	919.2	141.8
438.2	313.5	639.7	200.5	19.9	1172.0	23.3
442.2	356.8	595.1	212.3	33.3	1186.3	39.5
446.2	282.7	687.6	194.4	17.3	809.3	14.0
450.3	317.7	649.0	206.2	21.2	1185.5	25.1
454.3	273.9	709.0	194.2	10.8	930.9	10.1
458.3	338.0	685.2	231.6	77.8	1173.5	91.3
462.3	255.9	728.0	186.3	20.6	1143.1	23.5
466.3	255.8	731.9	187.2	10.0	1166.5	11.7
470.3	310.8	715.3	222.3	83.6	1095.6	91.6
474.4	333.2	716.7	238.8	59.6	1185.3	70.6
478.4	292.7	730.3	213.8	18.2	1184.6	21.6
482.4	275.9	760.8	209.9	53.0	1181.5	62.6
486.4	229.9	782.4	179.9	23.2	1104.2	25.6
490.4	305.0	775.5	236.5	70.3	1155.6	81.2
494.4	284.7	833.8	237.4	86.4	1026.3	88.7
498.4	243.6	774.8	188.7	14.2	1155.6	16.4
520.4	267.9	889.0	238.2	29.2	754.8	22.0
560.5	162.4	1028.7	167.1	234.8	393.5	92.4
600.5	229.7	1020.2	234.3	105.4	935.5	98.6
640.5	189.5	1031.6	195.5	21.3	449.8	9.6
680.5	189.8	1138.1	216.0	69.4	1076.7	74.7
720.5	164.9	1250.0	206.1	1664.7	288.1	479.6
760.5	184.6	1229.0	226.9	137.2	710.8	97.5
800.6	190.7	999.5	190.6	64.5	527.4	34.0
840.6	190.1	1073.2	204.0	60.8	1162.3	70.7
880.6	192.0	1064.3	204.3	95.6	848.0	81.1
920.6	219.3	959.3	210.4	37.7	1168.4	44.0
960.7	194.5	1145.2	222.7	1853.8	284.4	527.2
1000.7	199.1	1051.5	209.4	31.2	1180.8	36.8
1040.7	157.9	1055.4	166.6	91.9	270.3	24.8
1080.7	208.2	962.2	200.3	0.0	0.0	0.0

Rev. 2

Table 3-20 Break Mass and Energy Flow for the Long-term Cooling Phase of the DEPSG Break (Sheet 3 of 6)

Time (sec)	Break Flow (Reactor Vessel Side)			Break Flow (Steam Generator Side)		
	Mass (lbm/sec)	Enthalpy (Btu/lbm)	Energy (Thousand Btu/sec)	Mass (lbm/sec)	Enthalpy (Btu/lbm)	Energy (Thousand Btu/sec)
1120.7	184.4	1159.8	213.9	39.5	1179.4	46.6
1160.8	176.6	982.8	173.6	29.0	270.7	7.9
1200.8	236.0	1026.2	242.2	60.0	1038.2	62.3
1240.8	167.9	1075.9	180.6	290.0	337.9	98.0
1280.8	163.2	1029.3	168.0	125.9	271.6	34.2
1320.8	211.6	885.2	187.3	194.1	271.7	52.7
1360.8	193.7	889.7	172.3	69.7	305.1	21.3
1400.8	287.3	903.6	259.6	32.6	1180.6	38.5
1440.9	256.3	849.6	217.8	51.2	1180.5	60.4
1480.9	220.7	913.5	201.6	42.6	1146.0	48.8
1520.9	330.1	829.3	273.8	668.8	307.8	205.9
1560.9	295.8	799.8	236.6	387.0	368.2	142.5
1600.9	217.7	968.5	210.8	66.0	294.1	19.4
1641.0	215.4	913.6	196.8	27.9	1180.5	32.9
1681.0	258.7	865.0	223.8	52.0	1180.3	61.4
1721.0	232.5	837.3	194.7	12.7	1180.8	15.0
1761.0	219.7	890.0	195.5	25.4	1168.6	29.7
1801.0	215.3	921.5	198.4	0.2	269.9	0.1
1841.1	517.6	418.6	216.7	53.8	897.6	48.3
1881.1	212.3	823.0	174.7	56.1	1172.1	65.8
1921.1	178.0	907.3	161.5	8.5	1173.6	10.0
1961.1	151.5	974.9	147.7	34.9	1175.6	41.0
2001.1	943.9	275.0	259.6	93.3	1120.4	104.5
2041.2	125.8	1061.7	133.6	39.5	1175.4	46.4
2081.2	219.6	507.0	111.3	19.7	1181.2	23.3
2121.2	236.4	385.9	91.2	2.0	1179.1	2.4
2161.2	135.6	737.2	100.0	82.1	1141.7	93.7
2201.2	222.1	593.2	131.7	28.2	1181.2	33.3
2241.2	128.5	737.2	94.7	0.0	0.0	0.0
2281.3	403.6	345.1	139.3	24.2	1173.4	28.4
2321.3	387.3	359.3	139.2	27.2	1174.4	31.9
2361.3	188.5	588.3	110.9	10.6	1180.9	12.5
2401.3	162.8	596.0	97.0	1.8	1159.7	2.1
2441.3	143.6	584.1	83.9	2.9	1179.3	3.4
2481.3	133.8	685.6	91.7	25.7	1180.9	30.3
2521.4	127.5	708.1	90.3	78.1	1133.8	88.5
2561.4	234.3	436.5	102.3	22.5	1180.8	26.6

Rev. 2

Table 3-20 Break Mass and Energy Flow for the Long-term Cooling Phase of the DEPSG Break (Sheet 4 of 6)

Time (sec)	Break Flow (Reactor Vessel Side)			Break Flow (Steam Generator Side)		
	Mass (lbm/sec)	Enthalpy (Btu/lbm)	Energy (Thousand Btu/sec)	Mass (lbm/sec)	Enthalpy (Btu/lbm)	Energy (Thousand Btu/sec)
2601.4	122.7	876.1	107.5	19.3	1180.9	22.8
2641.4	329.9	376.5	124.2	26.3	1180.8	31.1
2681.4	204.7	550.3	112.6	14.1	1180.7	16.6
2721.4	201.5	552.5	111.3	14.3	1180.6	16.9
2761.4	204.5	541.2	110.7	14.8	1180.6	17.5
2801.4	201.5	541.8	109.2	14.9	1180.5	17.6
2841.4	205.6	527.7	108.5	15.0	1180.5	17.7
2881.4	203.5	528.3	107.5	14.6	1180.4	17.2
2921.5	197.6	536.8	106.1	13.7	1180.4	16.2
2961.5	304.1	373.6	113.6	24.7	1180.4	29.2
3001.6	368.9	339.3	125.2	28.2	1180.5	33.3
3201.6	152.9	648.0	99.1	22.4	1176.9	26.4
3401.9	463.1	272.3	126.1	3.5	1179.3	4.1
3602.0	294.1	408.0	120.0	34.4	1179.5	40.6
3802.1	276.8	408.2	113.0	11.6	1179.2	13.7
4002.2	208.4	441.0	91.9	20.5	1178.7	24.2
4202.4	193.7	438.0	84.8	0.0	0.0	0.0
4402.5	386.4	356.3	137.7	29.9	1178.4	35.2
4602.8	322.9	348.5	112.5	28.5	1178.3	33.6
4803.0	454.7	323.9	147.3	42.4	1177.9	49.9
5003.1	179.1	501.9	89.9	10.7	1177.5	12.6
5203.3	190.1	476.7	90.6	15.7	1177.5	18.5
5403.4	191.5	467.8	89.6	14.0	1176.4	16.5
5603.5	237.8	390.3	92.8	23.9	1175.6	28.1
5803.6	297.6	284.3	84.6	47.2	1107.3	52.3
6003.8	171.1	370.4	63.4	25.1	1176.0	29.5
6203.9	274.9	306.2	84.2	12.8	1174.6	15.0
6404.1	366.0	290.0	106.1	13.1	1176.1	15.4
6604.2	266.3	313.7	83.5	103.4	1048.9	108.5
6804.4	183.9	496.2	91.3	8.7	1176.0	10.2
7004.5	220.9	438.3	96.8	21.9	1175.9	25.8
7204.6	73.2	785.9	57.5	19.6	1175.8	23.0
7404.8	275.1	369.5	101.6	26.4	965.2	25.5
7605.0	182.9	479.9	87.8	7.7	1166.9	9.0
7805.2	211.2	370.4	78.2	0.0	0.0	0.0
8005.3	149.1	522.2	77.9	15.4	1175.2	18.1
8205.5	156.0	470.6	73.4	7.1	1174.9	8.3

Rev. 2

Table 3-20 Break Mass and Energy Flow for the Long-term Cooling Phase of the DEPSG Break (Sheet 5 of 6)

Time (sec)	Break Flow (Reactor Vessel Side)			Break Flow (Steam Generator Side)		
	Mass (lbm/sec)	Enthalpy (Btu/lbm)	Energy (Thousand Btu/sec)	Mass (lbm/sec)	Enthalpy (Btu/lbm)	Energy (Thousand Btu/sec)
8405.7	156.3	361.4	56.5	20.3	1174.9	23.9
8605.8	331.2	304.2	100.8	9.7	1174.0	11.4
8806.0	230.1	389.3	89.6	12.1	1110.4	13.4
9006.1	647.5	258.8	167.6	72.8	1173.9	85.5
9206.3	304.5	361.4	110.0	30.9	1173.8	36.3
9406.5	121.4	507.9	61.7	8.4	1165.8	9.8
9606.7	112.3	372.9	41.9	13.4	1173.9	15.7
9806.7	440.2	315.9	139.1	27.5	1173.9	32.3
10006.9	267.1	308.4	82.4	20.2	1165.8	23.5
12007.1	378.1	308.9	116.8	22.3	1172.6	26.1
14007.2	188.4	392.9	74.0	14.7	1105.2	16.2
16007.3	179.1	339.2	60.8	9.0	1159.5	10.4
18007.5	530.7	259.7	137.8	17.9	1170.1	20.9
20007.7	394.4	277.2	109.3	27.3	1164.9	31.8
22007.8	398.4	250.6	99.8	11.2	1168.0	13.1
24008.0	301.4	271.9	82.0	11.9	1068.0	12.7
26008.2	310.7	304.5	94.6	24.0	1165.8	28.0
28008.4	304.2	289.6	88.1	28.3	1139.7	32.3
30008.4	272.1	247.6	67.4	1.5	317.2	0.5
32008.6	200.9	301.6	60.6	14.2	1029.4	14.6
34008.7	40.7	580.2	23.6	0.1	218.1	0.0
36008.9	1096.6	210.1	230.4	5.6	1164.5	6.5
38009.1	76.0	581.2	44.2	8.6	1130.2	9.7
40009.3	434.7	207.5	90.2	11.3	1152.9	13.0
42009.4	128.3	366.3	47.0	4.1	1129.4	4.6
44009.6	933.0	210.4	196.3	1.7	1163.5	2.0
46009.7	0.0	0.0	0.0	26.5	894.8	23.7
48009.8	509.0	210.5	107.1	18.3	1105.4	20.2
50010.0	62.7	544.9	34.2	3.9	1162.5	4.5
52010.2	1164.9	202.6	236.0	6.9	1162.2	8.0
54010.3	394.7	206.1	81.3	24.4	1160.1	28.3
56010.5	181.1	319.0	57.8	10.1	1161.3	11.7
58010.6	259.6	205.5	53.3	12.3	1114.4	13.7
60010.9	78.5	368.4	28.9	1.8	1143.2	2.1
62011.0	297.4	204.5	60.8	7.9	1151.7	9.1
64011.2	0.0	0.0	0.0	76.2	906.3	69.1
66011.4	433.7	194.3	84.3	1.2	1160.9	1.4

Rev. 2

Table 3-20 Break Mass and Energy Flow for the Long-term Cooling Phase of the DEPSG Break (Sheet 6 of 6)

Time (sec)	Break Flow (Reactor Vessel Side)			Break Flow (Steam Generator Side)		
	Mass (lbm/sec)	Enthalpy (Btu/lbm)	Energy (Thousand Btu/sec)	Mass (lbm/sec)	Enthalpy (Btu/lbm)	Energy (Thousand Btu/sec)
68011.4	404.2	204.3	82.6	5.5	1160.9	6.4
70011.6	608.6	183.8	111.9	1.5	1160.5	1.7
72011.8	190.9	206.1	39.3	2.5	1140.8	2.9
74011.9	101.0	295.1	29.8	0.1	1140.3	0.1
76012.0	1078.9	188.1	202.9	4.8	1160.1	5.6
78012.1	475.9	185.4	88.2	1.2	1159.8	1.4
80012.2	0.0	0.0	0.0	91.0	881.2	80.2
82012.3	517.3	189.6	98.1	21.6	1159.6	25.0
84012.5	470.0	185.8	87.3	6.0	1158.6	7.0
86012.6	168.4	183.8	31.0	3.8	1159.7	4.4
88012.8	197.0	225.8	44.5	4.1	1158.5	4.7
90013.1	83.7	332.5	27.8	3.0	1156.5	3.5
92013.3	545.3	192.9	105.2	9.8	1093.7	10.7
94013.4	94.1	386.1	36.3	6.2	1158.6	7.2
96013.6	157.3	229.6	36.1	0.1	200.9	0.0
98013.8	114.7	178.1	20.4	27.6	1145.6	31.6
100000.0	410.8	182.6	75.0	3.0	949.8	2.8

Rev. 2

Table 3-21 Break Mass and Energy Flow for the Long-term Cooling Phase of the DEPSG Break (Sheet 1 of 23)

Time (sec)	Break Flow (Reactor Vessel Side)				Break Flow (Steam Generator Side)			
	Steam		Liquid		Steam		Liquid	
	Mass (lbm/sec)	Enthalpy (Btu/lbm)	Mass (lbm/sec)	Enthalpy (Btu/lbm)	Mass (lbm/sec)	Enthalpy (Btu/lbm)	Mass (lbm/sec)	Enthalpy (Btu/lbm)
266.0	81.8	1184.6	41.3	270.4	185.6	1199.1	0.6	267.6
267.0	114.2	1192.6	1263.7	277.8	465.1	1205.9	12.3	269.3
268.0	68.1	1208.8	5362.7	278.3	376.2	1204.0	183.5	269.4
269.0	52.2	1206.2	3192.5	278.5	368.1	1203.3	435.3	269.4
270.0	82.3	1232.4	2074.6	278.4	359.8	1202.8	922.2	271.7
271.0	165.4	1239.4	1581.6	279.5	248.3	1193.4	6194.5	276.5
272.0	240.4	1268.3	972.3	281.2	295.8	1187.8	6842.2	273.9
273.0	288.4	1275.1	618.9	283.8	277.2	1188.1	5117.8	271.8
274.0	318.2	1274.3	446.1	287.0	257.6	1189.3	3677.4	270.7
275.0	329.6	1272.5	340.6	290.2	299.6	1191.2	2432.6	270.7
276.0	334.6	1271.0	254.2	294.0	372.8	1191.3	2645.3	271.9
277.0	330.5	1267.4	194.0	297.2	420.6	1190.2	2980.2	272.6
278.0	312.5	1266.1	150.4	297.7	417.2	1191.0	2323.9	271.8
279.0	301.2	1269.3	206.0	280.4	399.7	1191.4	2233.7	271.7
280.0	294.4	1272.4	299.0	268.4	386.4	1191.4	2361.2	271.8
281.0	281.4	1272.6	394.0	259.9	379.8	1191.3	2313.3	271.7
282.0	264.0	1271.0	427.1	255.3	407.8	1191.7	1800.5	271.6
283.0	249.8	1269.7	334.7	255.6	556.8	1195.1	52.2	271.2
284.0	245.4	1271.2	198.4	257.0	416.6	1195.5	1066.3	272.4
285.0	237.0	1272.3	127.3	257.1	366.8	1192.6	2103.5	271.9
286.0	225.2	1273.1	87.7	256.6	353.3	1192.5	1396.3	271.1
287.0	210.9	1271.4	63.5	253.3	403.7	1194.2	614.6	270.9
288.0	211.7	1236.6	63.0	218.1	408.6	1195.8	35.8	270.1
289.0	210.3	1210.6	79.2	203.8	358.4	1196.0	413.0	271.0
290.0	199.6	1203.9	98.2	199.9	325.4	1195.5	524.4	270.4
291.0	191.2	1200.4	118.7	200.0	320.7	1195.8	398.0	270.3
292.0	179.4	1198.8	136.8	201.0	299.3	1196.0	318.5	270.1
293.0	172.9	1197.5	157.4	201.7	284.4	1196.3	259.0	270.0
294.0	168.1	1196.0	178.4	202.2	266.0	1196.7	221.3	269.9
295.0	164.9	1195.0	200.7	202.7	245.7	1196.7	289.8	269.8
296.0	160.9	1195.4	221.6	203.0	225.8	1196.7	332.8	269.8
297.0	157.2	1195.7	241.3	203.5	238.8	1196.0	370.5	269.9
298.1	153.1	1195.7	257.7	204.1	254.2	1195.7	170.2	269.9
299.1	149.0	1195.2	270.5	204.6	243.4	1196.7	5.6	269.7
300.1	145.1	1194.6	279.7	205.0	230.9	1196.7	5.5	269.6

Rev. 2

Table 3-21 Break Mass and Energy Flow for the Long-term Cooling Phase of the DEPSG Break (Sheet 2 of 23)

Time (sec)	Break Flow (Reactor Vessel Side)				Break Flow (Steam Generator Side)			
	Steam		Liquid		Steam		Liquid	
	Mass (lbm/sec)	Enthalpy (Btu/lbm)	Mass (lbm/sec)	Enthalpy (Btu/lbm)	Mass (lbm/sec)	Enthalpy (Btu/lbm)	Mass (lbm/sec)	Enthalpy (Btu/lbm)
301.1	141.6	1194.5	286.2	205.3	219.8	1196.7	5.4	269.7
302.1	138.1	1194.5	290.3	205.5	210.1	1196.7	5.2	269.6
303.1	134.8	1194.5	292.8	205.6	201.2	1196.6	4.9	269.6
304.1	131.9	1194.5	295.1	205.7	193.0	1196.5	4.6	269.6
305.1	128.9	1194.5	296.9	205.7	184.7	1196.4	4.2	269.6
306.1	126.1	1194.4	298.5	205.7	176.2	1196.4	3.6	269.7
307.1	123.4	1194.3	300.2	205.7	166.1	1196.3	24.0	269.5
308.1	121.1	1194.3	301.9	205.5	157.3	1194.5	134.3	269.5
309.1	118.2	1194.2	302.1	205.3	145.5	1194.3	103.5	269.4
310.1	116.0	1194.0	303.0	204.9	141.4	1194.4	85.3	269.4
311.1	114.9	1193.8	303.8	204.3	139.2	1194.4	69.0	269.4
312.1	114.2	1192.9	306.2	203.8	135.7	1194.5	58.6	269.3
313.1	118.6	1195.1	311.3	202.8	128.1	1194.6	42.7	269.3
314.1	120.1	1192.0	306.1	202.5	137.4	1194.4	57.0	269.3
315.1	127.0	1193.0	309.3	202.1	133.7	1194.4	50.4	269.3
316.1	129.7	1191.2	301.8	202.0	139.4	1194.2	65.1	269.4
317.1	131.2	1190.9	294.5	202.1	142.8	1194.0	68.0	269.3
318.1	131.3	1190.9	289.0	202.3	143.1	1193.8	81.5	269.3
319.1	131.2	1191.0	286.6	202.7	141.4	1193.7	76.5	269.4
320.1	131.4	1190.9	286.6	203.2	139.0	1193.6	71.9	269.3
321.1	131.6	1190.9	287.1	203.7	137.9	1193.4	89.0	269.3
322.1	131.5	1190.9	287.3	204.3	137.4	1193.2	105.3	269.3
323.1	131.1	1191.0	287.3	204.8	136.7	1193.0	110.6	269.3
324.1	130.6	1190.9	287.6	205.2	135.0	1193.0	103.7	269.3
325.1	130.3	1190.9	288.2	205.6	132.9	1192.9	94.0	269.3
326.1	130.1	1190.8	289.0	206.0	131.4	1192.8	93.8	269.3
327.1	129.8	1190.8	289.5	206.3	130.4	1192.7	100.8	269.3
328.1	129.4	1190.8	289.8	206.7	129.2	1192.5	102.2	269.3
329.1	129.0	1190.8	289.9	206.9	127.3	1192.4	97.1	269.3
330.1	128.8	1190.8	290.1	207.1	125.4	1192.4	91.9	269.2
331.1	128.6	1190.7	290.0	207.2	123.9	1192.3	90.9	269.2
332.1	128.4	1190.7	289.5	207.3	122.6	1192.1	92.6	269.2
333.1	128.2	1190.7	288.7	207.4	121.2	1192.0	92.0	269.2
334.1	127.9	1190.7	288.0	207.4	119.5	1192.0	87.3	269.2
335.1	127.7	1190.7	287.3	207.4	117.7	1191.9	81.5	269.2

Rev. 2

Table 3-21 Break Mass and Energy Flow for the Long-term Cooling Phase of the DEPSG Break (Sheet 3 of 23)

Time (sec)	Break Flow (Reactor Vessel Side)				Break Flow (Steam Generator Side)			
	Steam		Liquid		Steam		Liquid	
	Mass (lbm/sec)	Enthalpy (Btu/lbm)	Mass (lbm/sec)	Enthalpy (Btu/lbm)	Mass (lbm/sec)	Enthalpy (Btu/lbm)	Mass (lbm/sec)	Enthalpy (Btu/lbm)
336.1	127.6	1190.6	286.7	207.4	116.0	1191.8	77.1	269.2
337.1	127.4	1190.6	285.9	207.3	114.5	1191.7	74.1	269.2
338.1	127.2	1190.6	285.1	207.3	112.9	1191.7	70.3	269.1
339.1	127.0	1190.6	284.4	207.3	111.1	1191.6	65.2	269.1
340.1	126.8	1190.6	283.7	207.2	109.3	1191.5	59.8	269.1
341.1	126.6	1190.6	283.1	207.2	107.6	1191.4	55.3	269.1
342.1	126.5	1190.6	282.5	207.2	106.1	1191.3	52.2	269.1
343.1	126.3	1190.6	281.8	207.1	104.6	1191.3	48.9	269.1
344.1	126.1	1190.5	281.1	207.1	103.1	1191.2	45.4	269.1
345.1	126.0	1190.5	280.5	207.1	101.3	1191.1	41.9	269.0
346.1	125.8	1190.5	279.9	207.1	99.7	1191.0	38.9	269.0
347.1	125.7	1190.5	279.3	207.0	98.1	1191.0	36.1	269.0
348.1	125.6	1190.5	278.7	207.0	96.4	1190.9	33.3	269.0
349.1	125.5	1190.5	278.0	207.0	94.7	1190.9	30.2	269.0
350.1	125.4	1190.5	277.5	207.0	92.9	1190.8	27.4	269.0
351.1	125.3	1190.5	276.9	207.0	91.2	1190.7	24.8	269.0
352.1	125.2	1190.5	276.3	207.0	89.6	1190.7	22.4	268.9
353.1	125.2	1190.5	275.6	207.0	87.9	1190.5	20.1	269.0
354.1	125.1	1190.5	275.0	207.0	86.2	1190.5	17.8	269.0
355.1	125.1	1190.5	274.4	207.0	84.1	1190.4	15.2	268.9
356.1	125.2	1190.5	273.9	207.0	82.3	1190.4	13.7	268.9
357.1	125.2	1190.5	273.2	207.0	80.7	1190.3	12.7	268.9
358.1	125.2	1190.6	272.5	207.1	78.7	1190.2	11.6	268.9
359.1	125.3	1190.6	272.0	207.1	77.0	1190.2	10.2	268.7
360.1	125.5	1190.6	271.6	207.2	75.9	1190.1	8.9	268.9
361.1	125.6	1190.6	270.8	207.2	74.8	1190.1	7.8	269.0
362.1	125.6	1190.6	269.8	207.3	73.5	1190.0	6.8	268.7
363.1	125.5	1190.7	269.0	207.3	71.3	1189.9	5.6	268.8
364.1	125.6	1190.7	268.6	207.4	69.1	1189.8	4.4	268.9
365.1	125.8	1190.7	268.1	207.4	67.7	1189.9	3.5	268.6
366.1	125.8	1190.7	267.2	207.5	66.5	1189.8	2.9	268.9
367.1	125.7	1190.7	266.2	207.5	64.8	1189.7	2.1	268.8
368.1	125.8	1190.7	265.6	207.6	62.4	1189.7	1.2	268.0
369.1	126.0	1190.8	265.3	207.6	60.7	1189.9	0.7	269.9
370.1	126.1	1190.8	264.6	207.7	59.9	1190.1	0.5	266.5

Rev. 2

Table 3-21 Break Mass and Energy Flow for the Long-term Cooling Phase of the DEPSG Break (Sheet 4 of 23)

Time (sec)	Break Flow (Reactor Vessel Side)				Break Flow (Steam Generator Side)			
	Steam		Liquid		Steam		Liquid	
	Mass (lbm/sec)	Enthalpy (Btu/lbm)	Mass (lbm/sec)	Enthalpy (Btu/lbm)	Mass (lbm/sec)	Enthalpy (Btu/lbm)	Mass (lbm/sec)	Enthalpy (Btu/lbm)
371.1	126.0	1190.8	263.5	207.7	58.7	1190.3	0.3	274.4
372.1	125.9	1190.8	262.7	207.8	57.0	1190.4	0.0	0.0
373.1	126.2	1190.8	262.4	207.8	55.2	1190.5	0.0	0.0
374.1	126.6	1190.9	262.0	207.9	53.9	1190.5	0.0	0.0
375.1	126.5	1190.9	260.9	208.0	53.2	1190.4	0.0	0.0
376.1	126.3	1190.9	259.7	208.0	52.3	1190.4	0.0	0.0
377.1	126.3	1190.9	259.1	208.1	50.3	1190.4	0.0	0.0
378.1	126.6	1190.9	258.9	208.1	49.2	1190.3	0.0	0.0
379.1	126.8	1190.9	258.2	208.2	49.1	1190.2	0.0	0.0
380.1	126.3	1190.9	256.6	208.2	48.8	1190.2	0.0	0.0
381.1	125.8	1190.9	255.4	208.2	47.5	1190.1	0.0	0.0
382.1	125.8	1190.8	255.2	208.1	45.7	1190.0	0.0	0.0
383.1	126.7	1190.9	255.9	208.1	45.8	1190.0	0.0	0.0
384.1	127.0	1191.0	255.3	208.2	46.6	1189.9	0.0	0.0
385.1	124.7	1190.8	251.5	208.3	46.6	1189.9	0.0	0.0
386.1	122.1	1190.6	248.2	208.0	42.6	1189.8	0.0	0.0
387.1	122.6	1190.4	250.4	207.7	42.2	1189.8	0.0	0.0
388.1	124.6	1190.6	253.1	207.4	42.1	1189.7	0.0	0.0
389.1	144.0	1193.7	277.2	208.3	58.9	1189.7	0.1	273.4
390.1	155.0	1196.0	272.8	211.3	99.6	1189.2	4.3	268.6
391.1	152.6	1196.5	252.0	214.4	125.8	1187.6	94.2	268.8
392.1	152.3	1195.9	242.0	216.3	137.9	1186.2	217.1	268.8
393.1	150.6	1195.3	234.3	217.5	128.5	1185.4	347.0	268.8
394.1	143.5	1194.3	225.0	217.7	117.8	1185.3	332.5	268.7
395.1	126.8	1191.8	208.2	216.3	95.3	1186.3	51.7	268.5
396.1	125.1	1190.9	212.5	213.3	43.7	1186.7	3.2	268.4
397.1	126.8	1190.5	222.6	211.2	36.3	1187.2	0.1	280.4
398.1	127.1	1190.7	228.0	209.8	35.5	1187.7	0.0	0.0
399.1	123.2	1190.6	227.2	208.7	36.2	1188.0	0.0	0.0
400.1	112.4	1189.6	216.4	207.2	38.8	1188.3	0.0	0.0
401.1	114.7	1189.6	224.7	205.4	40.9	1188.3	0.0	0.0
402.1	132.3	1191.2	256.2	204.9	43.3	1188.5	0.0	0.0
403.1	148.3	1194.3	269.7	206.9	82.3	1188.2	1.4	267.8
404.1	159.8	1197.6	261.6	210.8	110.8	1187.8	9.1	268.6
405.1	162.6	1200.3	243.3	215.8	126.1	1186.5	112.0	268.7

Rev. 2

Table 3-21 Break Mass and Energy Flow for the Long-term Cooling Phase of the DEPSG Break (Sheet 5 of 23)

Time (sec)	Break Flow (Reactor Vessel Side)				Break Flow (Steam Generator Side)			
	Steam		Liquid		Steam		Liquid	
	Mass (lbm/sec)	Enthalpy (Btu/lbm)	Mass (lbm/sec)	Enthalpy (Btu/lbm)	Mass (lbm/sec)	Enthalpy (Btu/lbm)	Mass (lbm/sec)	Enthalpy (Btu/lbm)
406.1	149.7	1199.4	216.9	218.8	128.3	1184.9	277.4	268.7
407.1	143.8	1195.8	209.4	218.8	105.4	1185.3	191.4	268.5
408.1	140.9	1193.7	209.8	218.0	85.0	1185.9	73.0	268.5
409.2	136.7	1192.9	209.9	217.0	68.9	1186.2	21.5	268.4
410.2	125.5	1191.7	203.0	215.3	18.3	1186.5	1.9	269.0
411.2	116.4	1190.3	198.4	212.4	24.8	1186.5	0.2	262.6
412.2	119.1	1189.7	211.7	209.9	36.2	1187.1	0.0	0.0
413.2	116.8	1189.1	214.9	207.9	33.0	1187.3	0.0	0.0
414.2	112.8	1189.0	215.7	206.1	32.6	1187.6	0.0	0.0
415.2	105.9	1188.6	209.8	204.3	32.7	1187.6	0.0	0.0
416.2	121.3	1190.6	241.7	203.2	31.8	1187.7	0.0	0.0
417.2	142.0	1193.0	267.8	204.6	68.1	1187.7	0.2	265.5
418.2	156.1	1196.0	263.0	208.4	103.9	1187.1	2.9	268.7
419.2	165.1	1200.8	246.5	214.0	114.3	1186.8	25.0	268.5
420.2	155.1	1204.9	216.1	219.3	110.8	1185.5	98.2	268.6
421.2	140.7	1200.3	193.8	219.9	103.4	1184.9	110.6	268.5
422.2	151.4	1195.8	206.2	219.3	94.1	1185.1	81.5	268.5
423.2	155.7	1196.8	209.3	220.3	101.5	1184.9	111.1	268.6
424.2	141.5	1196.5	192.3	220.9	80.1	1184.6	94.2	268.4
425.2	116.6	1192.0	168.7	217.6	50.4	1185.2	15.0	268.3
426.2	117.8	1189.7	178.5	213.0	37.8	1185.5	2.0	268.6
427.2	115.2	1188.5	186.0	209.7	31.4	1185.7	0.1	272.5
428.2	112.6	1188.7	192.1	207.0	28.9	1186.2	0.0	0.0
429.2	102.8	1188.1	188.2	204.7	27.7	1186.4	0.0	0.0
430.2	105.9	1188.9	200.7	202.3	25.7	1186.6	0.0	0.0
431.2	128.1	1191.1	240.1	201.9	33.8	1186.7	0.0	0.0
432.2	142.8	1193.4	256.9	204.0	78.1	1186.7	1.0	269.7
433.2	153.2	1196.2	250.0	208.1	103.7	1186.2	3.1	268.1
434.2	164.5	1201.3	235.9	214.1	111.5	1186.0	21.7	268.5
435.2	161.1	1211.6	210.5	220.7	103.7	1185.2	66.9	268.5
436.2	139.7	1216.2	177.7	223.1	52.8	1184.7	38.6	268.1
437.2	138.3	1199.3	173.0	220.6	31.2	1185.1	5.4	268.2
438.2	136.5	1193.0	175.3	218.2	22.2	1185.2	0.9	268.0
439.2	133.3	1192.6	179.2	216.3	21.8	1185.6	0.1	263.5
440.2	113.0	1190.8	165.9	213.7	29.6	1185.9	0.0	0.0

Rev. 2

Table 3-21 Break Mass and Energy Flow for the Long-term Cooling Phase of the DEPSG Break (Sheet 6 of 23)

Time (sec)	Break Flow (Reactor Vessel Side)				Break Flow (Steam Generator Side)			
	Steam		Liquid		Steam		Liquid	
	Mass (lbm/sec)	Enthalpy (Btu/lbm)	Mass (lbm/sec)	Enthalpy (Btu/lbm)	Mass (lbm/sec)	Enthalpy (Btu/lbm)	Mass (lbm/sec)	Enthalpy (Btu/lbm)
441.2	117.9	1191.1	179.4	210.1	29.3	1186.0	0.0	0.0
442.2	136.3	1192.0	213.2	209.3	25.3	1186.3	0.0	0.0
443.2	149.7	1195.1	227.6	211.1	60.1	1186.3	0.0	0.0
444.2	162.1	1199.5	228.2	215.2	94.2	1186.2	4.0	268.3
445.2	164.9	1211.3	205.8	221.3	99.3	1185.3	35.3	268.4
446.2	142.8	1233.4	169.1	225.7	51.2	1184.7	26.8	268.2
447.2	134.3	1212.3	152.2	222.3	14.7	1185.1	2.9	268.4
448.2	134.1	1194.1	153.3	218.2	20.5	1185.1	0.5	266.0
449.3	129.6	1191.8	156.5	214.9	26.2	1185.3	0.1	266.2
450.3	130.9	1192.6	166.4	212.4	22.7	1185.7	0.0	0.0
451.3	145.9	1194.6	189.2	212.0	27.6	1185.8	0.0	0.0
452.3	159.5	1197.6	201.6	214.7	67.5	1186.0	0.0	0.0
453.3	168.3	1206.8	195.5	220.1	92.2	1185.5	16.0	268.4
454.3	143.9	1230.2	157.3	226.1	44.7	1184.8	14.2	268.3
455.3	133.8	1215.4	141.1	222.9	16.3	1185.0	1.2	267.9
456.3	136.4	1196.0	145.5	218.9	18.6	1184.9	0.2	272.0
457.3	142.1	1195.4	157.8	216.3	21.9	1185.3	0.0	0.0
458.3	159.1	1200.3	177.8	217.5	56.3	1185.6	0.1	269.5
459.3	164.7	1212.9	175.6	221.5	86.0	1185.3	13.6	268.4
460.3	160.7	1242.4	157.1	228.2	88.4	1184.4	49.1	268.3
461.3	130.3	1251.0	122.3	230.9	26.7	1184.2	13.6	268.3
462.3	134.9	1209.3	120.6	223.0	16.6	1184.5	2.2	268.4
463.3	138.1	1195.7	129.5	217.6	21.2	1184.7	0.5	266.0
464.3	160.8	1197.8	154.7	217.5	29.0	1185.0	0.1	273.1
465.3	164.8	1207.1	160.1	223.4	71.4	1185.1	2.7	268.4
466.3	138.1	1225.9	133.8	225.6	23.4	1184.8	1.7	267.7
467.3	132.6	1205.6	125.0	219.3	16.1	1185.0	0.1	267.1
468.3	134.4	1195.5	131.1	214.0	20.9	1185.1	0.0	0.0
469.3	157.7	1197.0	157.3	214.2	30.4	1185.4	0.0	0.0
470.3	166.7	1205.2	165.8	220.7	73.0	1185.3	2.2	268.5
471.3	140.9	1227.8	138.3	225.5	33.7	1184.8	2.7	267.7
472.3	132.2	1212.4	124.8	220.4	19.8	1185.0	0.1	275.0
473.3	135.4	1196.8	129.9	215.1	15.1	1185.1	0.0	0.0
474.4	160.0	1197.7	154.6	215.3	31.7	1185.3	0.0	0.0
475.4	167.6	1208.3	161.3	222.4	72.0	1185.2	2.2	267.6

Rev. 2

Table 3-21 Break Mass and Energy Flow for the Long-term Cooling Phase of the DEPSG Break (Sheet 7 of 23)

Time (sec)	Break Flow (Reactor Vessel Side)				Break Flow (Steam Generator Side)			
	Steam		Liquid		Steam		Liquid	
	Mass (lbm/sec)	Enthalpy (Btu/lbm)	Mass (lbm/sec)	Enthalpy (Btu/lbm)	Mass (lbm/sec)	Enthalpy (Btu/lbm)	Mass (lbm/sec)	Enthalpy (Btu/lbm)
476.4	140.4	1233.8	132.0	228.1	31.6	1184.6	2.6	268.4
477.4	132.1	1215.7	118.8	222.6	13.0	1185.0	0.1	276.5
478.4	137.9	1197.4	124.9	216.6	19.4	1184.9	0.0	0.0
479.4	160.0	1197.8	148.3	217.0	26.2	1185.2	0.0	0.0
480.4	165.2	1208.6	152.8	223.7	68.6	1185.2	1.1	268.4
481.4	140.8	1234.1	126.6	228.6	69.9	1184.7	8.1	268.3
482.4	139.1	1215.8	117.5	223.0	57.4	1184.5	2.3	268.6
483.4	155.1	1202.0	129.5	220.2	59.0	1184.8	0.4	268.7
484.4	171.0	1209.5	138.1	225.1	73.3	1184.6	9.5	268.1
485.4	151.2	1235.5	118.3	232.5	65.3	1184.0	24.0	268.2
486.4	127.3	1228.0	98.3	228.4	13.8	1184.0	5.5	268.1
487.4	129.4	1199.1	101.6	218.8	23.2	1184.1	1.1	268.6
488.4	144.0	1195.6	121.2	213.7	15.6	1184.1	0.2	260.5
489.4	160.1	1197.9	141.3	216.4	17.1	1184.5	0.0	0.0
490.4	163.2	1210.2	142.5	223.2	63.1	1184.7	0.6	268.3
491.4	152.8	1241.5	126.7	229.7	69.2	1184.4	6.4	268.2
492.4	140.8	1246.7	108.7	231.1	70.8	1184.1	10.9	268.2
493.4	155.3	1212.4	110.5	227.7	68.7	1184.1	7.8	268.4
494.4	170.0	1214.0	114.9	230.1	69.6	1184.1	9.6	268.3
495.4	161.8	1239.2	103.4	237.1	66.5	1183.8	16.9	268.3
496.4	131.7	1250.8	82.3	237.8	22.6	1183.6	6.2	268.1
497.4	130.1	1212.2	80.8	224.3	22.4	1183.6	1.3	268.7
498.4	134.4	1195.6	90.2	214.0	16.9	1183.5	0.6	266.6
499.4	152.4	1195.5	112.1	212.1	9.7	1183.4	0.4	269.9
500.4	166.9	1202.2	126.2	217.7	35.6	1183.6	0.7	267.4
510.4	151.0	1241.4	86.1	230.7	54.1	1182.8	225.1	268.5
520.4	158.7	1241.8	81.2	230.5	55.1	1182.5	64.1	268.4
530.4	159.0	1240.1	63.6	231.9	50.3	1182.2	80.4	268.4
540.4	152.2	1248.9	53.4	233.2	47.6	1182.2	131.0	268.5
550.4	155.3	1250.4	57.0	236.9	52.5	1181.9	196.3	268.7
560.5	155.8	1246.6	61.5	233.4	49.5	1181.9	61.4	268.6
570.5	153.4	1239.7	63.3	229.7	42.5	1181.9	51.6	268.5
580.5	153.1	1238.8	63.9	229.1	42.6	1181.6	91.2	268.5
590.5	159.3	1252.8	37.1	248.8	36.5	1181.6	67.7	268.6
600.5	155.5	1240.3	39.6	215.4	38.4	1181.1	331.2	269.1

Rev. 2

Table 3-21 Break Mass and Energy Flow for the Long-term Cooling Phase of the DEPSG Break (Sheet 8 of 23)

Time (sec)	Break Flow (Reactor Vessel Side)				Break Flow (Steam Generator Side)			
	Steam		Liquid		Steam		Liquid	
	Mass (lbm/sec)	Enthalpy (Btu/lbm)	Mass (lbm/sec)	Enthalpy (Btu/lbm)	Mass (lbm/sec)	Enthalpy (Btu/lbm)	Mass (lbm/sec)	Enthalpy (Btu/lbm)
610.5	154.3	1248.1	38.8	248.1	25.8	1181.7	5.6	268.6
620.5	163.3	1249.0	17.3	231.4	37.5	1181.4	179.0	268.8
630.5	151.3	1237.7	30.9	222.6	26.8	1181.4	6.2	268.7
640.5	157.7	1258.3	30.4	247.3	42.3	1181.3	270.7	269.0
650.5	161.7	1250.9	30.0	241.0	33.4	1181.3	9.8	268.7
660.5	154.8	1242.3	26.3	220.0	33.0	1180.9	214.3	269.0
670.5	151.6	1237.5	40.1	222.9	32.8	1180.9	119.7	268.8
680.5	160.5	1251.7	40.8	251.8	41.9	1181.0	17.0	268.9
690.5	166.0	1262.7	6.3	263.9	34.6	1180.9	316.3	269.6
700.5	155.6	1255.6	4.3	248.0	28.6	1180.9	50.3	269.0
710.5	152.3	1237.2	31.4	210.2	32.0	1180.5	126.9	269.0
720.5	163.6	1260.0	24.2	261.8	35.4	1181.0	135.1	269.4
730.5	152.4	1245.5	10.1	243.1	25.4	1180.6	159.9	269.5
740.5	160.0	1248.0	9.5	218.0	32.3	1180.8	230.5	269.4
750.5	155.0	1234.5	39.6	235.0	25.9	1180.6	3.0	269.0
760.6	161.3	1251.2	20.6	258.3	34.0	1181.1	2.8	268.9
770.6	155.4	1237.6	16.8	194.3	24.6	1180.6	474.7	269.9
780.6	145.7	1243.3	37.0	240.2	30.8	1180.8	1.4	269.3
790.6	150.6	1240.6	52.5	245.4	34.2	1180.9	2.7	269.3
800.6	153.4	1236.8	55.2	245.1	30.4	1180.9	8.9	269.4
810.6	161.7	1246.1	30.4	256.3	29.7	1180.7	142.1	269.7
820.6	154.2	1236.4	16.4	209.7	24.5	1180.4	552.3	270.0
830.6	159.9	1255.0	23.8	259.6	37.0	1180.8	13.6	269.4
840.6	145.0	1233.5	26.2	224.5	21.7	1180.4	123.5	269.5
850.6	149.6	1235.4	31.9	240.2	24.9	1180.6	0.4	270.1
860.6	158.8	1249.7	21.0	253.9	39.8	1180.8	387.9	270.0
870.6	149.4	1235.1	39.5	235.7	27.4	1180.5	0.7	269.0
880.6	150.2	1235.0	23.3	234.6	21.0	1180.6	68.4	269.6
890.6	153.1	1237.0	33.5	250.2	30.1	1180.6	214.8	269.8
900.6	151.6	1243.2	39.3	255.9	34.0	1180.4	37.6	269.6
910.6	155.5	1237.9	49.0	248.4	31.8	1180.4	52.3	269.8
920.6	148.7	1235.3	45.3	248.5	22.3	1180.3	29.2	269.7
930.6	143.4	1232.0	44.7	243.2	20.4	1180.4	0.1	271.9
940.6	160.3	1246.3	31.6	260.4	28.5	1180.8	467.6	270.5
950.7	158.1	1247.1	12.8	275.2	32.4	1180.4	44.0	270.0

Rev. 2

Table 3-21 Break Mass and Energy Flow for the Long-term Cooling Phase of the DEPSG Break (Sheet 9 of 23)

Time (sec)	Break Flow (Reactor Vessel Side)				Break Flow (Steam Generator Side)			
	Steam		Liquid		Steam		Liquid	
	Mass (lbm/sec)	Enthalpy (Btu/lbm)	Mass (lbm/sec)	Enthalpy (Btu/lbm)	Mass (lbm/sec)	Enthalpy (Btu/lbm)	Mass (lbm/sec)	Enthalpy (Btu/lbm)
960.7	161.9	1241.5	10.5	276.7	31.0	1180.4	213.6	270.3
970.7	148.0	1236.1	10.6	272.3	19.1	1180.1	209.3	270.6
980.7	150.0	1233.5	13.7	230.9	16.6	1180.9	66.5	270.1
990.7	147.8	1241.8	30.0	263.1	28.4	1180.2	12.2	269.8
1000.7	150.9	1232.7	35.5	251.3	26.4	1180.3	0.2	264.0
1010.7	157.5	1240.0	23.8	265.5	21.9	1180.7	432.1	270.6
1020.7	161.3	1236.2	29.3	256.7	36.0	1180.3	145.9	270.4
1030.7	148.8	1233.6	18.4	259.1	20.6	1180.1	66.4	270.3
1040.7	155.3	1240.8	32.2	243.9	18.2	1180.6	76.0	270.4
1050.7	159.8	1239.6	22.3	258.7	33.8	1180.2	132.2	270.5
1060.7	156.9	1241.5	3.3	264.6	27.5	1180.1	103.0	270.4
1070.7	153.9	1230.6	7.0	257.5	15.2	1180.6	525.8	271.1
1080.7	143.0	1231.8	35.5	248.9	27.2	1180.2	0.5	270.0
1090.7	147.9	1227.6	48.0	249.7	26.6	1180.2	0.1	267.3
1100.7	154.8	1236.0	13.4	266.1	20.8	1180.8	200.9	270.7
1110.7	164.0	1233.5	20.3	268.7	35.9	1180.2	119.9	270.9
1120.7	146.5	1229.1	16.9	268.8	21.3	1180.1	103.2	270.8
1130.7	158.9	1235.7	4.6	258.9	24.9	1180.6	374.1	271.1
1140.7	147.4	1221.2	35.7	245.2	30.1	1180.2	2.1	270.0
1150.7	141.5	1221.8	34.2	255.8	11.8	1179.8	26.5	270.8
1160.8	147.8	1226.4	42.3	249.0	21.0	1180.8	36.4	270.9
1170.8	144.9	1232.6	40.4	256.1	20.5	1179.9	9.6	270.4
1180.8	150.5	1233.1	54.9	246.0	23.4	1180.4	20.6	270.9
1190.8	161.3	1234.0	45.5	247.2	35.1	1180.2	83.5	271.1
1200.8	147.4	1233.0	42.2	243.6	21.0	1180.0	125.9	271.1
1210.8	163.4	1231.9	45.4	251.7	21.8	1180.3	314.2	271.5
1220.8	150.7	1231.2	43.8	242.2	18.2	1180.2	45.1	271.2
1230.8	155.7	1231.1	37.1	250.1	24.6	1180.5	82.4	271.3
1240.8	168.3	1230.9	39.3	263.8	39.2	1180.2	377.0	271.8
1250.8	151.5	1229.7	24.9	257.4	24.6	1180.2	12.8	271.4
1260.8	144.7	1226.3	30.2	256.6	16.7	1180.0	2.0	269.7
1270.8	149.9	1222.9	44.6	246.6	17.5	1180.9	131.4	271.6
1280.8	157.6	1226.2	42.3	258.7	32.6	1180.1	47.4	271.5
1290.8	149.5	1227.1	49.1	245.1	20.1	1179.9	43.4	271.5
1300.8	138.5	1217.9	55.5	249.9	14.8	1179.9	0.1	267.3

Rev. 2

Table 3-21 Break Mass and Energy Flow for the Long-term Cooling Phase of the DEPSG Break (Sheet 10 of 23)

Time (sec)	Break Flow (Reactor Vessel Side)				Break Flow (Steam Generator Side)			
	Steam		Liquid		Steam		Liquid	
	Mass (lbm/sec)	Enthalpy (Btu/lbm)	Mass (lbm/sec)	Enthalpy (Btu/lbm)	Mass (lbm/sec)	Enthalpy (Btu/lbm)	Mass (lbm/sec)	Enthalpy (Btu/lbm)
1310.8	147.2	1220.7	51.0	259.6	24.4	1180.2	0.0	0.0
1320.8	166.4	1224.4	82.1	241.2	17.2	1180.6	195.8	271.8
1330.8	161.5	1224.8	86.4	240.2	26.7	1180.2	70.4	271.8
1340.8	149.5	1223.7	57.5	241.8	20.1	1180.1	234.9	272.1
1350.8	165.1	1222.6	60.2	243.7	20.7	1180.5	116.9	272.0
1360.8	158.8	1223.1	65.6	245.6	24.4	1180.1	57.2	271.9
1370.8	154.1	1221.9	65.8	247.5	22.0	1180.1	24.9	271.9
1380.8	156.0	1220.8	66.2	241.2	7.4	1180.0	0.5	272.1
1390.9	151.1	1220.0	80.4	238.7	21.0	1180.1	0.0	0.0
1400.9	149.9	1219.9	81.7	244.1	20.9	1180.1	0.0	0.0
1410.9	149.2	1219.3	91.2	241.3	14.7	1180.1	7.3	271.6
1420.9	155.6	1218.1	95.5	239.6	18.0	1180.7	62.8	272.2
1430.9	164.9	1218.9	94.2	241.5	28.8	1180.1	70.9	272.3
1440.9	157.8	1217.2	84.6	239.5	19.7	1180.2	252.3	272.7
1450.9	161.0	1216.7	79.5	242.4	18.9	1180.2	0.0	0.0
1460.9	154.7	1216.0	80.5	241.1	19.0	1180.2	35.6	272.4
1470.9	158.8	1215.4	81.3	241.2	16.1	1180.1	1.4	271.4
1480.9	154.7	1214.6	85.9	242.1	13.1	1180.1	0.9	270.2
1490.9	150.4	1213.9	91.8	241.4	14.9	1180.4	0.1	269.0
1500.9	157.5	1213.9	98.4	242.8	19.7	1180.1	0.0	0.0
1510.9	157.0	1212.3	108.7	239.9	17.9	1180.5	45.4	272.8
1520.9	165.8	1212.8	112.0	241.4	28.8	1180.3	89.8	272.9
1530.9	162.8	1210.9	96.9	239.8	18.3	1180.5	376.9	273.3
1540.9	163.2	1210.5	78.6	243.9	16.6	1180.5	99.8	273.0
1550.9	159.0	1210.0	76.5	246.3	18.7	1180.4	20.3	272.8
1560.9	170.7	1209.8	86.8	247.1	27.1	1180.5	30.3	273.1
1570.9	160.3	1208.4	79.1	244.1	19.5	1180.4	180.1	273.2
1580.9	165.4	1208.0	77.6	245.9	18.6	1180.4	57.8	273.2
1590.9	166.6	1207.1	72.9	245.5	17.8	1180.6	172.8	273.4
1600.9	168.0	1206.2	62.3	249.5	21.4	1180.8	143.7	273.5
1611.0	168.4	1206.1	63.4	246.1	22.3	1180.4	46.4	273.4
1621.0	171.2	1205.8	62.9	248.3	26.7	1180.6	85.3	273.6
1631.0	163.2	1204.0	53.8	247.6	10.0	1180.2	106.9	273.7
1641.0	162.3	1204.3	70.0	242.3	15.3	1180.3	1.0	272.8
1651.0	157.7	1203.0	68.8	242.8	8.2	1180.8	1.0	273.7

Rev. 2

Table 3-21 Break Mass and Energy Flow for the Long-term Cooling Phase of the DEPSG Break (Sheet 11 of 23)

Time (sec)	Break Flow (Reactor Vessel Side)				Break Flow (Steam Generator Side)			
	Steam		Liquid		Steam		Liquid	
	Mass (lbm/sec)	Enthalpy (Btu/lbm)	Mass (lbm/sec)	Enthalpy (Btu/lbm)	Mass (lbm/sec)	Enthalpy (Btu/lbm)	Mass (lbm/sec)	Enthalpy (Btu/lbm)
1661.0	168.8	1203.5	77.2	244.7	29.9	1180.5	11.4	273.4
1671.0	158.5	1202.0	72.1	243.6	13.1	1180.3	64.0	273.8
1681.0	158.9	1201.5	74.6	243.7	14.7	1180.3	1.1	273.3
1691.0	162.6	1199.9	85.3	243.1	16.7	1180.9	38.5	274.0
1701.0	159.4	1200.4	82.3	243.3	18.6	1180.3	20.6	273.8
1711.0	160.6	1199.5	93.7	241.8	14.1	1180.4	0.2	275.0
1721.0	153.6	1199.2	90.3	244.5	16.3	1180.3	0.0	0.0
1731.0	155.3	1197.8	80.1	249.0	3.9	1180.6	0.0	0.0
1741.0	154.2	1198.1	78.9	251.9	10.9	1180.0	0.0	0.0
1751.0	151.6	1197.1	72.7	253.5	10.8	1180.5	0.1	275.1
1761.0	152.9	1196.6	78.7	250.5	13.3	1180.6	0.1	282.1
1771.0	160.7	1196.3	76.0	251.6	21.4	1180.4	0.1	269.1
1781.0	176.0	1195.1	60.5	246.5	35.6	1181.0	242.4	274.6
1791.0	162.8	1194.0	50.1	248.7	28.9	1180.9	30.5	274.6
1801.0	155.6	1192.7	33.8	242.4	33.1	1181.3	77.9	274.8
1811.1	134.2	1194.0	242.6	225.8	50.8	1180.9	14.9	274.8
1821.1	100.9	1189.9	278.4	230.4	28.5	1181.4	20.3	274.9
1831.1	133.0	1191.8	95.8	249.2	24.9	1180.6	0.2	266.7
1841.1	75.0	1192.8	913.1	239.9	62.0	1181.2	22.6	274.8
1851.1	130.4	1191.0	160.0	250.9	16.9	1180.8	0.7	274.5
1861.1	85.0	1189.7	397.5	252.3	48.6	1181.2	15.7	274.9
1871.1	111.0	1190.6	117.2	257.8	52.0	1181.1	8.3	274.9
1881.1	103.5	1190.2	230.8	259.7	28.4	1181.0	3.5	274.8
1891.1	126.5	1190.0	62.2	269.2	38.9	1181.1	3.0	274.8
1901.1	130.0	1189.4	55.4	267.0	24.4	1181.1	0.2	276.8
1911.1	129.3	1188.9	54.4	262.3	22.8	1181.1	0.1	274.5
1921.1	127.7	1188.6	53.2	259.5	20.7	1181.1	0.1	272.3
1931.1	125.2	1188.3	51.3	256.5	19.1	1181.1	0.1	279.2
1941.1	124.2	1188.3	45.1	254.9	20.7	1181.1	0.1	270.5
1951.1	121.9	1188.2	28.3	255.3	19.2	1181.1	0.1	280.7
1961.1	116.5	1188.0	27.7	245.0	18.9	1181.1	0.1	270.4
1971.1	105.8	1187.6	58.9	233.1	21.9	1181.1	1.1	275.0
1981.1	52.8	1188.7	595.3	224.5	66.6	1181.3	7.8	275.0
1991.1	70.5	1183.2	179.6	226.7	9.7	1180.4	0.0	0.0
2001.1	33.6	1187.1	1126.6	240.1	55.2	1181.3	6.9	274.8

Rev. 2

Table 3-21 Break Mass and Energy Flow for the Long-term Cooling Phase of the DEPSG Break (Sheet 12 of 23)

Time (sec)	Break Flow (Reactor Vessel Side)				Break Flow (Steam Generator Side)			
	Steam		Liquid		Steam		Liquid	
	Mass (lbm/sec)	Enthalpy (Btu/lbm)	Mass (lbm/sec)	Enthalpy (Btu/lbm)	Mass (lbm/sec)	Enthalpy (Btu/lbm)	Mass (lbm/sec)	Enthalpy (Btu/lbm)
2011.2	80.1	1186.9	353.8	243.8	50.6	1181.3	1.5	274.8
2021.2	105.3	1187.2	64.2	257.1	22.5	1181.2	0.2	274.2
2031.2	106.2	1187.0	41.1	263.6	20.0	1181.2	0.0	0.0
2041.2	105.5	1186.9	25.3	265.4	22.3	1181.2	0.0	0.0
2051.2	103.3	1186.8	18.2	264.7	22.9	1181.2	0.1	273.2
2061.2	94.7	1184.7	23.2	254.7	21.0	1181.2	0.2	274.3
2071.2	84.2	1184.0	79.7	232.5	20.0	1181.3	0.4	275.1
2081.2	58.7	1184.2	232.5	221.2	42.2	1181.2	1.9	274.5
2091.2	74.8	1183.2	102.9	217.7	30.8	1181.2	0.2	273.2
2101.2	85.3	1186.3	63.9	231.4	22.9	1181.2	0.0	0.0
2111.2	75.2	1184.1	127.2	230.6	18.5	1181.0	0.2	275.6
2121.2	48.7	1183.0	393.0	225.3	37.9	1181.2	2.7	274.5
2131.2	33.2	1183.0	745.7	232.7	46.2	1181.1	3.7	274.3
2141.2	64.4	1184.9	308.8	237.6	30.6	1181.3	0.0	0.0
2151.2	77.5	1183.7	126.7	243.3	18.6	1181.2	0.0	0.0
2161.2	74.3	1183.0	101.5	235.3	38.2	1181.2	1.1	274.4
2171.2	63.2	1181.9	175.4	223.6	31.4	1181.1	0.7	273.8
2181.2	58.3	1182.7	256.5	224.0	34.2	1181.2	0.9	274.2
2191.2	65.1	1182.9	182.2	232.6	27.3	1181.1	0.4	274.5
2201.2	64.6	1183.3	263.3	235.4	31.2	1181.2	0.4	274.2
2211.2	69.0	1183.7	157.1	235.3	29.4	1181.2	0.6	273.9
2221.2	67.7	1183.2	228.5	231.0	38.1	1181.1	0.9	273.5
2231.2	63.2	1185.0	251.1	230.5	32.9	1181.2	1.1	273.9
2241.2	69.0	1185.0	167.6	229.7	45.3	1181.1	2.2	273.9
2251.3	50.6	1185.2	292.6	227.8	44.1	1181.1	1.7	273.6
2261.3	50.7	1185.9	366.7	230.3	30.0	1181.1	0.1	276.3
2271.3	72.9	1184.7	113.6	238.8	25.2	1181.1	0.1	273.0
2281.3	65.5	1183.8	121.1	235.6	20.2	1181.1	0.5	273.9
2291.3	37.9	1185.3	670.5	230.1	52.4	1181.0	2.2	273.4
2301.3	61.3	1184.1	200.7	234.1	27.8	1181.2	0.1	271.9
2311.3	72.9	1184.6	64.8	243.4	26.0	1181.1	0.0	0.0
2321.3	63.1	1183.2	69.4	240.2	19.6	1181.0	0.8	273.1
2331.3	27.7	1185.7	878.0	233.0	55.3	1181.0	2.2	273.3
2341.3	64.2	1184.2	269.3	235.8	27.6	1181.1	0.0	0.0
2351.3	75.8	1184.2	57.7	246.2	27.7	1181.1	0.2	272.1

Rev. 2

Table 3-21 Break Mass and Energy Flow for the Long-term Cooling Phase of the DEPSG Break (Sheet 13 of 23)

Time (sec)	Break Flow (Reactor Vessel Side)				Break Flow (Steam Generator Side)			
	Steam		Liquid		Steam		Liquid	
	Mass (lbm/sec)	Enthalpy (Btu/lbm)	Mass (lbm/sec)	Enthalpy (Btu/lbm)	Mass (lbm/sec)	Enthalpy (Btu/lbm)	Mass (lbm/sec)	Enthalpy (Btu/lbm)
2361.3	72.1	1184.2	119.8	236.4	26.8	1181.0	0.1	271.2
2371.3	67.1	1184.4	140.3	232.9	27.6	1181.1	0.1	275.9
2381.3	67.4	1184.2	102.6	234.3	29.8	1181.0	0.5	273.0
2391.3	48.3	1184.2	266.2	229.6	46.8	1181.0	1.4	273.0
2401.3	46.6	1184.5	270.5	230.8	36.8	1181.0	0.7	273.0
2411.3	59.1	1184.3	208.6	232.9	31.8	1181.0	0.5	272.7
2421.3	61.9	1184.2	229.2	231.6	32.4	1181.0	0.5	273.0
2431.3	62.3	1183.9	220.4	229.0	30.0	1181.0	0.4	273.1
2441.3	61.3	1183.8	134.5	229.5	30.0	1181.0	0.5	272.0
2451.3	50.1	1184.4	299.8	228.1	45.2	1180.9	1.2	272.8
2461.3	53.2	1184.0	174.3	229.1	32.6	1181.0	0.5	272.6
2471.3	57.7	1184.0	232.7	228.8	30.9	1180.9	0.3	272.7
2481.3	60.9	1184.1	215.5	227.5	33.6	1181.0	0.1	271.2
2491.4	54.1	1182.9	165.7	229.8	20.4	1180.8	0.0	0.0
2501.4	30.0	1183.6	610.5	228.2	46.6	1180.9	1.7	272.3
2511.4	52.3	1183.5	216.2	232.3	33.0	1180.9	0.1	276.0
2521.4	68.5	1183.4	77.1	238.0	30.0	1181.0	0.3	272.3
2531.4	47.1	1182.6	292.7	232.9	16.4	1180.4	0.1	273.0
2541.4	29.5	1183.4	590.9	232.6	48.3	1180.9	1.6	272.2
2551.4	63.9	1183.0	118.8	237.5	19.7	1180.9	0.0	0.0
2561.4	63.4	1183.2	166.3	236.1	28.0	1180.9	0.1	270.6
2571.4	35.0	1183.9	278.8	233.5	42.9	1180.8	1.1	272.4
2581.4	43.8	1183.9	341.1	238.0	38.3	1180.8	2.2	272.0
2591.4	57.2	1183.9	76.0	238.0	33.0	1180.8	0.0	0.0
2601.4	74.7	1183.5	42.8	235.3	20.4	1180.9	0.0	0.0
2611.4	81.7	1182.9	32.9	233.1	19.3	1180.8	0.0	0.0
2621.4	79.3	1183.1	17.5	232.3	20.6	1180.9	0.0	0.0
2631.4	75.1	1183.2	51.7	208.7	22.0	1180.8	0.0	0.0
2641.4	66.1	1183.3	208.2	205.1	24.8	1180.8	0.0	0.0
2651.4	67.2	1183.3	206.0	204.1	26.1	1180.7	0.0	0.0
2661.4	64.5	1183.3	222.6	202.3	27.1	1180.8	0.0	0.0
2671.4	69.1	1183.0	268.6	201.1	24.4	1180.7	0.0	0.0
2681.4	70.7	1182.8	220.0	200.4	22.1	1180.8	0.0	0.0
2691.4	67.5	1182.9	238.1	199.8	24.5	1180.7	0.0	0.0
2701.4	67.5	1183.1	249.3	199.3	27.9	1180.7	0.0	0.0

Rev. 2

Table 3-21 Break Mass and Energy Flow for the Long-term Cooling Phase of the DEPSG Break (Sheet 14 of 23)

Time (sec)	Break Flow (Reactor Vessel Side)				Break Flow (Steam Generator Side)			
	Steam		Liquid		Steam		Liquid	
	Mass (lbm/sec)	Enthalpy (Btu/lbm)	Mass (lbm/sec)	Enthalpy (Btu/lbm)	Mass (lbm/sec)	Enthalpy (Btu/lbm)	Mass (lbm/sec)	Enthalpy (Btu/lbm)
2711.4	68.8	1182.8	232.9	198.8	25.0	1180.7	0.0	0.0
2721.4	69.4	1182.8	213.3	198.3	22.4	1180.6	0.0	0.0
2731.4	67.0	1182.8	228.6	197.7	24.3	1180.7	0.0	0.0
2741.4	67.0	1183.0	249.6	197.4	28.0	1180.6	0.0	0.0
2751.4	67.9	1182.8	234.8	197.1	24.8	1180.6	0.0	0.0
2761.4	68.2	1182.8	212.8	197.0	22.6	1180.6	0.0	0.0
2771.4	65.8	1182.7	229.2	196.7	24.5	1180.6	0.0	0.0
2781.4	65.9	1182.9	248.7	196.5	27.9	1180.6	0.0	0.0
2791.4	67.0	1182.7	237.8	196.3	24.6	1180.6	0.0	0.0
2801.4	67.2	1182.7	216.9	196.2	22.5	1180.5	0.0	0.0
2811.4	64.6	1182.6	233.2	196.1	24.7	1180.6	0.0	0.0
2821.4	64.6	1182.9	251.7	196.1	28.1	1180.5	0.0	0.0
2831.4	65.9	1182.7	239.3	196.0	24.6	1180.6	0.0	0.0
2841.4	66.4	1182.5	218.5	195.9	22.3	1180.5	0.0	0.0
2851.4	63.7	1182.6	236.5	195.9	24.6	1180.5	0.0	0.0
2861.4	63.7	1182.8	252.2	195.9	28.2	1180.5	0.0	0.0
2871.4	64.8	1182.6	239.2	195.9	24.8	1180.5	0.0	0.0
2881.4	65.2	1182.5	217.7	195.9	22.5	1180.5	0.0	0.0
2891.5	63.0	1182.5	234.0	195.9	24.4	1180.5	0.0	0.0
2901.5	62.6	1182.6	256.5	195.9	28.1	1180.5	0.0	0.0
2911.5	63.7	1182.5	244.0	195.9	24.9	1180.4	0.0	0.0
2921.5	64.2	1182.3	222.1	196.0	22.5	1180.5	0.0	0.0
2931.5	61.7	1182.4	237.5	196.0	24.7	1180.4	0.0	0.0
2941.5	62.5	1182.6	247.3	196.0	26.9	1180.4	0.0	0.0
2951.5	63.8	1182.3	235.4	196.0	23.9	1180.4	0.0	0.0
2961.5	62.3	1182.3	229.7	196.0	22.7	1180.4	0.0	0.0
2971.5	60.5	1182.5	243.2	196.1	25.7	1180.5	0.0	0.0
2981.5	62.3	1182.4	257.5	196.2	27.1	1180.5	0.0	0.0
2991.5	62.7	1182.3	226.4	196.2	21.7	1180.5	0.0	0.0
3001.6	61.3	1182.3	231.2	196.3	23.9	1180.6	0.0	0.0
3051.6	33.6	1182.6	441.1	211.2	29.7	1180.3	2.5	270.1
3101.6	26.4	1182.7	498.5	235.0	28.7	1180.3	0.7	269.7
3151.6	65.7	1181.8	21.8	245.2	19.1	1180.2	0.0	0.0
3201.7	45.3	1181.8	114.5	232.7	28.6	1180.1	0.2	270.0
3251.7	56.0	1181.4	210.1	220.4	23.7	1180.1	0.0	0.0

Rev. 2

Table 3-21 Break Mass and Energy Flow for the Long-term Cooling Phase of the DEPSG Break (Sheet 15 of 23)

Time (sec)	Break Flow (Reactor Vessel Side)				Break Flow (Steam Generator Side)			
	Steam		Liquid		Steam		Liquid	
	Mass (lbm/sec)	Enthalpy (Btu/lbm)	Mass (lbm/sec)	Enthalpy (Btu/lbm)	Mass (lbm/sec)	Enthalpy (Btu/lbm)	Mass (lbm/sec)	Enthalpy (Btu/lbm)
3301.7	52.9	1181.7	246.4	224.6	23.2	1180.0	0.1	269.0
3351.8	58.0	1181.3	219.7	210.8	23.8	1180.0	0.0	0.0
3401.9	38.6	1181.6	266.3	219.2	17.2	1179.8	0.6	268.0
3451.9	32.2	1181.7	510.7	241.1	33.7	1179.8	1.5	267.9
3502.0	35.8	1181.3	263.4	243.0	37.1	1179.7	0.9	267.4
3552.0	54.5	1181.0	87.1	241.1	22.0	1179.7	0.0	0.0
3602.0	56.1	1180.8	132.0	227.4	22.6	1179.6	0.0	0.0
3652.0	54.3	1180.6	235.6	212.5	23.1	1179.6	0.0	0.0
3702.1	40.4	1180.8	292.1	217.9	30.7	1179.4	0.6	266.7
3752.1	48.8	1180.5	259.6	222.0	25.4	1179.3	0.5	266.6
3802.1	53.8	1180.5	232.4	213.6	23.5	1179.4	0.0	0.0
3852.1	42.3	1180.3	317.9	213.8	27.3	1179.2	0.6	266.0
3902.1	38.4	1180.8	296.0	227.7	25.7	1179.2	0.4	266.1
3952.2	54.0	1180.4	177.6	218.6	21.9	1179.2	0.0	0.0
4002.3	49.1	1180.1	251.0	216.4	22.3	1179.0	0.1	268.6
4052.3	51.2	1180.2	234.9	214.6	21.8	1179.0	0.3	265.0
4102.3	39.3	1181.2	321.4	217.0	27.2	1178.9	2.1	264.8
4152.3	40.8	1180.8	277.4	226.0	26.2	1178.8	0.9	264.8
4202.4	39.0	1179.9	235.3	229.8	24.0	1178.7	0.3	264.6
4252.4	41.8	1179.8	246.5	229.3	26.3	1178.7	0.3	264.2
4302.5	44.6	1179.8	238.4	228.3	23.6	1178.7	0.1	264.8
4352.5	49.9	1179.7	246.2	221.1	22.1	1178.6	0.1	264.1
4402.5	49.8	1179.7	235.3	216.9	21.3	1178.5	0.0	0.0
4452.6	50.7	1179.6	262.1	215.1	21.4	1178.5	0.0	0.0
4502.6	47.2	1179.5	233.7	216.1	23.6	1178.4	0.5	263.3
4552.7	36.1	1179.9	295.3	222.1	26.1	1178.3	2.1	263.1
4602.8	42.5	1179.8	246.0	225.9	23.4	1178.3	0.4	263.3
4652.8	43.0	1179.9	260.2	221.0	22.3	1178.2	1.5	262.4
4702.8	39.5	1179.9	285.4	229.1	21.6	1178.1	0.3	262.7
4752.9	39.8	1180.1	252.0	230.4	27.7	1178.1	1.6	262.4
4803.0	47.6	1179.2	229.3	222.5	22.2	1178.1	0.1	262.3
4853.0	46.4	1179.1	232.8	219.6	21.2	1178.0	0.2	261.7
4903.0	46.2	1179.1	288.7	218.5	23.0	1178.0	0.2	262.1
4953.1	48.0	1178.9	254.0	217.0	22.2	1178.0	0.0	0.0
5003.1	49.8	1178.9	239.5	216.1	19.9	1177.8	0.0	0.0

Rev. 2

Table 3-21 Break Mass and Energy Flow for the Long-term Cooling Phase of the DEPSG Break (Sheet 16 of 23)

Time (sec)	Break Flow (Reactor Vessel Side)				Break Flow (Steam Generator Side)			
	Steam		Liquid		Steam		Liquid	
	Mass (lbm/sec)	Enthalpy (Btu/lbm)	Mass (lbm/sec)	Enthalpy (Btu/lbm)	Mass (lbm/sec)	Enthalpy (Btu/lbm)	Mass (lbm/sec)	Enthalpy (Btu/lbm)
5053.2	47.4	1179.0	240.6	215.6	21.1	1177.8	0.0	0.0
5103.2	43.2	1178.7	285.2	218.8	17.4	1177.6	0.3	261.8
5153.3	47.4	1178.8	242.8	222.0	18.4	1177.5	0.1	261.9
5203.3	46.2	1178.7	261.1	218.7	23.3	1177.6	0.7	261.0
5253.3	41.5	1178.8	257.7	219.1	22.1	1177.6	0.4	260.1
5303.3	34.0	1179.5	294.4	226.2	24.5	1177.5	1.7	260.6
5353.4	43.6	1178.5	251.2	228.0	19.8	1177.3	0.0	0.0
5403.4	47.9	1178.5	223.9	221.9	20.5	1177.5	0.0	0.0
5453.5	43.7	1178.5	262.4	219.4	20.9	1177.4	0.0	0.0
5503.5	43.4	1178.4	268.1	223.1	19.8	1177.3	0.2	259.4
5553.5	41.1	1178.4	276.7	221.1	22.9	1177.3	0.6	259.8
5603.5	46.6	1178.3	237.4	221.1	19.4	1177.2	0.0	0.0
5653.5	42.6	1178.3	263.9	220.1	20.6	1177.1	0.0	0.0
5703.5	33.8	1178.1	284.3	225.9	25.2	1177.0	1.5	259.2
5753.5	43.5	1178.1	215.1	225.2	20.0	1177.2	0.3	259.5
5803.6	36.5	1178.1	297.7	225.4	24.4	1177.0	1.7	258.7
5853.7	39.3	1178.0	250.4	228.8	20.0	1176.9	0.6	258.8
5903.7	36.6	1178.0	270.7	231.5	23.8	1177.0	1.1	258.6
5953.8	40.3	1178.0	252.1	227.8	21.6	1176.9	0.2	258.4
6003.8	46.6	1177.8	230.1	222.7	17.6	1176.8	0.0	0.0
6053.8	31.4	1178.2	364.6	224.9	23.9	1176.7	1.0	258.2
6103.9	44.2	1177.9	197.9	231.0	19.6	1176.8	0.0	0.0
6153.9	44.5	1177.8	232.2	223.9	19.8	1176.8	0.0	0.0
6203.9	39.5	1177.6	275.2	222.7	19.5	1176.7	0.2	257.7
6254.0	28.5	1177.5	316.7	230.8	25.2	1176.6	1.7	257.5
6304.1	36.2	1178.2	272.3	234.1	23.1	1176.6	0.5	257.1
6354.1	44.6	1177.5	219.2	228.2	19.0	1176.6	0.0	0.0
6404.1	41.3	1177.4	251.3	224.2	18.3	1176.5	0.0	0.0
6454.1	30.8	1177.9	352.8	231.4	25.6	1176.3	1.5	257.0
6504.1	45.8	1177.4	169.0	228.4	18.8	1176.5	0.0	0.0
6554.1	44.4	1177.3	218.4	223.8	17.8	1176.3	0.0	0.0
6604.2	36.2	1177.3	298.2	224.5	21.4	1176.3	1.0	256.6
6654.3	37.8	1177.3	278.4	228.4	21.6	1176.1	1.0	256.1
6704.3	41.3	1177.2	254.0	224.7	17.1	1176.2	0.0	0.0
6754.3	35.6	1177.3	291.2	225.6	23.9	1176.2	1.2	256.2

Rev. 2

Table 3-21 Break Mass and Energy Flow for the Long-term Cooling Phase of the DEPSG Break (Sheet 17 of 23)

Time (sec)	Break Flow (Reactor Vessel Side)				Break Flow (Steam Generator Side)			
	Steam		Liquid		Steam		Liquid	
	Mass (lbm/sec)	Enthalpy (Btu/lbm)	Mass (lbm/sec)	Enthalpy (Btu/lbm)	Mass (lbm/sec)	Enthalpy (Btu/lbm)	Mass (lbm/sec)	Enthalpy (Btu/lbm)
6804.4	42.4	1177.3	246.3	229.2	17.3	1176.1	0.1	255.7
6854.4	43.7	1177.1	237.4	224.6	18.4	1176.1	0.0	0.0
6904.4	38.5	1177.1	258.7	223.3	20.0	1176.1	0.7	255.9
6954.4	32.5	1177.5	343.3	229.4	22.1	1175.9	1.8	255.4
7004.5	43.9	1177.1	190.0	228.5	18.4	1176.0	0.0	0.0
7054.6	41.7	1176.9	225.0	224.7	18.1	1175.9	0.0	0.0
7104.6	32.4	1176.9	303.9	227.4	22.6	1175.8	0.9	255.3
7154.6	18.0	1177.2	564.5	235.4	25.8	1175.8	2.3	255.0
7204.7	45.4	1176.8	49.8	241.7	19.7	1175.7	0.2	254.7
7254.7	43.4	1176.8	157.7	228.7	17.5	1175.8	0.0	0.0
7304.7	41.6	1176.6	231.8	225.2	18.3	1175.8	0.0	0.0
7354.8	32.2	1176.6	302.3	226.9	20.2	1175.7	0.8	254.6
7404.8	35.3	1176.6	350.4	228.9	23.9	1175.6	1.8	254.4
7454.8	39.1	1176.6	224.5	227.9	19.7	1175.7	0.2	254.4
7504.8	41.1	1176.6	253.5	224.8	17.4	1175.5	0.0	0.0
7554.9	32.1	1176.6	362.0	226.4	20.3	1175.5	1.2	254.1
7605.0	39.2	1176.5	191.3	231.4	20.3	1175.6	0.6	254.0
7655.0	41.4	1176.4	235.9	226.1	17.0	1175.3	0.0	0.0
7705.1	36.8	1176.3	285.4	225.9	19.2	1175.3	0.8	253.7
7755.2	40.7	1176.4	261.9	226.7	18.4	1175.4	0.0	0.0
7805.2	39.9	1176.3	261.8	224.3	18.3	1175.4	0.0	0.0
7855.2	36.0	1176.3	272.9	225.7	21.3	1175.3	1.2	253.4
7905.2	32.1	1176.4	269.5	227.0	23.4	1175.2	3.1	253.1
7955.3	33.6	1176.4	250.2	229.0	21.1	1175.3	1.2	253.2
8005.3	34.8	1176.2	273.5	227.2	22.4	1175.2	1.0	253.0
8055.3	27.9	1176.6	292.1	230.4	22.5	1175.2	2.1	252.9
8105.4	33.0	1176.3	279.6	232.3	20.4	1175.1	1.4	252.8
8155.5	40.3	1176.4	210.9	232.3	17.5	1175.0	0.0	0.0
8205.5	39.9	1176.1	226.9	226.6	17.4	1175.0	0.0	0.0
8255.6	34.1	1175.9	291.0	227.2	16.9	1175.0	0.1	253.3
8305.6	29.1	1176.5	344.1	231.7	24.5	1175.0	3.9	252.3
8355.6	33.0	1176.4	263.2	233.3	21.3	1175.0	1.6	252.1
8405.7	32.5	1176.2	210.8	233.8	22.4	1175.0	1.8	252.1
8455.7	30.4	1176.0	292.5	232.7	21.9	1174.9	1.2	252.0
8505.7	25.7	1175.7	342.5	235.8	25.8	1174.9	1.6	251.8

Rev. 2

Table 3-21 Break Mass and Energy Flow for the Long-term Cooling Phase of the DEPSG Break (Sheet 18 of 23)

Time (sec)	Break Flow (Reactor Vessel Side)				Break Flow (Steam Generator Side)			
	Steam		Liquid		Steam		Liquid	
	Mass (lbm/sec)	Enthalpy (Btu/lbm)	Mass (lbm/sec)	Enthalpy (Btu/lbm)	Mass (lbm/sec)	Enthalpy (Btu/lbm)	Mass (lbm/sec)	Enthalpy (Btu/lbm)
8555.8	35.0	1175.8	210.5	233.3	21.2	1174.9	0.6	251.7
8605.9	28.0	1175.8	313.0	232.6	21.6	1174.8	1.4	251.6
8655.9	35.4	1175.8	214.5	235.9	20.3	1174.7	0.3	251.4
8706.0	39.4	1175.6	243.6	228.7	17.4	1174.8	0.0	0.0
8756.0	37.7	1175.6	262.5	226.2	16.3	1174.6	0.0	0.0
8806.0	38.1	1175.5	281.6	225.7	17.0	1174.7	0.1	251.6
8856.0	38.8	1175.5	269.9	225.1	16.6	1174.5	0.1	251.3
8906.1	34.6	1175.5	268.5	226.6	17.9	1174.4	0.8	250.9
8956.1	29.7	1175.5	280.2	231.4	22.4	1174.5	1.2	250.9
9006.1	32.6	1175.5	309.5	230.5	18.5	1174.5	0.6	250.8
9056.2	35.4	1175.7	222.8	232.6	21.7	1174.4	0.9	250.7
9106.2	38.8	1175.4	231.0	227.2	16.9	1174.5	0.0	0.0
9156.2	35.2	1175.4	271.3	225.5	17.3	1174.4	0.0	0.0
9206.3	28.2	1175.7	330.8	230.2	23.3	1174.5	2.1	250.4
9256.4	40.1	1175.3	212.3	227.8	16.0	1174.3	0.0	0.0
9306.4	37.8	1175.3	263.5	225.3	16.6	1174.3	0.0	0.0
9356.4	29.8	1175.2	313.4	227.1	23.2	1174.3	2.0	250.2
9406.5	30.0	1175.2	272.3	231.4	20.1	1174.3	0.8	249.9
9456.5	31.6	1175.2	264.8	229.3	20.9	1174.2	1.5	249.9
9506.5	27.8	1175.4	287.5	234.1	19.4	1174.2	1.0	249.6
9556.6	39.5	1175.1	217.9	230.2	17.3	1174.2	0.0	0.0
9606.7	36.1	1175.1	253.0	226.4	16.9	1174.1	0.0	0.0
9656.7	29.3	1175.1	307.2	228.7	20.5	1174.1	1.6	249.6
9706.7	33.6	1175.0	228.5	230.7	18.4	1174.0	0.6	249.1
9756.7	27.5	1175.5	299.2	230.7	23.2	1174.0	1.5	248.9
9806.7	37.5	1175.0	259.2	229.2	16.7	1174.0	0.2	249.1
9856.8	38.4	1174.8	236.0	225.8	17.0	1174.0	0.0	0.0
9906.8	32.2	1174.9	316.7	225.6	18.3	1173.9	1.3	249.2
9956.9	27.1	1174.9	302.6	230.9	20.7	1174.0	0.7	248.8
10006.9	23.7	1175.3	349.8	235.4	23.1	1173.9	2.7	248.7
10507.0	32.5	1174.8	260.3	229.6	19.0	1173.7	0.7	248.2
11007.0	32.3	1174.5	270.3	227.5	18.2	1173.5	1.0	247.3
11507.1	32.3	1174.2	270.3	226.8	17.7	1173.2	0.7	246.5
12007.1	30.6	1173.9	272.2	227.3	18.7	1172.9	1.1	245.8
12507.1	29.4	1173.8	277.1	228.1	18.3	1172.7	1.1	244.9

Rev. 2

Table 3-21 Break Mass and Energy Flow for the Long-term Cooling Phase of the DEPSG Break (Sheet 19 of 23)

Time (sec)	Break Flow (Reactor Vessel Side)				Break Flow (Steam Generator Side)			
	Steam		Liquid		Steam		Liquid	
	Mass (lbm/sec)	Enthalpy (Btu/lbm)	Mass (lbm/sec)	Enthalpy (Btu/lbm)	Mass (lbm/sec)	Enthalpy (Btu/lbm)	Mass (lbm/sec)	Enthalpy (Btu/lbm)
13007.1	31.0	1173.5	271.5	224.8	17.5	1172.4	0.8	244.0
13507.1	28.2	1173.3	282.6	226.4	18.1	1172.2	1.4	243.3
14007.2	28.6	1173.0	274.9	225.4	17.9	1172.0	1.1	242.6
14507.2	27.0	1172.9	278.1	226.8	18.1	1171.7	1.4	241.8
15007.2	26.5	1172.6	273.9	227.3	18.0	1171.5	1.3	241.0
15507.3	27.2	1172.3	280.0	223.5	17.4	1171.3	1.2	240.3
16007.3	27.5	1172.1	271.5	223.2	17.1	1171.1	1.0	239.7
16507.4	25.2	1171.9	290.1	222.9	17.5	1170.9	1.4	239.1
17007.4	26.9	1171.7	272.3	220.2	16.8	1170.7	1.1	238.4
17507.4	26.7	1171.5	273.7	220.2	16.2	1170.4	1.0	237.8
18007.5	23.5	1171.4	288.5	223.0	17.4	1170.3	1.8	237.2
18507.6	24.2	1171.1	279.4	222.1	17.3	1170.1	1.4	236.4
19007.6	25.5	1170.9	282.8	217.1	16.3	1169.8	1.5	235.9
19507.7	23.4	1170.8	289.7	220.1	16.4	1169.6	1.3	235.3
20007.7	25.0	1170.4	263.0	219.9	16.1	1169.5	1.2	234.7
20507.7	23.9	1170.4	302.8	214.5	16.0	1169.3	1.5	234.1
21007.8	21.9	1170.2	279.3	218.6	17.2	1169.2	1.8	233.6
21507.8	22.9	1170.0	285.0	216.1	16.0	1168.9	1.3	233.0
22007.8	21.5	1169.9	300.2	216.6	16.9	1168.8	2.2	232.4
22507.9	24.4	1169.6	273.7	215.1	14.4	1168.6	1.0	231.9
23008.0	22.0	1169.5	291.1	214.4	16.0	1168.5	2.0	231.5
23508.0	23.6	1169.3	263.6	216.0	14.5	1168.3	1.2	230.8
24008.0	22.6	1169.1	284.3	210.5	15.7	1168.1	2.0	230.6
24508.1	22.4	1169.0	294.3	215.4	13.8	1167.9	1.6	230.1
25008.1	21.8	1168.9	291.7	210.5	15.2	1167.8	2.0	229.6
25508.1	20.8	1168.8	292.7	210.7	15.9	1167.7	2.3	229.2
26008.2	20.3	1168.6	286.6	214.4	15.4	1167.6	2.0	228.6
26508.3	19.6	1168.5	291.7	210.8	16.3	1167.4	2.6	228.3
27008.4	20.3	1168.3	270.9	210.0	16.1	1167.3	2.0	227.9
27508.4	20.6	1168.1	297.0	206.6	15.1	1167.1	2.1	227.6
28008.4	20.8	1168.1	285.6	205.5	15.4	1167.0	2.0	227.2
28508.4	22.0	1167.9	281.7	205.0	13.7	1166.9	2.1	226.8
29008.4	20.8	1167.9	299.8	203.8	13.9	1166.7	2.2	226.5
29508.4	20.1	1167.7	304.9	203.1	15.3	1166.7	2.6	226.1
30008.4	21.8	1167.5	264.2	200.8	13.9	1166.6	2.1	225.8

Rev. 2

Table 3-21 Break Mass and Energy Flow for the Long-term Cooling Phase of the DEPSG Break (Sheet 20 of 23)

Time (sec)	Break Flow (Reactor Vessel Side)				Break Flow (Steam Generator Side)			
	Steam		Liquid		Steam		Liquid	
	Mass (lbm/sec)	Enthalpy (Btu/lbm)	Mass (lbm/sec)	Enthalpy (Btu/lbm)	Mass (lbm/sec)	Enthalpy (Btu/lbm)	Mass (lbm/sec)	Enthalpy (Btu/lbm)
30508.5	20.3	1167.5	311.2	202.2	13.8	1166.4	2.0	225.4
31008.5	20.4	1167.3	271.7	204.6	14.1	1166.3	2.1	225.0
31508.5	18.4	1167.2	299.5	203.2	15.3	1166.2	2.4	224.8
32008.6	18.0	1167.0	289.0	202.7	15.2	1166.1	2.5	224.4
32508.6	20.4	1166.9	281.8	199.6	13.6	1166.0	2.2	224.0
33008.6	17.9	1167.0	328.9	203.7	13.4	1165.8	2.0	223.5
33508.6	18.1	1166.8	280.8	200.6	14.7	1165.7	2.2	223.2
34008.7	18.4	1166.7	297.7	201.7	14.0	1165.6	2.5	222.8
34508.7	18.4	1166.5	283.2	199.5	13.7	1165.5	2.0	222.5
35008.7	17.4	1166.4	300.2	200.4	14.4	1165.4	2.5	222.2
35508.8	15.3	1166.3	297.1	206.1	14.4	1165.3	2.6	221.8
36008.9	17.9	1166.0	299.3	200.7	12.6	1165.1	1.7	221.4
36508.9	19.1	1166.0	277.3	195.8	13.8	1165.1	2.2	221.2
37009.0	17.8	1166.0	297.6	198.7	12.8	1165.0	2.0	220.9
37509.0	16.6	1165.8	287.1	199.7	14.0	1164.9	2.4	220.5
38009.1	16.0	1165.7	315.8	199.1	12.8	1164.8	2.0	220.2
38509.1	15.5	1165.7	317.9	201.5	13.2	1164.6	1.9	219.8
39009.2	15.8	1165.5	300.8	198.6	13.2	1164.5	2.0	219.3
39509.3	17.1	1165.5	285.0	197.7	11.1	1164.4	1.3	219.1
40009.3	16.3	1165.3	284.5	199.5	13.5	1164.3	1.9	218.9
40509.3	16.6	1165.3	279.7	198.4	12.3	1164.1	2.0	218.5
41009.3	14.4	1165.1	325.8	197.2	12.9	1164.1	2.1	218.4
41509.3	15.9	1165.0	291.0	193.9	12.8	1164.0	2.3	218.1
42009.4	16.3	1164.9	289.5	198.7	11.3	1163.9	1.6	217.7
42509.4	14.3	1164.9	333.4	196.1	12.1	1163.8	2.2	217.5
43009.5	14.6	1164.7	287.5	195.5	13.2	1163.8	2.6	217.3
43509.5	13.7	1164.6	336.2	201.2	11.6	1163.7	1.8	217.1
44009.6	14.3	1164.4	270.7	199.3	11.4	1163.6	1.7	216.6
44509.6	15.2	1164.3	271.8	202.6	12.2	1163.4	1.9	216.2
45009.6	13.3	1164.4	307.7	194.7	13.1	1163.4	2.3	216.0
45509.7	12.1	1164.4	327.7	194.1	13.5	1163.4	3.1	216.0
46009.7	14.3	1164.3	292.2	194.0	12.2	1163.2	1.8	215.7
46509.7	13.8	1164.2	292.2	193.0	12.8	1163.2	2.5	215.5
47009.8	10.2	1163.9	307.0	201.0	14.5	1163.2	3.3	215.3
47509.8	13.1	1163.8	294.2	198.5	12.0	1163.0	1.7	214.9

Rev. 2

Table 3-21 Break Mass and Energy Flow for the Long-term Cooling Phase of the DEPSG Break (Sheet 21 of 23)

Time (sec)	Break Flow (Reactor Vessel Side)				Break Flow (Steam Generator Side)			
	Steam		Liquid		Steam		Liquid	
	Mass (lbm/sec)	Enthalpy (Btu/lbm)	Mass (lbm/sec)	Enthalpy (Btu/lbm)	Mass (lbm/sec)	Enthalpy (Btu/lbm)	Mass (lbm/sec)	Enthalpy (Btu/lbm)
48009.8	10.2	1163.8	318.8	196.1	13.2	1163.0	2.3	214.7
48509.9	13.3	1163.6	297.1	197.7	11.0	1162.8	1.8	214.4
49009.9	14.5	1163.7	284.8	190.4	11.0	1162.6	1.9	214.2
49509.9	12.2	1163.7	323.8	199.0	11.6	1162.6	1.7	214.0
50010.0	12.4	1163.7	317.1	190.7	12.2	1162.6	2.4	214.0
50510.0	12.6	1163.5	278.3	193.6	12.6	1162.7	2.3	213.8
51010.1	11.2	1163.4	318.2	197.0	11.3	1162.5	1.6	213.4
51510.2	10.9	1163.3	333.9	198.6	10.8	1162.3	1.5	213.1
52010.2	13.4	1163.3	284.7	192.1	10.9	1162.3	1.9	213.0
52510.2	12.7	1163.3	276.2	195.1	11.4	1162.3	2.1	212.8
53010.2	9.9	1162.9	339.7	199.5	10.5	1162.2	1.8	212.5
53510.3	10.3	1162.8	306.5	200.0	11.2	1162.2	1.8	212.2
54010.3	11.0	1162.7	277.5	198.4	11.8	1162.0	2.0	212.0
54510.4	10.4	1162.9	336.1	193.1	10.5	1162.0	2.1	211.8
55010.4	11.4	1162.8	309.6	196.0	10.6	1161.8	1.3	211.6
55510.4	12.1	1162.9	289.1	193.1	9.7	1161.8	1.3	211.5
56010.5	11.9	1162.8	316.6	192.0	10.0	1161.7	2.1	211.5
56510.5	11.6	1162.5	280.2	195.9	11.3	1161.8	2.2	211.3
57010.5	8.6	1162.6	324.8	190.5	12.9	1161.8	2.6	211.3
57510.6	11.8	1162.7	310.2	192.1	9.2	1161.6	1.0	211.0
58010.6	11.1	1162.5	288.1	194.3	10.8	1161.6	1.7	210.8
58510.7	10.8	1162.3	325.8	196.2	8.6	1161.4	1.2	210.5
59010.8	9.8	1162.3	304.9	191.2	11.8	1161.5	2.1	210.6
59510.8	9.2	1162.4	319.2	193.5	10.3	1161.4	2.0	210.2
60010.9	10.3	1162.4	298.0	187.5	12.1	1161.4	2.9	210.3
60510.9	8.9	1162.5	304.4	189.7	12.4	1161.5	2.4	210.2
61011.0	9.1	1162.3	314.8	186.6	12.1	1161.4	2.5	210.3
61511.0	9.0	1162.2	290.3	187.4	11.8	1161.4	2.4	210.2
62011.0	8.5	1162.1	310.4	188.5	13.2	1161.4	2.9	210.0
62511.1	8.3	1162.1	309.0	189.4	12.2	1161.3	2.7	209.8
63011.1	11.4	1162.2	298.3	185.6	9.8	1161.2	1.3	209.7
63511.2	9.7	1162.2	315.2	185.2	11.6	1161.2	2.5	209.6
64011.2	8.2	1162.1	330.6	187.5	11.3	1161.2	2.7	209.6
64511.2	9.4	1162.0	297.7	187.6	11.3	1161.2	1.7	209.4
65011.3	9.7	1162.0	293.1	187.3	10.7	1161.0	2.1	209.1

Rev. 2

Table 3-21 Break Mass and Energy Flow for the Long-term Cooling Phase of the DEPSG Break (Sheet 22 of 23)

Time (sec)	Break Flow (Reactor Vessel Side)				Break Flow (Steam Generator Side)			
	Steam		Liquid		Steam		Liquid	
	Mass (lbm/sec)	Enthalpy (Btu/lbm)	Mass (lbm/sec)	Enthalpy (Btu/lbm)	Mass (lbm/sec)	Enthalpy (Btu/lbm)	Mass (lbm/sec)	Enthalpy (Btu/lbm)
65511.3	7.3	1161.9	322.3	187.9	12.4	1161.1	2.7	209.1
66011.4	10.4	1161.8	310.7	187.1	9.2	1160.9	1.1	208.9
66511.4	7.5	1161.6	313.4	187.3	12.3	1161.0	2.6	208.9
67011.4	10.6	1161.6	288.4	188.6	9.1	1160.9	1.3	208.6
67511.4	7.0	1161.9	328.5	188.5	11.2	1160.9	2.2	208.5
68011.4	7.3	1161.6	312.6	187.6	12.4	1160.9	2.3	208.4
68511.5	7.2	1161.7	305.5	187.7	12.0	1160.8	2.1	208.2
69011.5	8.9	1161.7	298.7	185.4	11.5	1160.8	2.2	208.3
69511.5	7.9	1161.6	339.8	189.7	8.0	1160.5	0.9	207.8
70011.6	10.7	1161.3	294.3	189.5	8.5	1160.5	1.2	207.7
70511.6	7.8	1161.6	335.0	184.5	10.5	1160.5	2.0	207.8
71011.6	8.9	1161.6	297.6	184.0	10.8	1160.6	2.2	207.7
71511.7	7.2	1161.5	328.0	187.1	10.5	1160.6	1.8	207.7
72011.8	7.8	1161.6	302.6	187.9	10.7	1160.5	2.0	207.4
72511.8	6.3	1161.3	315.1	187.0	11.7	1160.6	2.5	207.4
73011.8	8.8	1161.0	296.3	184.2	10.2	1160.5	1.6	207.3
73511.9	8.1	1161.2	296.0	184.3	11.2	1160.5	1.7	207.4
74011.9	8.2	1161.5	327.8	183.3	8.4	1160.3	1.4	207.2
74511.9	9.1	1161.3	294.9	185.9	10.5	1160.3	2.2	207.1
75012.0	8.7	1161.4	334.9	184.5	8.3	1160.2	1.3	206.9
75512.0	8.0	1161.3	319.4	183.1	9.8	1160.3	1.9	206.9
76012.0	9.0	1161.2	302.6	182.3	9.1	1160.2	1.5	206.8
76512.1	7.8	1161.2	303.2	184.3	11.2	1160.3	2.4	206.8
77012.1	7.2	1160.9	321.4	184.5	9.9	1160.2	1.7	206.7
77512.1	8.0	1161.5	303.2	184.6	8.8	1160.1	1.5	206.4
78012.1	9.2	1161.2	311.1	181.5	8.7	1160.0	1.4	206.3
78512.2	7.0	1161.2	321.7	181.8	10.9	1160.1	1.9	206.5
79012.2	7.2	1161.2	317.8	183.0	11.0	1160.2	2.0	206.5
79512.2	8.5	1161.3	306.4	179.5	8.4	1160.0	1.3	206.3
80012.2	8.7	1161.3	326.5	180.9	9.4	1159.9	2.2	206.2
80512.2	8.2	1160.8	295.9	181.3	10.3	1160.0	1.7	206.2
81012.3	7.5	1161.0	319.6	179.9	9.1	1160.0	1.5	206.2
81512.3	7.0	1161.3	324.8	184.1	9.5	1159.9	1.2	205.8
82012.3	9.4	1161.0	303.3	182.4	7.8	1159.7	0.7	205.7
82512.3	8.5	1161.0	325.2	180.3	8.2	1159.7	1.4	205.8

Rev. 2

Table 3-21 Break Mass and Energy Flow for the Long-term Cooling Phase of the DEPSG Break (Sheet 23 of 23)

Time (sec)	Break Flow (Reactor Vessel Side)				Break Flow (Steam Generator Side)			
	Steam		Liquid		Steam		Liquid	
	Mass (lbm/sec)	Enthalpy (Btu/lbm)	Mass (lbm/sec)	Enthalpy (Btu/lbm)	Mass (lbm/sec)	Enthalpy (Btu/lbm)	Mass (lbm/sec)	Enthalpy (Btu/lbm)
83012.4	7.6	1160.8	323.0	185.6	8.3	1159.8	1.1	205.6
83512.4	6.1	1160.7	312.6	186.5	10.0	1159.8	1.8	205.4
84012.5	8.1	1160.6	284.1	179.7	9.7	1159.8	1.8	205.6
84512.5	6.8	1160.8	330.2	177.7	10.2	1159.9	2.2	205.6
85012.5	8.1	1160.8	295.6	177.8	10.0	1159.8	1.9	205.6
85512.5	7.4	1160.6	323.0	180.0	9.7	1159.9	1.9	205.7
86012.6	6.4	1160.7	325.6	177.8	9.5	1159.8	1.6	205.5
86512.6	8.5	1160.7	290.3	178.2	9.1	1159.7	1.5	205.4
87012.7	6.2	1160.7	318.7	177.6	10.8	1159.8	2.1	205.4
87512.8	8.7	1160.6	311.1	174.2	8.7	1159.7	1.4	205.3
88012.8	7.7	1161.0	334.9	179.9	8.6	1159.6	1.5	205.3
88512.9	8.5	1160.8	311.5	179.9	6.9	1159.4	0.8	205.0
89013.0	8.3	1160.7	323.9	180.3	8.2	1159.5	1.2	205.0
89513.0	8.3	1160.7	311.3	179.4	7.5	1159.5	0.9	205.1
90013.1	6.8	1160.8	312.5	183.4	8.9	1159.5	1.3	204.7
90513.1	7.4	1160.6	309.4	177.1	9.2	1159.5	1.5	204.7
91013.2	6.0	1160.8	326.2	181.6	8.5	1159.5	1.7	204.7
91513.2	7.8	1160.5	318.1	178.2	8.4	1159.4	1.3	204.6
92013.3	8.0	1160.6	308.9	181.9	6.7	1159.1	0.5	204.1
92513.3	7.1	1160.6	323.1	180.4	8.6	1159.4	2.0	204.4
93013.4	6.9	1160.4	304.0	180.4	8.7	1159.3	1.2	204.4
93513.4	5.9	1160.2	323.9	179.0	9.8	1159.4	1.6	204.3
94013.4	8.3	1160.2	301.5	176.4	7.3	1159.3	1.2	204.4
94513.5	7.1	1160.4	328.1	175.9	8.5	1159.2	1.3	204.4
95013.5	8.3	1160.5	309.5	178.8	7.1	1159.1	0.6	204.2
95513.5	9.2	1160.6	318.1	175.0	6.7	1158.9	0.7	204.0
96013.6	8.6	1160.7	322.2	177.6	6.6	1159.0	0.7	204.2
96513.7	9.3	1160.7	311.3	174.4	6.8	1159.0	1.1	204.0
97013.7	7.8	1160.7	328.0	181.0	6.9	1159.1	0.8	204.0
97513.8	9.0	1160.3	294.4	174.3	7.9	1159.1	1.5	204.1
98013.8	6.4	1160.2	336.5	174.8	9.4	1159.4	2.2	204.3
98513.8	6.0	1160.1	312.2	174.9	9.4	1159.3	1.6	204.2
99013.9	8.3	1160.3	302.2	175.1	8.0	1159.2	1.0	204.0
99514.0	6.9	1160.4	320.9	174.8	7.7	1159.1	1.0	203.9
100000.0	7.6	1160.4	324.2	178.1	6.7	1158.9	0.6	203.6

Rev. 2

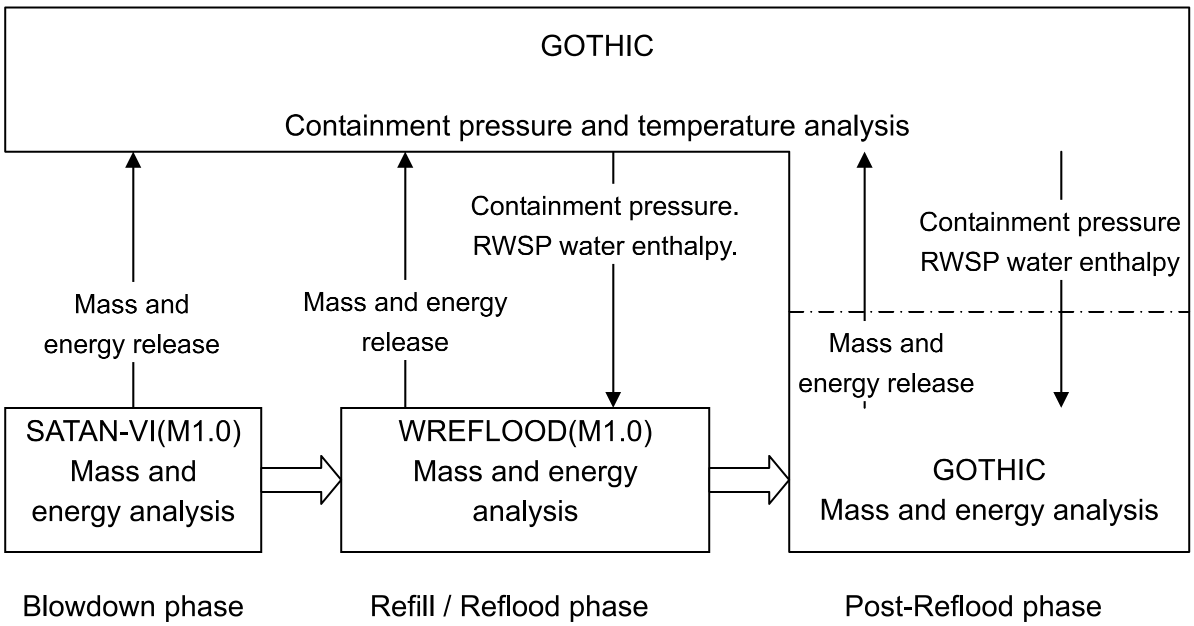

Figure 3-1 The Calculation Code System for Mass and Energy Release and Containment Response Analyses

Rev. 2

Figure 3-2 Noding Diagram of SATAN-VI
(Blowdown Phase Mass and Energy Release Analysis)
(Reference 2)

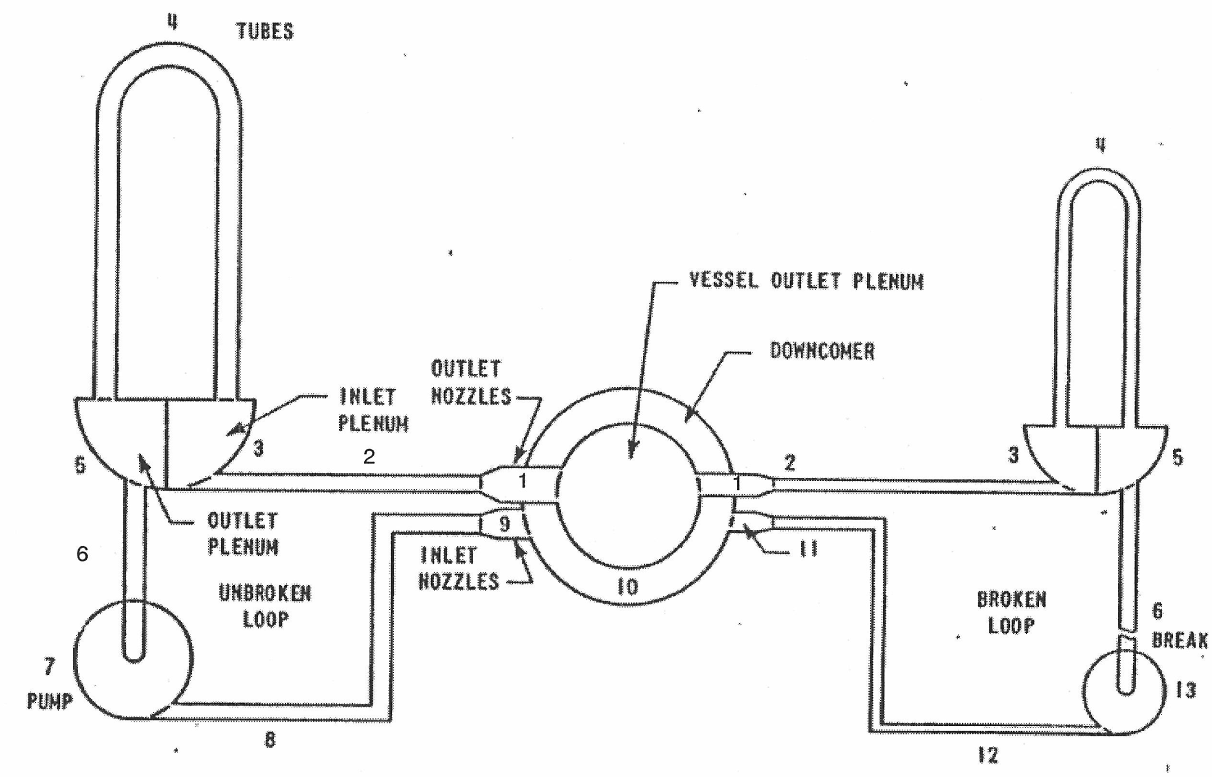

Figure 3-3 Noding Diagram of WREFLOOD
(Reflood Phase Mass and Energy Release Analysis)
(Reference 2)

Rev. 2

Figure 3-4 Characteristics of Flow Damper

Rev. 2

Figure 3-5 Cavitation Factor during Blowdown Phase

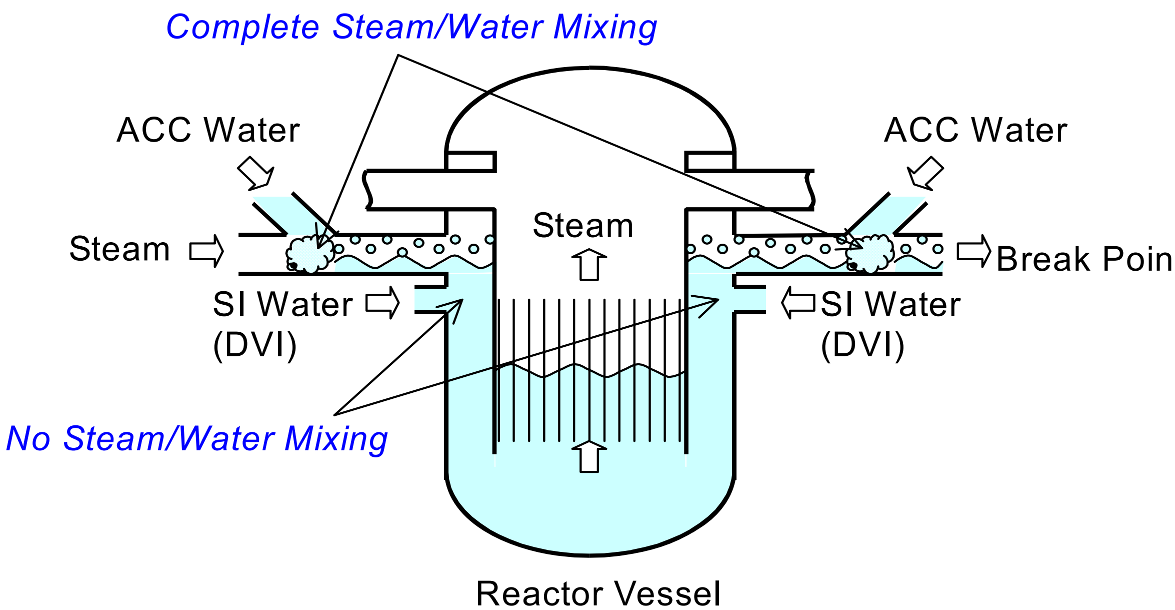

Figure 3-6 Steam/Water Mixing Model for Direct Vessel Injection (DVI)

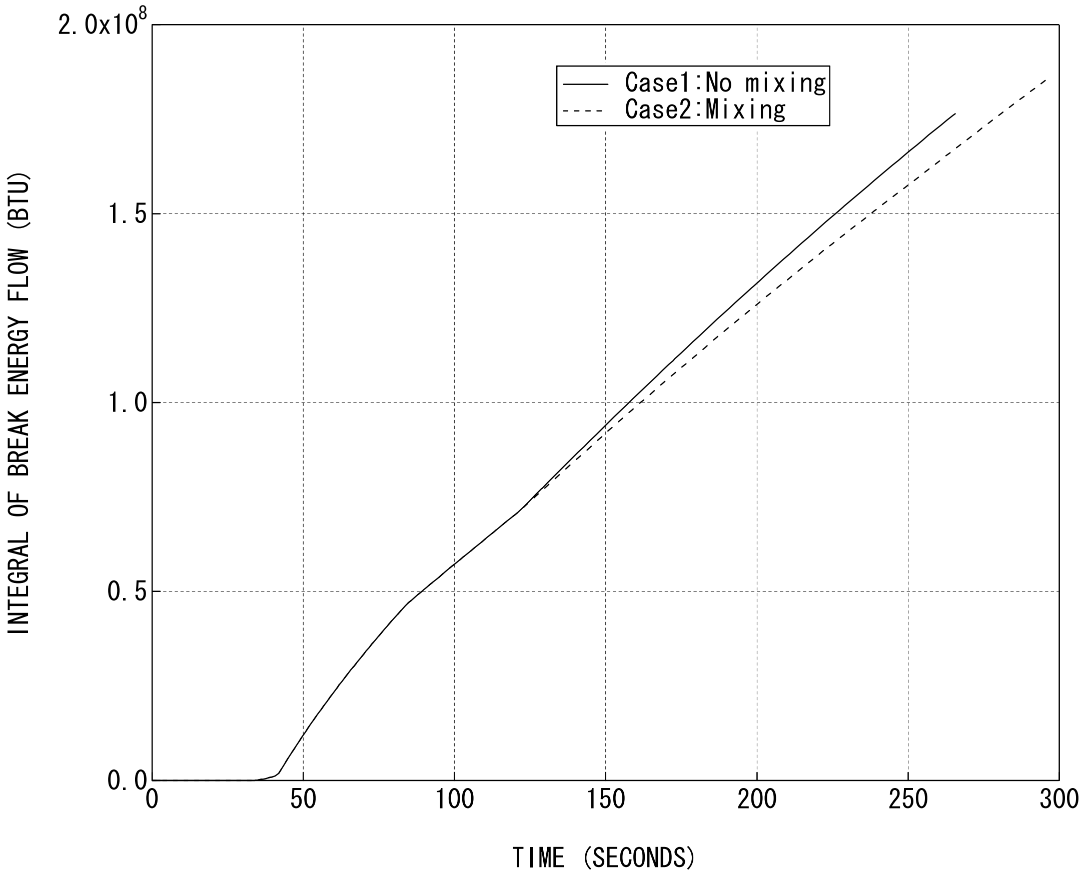

Rev. 1

Figure 3-7 Sensitivity Analysis Result about Steam/Water Mixing Model at DVI (Calculated by the WREFLOOD(M1.0) code)

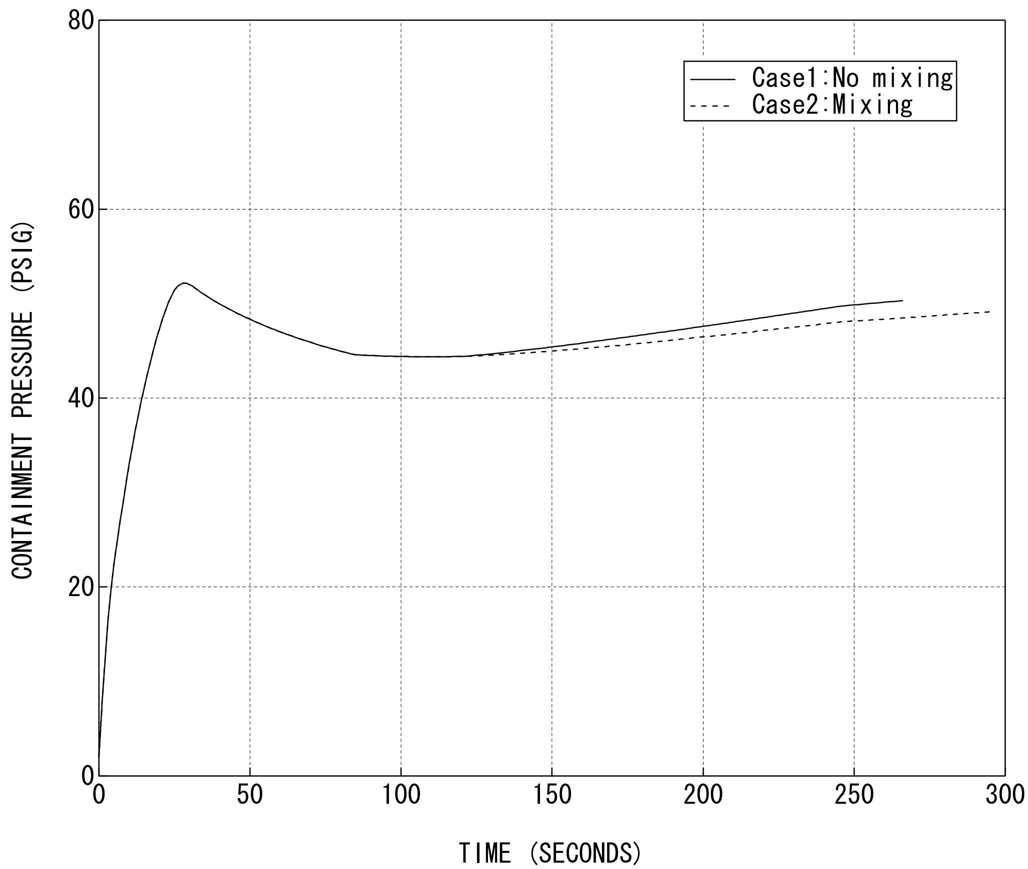

Rev. 1

Figure 3-8 Sensitivity Analysis Result about Steam/Water Mixing Model at DVI (Calculated by the GOTHIC code)

Reflood phenomena related to Neutron Reflector

・Metal heat release from thick metal structure

・Affects on Vin (core flooding rate) and Fout (core carry-over fraction)

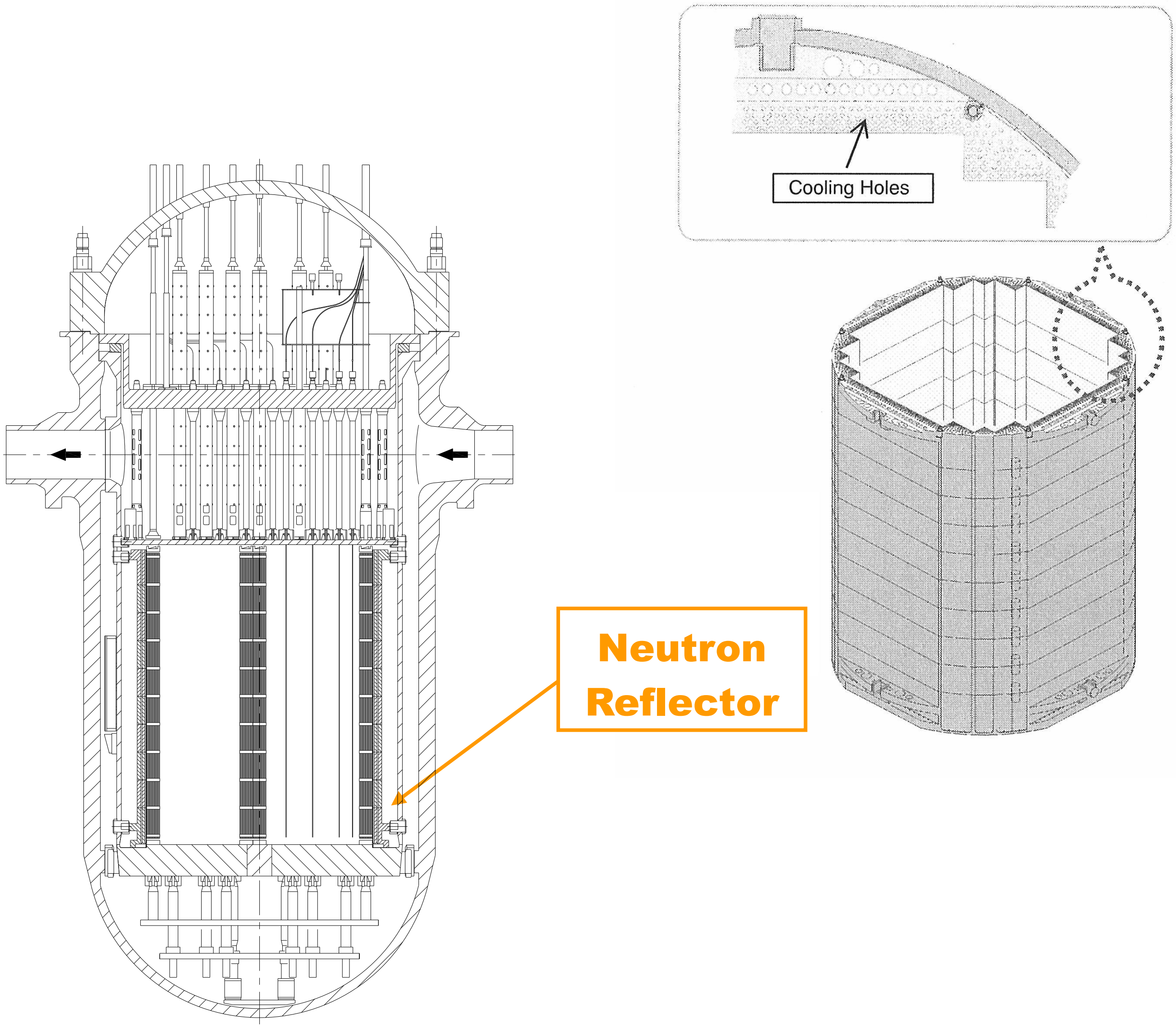

Figure 3-9 Reflood Phenomena Related to Neutron Reflector

(Reference 4)

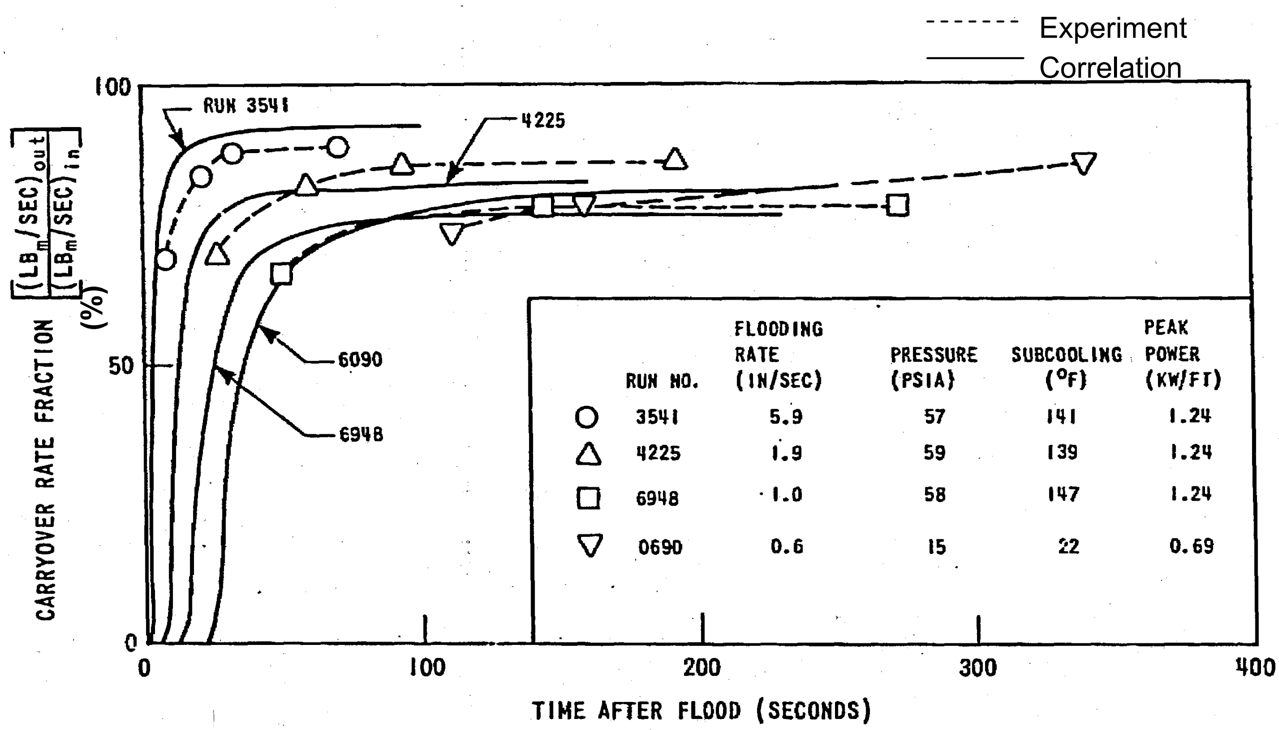

Figure 3-10 Comparison of Carryover Rate Fraction between Correlation and PWR-FLECHT Data

(Reference 4.)

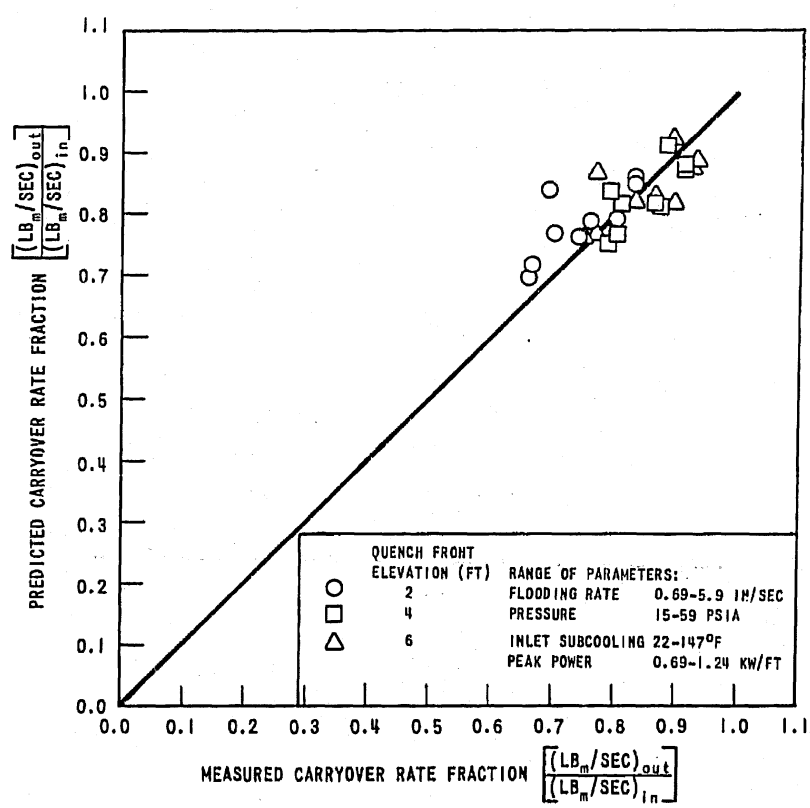

Figure 3-11 Comparison of Measured and Predicted Carryover Rate Fraction
(Reference 4.)

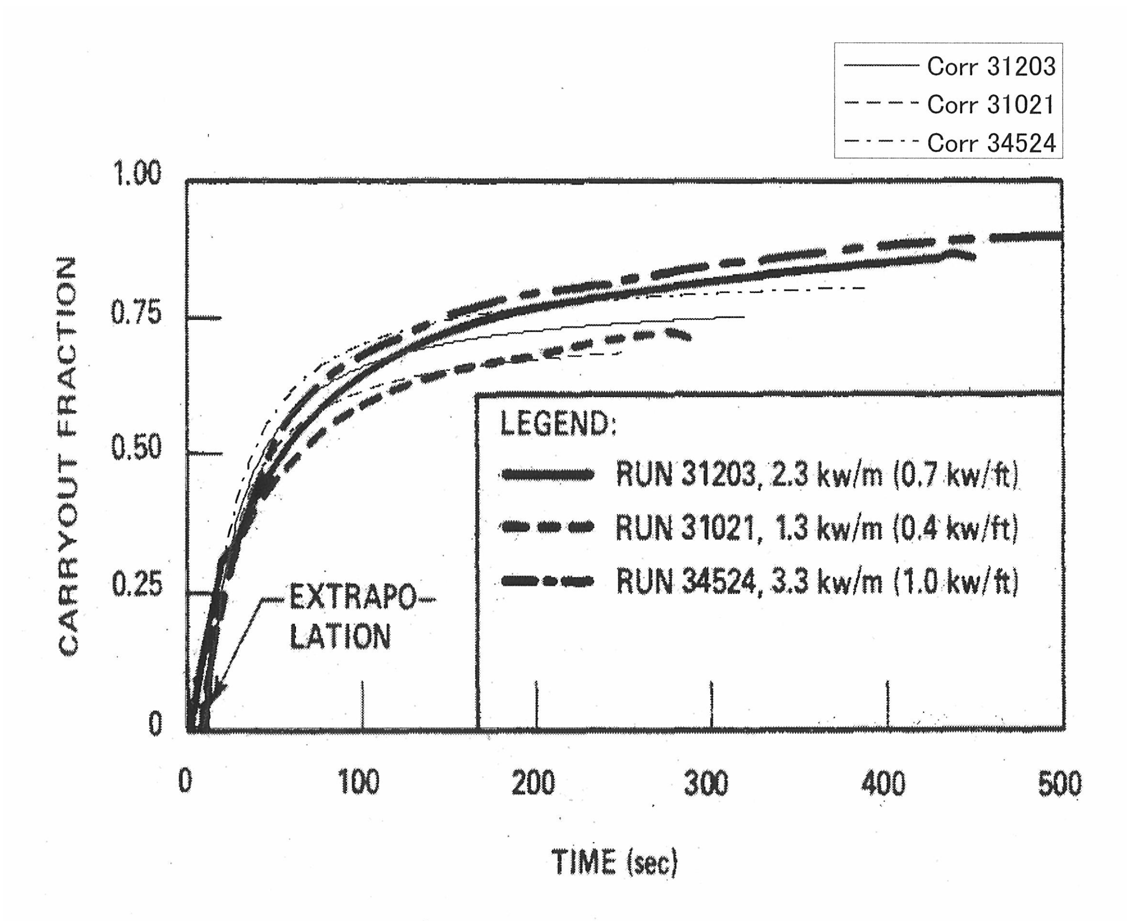

Figure 3-12 Peak Power Effects on Carryout Fraction Comparison of Correlation with FLECHT SEASET Data
(Reference 17)

Figure 3-13 Noding Diagram of GOTHIC
(Post-reflood Phase Mass and Energy Release Analysis)

Rev. 2

Figure 3-14 Core Decay Heat Curve

Rev. 2

Figure 3-15 Heat Transfer Selection Logic

Rev. 2

Figure 3-16 Concept of two-phase level of the vessel by GOTHIC

Rev. 2

Figure 3-17 Noding Diagram of US-APWR Containment Integrity Analysis for Loss-of-Coolant Accident

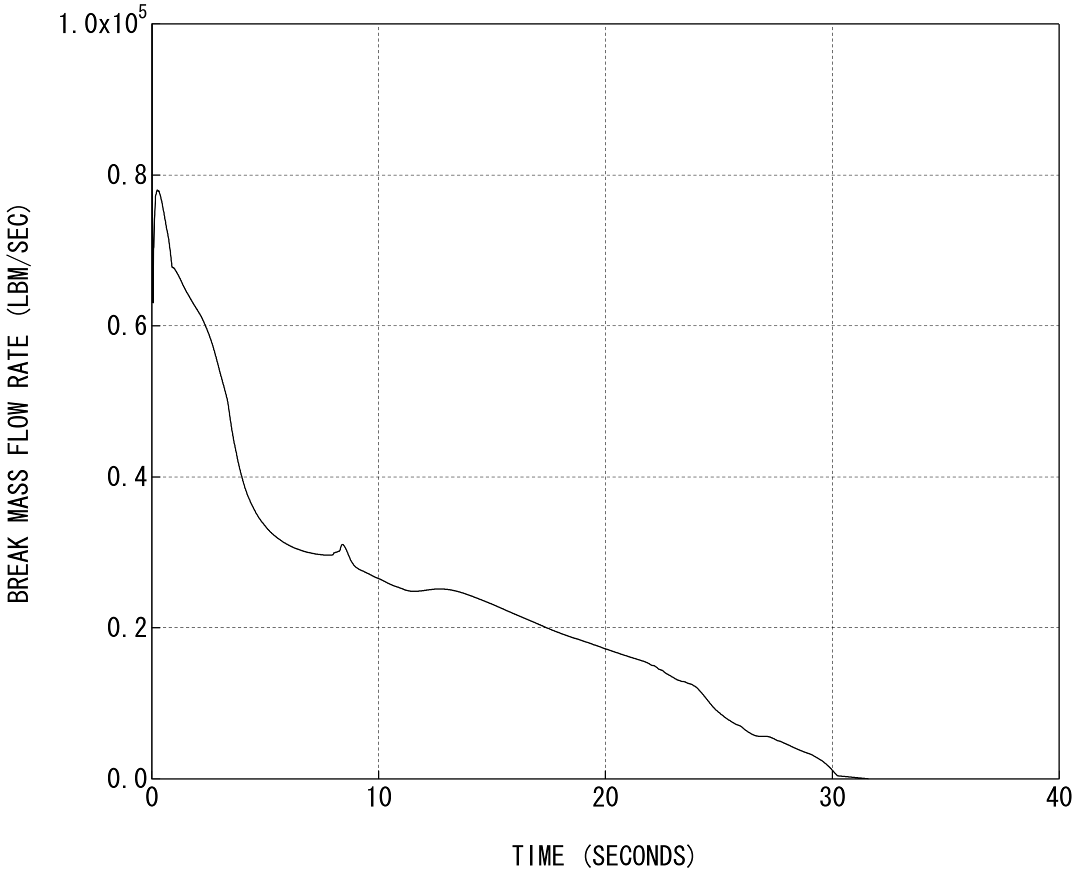

Rev. 1

Figure 3-18 Break Mass Flow Rate (Blowdown Phase)
(Calculated by the SATAN-VI(M1.0) code)

Rev. 1

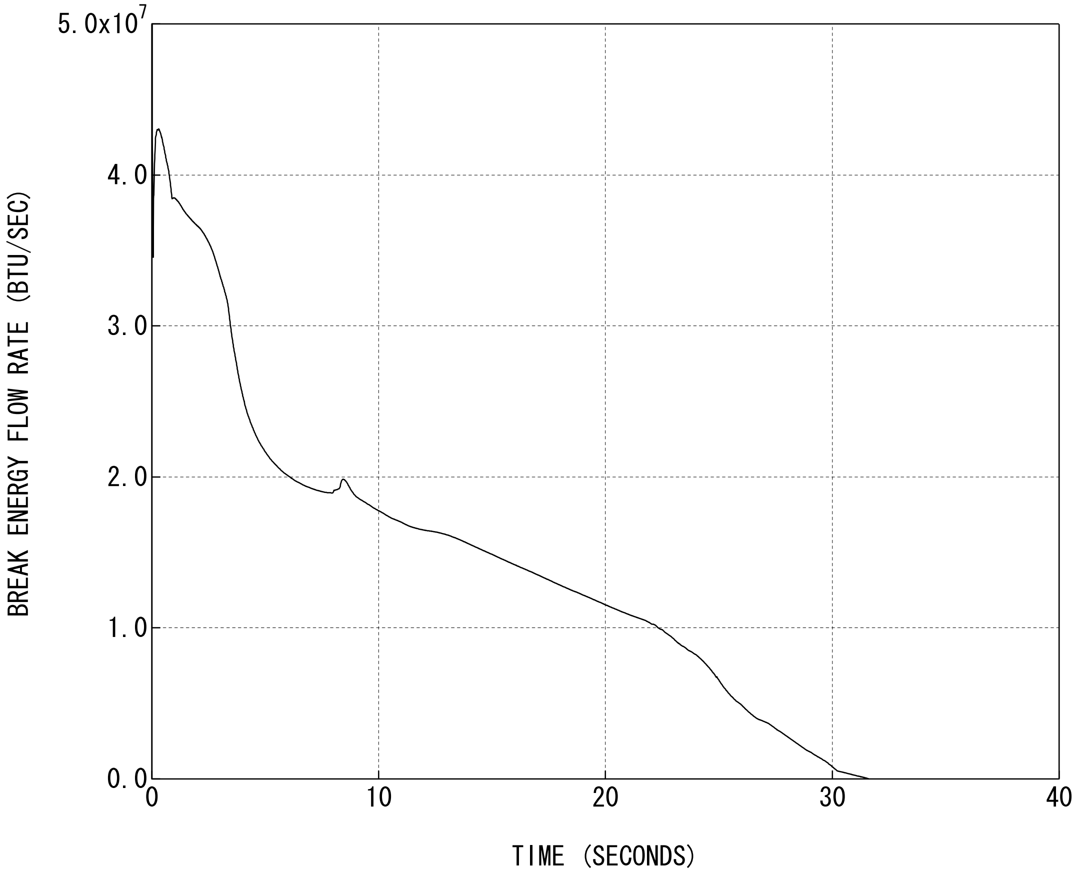

**Figure 3-19 Break Energy Flow Rate (Blowdown Phase)
(Calculated by the SATAN-VI(M1.0) code)**

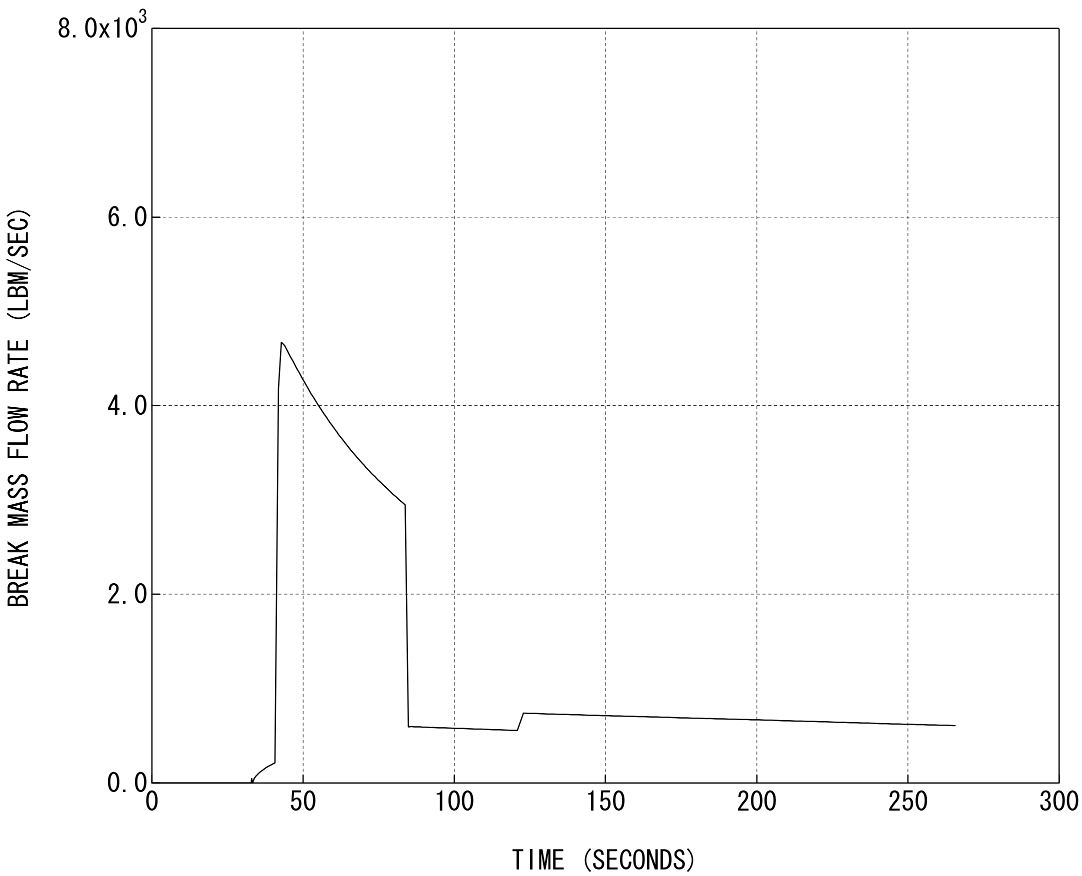

Rev. 1

Figure 3-20 Break Mass Flow Rate (Reflood Phase)
(Calculated by the WREFLOOD(M1.0) code)

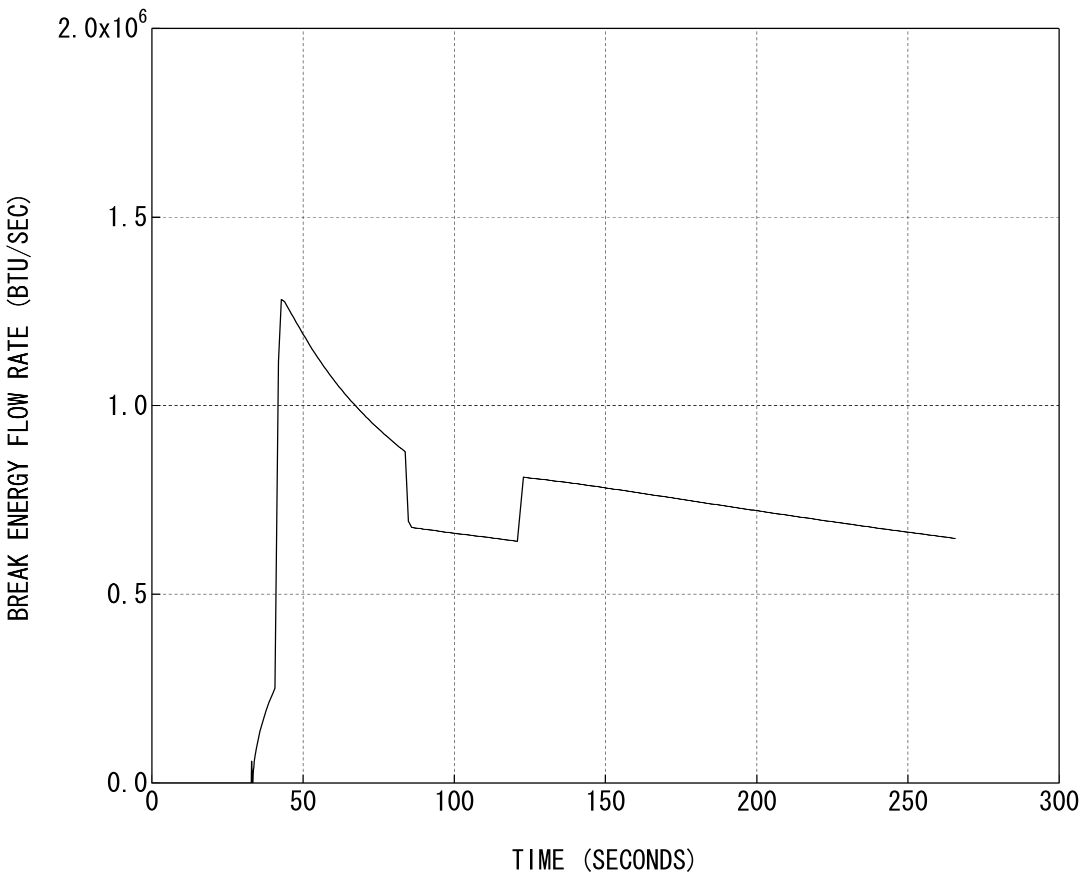

Rev. 1

**Figure 3-21 Break Energy Flow Rate (Reflood Phase)
(Calculated by the WREFLOOD(M1.0) code)**

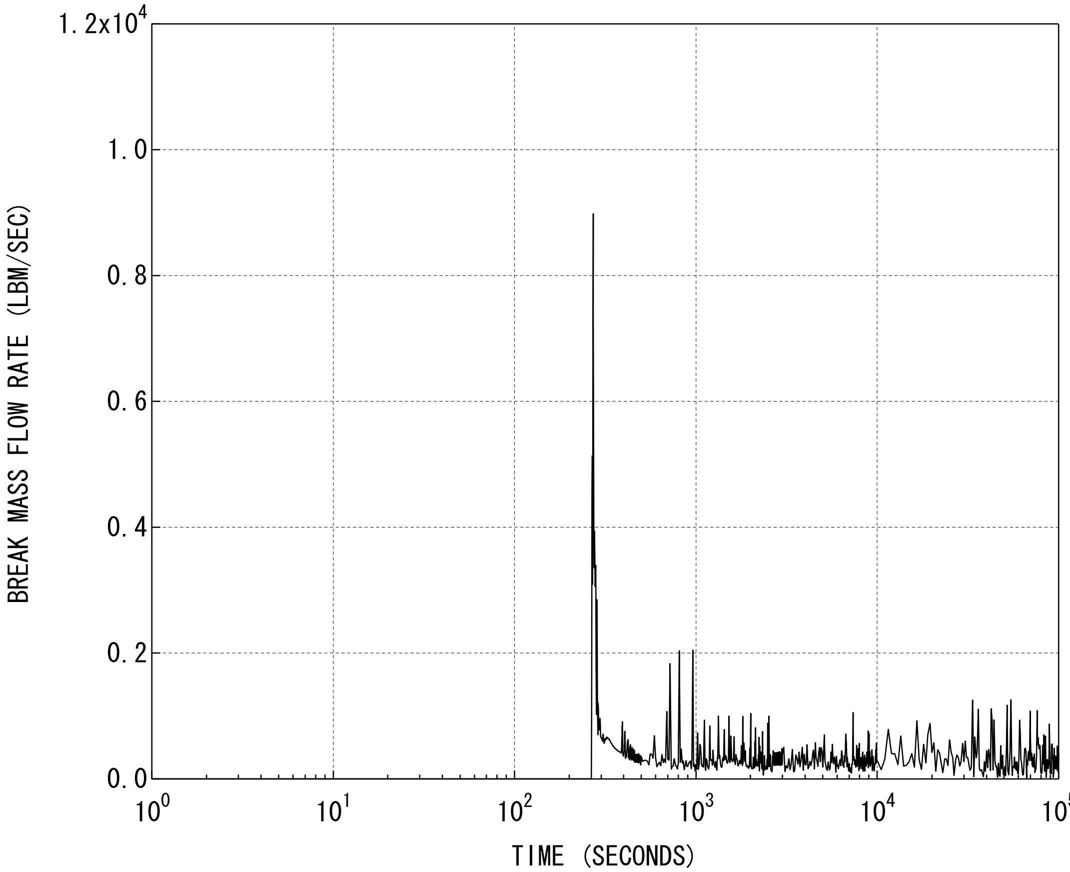

Rev. 1

Figure 3-22 Break Mass Flow Rate (Post-reflood Phase) (Calculated by the GOTHIC code)

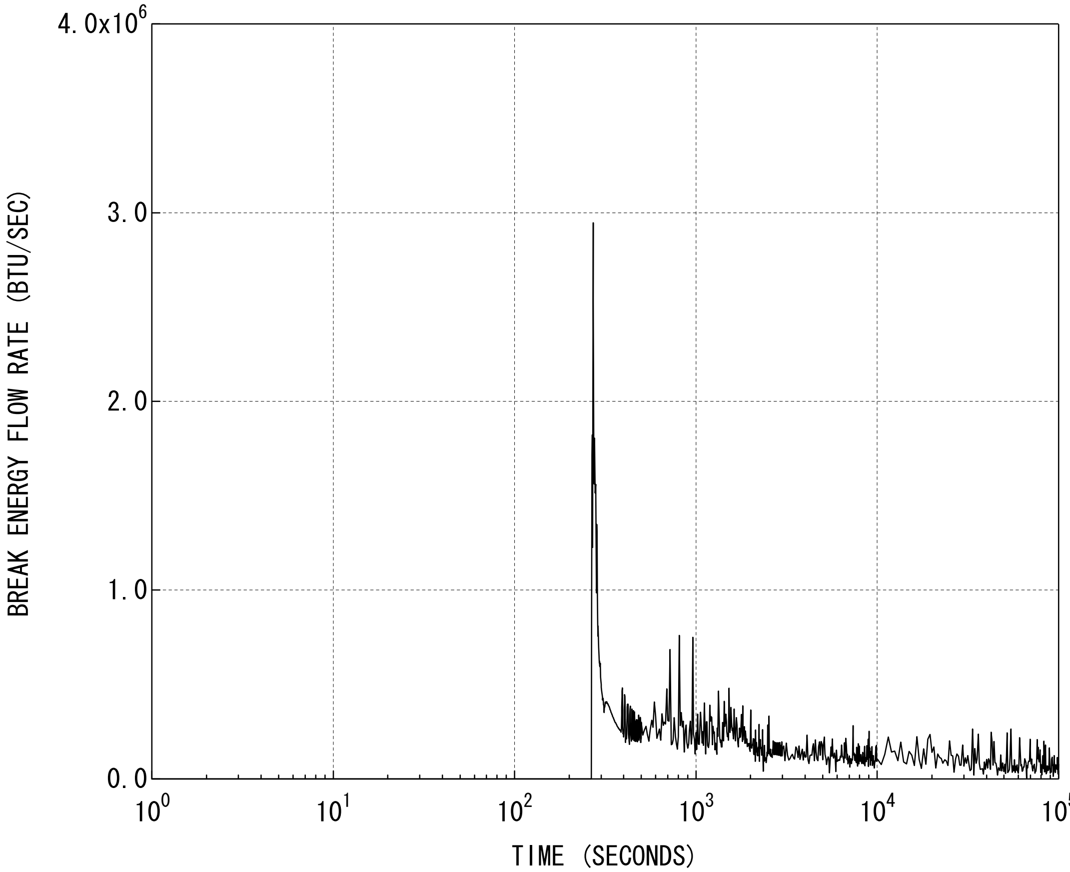

Rev. 1

Figure 3-23 Break Energy Flow Rate (Post-reflood Phase) (Calculated by the GOTHIC code)

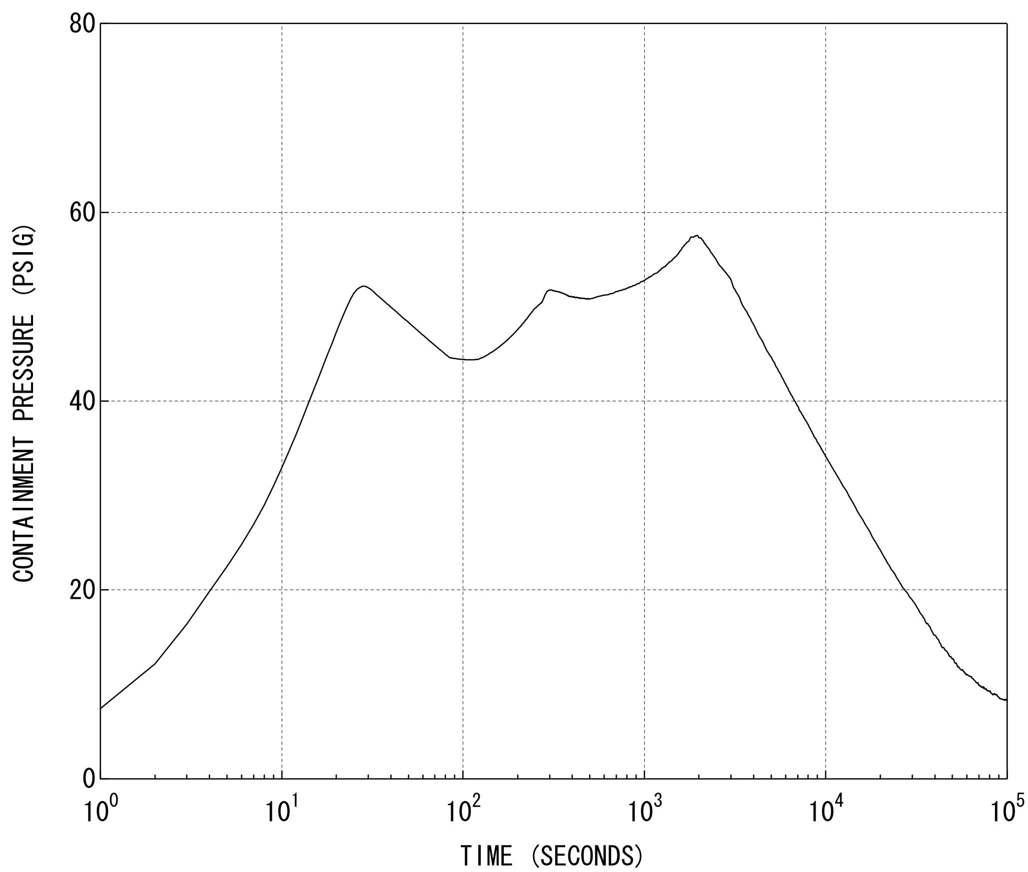

Rev. 1

Figure 3-24 Containment Pressure
(Calculated by the GOTHIC code)

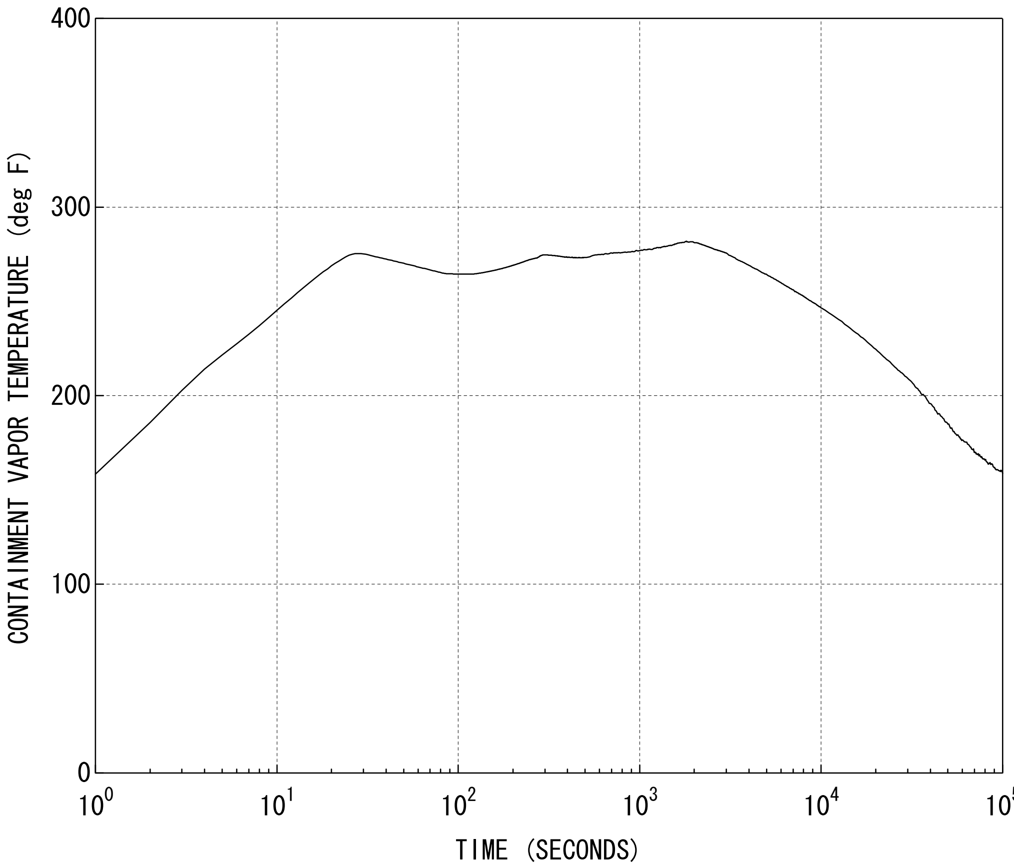

Rev. 1

Figure 3-25 Containment Temperature (Vapor Phase) (Calculated by the GOTHIC code)

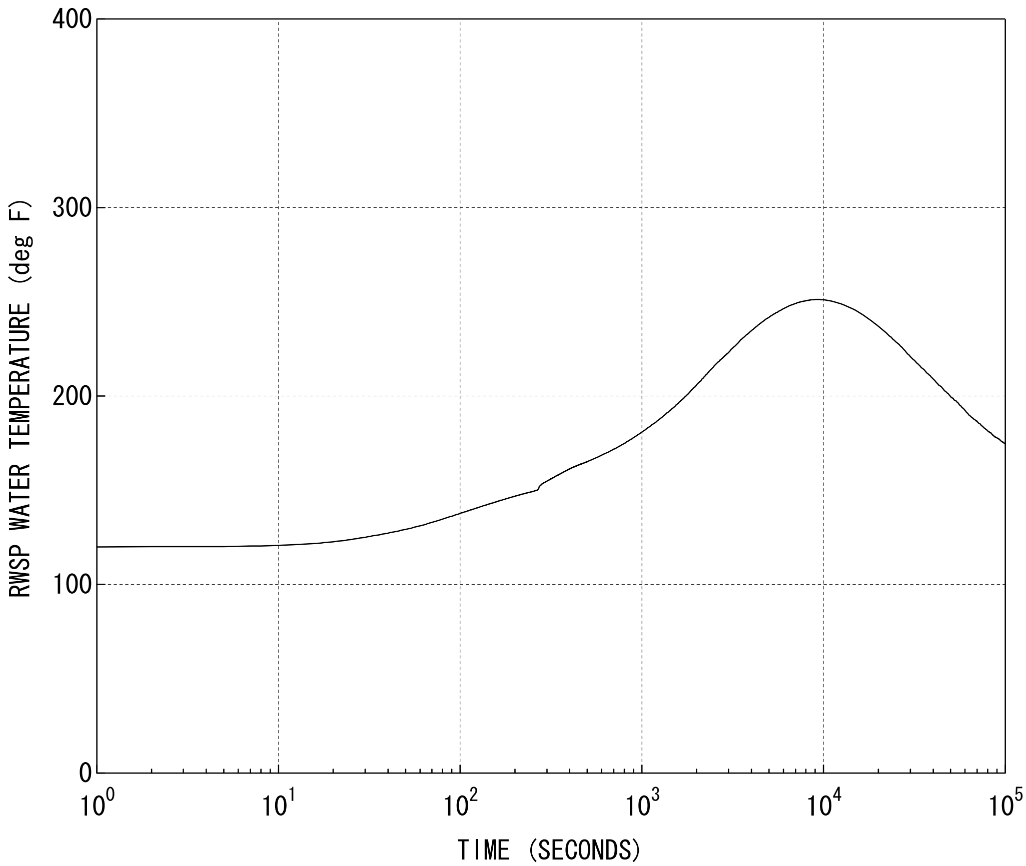

Rev. 2

Figure 3-26 RWSP Water Temperature (Calculated by the GOTHIC code)

Rev. 2

Figure 3-27 Transient of Total Vapor Volume Fraction in Hot Leg Inlet

Note: Both Void in the Pool and Separated Vapor Region are Considered, see Figure 3-16

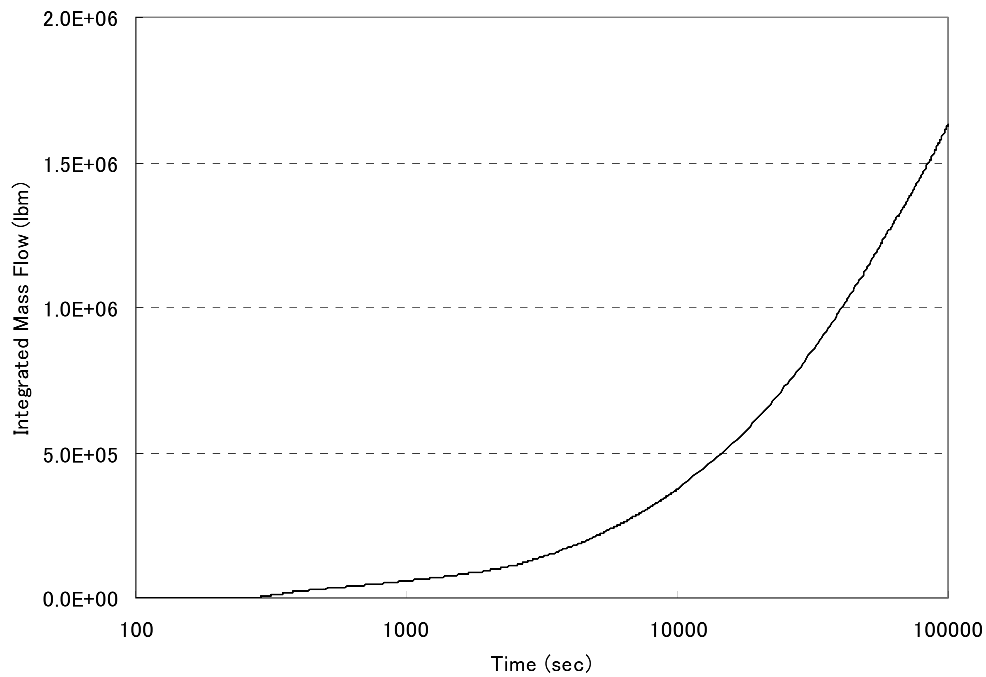

Rev. 2

Figure 3-28 Integrated Vapor Mass Flow Rate into SG (Intact Loop)

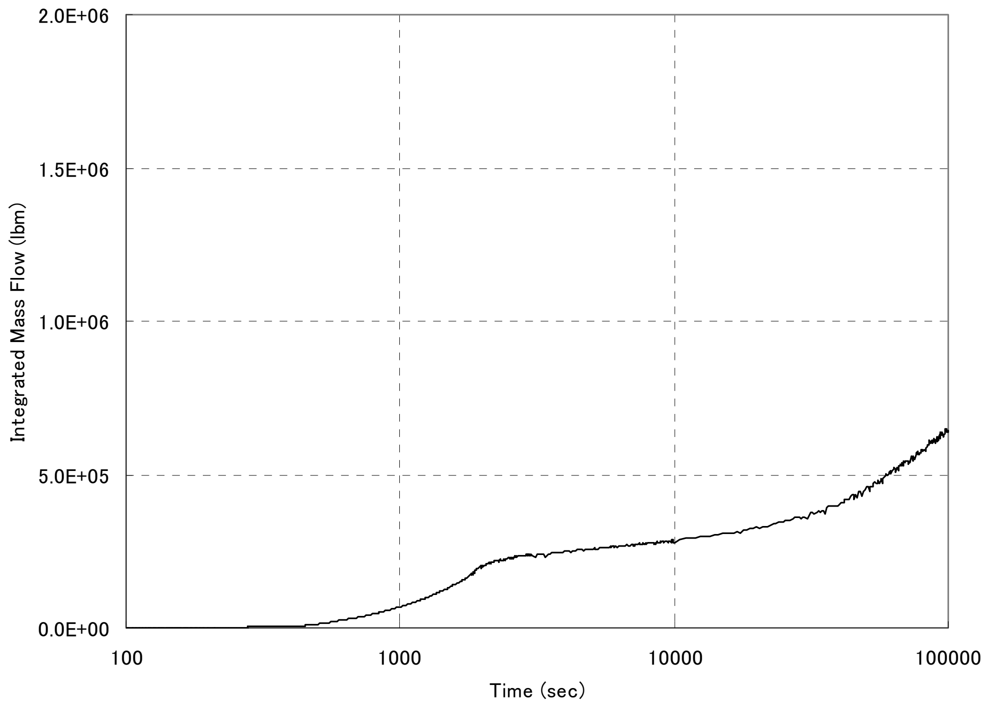

Rev. 2

Figure 3-29 Integrated Liquid Mass Flow Rate into SG (Intact Loop)

Notes: Drop Including

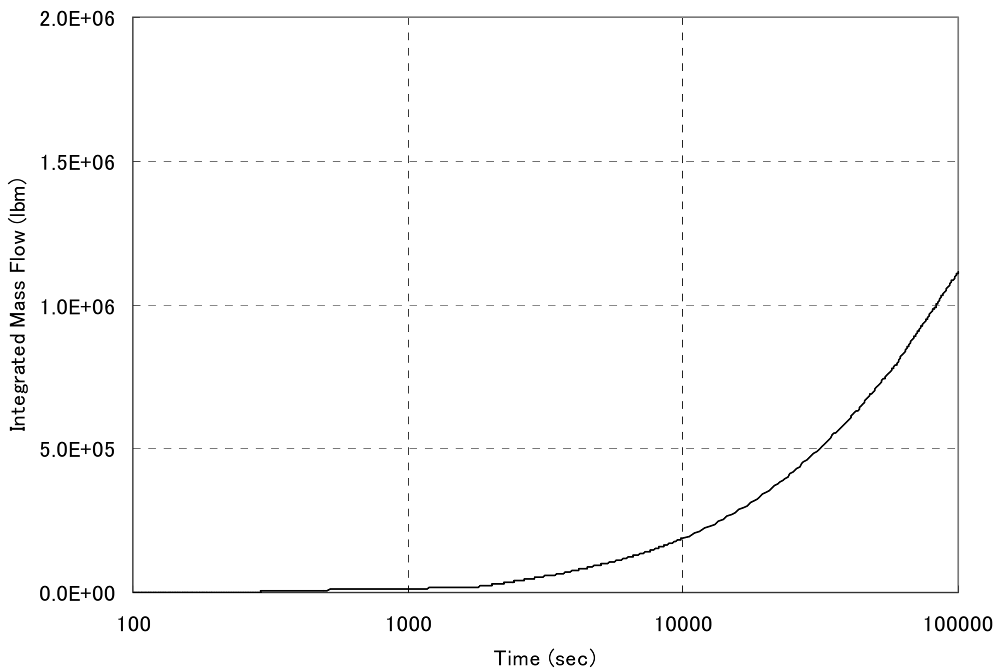

Rev. 2

Figure 3-30 Integrated Vapor Mass Flow Rate into SG (Broken Loop)

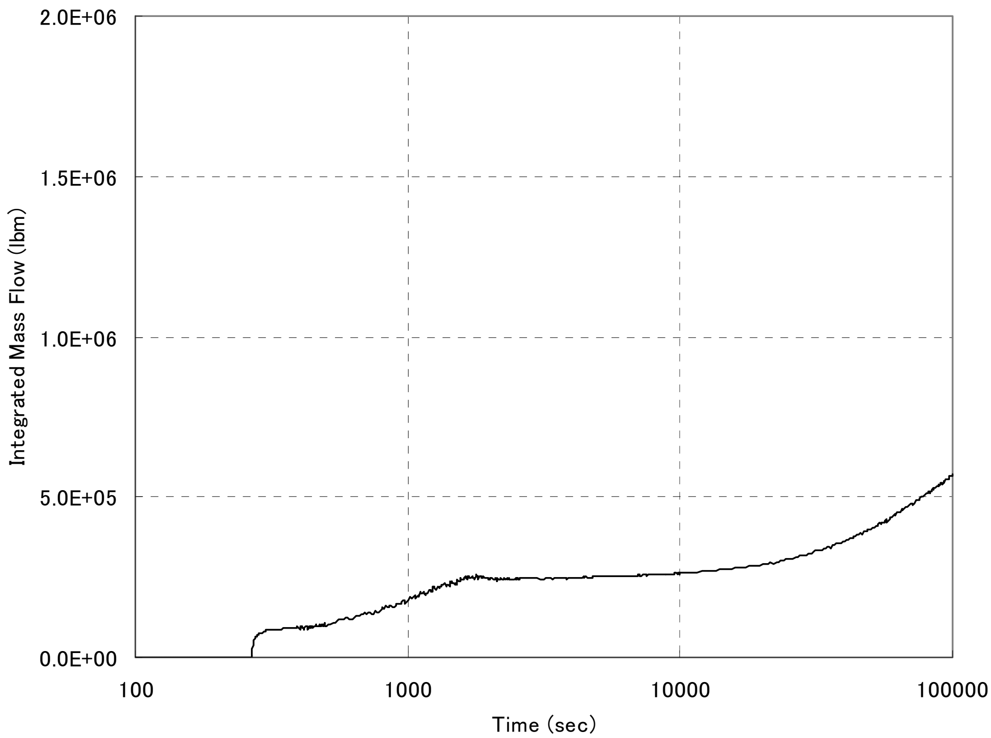

Rev. 2

Figure 3-31 Integrated Liquid Mass Flow Rate into SG (Broken Loop)

Notes: Drop Including

Rev. 2

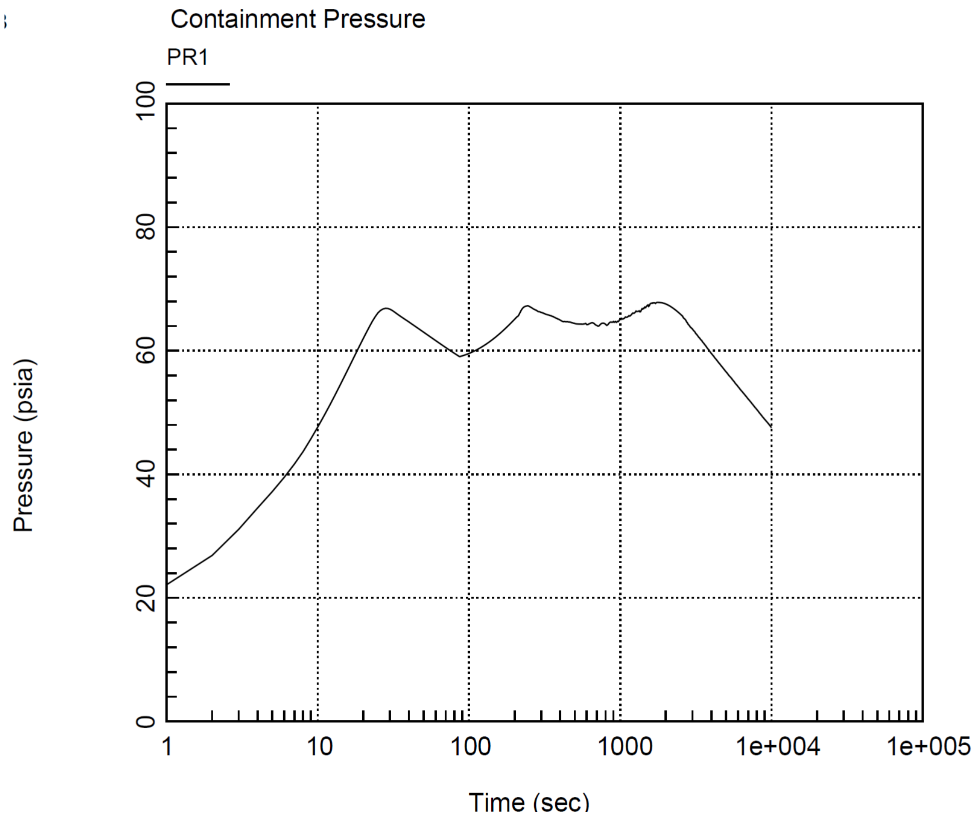

Figure 3-32 Containment Pressure for DEPSG Break with Maximum Safety Injection

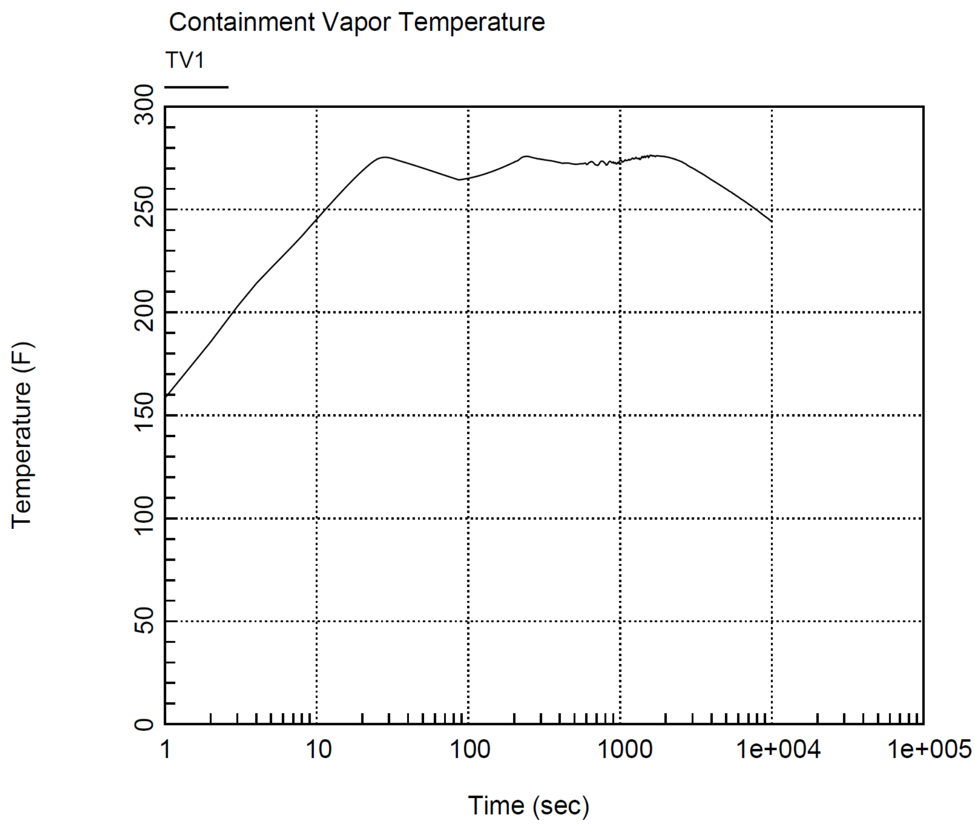

Rev. 2

Figure 3-33 Containment Atmospheric Temperature for DEPSG Break with Maximum Safety Injection

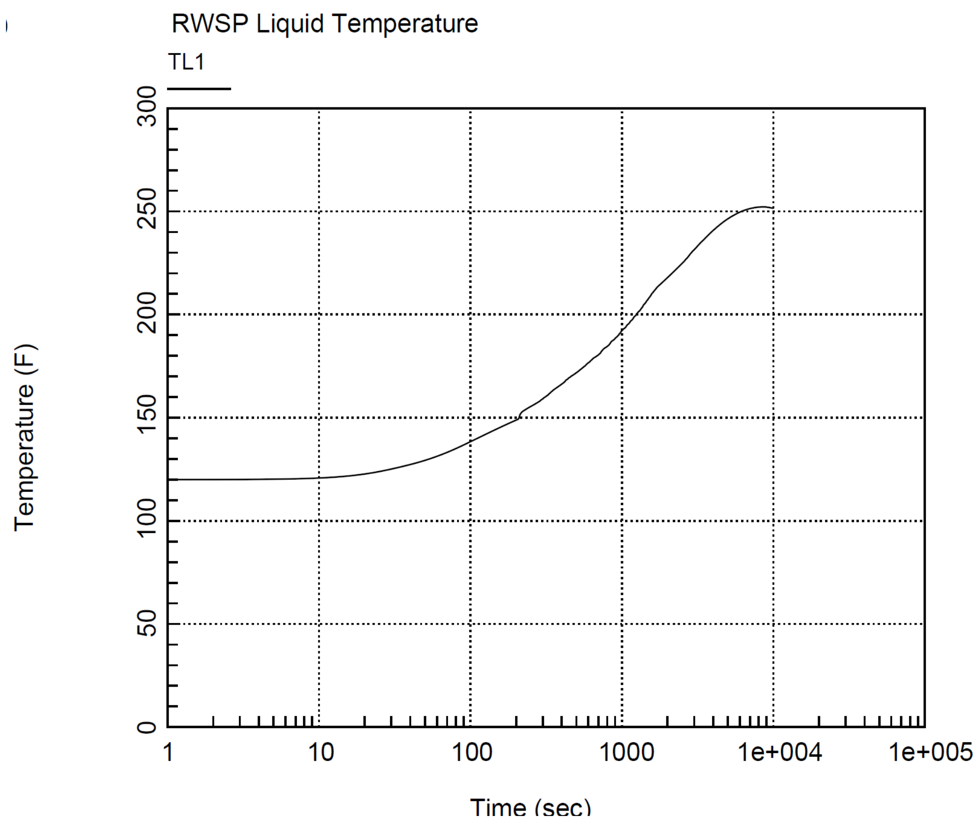

Figure 3-34 RWSP Water Temperature for DEPSG Break with Maximum Safety Injection

Rev. 2

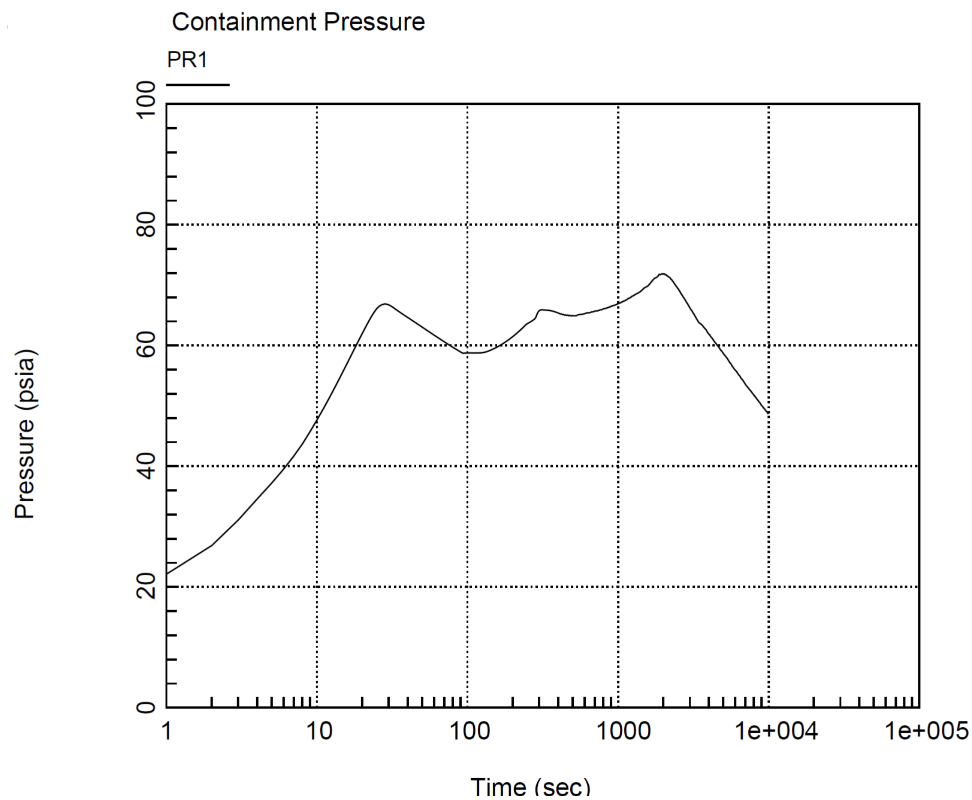

Rev. 2

Figure 3-35 Containment Pressure for DEPSG Break with Maximum Accumulator Water

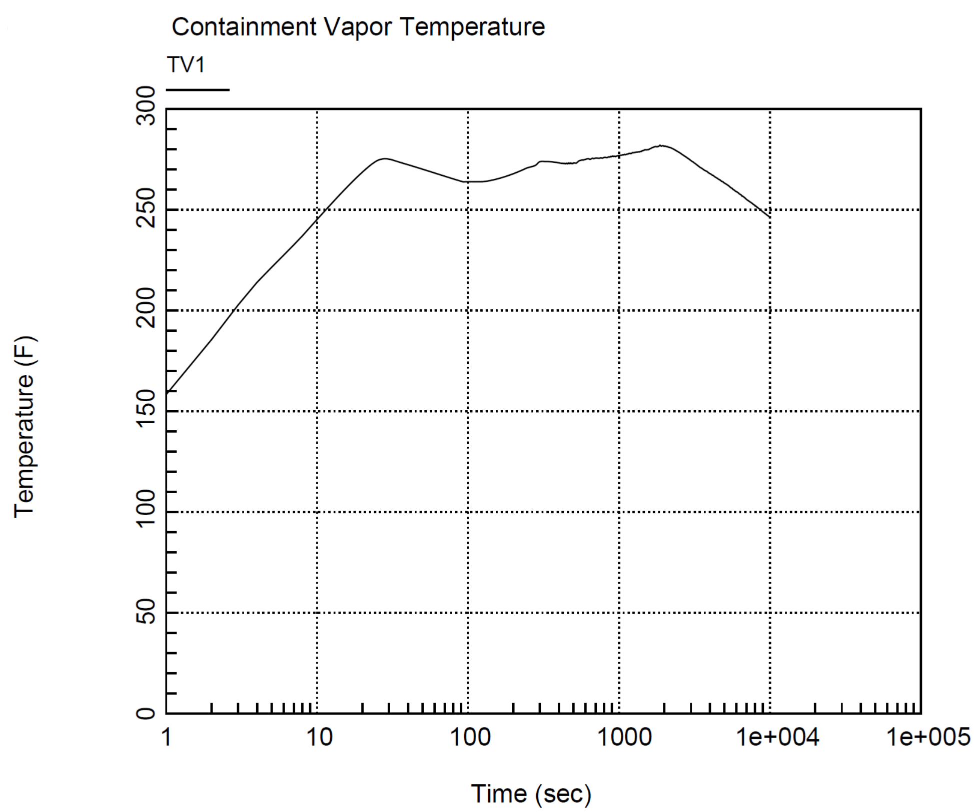

Rev. 2

Figure 3-36 Containment Atmospheric Temperature for DEPSG Break with Maximum Accumulator Water

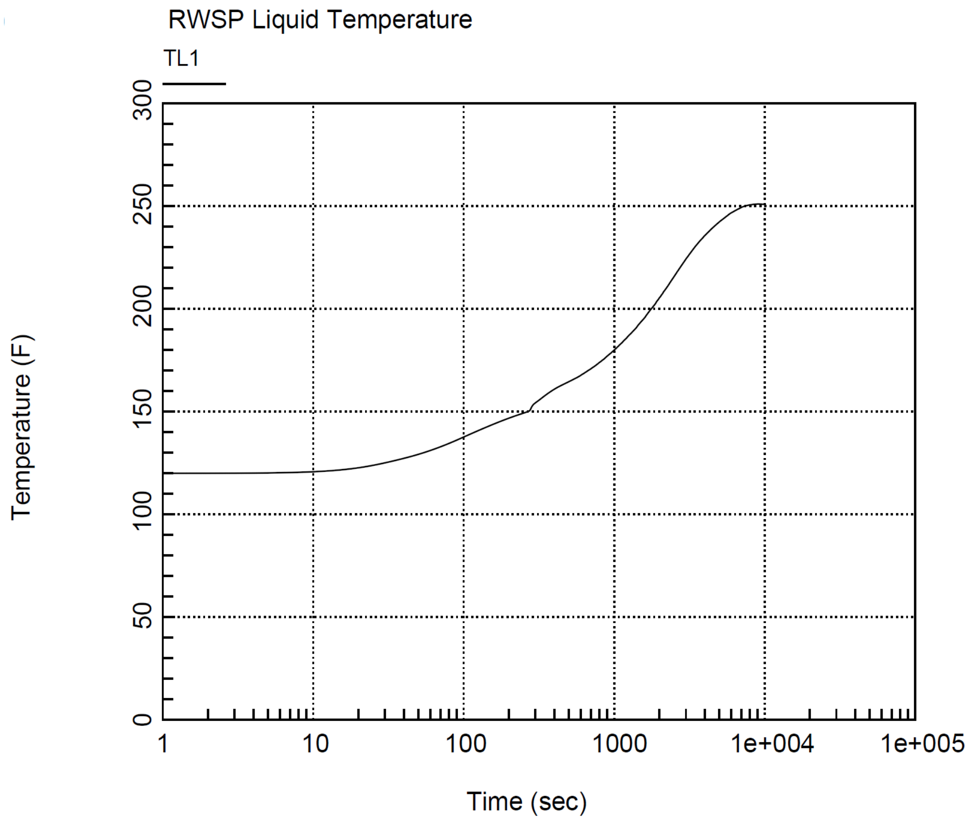

Rev. 2

Figure 3-37 RWSP Water Temperature for DEPSG Break with Maximum Accumulator Water

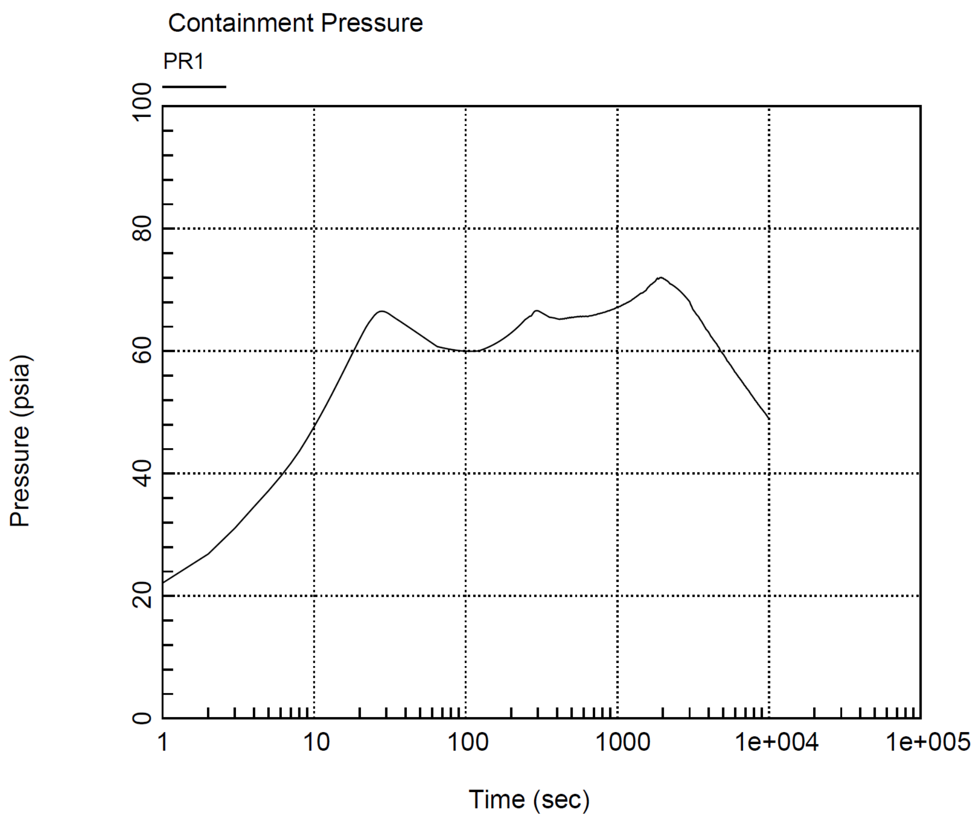

Rev. 2

Figure 3-38 Containment Pressure for DEPSG Break with Maximum Accumulator Flowrate

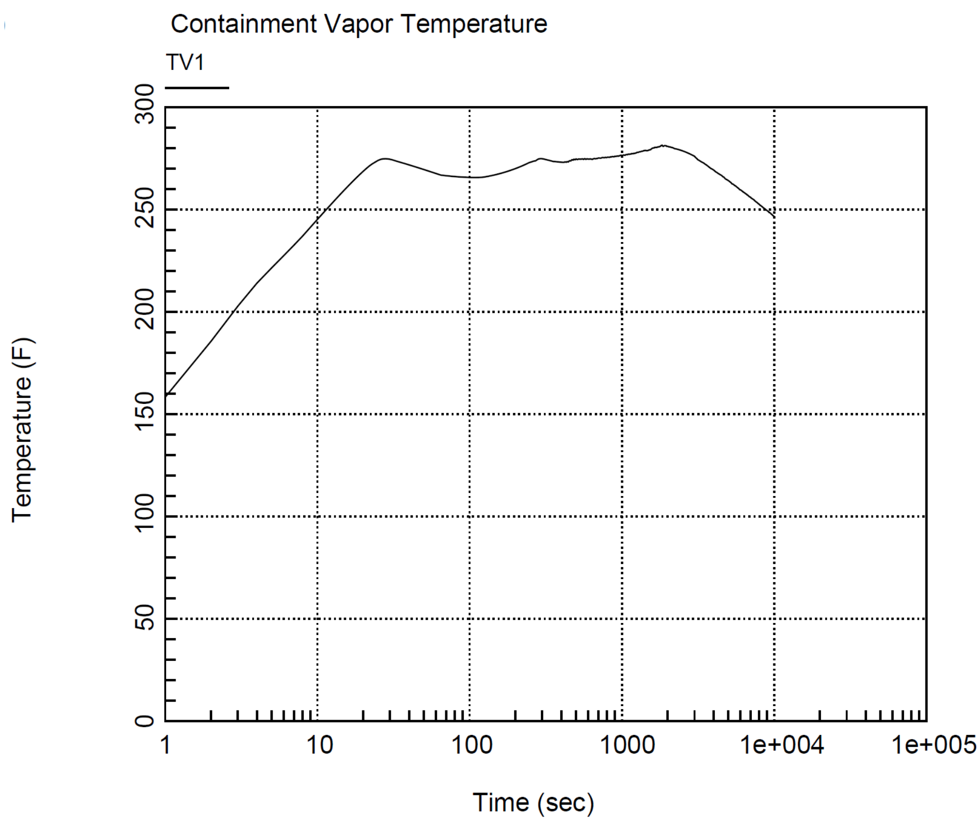

Rev. 2

Figure 3-39 Containment Atmospheric Temperature for DEPSG Break with Maximum Accumulator Flowrate

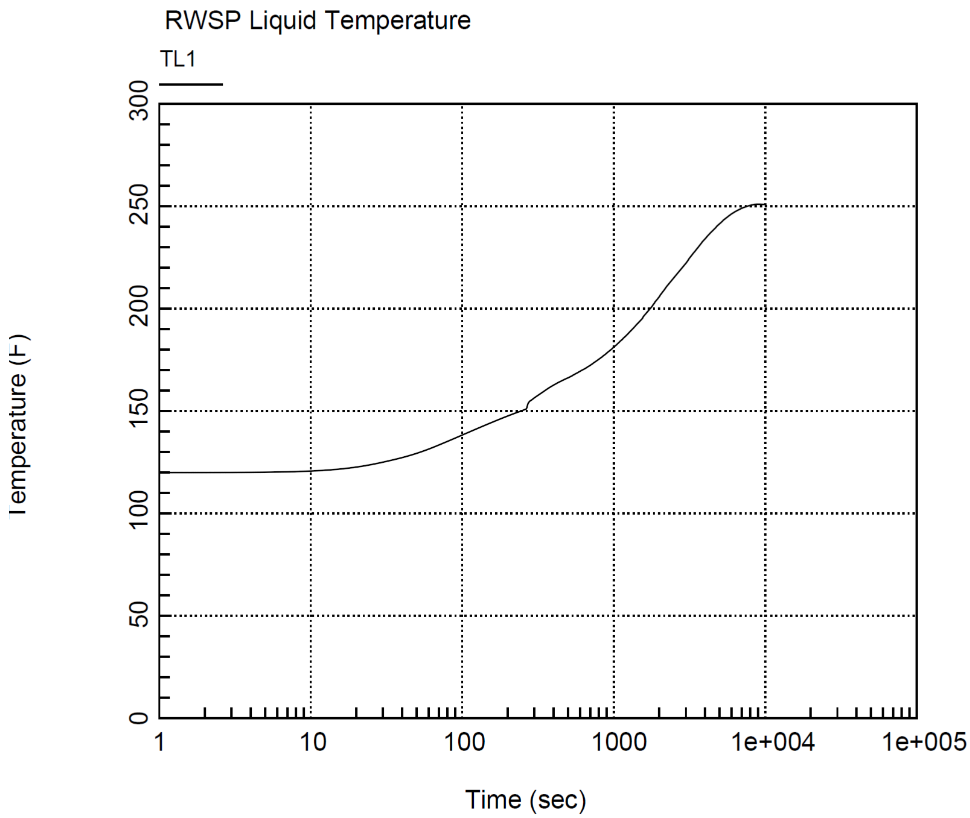

Rev. 2

Figure 3-40 RWSP Water Temperature for DEPSG Break with Maximum Accumulator Flowrate

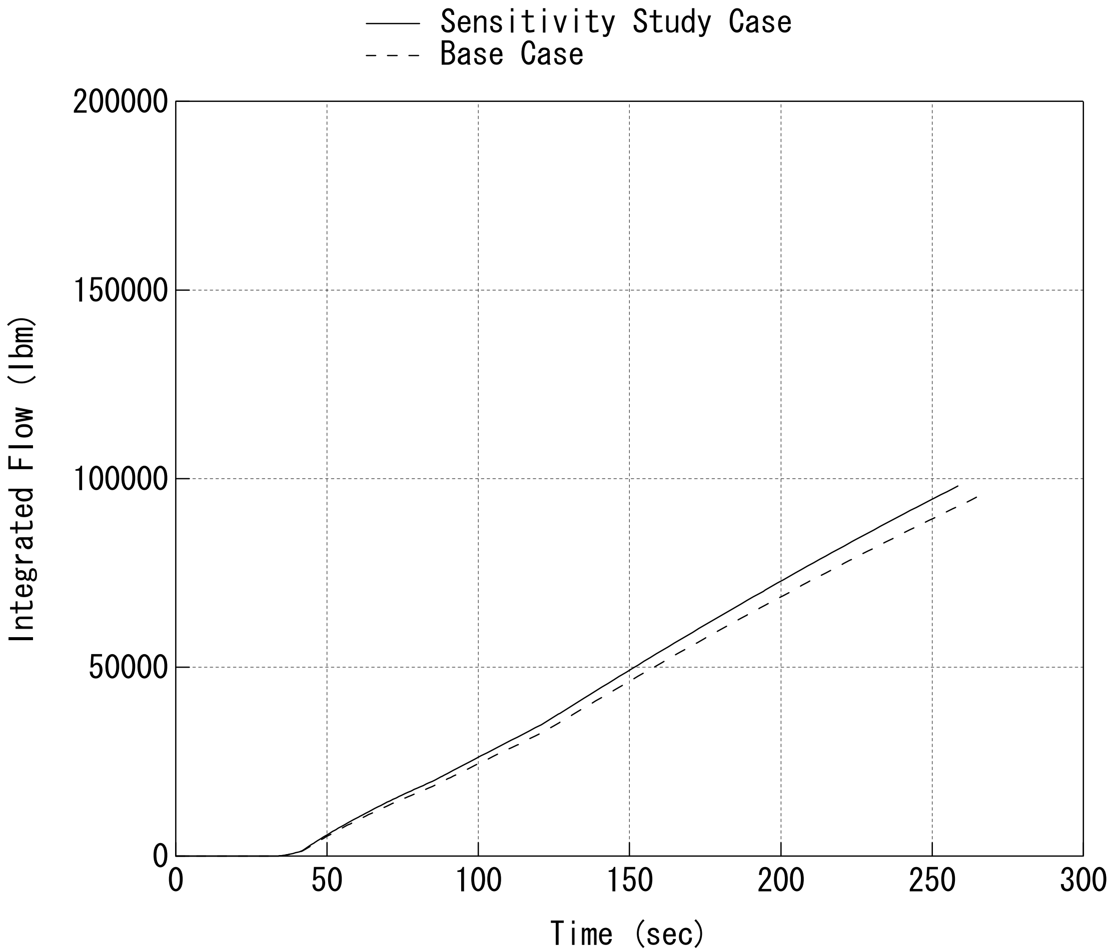

Rev. 2

Figure 3-41 Integral of Broken Loop SG Side Break Flow from WREFLOOD

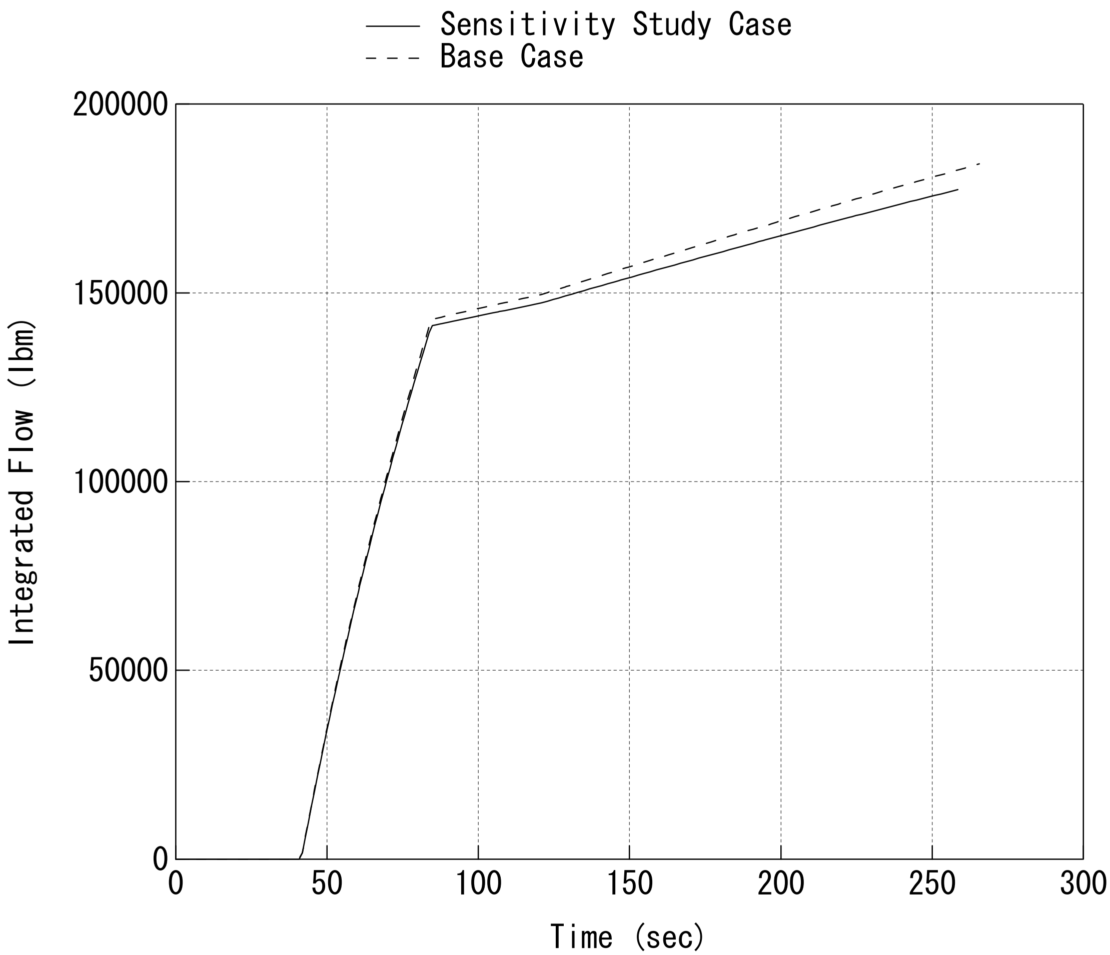

Rev. 2

Figure 3-42 Integral of Broken Loop RCP Side Break Flow from WREFLOOD

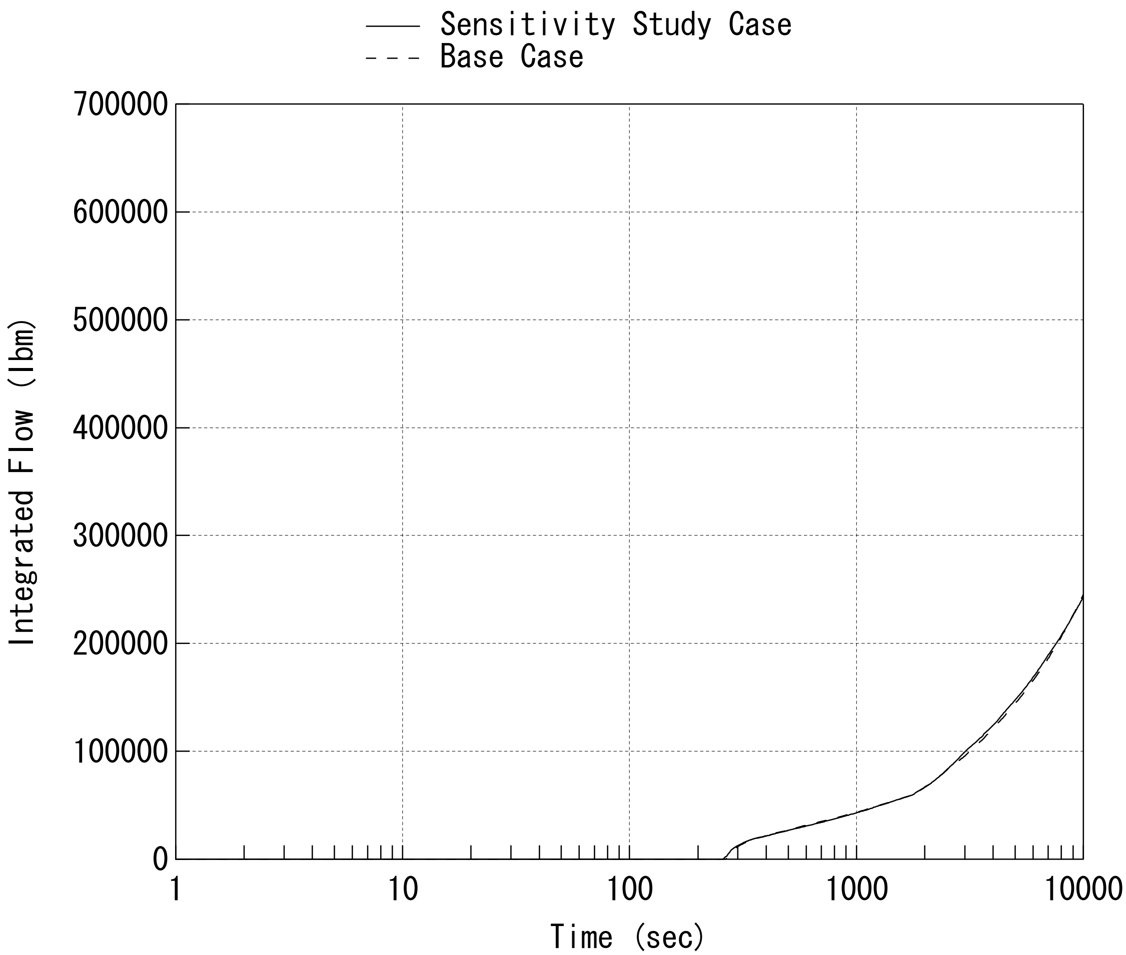

Rev. 2

Figure 3-43 Integral of Broken Loop SG Side Steam Flow from GOTHIC

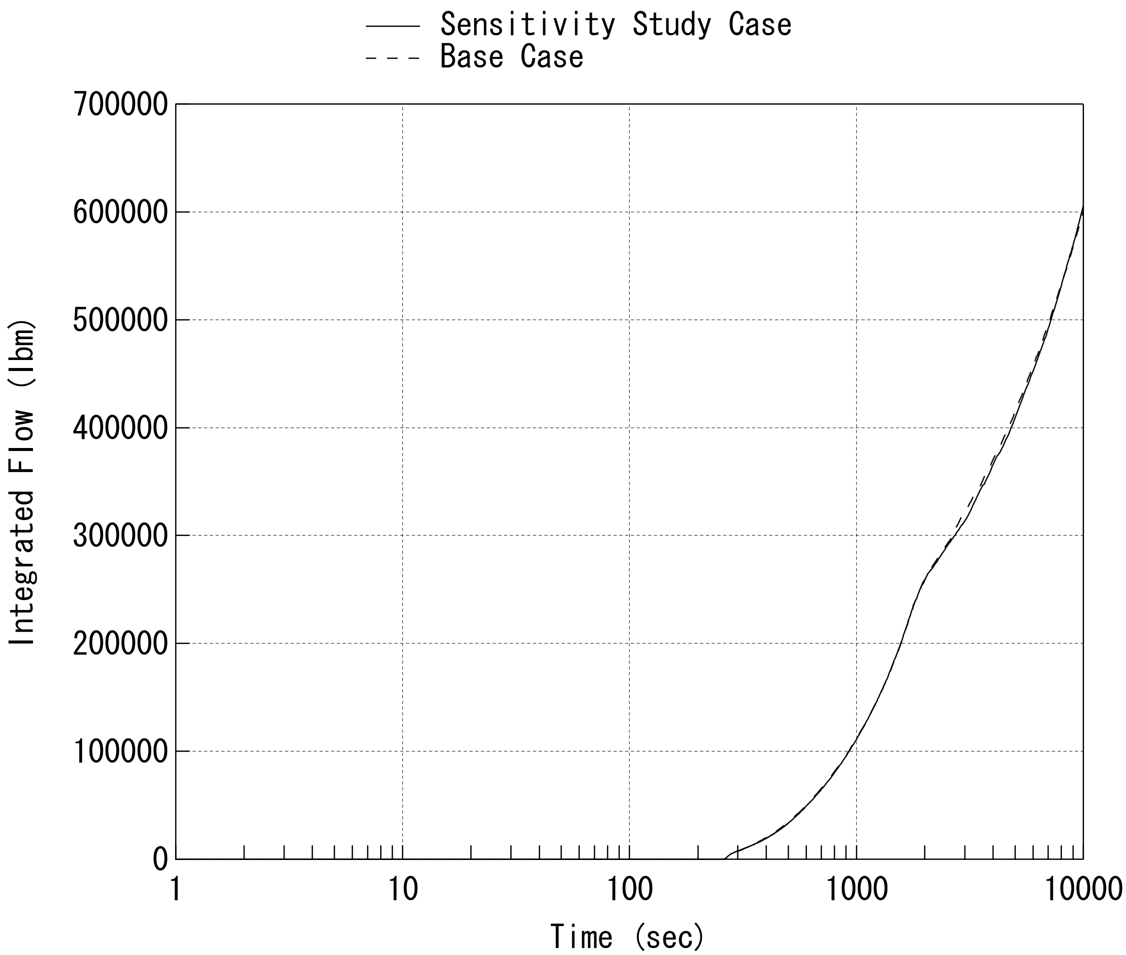

Rev. 2

Figure 3-44 Integral of Broken Loop RCP Side Steam Flow from GOTHIC

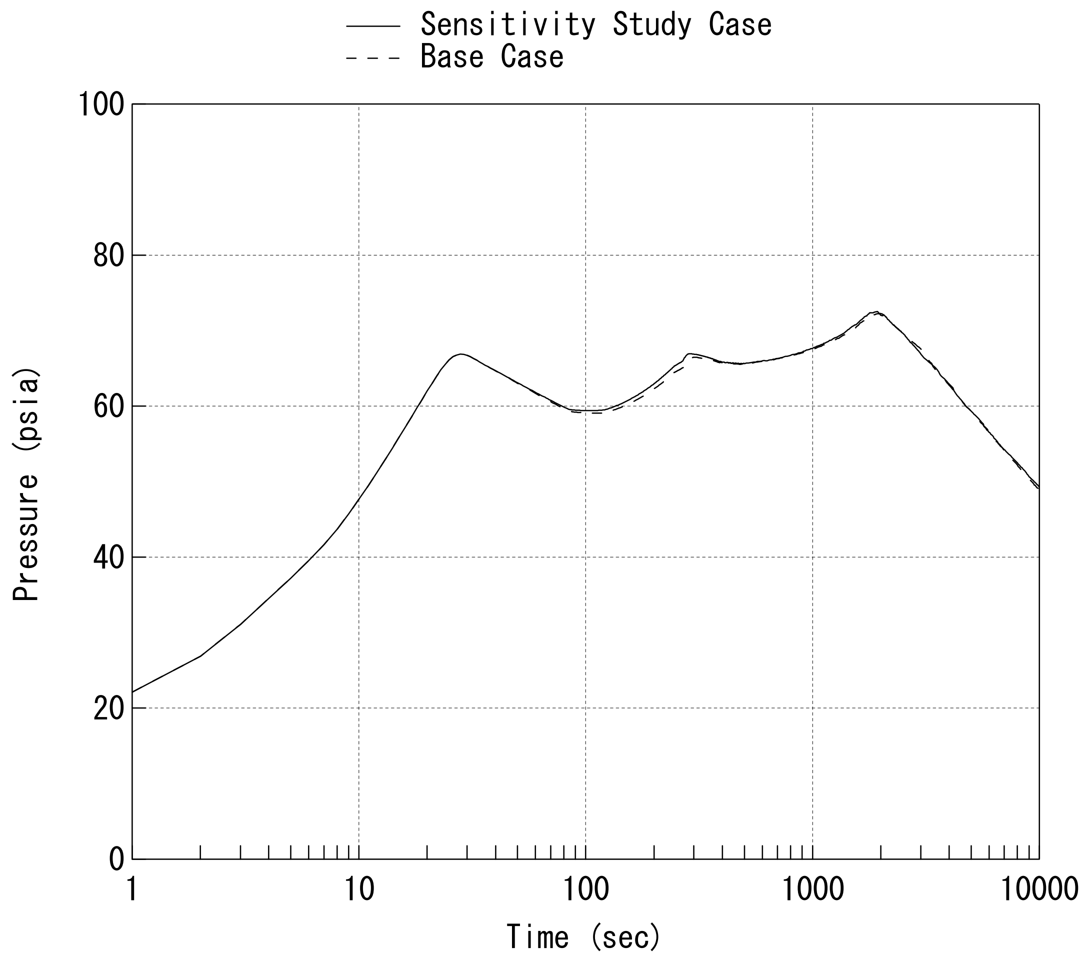

Rev. 2

Figure 3-45 Containment Pressure

Rev. 2

Figure 3-46 Noding Diagram of GOTHIC for Simulation of Loop Seal Formation in Intact Loop

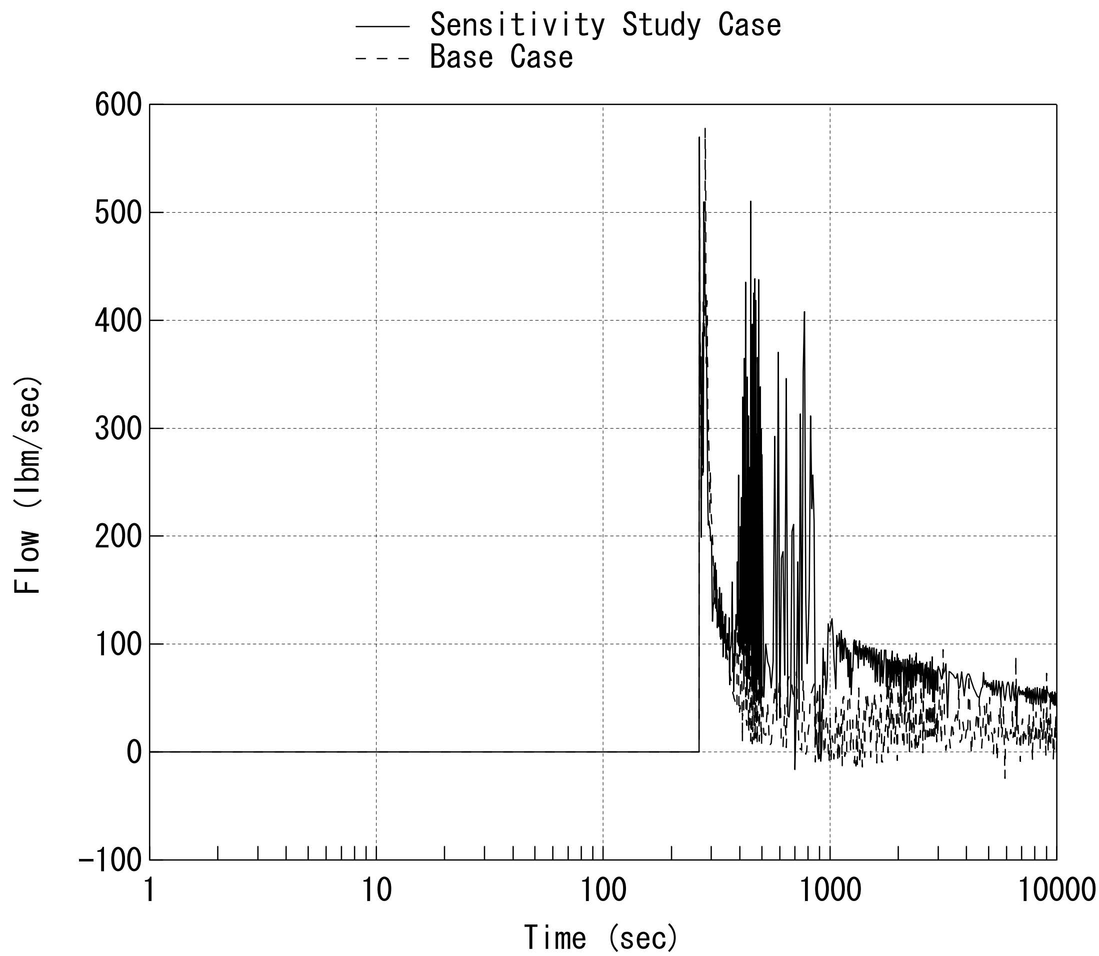

Rev. 2

Figure 3-47 Break Steam Flow from Broken Loop SG Side

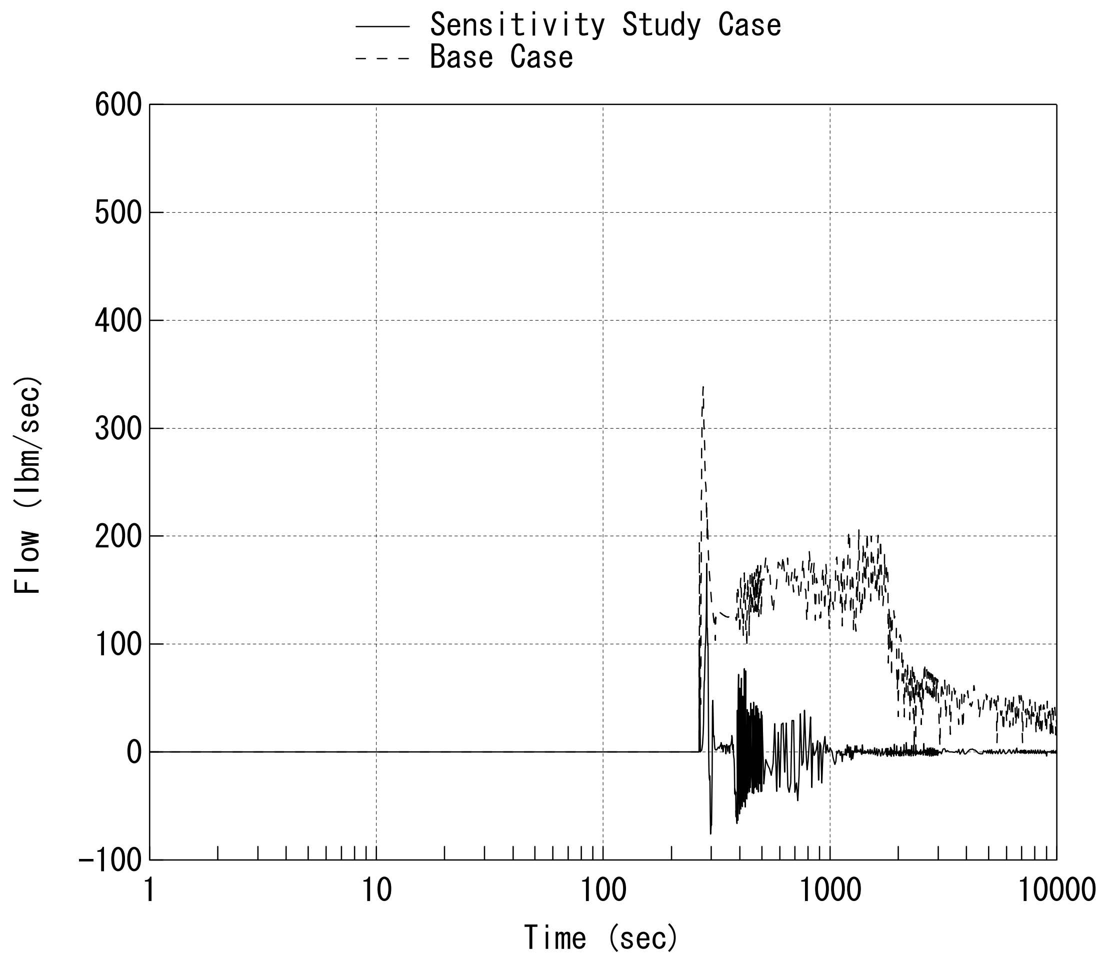

Rev. 2

Figure 3-48 Break Steam Flow from Broken Loop RCP Side

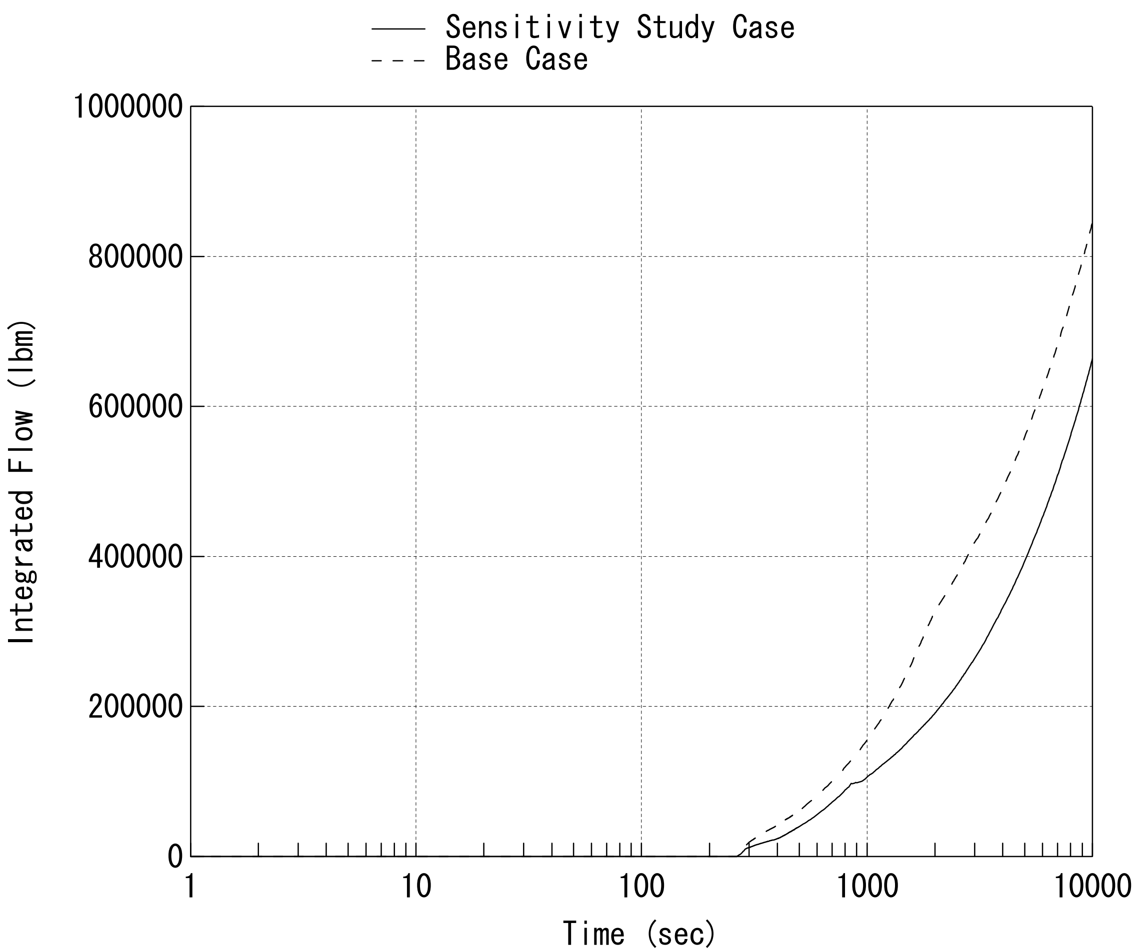

Figure 3-49 Integral of Total Steam Flow to the Containment

Rev. 2

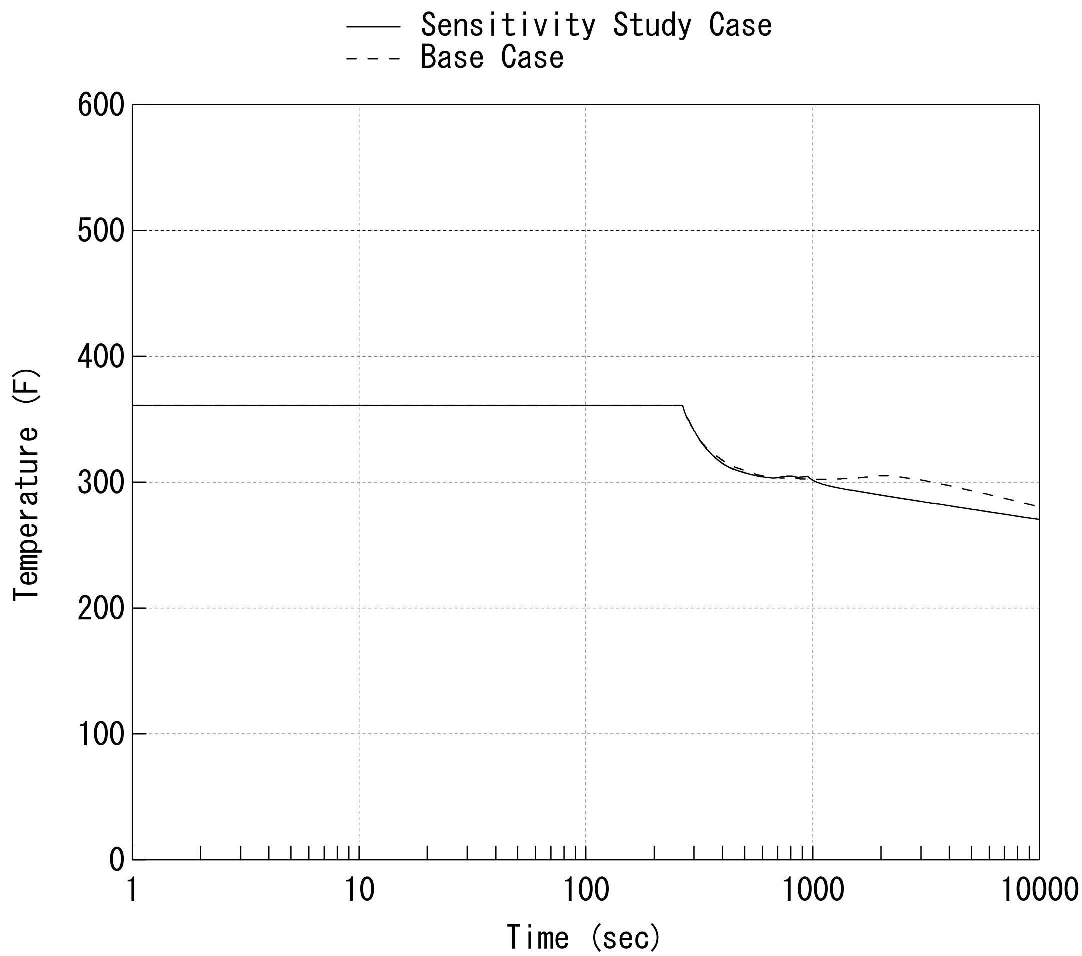

Rev. 2

Figure 3-50 Broken Loop SG Secondary Side Temperature

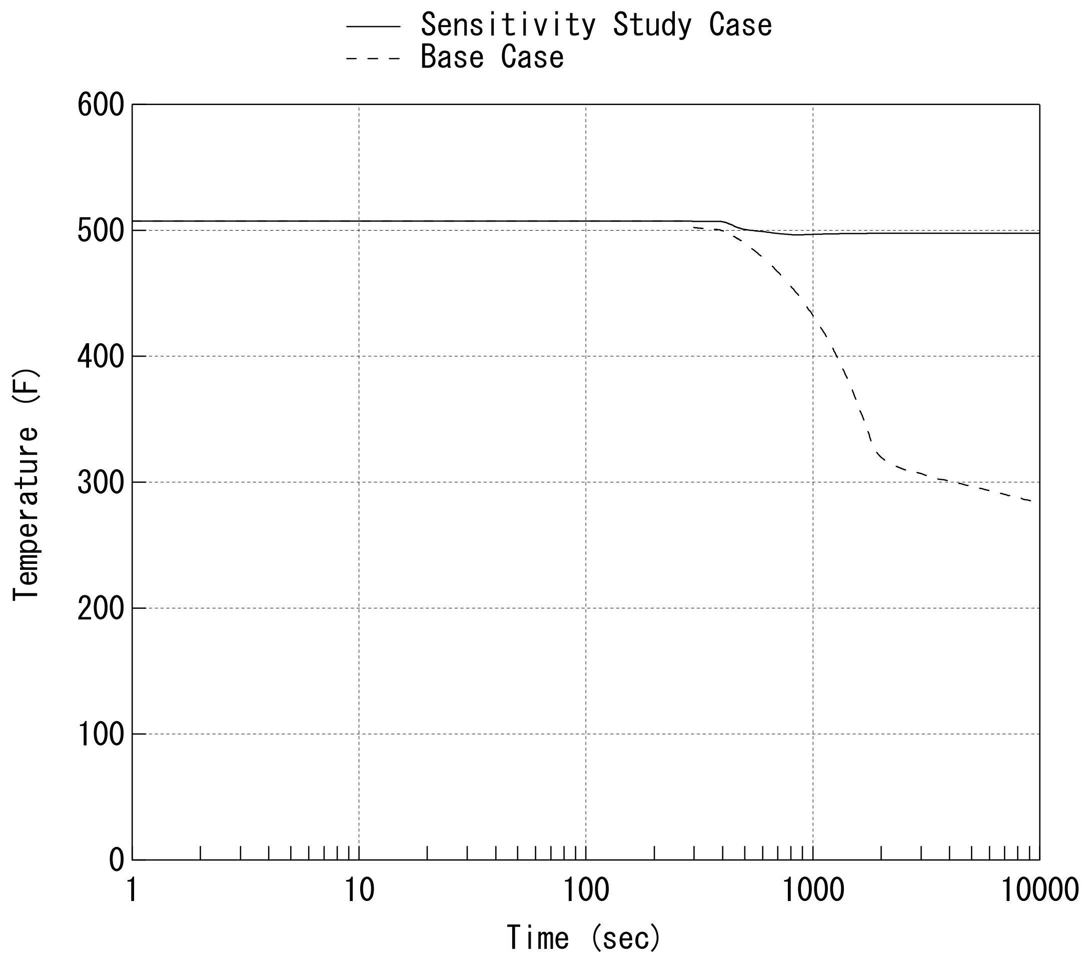

Rev. 2

Figure 3-51 Intact Loop SG Secondary Side Temperature

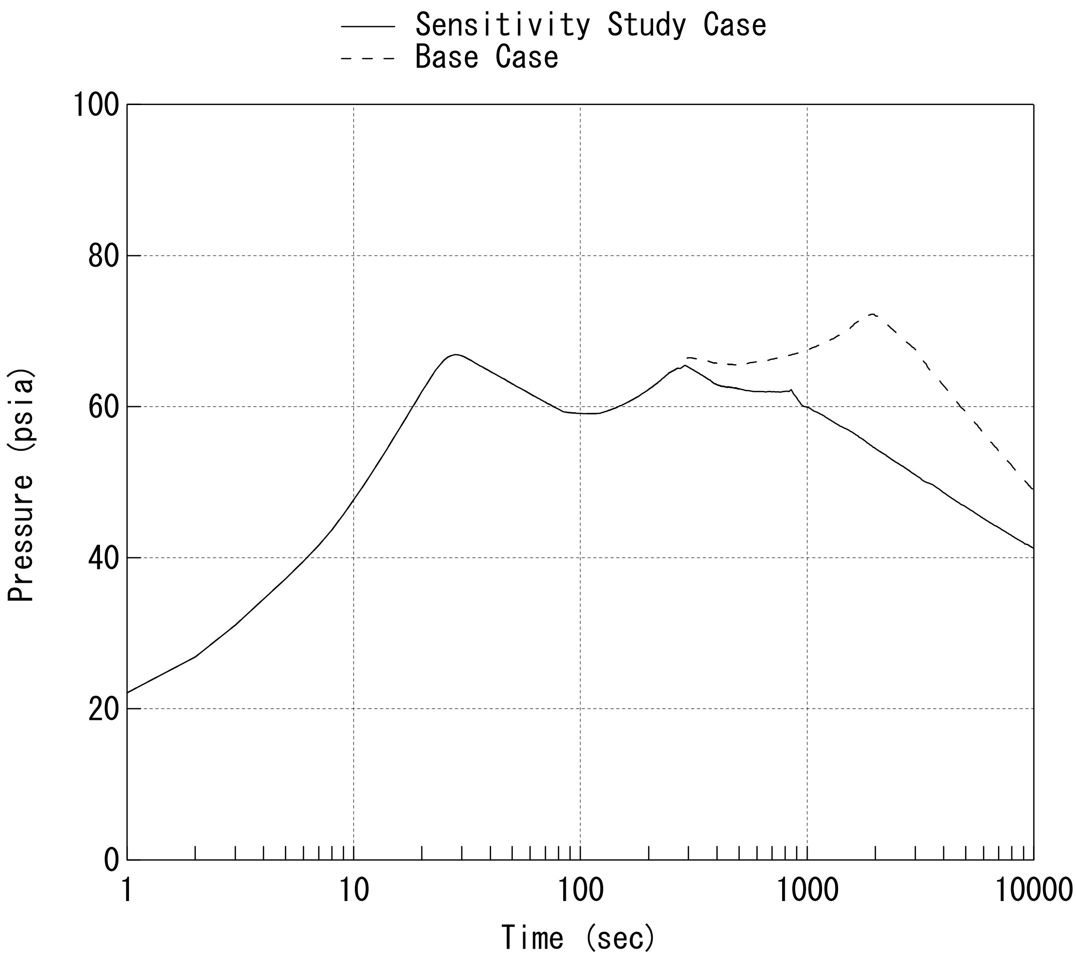

Rev. 2

Figure 3-52 Containment Pressure

Rev. 2

Figure 3-53 Integral of Steam Release Rate after Peak Pressure

Figure 3-54 GOTHIC Model for Eliminating Effects of Oscillation

Rev. 2

Rev. 2

Figure 3-55 Sensitivity for Initial Conditions

Rev. 2

Figure 3-56 Integrated Mass Flow Rates at Junction between Downcomer and Lower Plenum

Rev. 2

Figure 3-57 Sensitivity of Lag Constants on Lower plenum Inlet Flow

Rev. 2

Figure 3-58 Sensitivity of Lag Constants on Containment Pressure

Rev. 2

Figure 3-59 Differential Pressure between Downcomer and Lower Plenum

Rev. 2

Figure 3-60 SG secondary Side Fluid Temperature

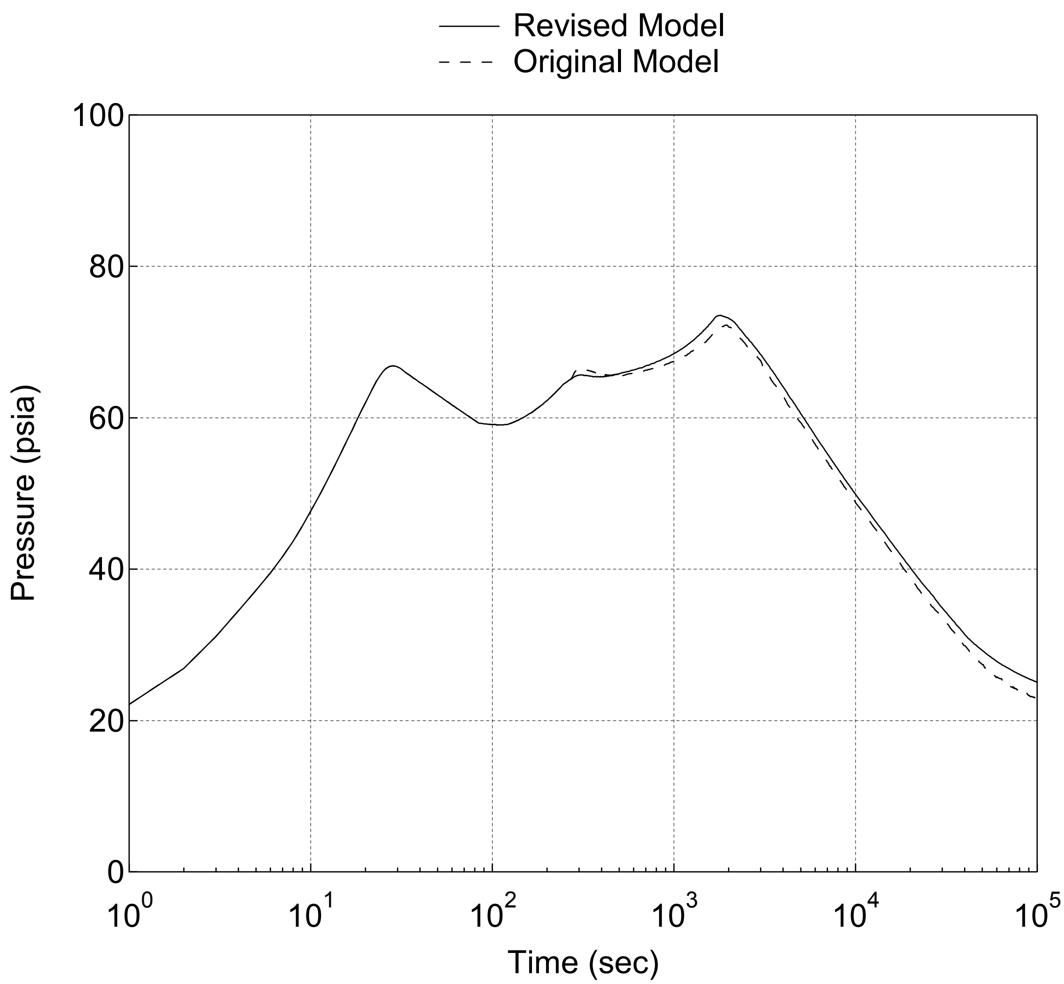

Figure 3-61 Containment Pressure Using Proposed Model

Rev. 2

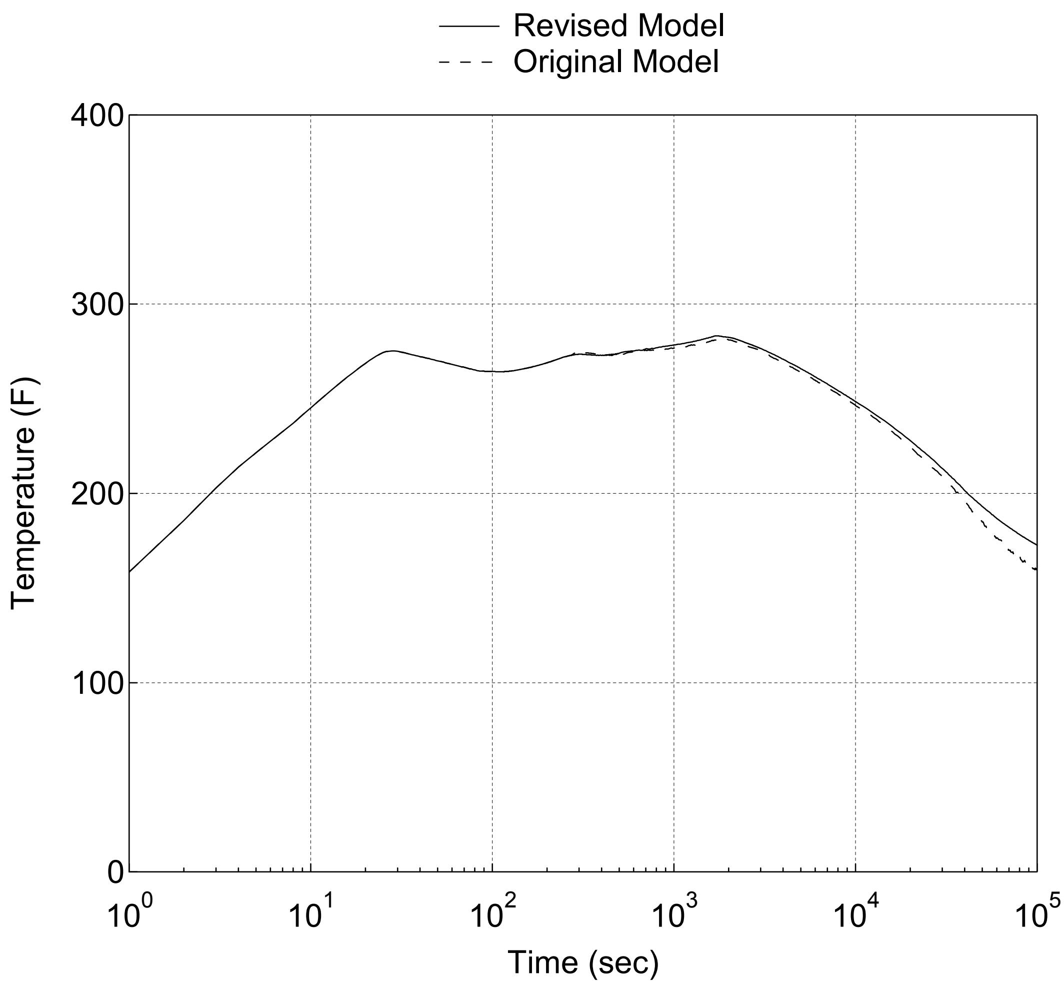

Rev. 2

Figure 3-62 Containment Atmospheric Temperature Using Proposed Model

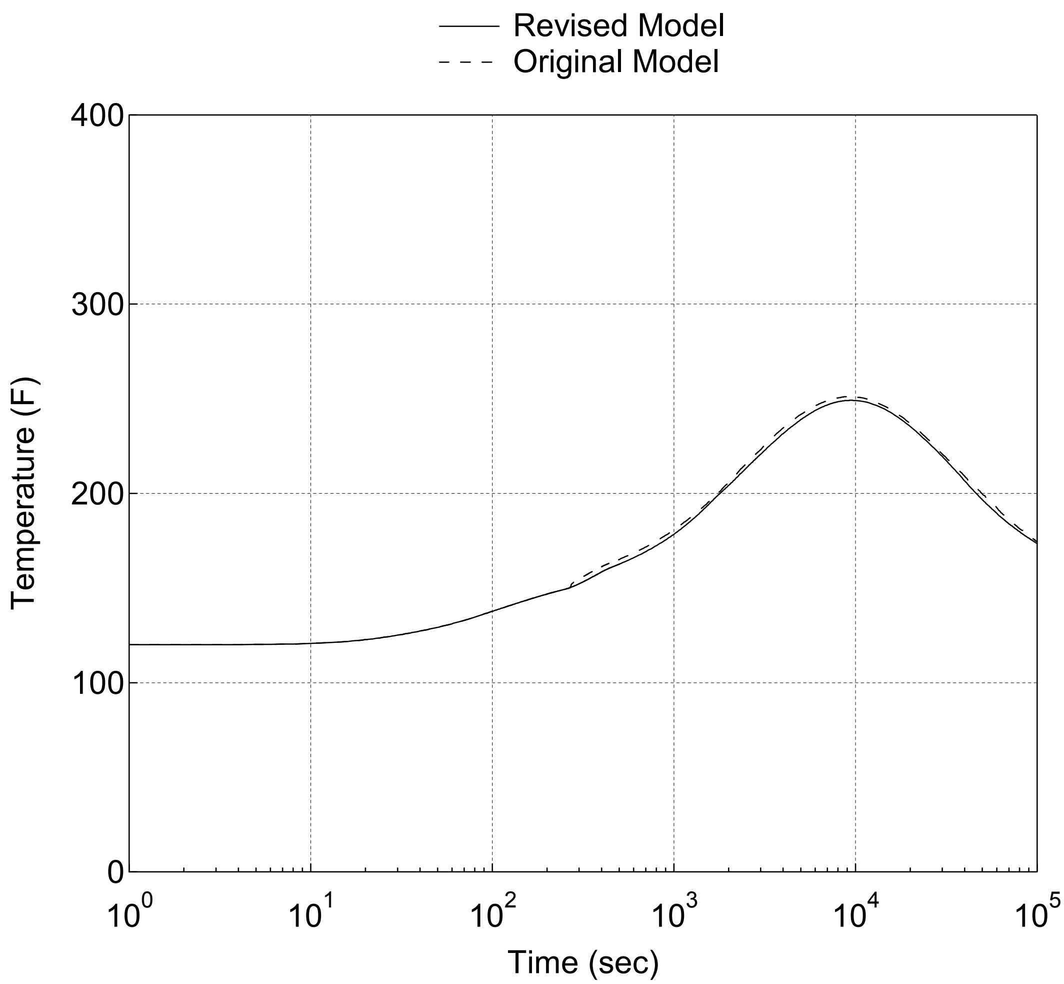

Rev. 2

Figure 3-63 Containment RWSP Water Temperature Using Proposed Model

Rev. 2

Figure 3-64 Integrated of Mass Flow Rates at Junction between Downcomer and Lower Plenum Using Proposed Model

4.0 CONCLUSIONS

The US-APWR, an advanced PWR with improved design, is retaining many basic features of the existing 4-loop PWR. Therefore the methodology for calculation of mass and energy release to the containment following a design basis loss-of-coolant accident has been developed based on the approved one for the existing PWR with minor modifications to address specific features of the US-APWR.

For Blowdown and Reflood phases, SATAN-VI and WREFLOOD (Reference 2) is utilized with minor modifications for the US-APWR design features, respectively. SATAN-VI was modified for the advanced accumulator and so was WREFLOOD for the advanced accumulator, no steam water mixing of direct vessel injection, the refueling water storage pit and the neutron reflector. All the modifications were confirmed to be appropriate by either test calculations or sensitivity studies.

For post-reflood phase, the GOTHIC code, which has also been already approved by the NRC (Reference 8), is utilized with no modification. Rev. 2

A sample analysis of the US-APWR with the methodology was performed for the large break LOCA, and a reasonable transient behavior was obtained.

The US-APWR mass and energy release analysis methodology is thus established and will be used when determining maximum containment pressure and temperature following a loss-of-coolant accident.

5.0 REFERENCES

1. NUREG-0800 : STANDARD REVIEW PLAN "6.2.1.3 MASS AND ENERGY RELEASE ANALYSIS FOR POSTULATED LOSS-OF-COOLANT ACCIDENTS (LOCAs)"

2. "Westinghouse LOCA Mass and Energy Release Model for Containment Design March 1979 Version," WCAP-10325-P-A, May, 1983.

3. Bordelon, F. M., et. al., "SATAN-VI Program: Comprehensive Space-Time Dependent Analysis of Loss-of-Coolant," WCAP-8302 (Proprietary Version), WCAP-8306 (Non-Proprietary Version), June 1974.

4. Kelly, R.D., et. al, "Calculational Model for Core Reflooding after a Loss-of-Coolant Accident (WREFLOOD Code)," WCAP-8170 (Proprietary Version), WCAP-8171 (Non-Proprietary Version), June 1974.

5. "GOTHIC Containment Analysis Package User Manual, Version 7.2a(QA)," NAI 8907-02 Rev 17, January 2006.

6. "GOTHIC Containment Analysis Package Technical Manual, Version 7.2a(QA)," NAI 8907-06 Rev 16, January 2006.

7. "GOTHIC Containment Analysis Package Qualification Report, Version 7.2a(QA)," NAI 8907-09 Rev 9, January 2006.

8. Letter from Gerald T. Bischof (Virginia Electric and Power Company) to United States Nuclear Regulatory Commission dated November 6, 2006, Transmittal of Approved Topical Report DOM-NAF-3 NP-A, "GOTHIC Methodology for Analyzing the Response to Postulated Pipe Ruptures inside Containment." ADAMS Accession No. ML063190467.

9. Cunningham, J.P. and H.C. Yeh, "Experiments and Correlation for PWR Small Break LOCA Conditions," ANS Transactions, Vol. 17, 1973, p369-370.

10. Lilly, G.P. and L.E. Hochreiter, "Mixing of Emergency Core Cooling Water with Steam: 1/3 Scale Test and Summary," EPRI 294-2, Electric Power Research Institute, June 1975.

11. ANS-5.1-1979, "American National Standard for Decay Heat Power in Light-Water Reactors," August 1979.

12. Letter from N Kalyanam (NRR) to James Scarola (Progress Energy) dated October 12, 2001, "Shearon Harris Nuclear Power Plant Unit 1 – Issuance of Amendment Re: Steam Generator Replacement and Power Uprate (TAC NOS. MB0199 AND MB0782)." ADAMS Accession No. ML012830516.

13. Letter from N. Kalyanam (NRR) to Charles M. Dugger (Entergy Operations) dated July 6, 2000, "Waterford Steam Electric Station, Unit 3 – Issuance of Amendment Re: Reduction in Operable Containment Fan Coolers in the Containment Cooling System (TAC NO. MA6997)." ADAMS Accession No. ML003731172

14. "The Advanced Accumulator," MUAP-07001-R1, January 2007

15. Bajorek, S. M., et al., 1998, “Code Qualification Document for Best Estimate LOCA Analysis,” WCAP-12945-P-A, Volume 1, Revision 2, and Volumes 2 through 5, Revision 1, and WCAP-14747 (Non-Proprietary).

16. F.F. Cadek, D.P. Dominicis, R.H. Leyse, “PWR FLECHT (Full Length Emergency Cooling Heat Transfer) Final Report,” WCAP 7665, April 1971.

17. N. Lee, S. Wong, L. E. Hochreiter, “PWR FLECHT SEASET Unblocked Bundle, Forced and Gravity Reflood Task Data Evaluation and Analysis Report,” NUREG/CR-2256, EPRI NP-2013, WCAP-9891, November 1981.

18. Dittus, F.W. and L.M.K. Boelter, University of California Publ, Eng,2,443,1930.

19. Chen,J.C.,”A Correlation for Boiling Heat Transfer to Saturated Fluids in convective flow “,ASME 63-HT-34,American Society of Mechanical Engineers,1963.

20. R.C. Howard and L. E. Hochreiter, “PWR FLECHT SEASET Steam Generator Separte Effects task Data Analysis and Evaluation Report” NRC/EPRI/Westinghuse-9,June 1981.

21. “Large Break LOCA Code Applicability Report for US-APWR ,” MUAP-07011(R0), July 2007

Rev 2

Appendix A The Advanced Accumulator Model Built into the SATAN-VI Code

The accumulator flow is calculated in subroutine of SATAN-VI. The advanced accumulator model for US-APWR was built into this subroutine. The configuration of the advanced accumulator model for SATAN-VI(M1.0) is shown in Figure A-1.

It is necessary to estimate the pressure at the flow damper outlet P_o to calculate the resistance coefficient of flow damper K_D. Therefore it is necessary to define the pressure at the flow damper outlet P_o, that is defined as follows,

(A-1)

The momentum equation in the SATAN-VI code is considered the inertia force (Reference 3).

The cavitation factor σ_v is calculated from the flow condition at ACC tank and flow damper outlet as follows,

(A-2)

The flow rate coefficient C_v is calculated using the following correlations obtained from test data which cover the range of applicability for the US-APWR design.

$$\begin{cases} C_v^i = 0.7787 - 0.6889\exp\left(-0.5238\sigma_v^i\right) & \text{(For large flow rate)} \\ C_v^i = 0.07197 - 0.01904\exp\left(-6.818\sigma_v^i\right) & \text{(For small flow rate)} \end{cases} \quad \textbf{(A-3)}$$

C_v is converted to the resistance coefficient of flow damper K_D.

$$K_D^i = 1 \Big/ \left(C_v^i\right)^2 \quad \textbf{(A-4)}$$

(A-5)

Total resistance coefficient for ACC system is calculated from K_D and following equation.

$$K_{ACC} = K_D + K_p \quad \textbf{(A-6)}$$

K_{ACC} : Total resistance coefficient of the flow damper and injection piping

The calculation flowchart of advanced accumulator model in SATAN-VI(M1.0) is shown in Figure A-2.

Figure A-1 The Configuration of Advanced ACC Model

Figure A-2 Calculation Flowchart of Advanced ACC Model in SATAN-VI(M1.0)

Appendix B The Advanced Accumulator Model Built into the WREFLOOD Code

The accumulator flow is calculated in subroutine[ ] of WREFLOOD. The advanced accumulator model for US-APWR was built into this subroutine. The configuration of the advanced accumulator model for WREFLOOD(M1.0) is shown in Figure B-1.

The velocity of the injection piping V_p is calculated as follows,

[ ] **(B-1)**

[ ] Therefore the equation for calculation of V_p is shown in equation B-1.

It is necessary to estimate the pressure at the flow damper outlet P_o to calculate the resistance coefficient of flow damper K_D.[ ] Therefore it is necessary to define the pressure at the flow damper outlet P_o, that is defined as follows,

[ ] **(B-2)**

The cavitation factor σ_v is calculated from the flow condition at ACC tank and flow damper outlet as follows,

(B-3)

The flow rate coefficient C_v is calculated using the following correlations obtained from test data which cover the range of applicability for US-APWR design.

$$\begin{cases} C_v^i = 0.7787 - 0.6889\exp\left(-0.5238\sigma_v^i\right) & \text{(For large flow rate)} \\ C_v^i = 0.07197 - 0.01904\exp\left(-6.818\sigma_v^i\right) & \text{(For small flow rate)} \end{cases} \quad \textbf{(B-4)}$$

C_v is converted to the resistance coefficient of flow damper K_D.

$$K_D^i = 1 \Big/ \left(C_v^i\right)^2 \quad \textbf{(B-5)}$$

Total resistance coefficient for ACC system is calculated from K_D and following equation.

$$K_{ACC} = K_D + K_p \quad \textbf{(B-6)}$$

K_{ACC} : Total resistance coefficient of the flow damper and injection piping

The calculation flowchart of advanced accumulator model in WREFLOOD(M1.0) is shown in Figure B-2.

Figure B-1 The Configuration of Advanced ACC Model

Figure B-2 Calculation Flowchart of Advanced ACC Model in WREFLOOD(M1.0)

Appendix C Validation of the NR Model for the Mass and Energy Evaluation

C.1 Introduction

C.2 Process for the Evaluation

C.3 Results of the Evaluation

C.4 Conclusions

Figure C-1 WCOBRA/TRAC Noding Diagram for the NR

Rev. 1

Figure C-2 Inlet and Outlet Pressure of the NR

Rev. 1

Figure C-3 Inlet Enthalpy of the NR

Rev. 1

Figure C-4 Temperature Distribution of the NR at the End of Reflood

Rev. 1

Figure C-5 Integral of Reflooding Rate

Rev. 1

Figure C-6 Integral of Reflooding Rate Times Mass Effluence Fraction

Rev. 1

Figure C-7 NR Outlet Mass Flow Rate with WCOBRA/TRAC

Rev. 1

Figure C-8 Collapsed Liquid Level

Appendix D Pump Discharge Break Analysis

As mentioned in Subsection 3.4.2.4, containment analyses for the limiting pump-suction break and the cold-leg pump discharge break are performed using a more realistic GOTHIC model within the expected parameter ranges in order to demonstrate the conservativeness of the GOTHIC model and the actual relation between both break cases. The following shows the details of the study.

Rev. 2

Rev. 2

Rev.2

D.2 Analyses

The containment analyses for the limiting pump-suction break and the cold leg (pump discharge) break have been performed using the above described GOTHIC realistic model. The relevant modeling assumptions for each model are summarized in Table D-1. Figures D-4 and D-5 illustrate the GOTHIC noding for the more realistic analyses for the pump suction break and the cold leg (pump discharge), respectively. The methodology for the blowdown and reflood phase is the same as the evaluation model.

Initial containment conditions, chosen conservatively for the evaluations, are listed in Table D-2. Assumptions for the containment heat removal and the SI system operability are shown in Table D-3.

Summary results for each LOCA analyzed are presented in Table D-4 and compared with the limiting pump suction break case with the evaluation model. The containment pressures and vapor temperatures are compared in Figures D-6 and D-7, respectively.
Comparison of results for the limiting pump suction break using the evaluation model and the realistic model demonstrates large conservatism in the evaluation model. Also, comparison of results for the pump suction break and the cold leg (pump discharge) break using the more realistic model demonstrates that the pump suction is the limiting break location.

During the post-reflood period, the cold leg break is found to give higher containment pressure rise than the pump suction break because of earlier heat release from the secondary side of the intact loop SG. However, since the increase of the containment pressure is small enough, the peak pressure for the cold leg break is still less than the peak pressure at the end of reflood for the pump suction break. Rev.2

D.3 Conclusion

For the limiting pump suction break, accumulator water injected into the pump-discharge side does not spill directly from the break. It has been demonstrated with the analyses simulating realistic phenomena that the cold leg (pump-discharge) break, where spillage of the broken loop accumulator is possible, is much less limiting in terms of the overall containment peak pressure than the pump suction break.

D.4 References

D-1 H. C. Yeh, “Modification of Void Fraction Correlation”, Proceedings of 4th International Topical Meeting on Nuclear Thermal Hydraulics, Operations and Safety, Volume 1, Taipei, Taiwan, April 5-9, 1994.ANS Transactions, Vol. 17, 1973, p369-370.

Table D-1 Comparison between Evaluation Model and Realistic Model with GOTHIC

Rev.2

Table D-2 Initial Conditions for Containment Pressure Analytical Model

Parameters	Value	Setting for Conservatism
A. Reactor Coolant System		
1. Reactor Power Level, MWt	4,451×1.02	Max (102%)
2. Average Coolant Temperature, °F	587.8	Max
3. Mass of Reactor Coolant System Liquid, lbm	7.42×10^{5}	Max
4. Mass of Reactor Coolant System Steam, lbm	1.02×10^{4}	
5. Liquid Plus Steam Energy,* Btu	4.41×10^{8}	Max
B. Containment		
1. Pressure, psig	2	Max
2. Temperature, °F	120	Max
3. Relative Humidity, %	0	Min
4. Service Water Temperature, °F	95	Max
5. Refueling Water Temperature, °F	120	Max
6. Outside Temperature, °F	Not Considered	Thermal Insulation is Assumed.
C. Stored Water (as applicable)		
1. RWSP water volume, ft^3** (gallon)	44,000 (329,000)	Min
2. Accumulators water volume, ft^3	1.03×10^{4}	Min

Notes:
* All energies are relative to 32°F [0°C].
** This includes RWSP minimum inventory and return water, plus a safety margin, but does not include the ineffective pool volume.

Rev.2

Table D-3 Engineered Safety Feature Systems Information

US APWR Specification	Value	
	Full Capacity	Value Used for Containment Design Evaluation
I. Passive Safety Injection System		
A. Number of Accumulators	4	4
B. Pressure, psig	695	586
II. Active Safety Injection Systems		
A. High Head Injection System (HHIS)		
1. Number of Lines	4	2
2. Number of Pumps	4	2
3. Flow Rate, gpm/train *	1,540	1,259
4. Response Time, sec (after analytical limit of SI signal reached)	3 (Offsite Power Available)	118
III. Containment Spray System (CSS)		
A. Number of Lines	4	2
B. Number of Pumps	4	2
C. Number of Headers	1	1
D. Flow Rate, gpm	9,800 (4 pumps)	5,290 (2 pumps)
E. Response Time, sec (after analytical limit of SI signal reached)	5 (Offsite Power Available)	243
IV. Refueling Water Storage Pit (RWSP)		
A. Liquid volume. Gallons	651,000	329,000
B. Liquid surface area ,ft^2	4,985	Interface Area is Ignored
V. Containment		
A. Free Volume (Air Volume), ft^3	2,800,000	2,743,000

Rev.2

Notes:
* HHIS flow rate is the value when RCS pressure is at 0psig.
Hot leg switch-over is conservatively not assumed, which leads to ignoring steam condensation with the hot leg injection.

Table D-4 Summary of Analysis Results

Rev.2

Rev.2

Figure D-1 Concept of Two-phase Level of the Vessel by GOTHIC

Rev.2

Figure D-2 Core Power Shape for the Realistic Analysis

Figure D-3 Core Void Profile

Rev.2

Figure D-4 Noding Diagram of GOTHIC for Realistic Analysis Pump Suction Break Case

Rev.2

Figure D-5 Noding Diagram of GOTHIC for Realistic Analysis Cold Leg (Pump Discharge) Break Case

Rev.2

Figure D-6 Comparison of Containment Pressure vs. Time

Rev.2

Figure D-7 Comparison of Containment Atmospheric Temperature vs. Time

Appendix E Effects of Flow Oscillation

Rev. 2

Rev. 2

Rev. 2

Figure E-1 Integral of Mass Flow Rate between Downcomer and Lower Plenum

Rev. 2

Figure E-2 Containment Pressure

Rev. 2

Figure E-3 Temperature of Injected Water and Lower Plenum Water

Rev. 2

Figure E-4 Differential Pressure between Downcomer and Lower Plenum

Appendix F Responses to NRC's Requests for Additional Information

Table of Contents

Rev. 2

INTRODUCTION

The following NRC's RAIs concerning the topical report, MUAP-07012-P(R0), "LOCA Mass and Energy Release Analysis Code Applicability Report for US-APWR" are responded to in the referenced reports below.

- "REQUEST FOR ADDITIONAL INFORMATION ON MASS AND ENERGY RELEASE ANALYSIS CODE APPLICABILITY FOR US-APWR TOPICAL REPORT MUAP-07012-P" dated December 31, 2007
- "A FOLLOW-UP REQUEST FOR ADDITIONAL INFORMATION ON MASS AND ENERGY RELEASE ANALYSIS CODE APPLICABILITY FOR US-APWR TOPICAL REPORT MUAP-07012-P" dated January 30, 2008

References 1 through 3 are integrated into Reference 4. Reference 4 also provides response to the requests related to flow oscillation in the GOTHIC calculation received at the beginning of March 2008.

This appendix provides the contents in Reference 4. Table F-1 shows the status for the responses to the requests on the topical report. The responses are incorporated into the body of this topical report as shown in Table F-1.

References Rev. 2

1. "MHI's Responses to NRC's Requests for Additional Information on Topical Report MUAP-07012-P(R0) LOCA Mass and Energy Release Analysis Code Applicability Report for US-APWR," UAP-HF-08033-P(Proprietary), UAP-HF-08033-NP(Non-Proprietary), January 2008.

2. "MHI's Second Responses to NRC's Requests for Additional Information on Topical Report MUAP-07012-P(R0) LOCA Mass and Energy Release Analysis Code Applicability Report for US-APWR," UAP-HF-08049-P(Proprietary), UAP-HF-08049-NP(Non-Proprietary), February 2008.

3. "MHI's Response to NRC's Follow-Up Request for Additional Information on Mass and Energy Release Analysis Code Applicability for US-APWR Topical Report MUAP-07012-P," UAP-HF-08048-P(Proprietary), UAP-HF-08048-NP(Non-Proprietary), February 2008.

4. "Response Package to NRC's Requests for Additional Information on Topical Report MUAP-07012-P(R0) LOCA Mass and Energy Release Analysis Code Applicability for US-APWR," UAP-HF-08083-P(Proprietary) Rev. 1, UAP-HF-08083-NP(Non-Proprietary) Rev.1, May 2008.

Table F-1 Status for Responses to RAIs

Item No.	Status for Responses	Revision of Topical Report to be Submitted	
RAIs dated December 31, 2007			
1a	Same as UAP-HF-08033	Included in	Subsection 3.2.3.1
1b	Same as UAP-HF-08033		Subsection 3.2.3.1
2	Same as UAP-HF-08033		Subsection 3.3.2.2(7)
3	Same as UAP-HF-08033		Subsection 3.4.2.1
4	Same as UAP-HF-08033		Subsection 3.4.1
5	Same as UAP-HF-08033		Subsection 3.4.1
6	Same as UAP-HF-08033		Subsection 3.2.3
7	Same as UAP-HF-08033		Subsection 3.4.1
8	Same as UAP-HF-08049		Subsection 3.4.2.2
9	Same as UAP-HF-08033		Subsection 3.2.1
10	Same as UAP-HF-08033	Not Applicable	
11a	Same as UAP-HF-08049	Included in	Subsection 3.4.2.2
11b	Same as UAP-HF-08033		Subsection 3.3.2.2(8)
11c	Same as UAP-HF-08033		Subsection 3.3.2.2(3)
11d	Same as UAP-HF-08033		Subsection 3.3.2.2(4)
11e	Same as UAP-HF-08033		Subsection 3.3.2.2(3)
11f	Same as UAP-HF-08033		Subsection 3.3.2.2(3)
11g	Same as UAP-HF-08033		Subsection 3.3.2.2(3)
11h	Same as UAP-HF-08033		Subsection 3.3.2.2(3)
11i	Same as UAP-HF-08033		Subsection 3.3.2.2(1)
11j	Same as UAP-HF-08033		Subsection 3.3.2.2(5)
11k	Same as UAP-HF-08049		Subsection 3.4.2.3
12	Same as UAP-HF-08033		Subsection 3.4.1
13	Same as UAP-HF-08033		Subsection 3.4.1
14	Response in UAP-HF-08033 is supplemented		Subsection 3.4.1
15	Same as UAP-HF-08033		Subsection 3.2.3.2
16	Same as UAP-HF-08049		Subsection 3.4.2.4 Appendix D
17	Same as UAP-HF-08049		Subsection 3.4.2.4 Appendix D
18	Same as UAP-HF-08033		Subsection 3.2.3.6
Follow-up Request dated January 30, 2008			
19	Same as UAP-HF-08048	Not Applicable	
Requests in March, 2008			
20	Provided in this report	Included in	Subsection 3.4.2.5 Subsection 3.4.3 Appendix E
21	Response provided in this report		Subsection 3.3.2.2(7)

Rev. 2

1.0 Responses to RAIs dated December 31, 2007

Item 1

Beginning on page 3-3, modeling of the advanced accumulator within the SATAN-IV and WREFLOOD computer codes is described.

Item 1a

Please describe any differences between this modeling and the advanced accumulator model in WCOBRA/TRAC that will be used to show compliance with 10CFR50.46. If differences exist, justify that the effect will lead to conservative containment analyses. If there are no significant differences, the staff plans to perform only one review for the advanced accumulator model in all 3 computer codes.

RESPONSE

The equations used to calculate the accumulator performance are identical for all three codes and there are no significant differences that affect the calculated accumulator flow rate. The main difference in modeling of the accumulator among these codes is that the accumulator injection line is treated as a path in the model for SATAN-VI and WREFLOOD while it is explicitly modeled as a control volume with multiple cells for WCOBRA/TRAC. Therefore, the flow damper outlet pressure, P_D, used in the following equation for the cavitation factor has to be calculated with an iterative scheme in the SATAN-VI and WREFLOOD as described in Appendix A and Appendix B of the topical report, while P_D is obtained from the pressure of the cell next to the accumulator tank in the WCOBRA/TRAC calculation. Rev. 2

In calculating P_D with the iterative scheme, accumulator flow is assumed to be quasi-steady, as explained in the response to Item 1b.

$$\sigma_v = \frac{P_D + P_{at} - P_v}{\left(P_{gas} + \rho g H_t\right) - \left(P_D + \frac{\rho V_D^2}{2} + \rho g H_D\right)}$$

σ_v : Cavitation factor
P_{at} : Atmospheric pressure
P_D : Flow damper outlet pressure (gage)
P_{gas} : Gas pressure in accumulator (gage)
P_v : Saturated vapor pressure
V_D : Fluid velocity of the injection piping
ρ : Density of water
g : Acceleration of gravity
H_t : Difference in height between accumulator water level and vortex chamber
H_D : Difference in height between flow damper outlet piping and vortex chamber

Item 1b

The description of the advanced accumulator flow model appears to be quasi-steady so as not to account for fluid inertia in the injection path. Please provide a discussion on the effect of not including injection path fluid inertia on the containment analysis.

RESPONSE

Fluid inertia effects are potentially significant only when the rate of change of the flow rate is large. So the discussion here is focused on the blowdown phase. Fluid inertia in the injection path is accounted for in the momentum equation of the SATAN code. However, it is not accounted for to calculate the resistance of the flow damper.

Fluid inertia affects the cavitation factor, σ_v, through the damper exit pressure, P_D, as described in the response to Item 1a.

Figure 1-1 shows the relation between σ_v and flow rate coefficient, Cv. The resistance of the flow damper, K, is related to Cv by $K=1.0/Cv^2$. The upper curve gives the relation between σ_v and Cv for the large-flow phase, which covers the blowdown phase. This curve indicates that Cv is essentially unaffected by changes in σ_v when σ_v is larger than around 5.

Figure 1-2 shows the transient of σ_v of the intact-loop accumulator during the blowdown phase, which indicates that σ_v is large enough not to affect Cv especially in the early blowdown phase when the effect of fluid inertia is large. This demonstrates that even if P_D is changed by fluid inertia, in turn leading to a change of σ_v, Cv is not affected. Rev. 2

Figure 1-1 Characteristics of Flow Damper

Rev. 2

Figure 1-2 Cavitation Factor during Blowdown Phase

Item 2

On page 3-3 the advanced accumulator model that is built into SATAN-VI and WREFLOOD is described. On page 3-15 injection of accumulator water into a cold leg using the US-APWR GOTHIC model is discussed. Has GOTHIC also been modified to include a model of the advanced accumulator? If so please describe this model and justify that it is conservative for containment analysis.

RESPONSE

GOTHIC has not been modified to include a model of the advanced accumulator because during the post-reflood phase the accumulator operates in the low flow mode, in which the flow resistance is nearly constant. The accumulator is modeled using basic GOTHIC modeling elements. The model includes the accumulator tank with the end of reflood water inventory and gas pressure specified. The flow from the accumulator is calculated by GOTHIC for the flow path connecting the accumulator to the cold leg with an constant resistance factor, whose value is calculated at the end of reflood in WREFLOOD (M1.0). Uncertainty of the flow resistance is included in the sensitivity studies for accumulator parameters.

Table 2-1 shows the result of the hand calculation using characteristics of the accumulator flow damper in order to confirm that the resistance factor at the end of reflood is appropriate on the accumulator conditions during long-term cooling period. The hand calculation was performed with the method described in Appendix B of the topical report. This result indicates that the flow resistance inputted in GOTHIC is consistent with the calculated value using accumulator conditions during long-term period. Rev. 2

Table 2-1 Hand Calculation of Accumulator Resistance Coefficient

Item 3

On page 3-5 it is stated that the treatment of uncertainties in the accumulator initial conditions (pressure, water mass and the injection pipe resistance) will be established by sensitivity studies. When will these sensitivity studies, as they relate to containment analysis, be completed and submitted for NRC staff review?

RESPONSE

These sensitivity studies are described in Subsection 6.2.1.1.3.4 of the US-APWR DCD.

The analyzed conditions and the results of the sensitivity studies are shown in Table 3-1. For the limiting case, minimum accumulator water volume and pressure and maximum injection resistance are assumed, to minimize steam condensation by the injected water. Sensitivity analyses demonstrate that the accumulator water volume, pressure, and injection resistance assumed for the limiting case give the most severe results. These parameters, however, do not have a large effect on the peak containment pressure and temperature because the peak pressure appears in the long term cooling phase, when steam condensation resulting from the accumulator water injection is relatively small compared to that in the reflood phase.

Table 3-1 Summary of Sensitivity of ECCS Conditions on the Containment Pressure and Temperature

Case	Limiting Case	Accumulator Max Water	Accumulator Max Flow
Break Location	Pump Suction	Pump Suction	Pump Suction
Break Size and Type	C_D=1.0 Double Ended Guillotine	C_D=1.0 Double Ended Guillotine	C_D=1.0 Double Ended Guillotine
Offsite Power	Lost	Lost	Lost
Assumption for Out of service*	1 Emergency Generator	1 Emergency Generator	1 Emergency Generator
Single Failure	1 Emergency Generator	1 Emergency Generator	1 Emergency Generator
Safety Injection	2 SIP Operation Minimum Safeguard	2 SIP Operation Minimum Safeguard	2 SIP Operation Minimum Safeguard
Accumulator Water Volume	Minimum	Maximum	Minimum
Accumulator Pressure	Minimum	Minimum	Maximum
Accumulator Line Resistance	Maximum	Maximum	Minimum
Peak Pressure, psia (psig)	72.2 (57.5)	71.9 (57.2)	72.1 (57.4)
Peak Atmospheric Temperature, °F	282	282	281
Peak RWSP Water Temperature, °F	251	251	251
24 hours Pressure, psia (psig)	23.6 (8.9)	Expected to be sufficiently low	Expected to be sufficiently low

* Out of service basis for the limiting conditions (maintenance or operation surveillance)

Rev. 2

Item 4

The topical report states that the SATAN-VI(M1.0) computer code will be used to describe the blowdown portion of a LOCA and the WREFLOOD(M1.0) computer code will be used to describe the reflood portion. Please describe the transition between the SATAN-VI(M1.0) and WREFLOOD(M1.0) analyses in greater detail. For the sample calculation in MUAP-07012, provide the reactor system water mass and temperature, temperature of the fuel in the core, the neutron reflector, reactor vessel heavy metal, steam generator heavy metal and steam generator water mass and temperature at the time of transition.

RESPONSE

The blowdown period is defined as the time from the accident inception, at steady state 102 % power operation, to the time that the Reactor Coolant System has depressurized to the containment pressure. The refill period is defined as the period from the end of blowdown to the time that the vessel lower plenum has been refilled by the ECCS. The reflood period is defined to the period from the time when water enters the active core to the time that the reactor core is quenched.

The SATAN-VI computer code has a model for calculating counterflow conditions in vertical flow paths by utilizing a drift flux approach. The most significant use of this model is in the calculation of sustained downflow of the accumulator water in the downcomer (called end of bypass). It is used to more accurately calculate the water inventory in the vessel at end of blowdown. This model is incorporated to comply with the requirements of 10 CFR 50.46 and does not affect the mass and energy release results significantly since the reactor vessel lower plenum is conservatively assumed to be full at the end of blowdown. That is, the refill period is conservatively assumed to be 0 seconds. This assumption is in conformance with Acceptance Criterion 1.C.iii. of SRP 6.2.1.3. Rev. 2

WREFLOOD reads temperatures and mass inventory at the end of blowdown period from SATAN-VI (1.0). Then the code calculates the transient for the refill period during which the water level in the reactor vessel increases due to the ECCS injection, until it reaches the bottom of the fuel rods. With this calculation, the vessel inventory and the parameters related to the ECCS are updated. The problem time, however, is retained at the end of blowdown. Then calculation for reflood period starts.

The reactor system water mass and temperature, temperature of the fuel in the core, the neutron reflector, reactor vessel heavy metal, steam generator heavy metal and steam generator water mass and temperature at the time of transition for the limiting case in the US-APWR DCD are provided in Table 4-1.

Table 4-1 Water Mass and RCS Temperature Transient

Rev. 2

Item 5

The staff could not find a description of treatment for the refill period following a LOCA in the topical report. Please describe treatment of this period of analysis and justify that this treatment is conservative.

RESPONSE

As described in the response to Item 4, the refill period is conservatively assumed to be zero seconds to initiate mass and energy release with the core reflood earlier.

Item 6

The topical reports described modeling of the advanced accumulator in SATAN-VI and WREFLOOD to produce the (M1.0) versions of the code. Please describe all other changes in SATAN-VI and WREFLOOD and justify that they are conservative for containment analysis.

RESPONSE

SATAN Changes (1 item):

(1) Modification of initial Neutron Reflector (NR) metal temperature.
NR is modeled using metal model in SATAN-VI. In the normal power operation, the neutron reflector metal temperature is higher than the coolant temperature due to the heat generated by gamma ray absorption. SATAN-VI is modified to allow different initial temperatures for the metal and fluid.

Rev. 2

WREFLOOD Changes (5 items):

(1) Steam-Water Mixing model in WREFLOOD
High pressure SI of the US-APWR injects directly into the reactor vessel downcomer (DVI). The nozzle elevation in the downcomer is almost same as the bottom of the inlet nozzle as shown in Figure 2-4 of the topical report. Hence, SI water readily mixes with accumulated water in the downcomer when the downcomer is full. Contact between the injected water and steam from the intact loop is very limited in this situation.

Consequently, it is assumed that no mixing of the DVI water with the steam in the downcomer. This assumption is actually implemented in WREFLOOD (M1.0) by a revision of the mass and energy balance for the downcomer. Complete mixing of DVI flow and water flow from the intact loop is assumed for calculating the enthalpy of the water entering the downcomer. All flow from DVI and the intact loop is added to the downcomer water when the downcomer is not full. When the downcomer is full, the combined DVI and intact loop flow that is in excess of the core inlet flow is spilled to the containment. The enthalpy of this spillage is the mixture enthalpy of the combined DVI and intact loop water flow. Steam flow from the intact loop passes the downcomer with no interaction with DVI flow. Condensation due to direct contact of DVI water flow with steam flow from the intact loop in the downcomer is disregarded.

The treatment of the DVI injection is conservative since any condensation potential of the DVI is reduced in WREFLOOD (M1.0).

(2) Modification of neutron reflector (NR) metal heat

[

] Validity of the modeling approach for a conservative analysis is confirmed in Appendix C of the topical report.

(3) Coupling of WREFLOOD with GOTHIC

US-APWR has RWSP in the containment and the RWSP is water source of the high head injection system. RWSP water temperature changes during LOCA transient. Hence, coupled calculation of WREFLOOD with GOTHIC is enabled to make the injected water temperature consistent with RWSP temperature calculated in GOTHIC.

Communication between WREFLOOD and GOTHIC is conducted by the existing IPC (Inter-Process Communication) function of GOTHIC and no modification of GOTHIC is required. WREFLOOD is modified by the addition of two subroutines to communicate with GOTHIC and code logic to set the current containment pressure and RWSP water temperature in WREFLOOD to match the current GOTHIC calculated values.

Data transferred from WREFLOOD to GOTHIC are as follows: Rev. 2

WREFLOOD time
Break flow (SG side)
Break flow enthalpy (SG side)
Break flow (RCP side)
Break flow enthalpy (RCP side)
DVI flow
Spilt flow
Spilt flow enthalpy

Data transferred from GOTHIC to WREFLOOD are as follows:

GOTHIC time
Containment pressure
RWSP water enthalpy

Validation of this function is confirmed by comparing transferred data in both sender and receiver sides.

(4) Modification of core fuel rod numbers

(5) Modification of FOUT correlation.

The FOUT correlation calculates the fraction of core total outlet mass flow to the inlet mass flow, F_{out}. In WREFLOOD (M1.0) the input parameters to FOUT are modified for conservatism as follows:

The above description is included in Subsection 3.2.3.5 of the topical report.

Item 7

The topical report references NRC staff approved Westinghouse methodology described in WCAP-10325-P-A. The WCAP provides lists of modeling options that were utilized in tables 1 through 4. Please provide comparisons of the options in these tables to those selected for analysis of USA-PWR. If differences exist, justify that the selected options are conservative. Rev. 2

RESPONSE

Comparisons of the options in the tables (7-1 through 7-4) to those selected for analysis of US-APWR are provided below. They show that, except for table 7-4, standard model options are used for the US-APWR. In table 7-4, PREF and HINJ are supplied from GOTHIC calculated values, since they are available through the simultaneous calculation with GOTHIC. The GOTHIC model is constructed to give conservatively high values for the containment pressure and RWSP enthalpy.

Table 7-1 Model Differences between SATAN V , SATAN VI and SATAN VI (M1.0)

	SATAN V	SATAN VI	SATAN VI (M1.0)
Drift Flux Model	No	Yes	Yes
Momentum Flux	No	Yes	Yes
Two Phase Pump Model	Simplified Model	Dynamic 2 ϕ Pump Model	Dynamic 2 ϕ Pump Model
Core Heat Release Model	Externally Calculated	Internally Calculated	Internally Calculated
Wall Heat Transfer Correlation (Nucleate Boiling)	Jens-Lottes	Thom	Thom
Thin Metal Heat Release Model	Externally Calculated	Internally Calculated	Internally Calculated
Film Boiling Heat Transfer Correlation	Dougall-Rohsenow	Westinghouse Transition Boiling	Westinghouse Transition Boiling

Table 7-2 SATAN VI and SATAN VI (M1.0) Comparisons of Significant Standard Inputs for ECCS & MASS/ENERGY RELEASE ANALYSES

Rev. 2

Input	Appendix K ECCS Analysis	Mass & Energy Release Analysis SATAN VI	Mass & Energy Release Analysis SATAN VI (M1.0)
IMAX	49	71	71
IUCP	0	1	1
IDNB	3	2	2
NCORE	8	2	2
NCHAN	2	1	1
NHOT(1)	6	1	1
PCONT	Minimum Value	Maximum Value	Maximum Value
VWABG1	Intact Loop	Broken Loop	Broken Loop
VWABG2	Broken Loop	Intact Loop	Intact Loop
DNBR	1	0.7	0.7
CON(1)	1	0	0
CON(2)	1	0	0
CON(7)	1	0	0
CON(8)	0	1	1
CON(13)	Minimum Value	Maximum Value	Maximum Value

Table 7-3 MODEL DIFFERENCES BETWEEN VERSIONS OF WREFLOOD

	WREFLOOD(IAC)	**WREFLOOD(FAC)**	**WREFLOOD(M1.0)**
Injection Section Pressure Drop	No	Yes – Not Used for M & E Analyses	Yes – Not Used for M & E Analyses
Injection section Steam/Water Mixing	No	Yes	Yes – for Accumulator Injection No – for HHIS (DVI Injection)
Two Phase Pressure Drop Multiplier	No	Yes	Yes

Table 7-4 Comparisons of Significant Standard REFLOOD Inputs for ECCS and Mass & Energy Release Analysis

Input	ECCS value	M & E Value (WREFLOOD)	M & E Value (WREFLOOD (M1.0))	Comment
ITSAT	3	4	4	This input when set to a value of 4 defines the case as a mass & energy release analysis.
IPMP	0	1	1	Reactor Coolant Pumps homologous curves are used for M & E analyses.
PREF	Calculated Containment Pressure	Containment Design Pressure	Calculated Containment Pressure	Calculated containment pressure is conservatively high.
HINJ	Minimum RWSP Water Enthalpy	Maximum RWSP Water Enthalpy	Calculated RWSP Water Enthalpy	Maximum initial RWSP water enthalpy is used.

Rev. 2

Item 8

Steam flow to the containment using the WREFLOOD code will be dependant on the piping resistances assumed for the reactor system. Please quantify the degree of conservatism which will be used in selecting piping resistances for the containment analysis.

RESPONSE

WREFLOOD analysis uses best estimate design value of primary loop piping resistance. A sensitivity analysis was performed to confirm quantitative effect of piping resistance error on the containment pressure. The sensitivity study used 20% lower piping resistance. In the sensitivity study GOTHIC loop resistance is also reduced 20% and analysis results show the effect of the reduced loop resistance both in reflood and post-reflood phases.

The following parameters from the sensitivity study are shown in Figure 8-1 to Figure 8-5 in comparison to the base case.

Integral of broken loop SG side break flow from WREFLOOD (Figure 8-1)
Integral of broken loop RCP side break flow from WREFLOOD (Figure 8-2)
Integral of broken loop SG side steam flow from GOTHIC (Figure 8-3)
Integral of broken loop RCP side steam flow from GOTHIC (Figure 8-4)
Containment pressure (Figure 8-5)

Results of the sensitivity study show slightly larger steam flow to the containment than the base case as shown in Figure 8-1 to Figure 8-4. The peak containment pressure is about 72.5 psia and is 0.3 psi higher than the base case as shown in Figure 8-5. The peak pressure is substantially lower than the design pressure. The effect of 20% lower loop resistance on the peak containment pressure is small, because most of the loop resistance is due to the RCP and piping resistance is relatively small. Rev. 2

This increase in the peak containment pressure due to lower primary loop resistance is small relative to the identified conservative margin in peak pressure[ ] as described in the response to Items 16 and 17.

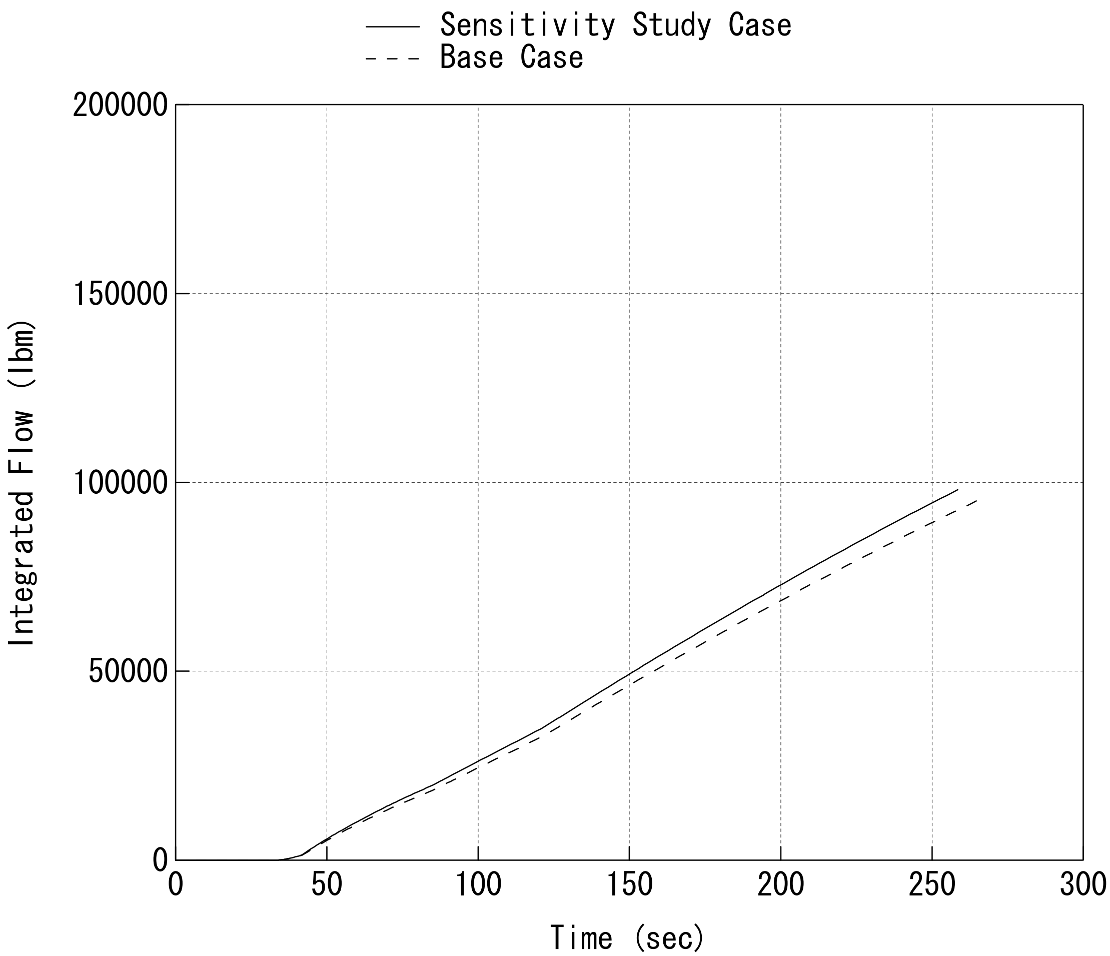

Figure 8-1 Integral of Broken Loop SG Side Break Flow from WREFLOOD

Rev. 2

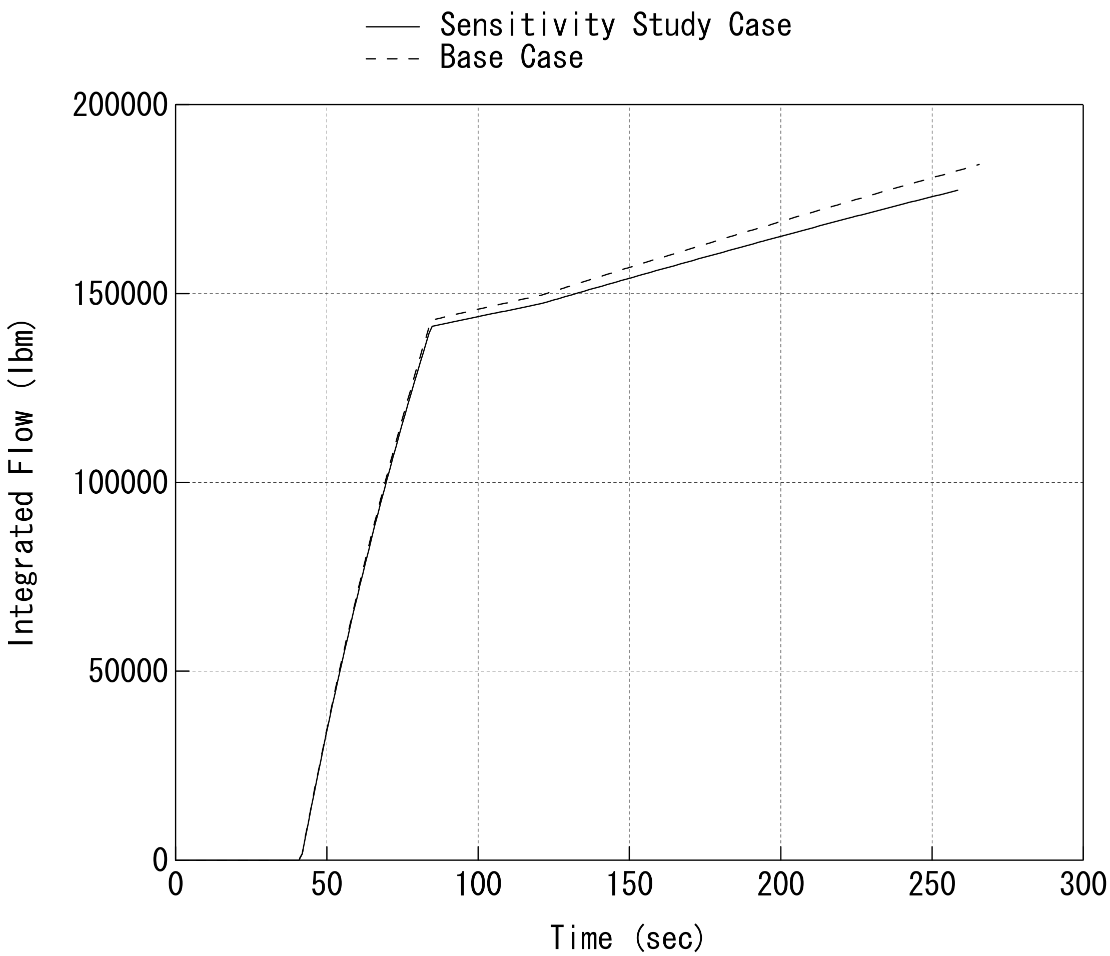

Figure 8-2 Integral of Broken Loop RCP Side Break Flow from WREFLOOD

Rev. 2

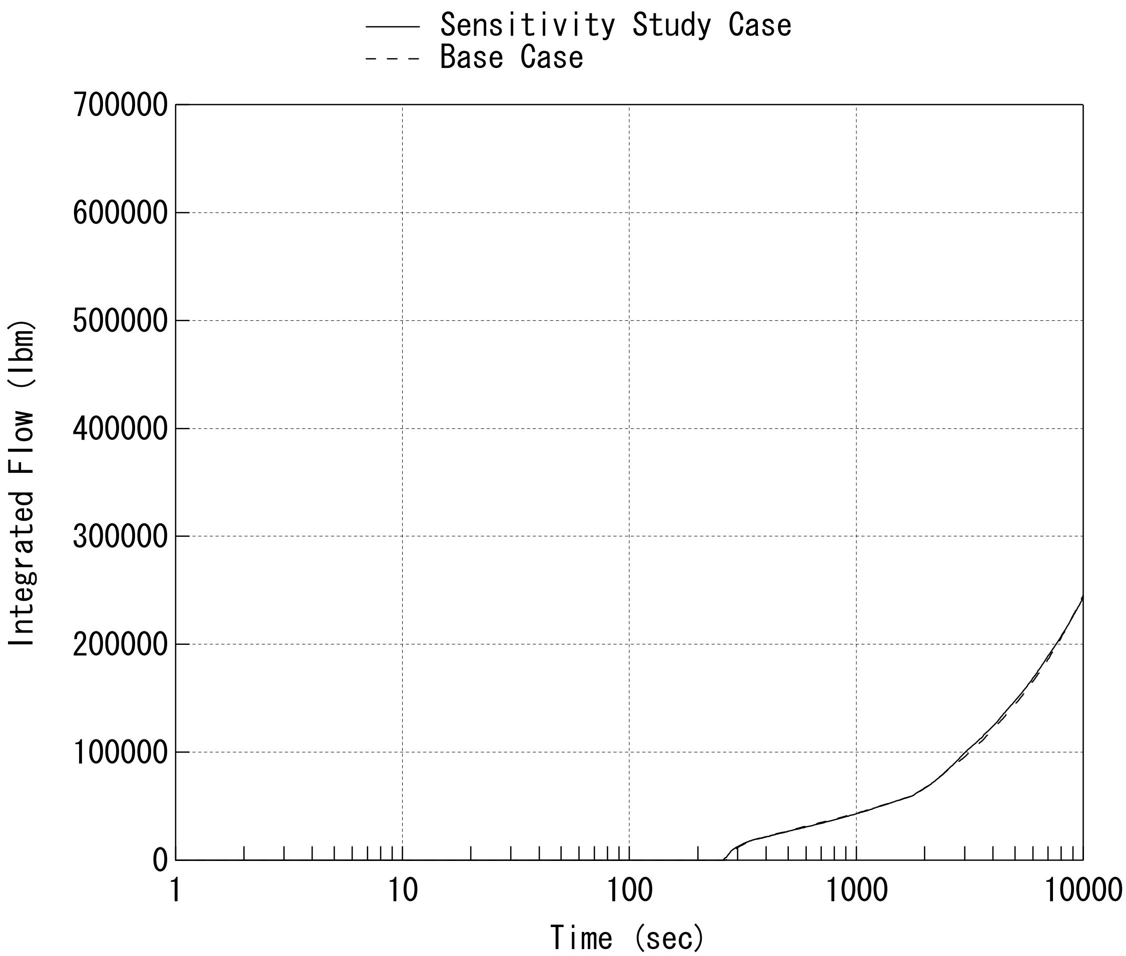

Figure 8-3 Integral of Broken Loop SG Side Steam Flow from GOTHIC

Rev. 2

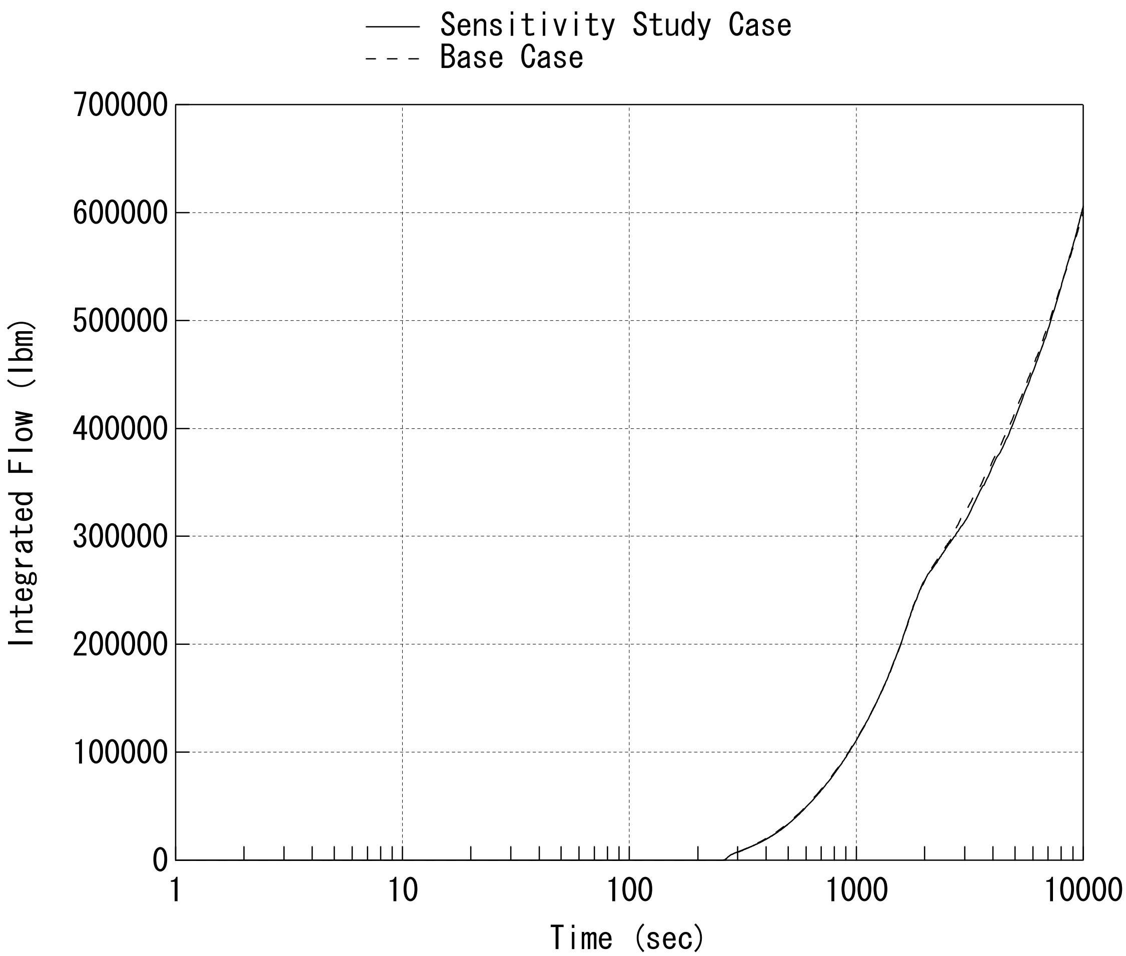

Figure 8-4 Integral of Broken Loop RCP Side Steam Flow from GOTHIC

Rev. 2

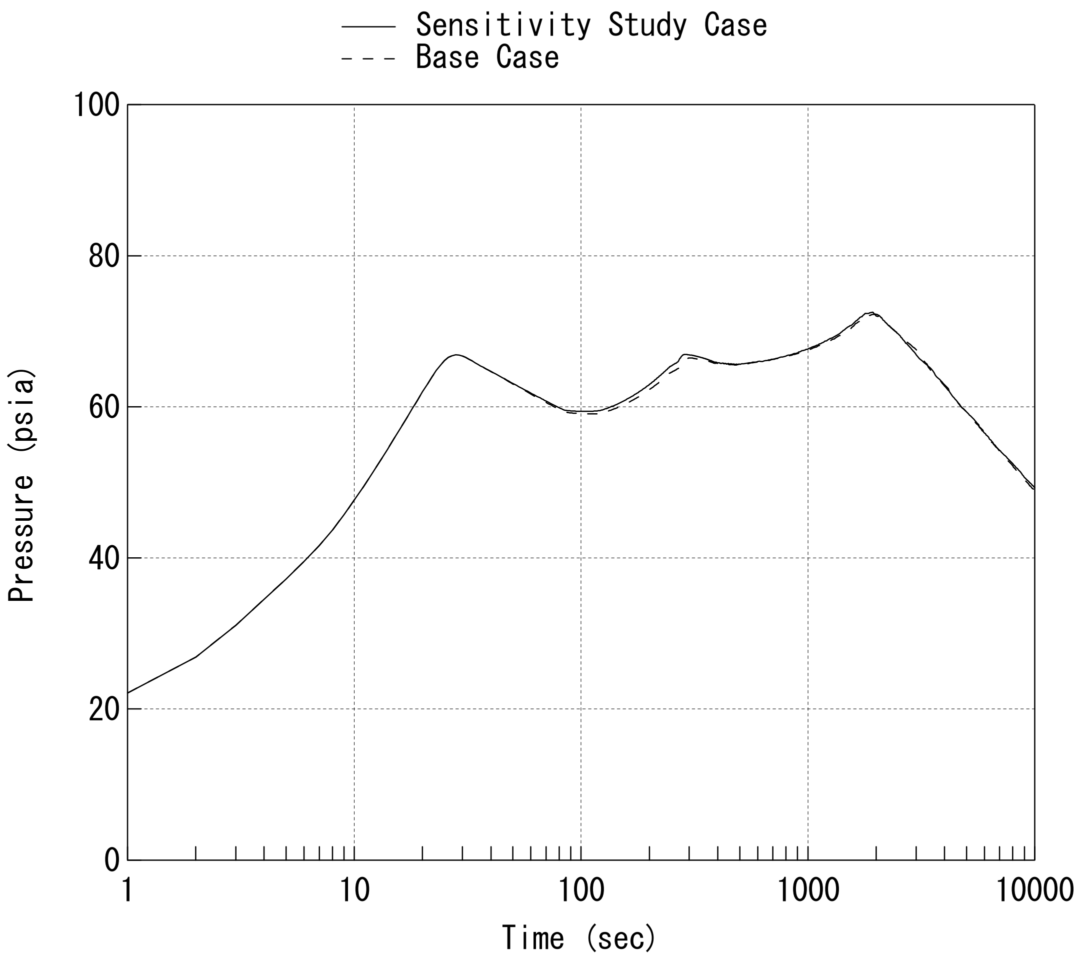

Figure 8-5 Containment Pressure

Rev. 2

Item 9

Figure 3-2 provides the SATAN-VI noding diagram for US-APWR. Please identify the nodes by which flow from the accumulators and the HHIS enters the reactor system.

RESPONSE

Figure 9-1 shows the SATAN-VI noding diagram for US-APWR with the accumulator injection paths. [ ] The high head injection is conservatively assumed unavailable during the blowdown phase along with the assumption of loss of offsite power.

Rev. 2

Figure 9-1 Noding Diagram of SATAN-VI
(Blowdown Phase Mass and Energy Release Analysis)

Item 10

Starting on page 3-12 a brief description of the GOTHIC containment model is presented. When will the detailed containment model be provided for staff review?

RESPONSE

The brief description of the GOTHIC containment model is presented for information. A detailed containment model is provided in the DCD.

Item 11

Starting on page 3-13 the GOTHIC model for predicting mass and energy release is described. Please describe the GOTHIC model in greater detail including the following considerations:

Item 11-a

Steam flow to the containment using the GOTHIC reactor system model will be dependant on the piping resistances assumed for the reactor system. Please quantify the degree of conservatism which will be used in selecting piping resistances for the containment analysis.

RESPONSE

GOTHIC loop resistances are best estimate values and as described in response to Item 8, the effect of lower loop resistance is small relative to conservatism in the peak pressure due to other modeling assumptions as described in the response to Items 16 and 17.

Rev. 2

Sensitivity studies to confirm effect of the conservativeness are performed and peak containment pressure reduction in the post-reflood phase is[ ]. This peak containment pressure reduction well surpasses pressure rise due to conservative loop resistance and US-APWR analysis model still has sufficient conservatism.

Item 11-b

The GOTHIC computer code provides very versatile methodology which gives many options to the users. Please identify all options selected that are relevant to mass and energy release calculations and justify that they are conservative.

RESPONSE

The GOTHIC model for the long term mass and energy release is based on the approach used for the Surry Nuclear Plant (Ref. 1). In the Surry analysis, it was shown that the methodology gave a mass and energy release rate that was very close to that calculated using the Westinghouse methodology (Ref. 1) which is conservative.

The peak containment pressure is determined mainly by the rate of energy release from the secondary side of the steam generators. From the FLECHT SEASET Steam Generator Separate Effects Tests (Ref. 2), it is apparent that the heat release rate from the steam generators is dominated by the rate of water delivery to the SG primary side. As long as the SGs are hotter than the primary system, the heat from the secondary side is enough to boil all of the water that enters the SG tubes. Heat transfer to the generated steam is relatively small. Therefore, the mass and energy release is primarily a function of the buoyancy driven water flow through the intact and broken loops and the amount of water that is carried from the core and into the SG tubes. Based on these observations, the predicted mass and energy release may be influenced by

- Noding of the SG primary side
- Noding of the SG secondary side
- Noding of the hot legs
- Noding of the SG inlet riser and inlet plenum
- Core and Upper Plenum noding
- Hydraulic diameter for the core and upper plenum nodes
- Loop resistance factors
- Flow Path stratified flow option
- Flow Path momentum transport option
- Flow Path compressibility option
- Liquid/Vapor Interface Area

Rev. 2

Rev. 2

Based on the above models, the long term mass and energy will be conservatively predicted by GOTHIC. The following options relevant to mass and energy release calculations are identified for each node and junction in Table 11-b-1 and Table 11-b-2.

For Volumes, see Table 11-b-1 (1/2):

For Flow Paths, see Table 11-b-1 (2/2):

References

1. Letter from Gerald T. Bischof (Virginia Electric and Power Company) to United States Nuclear Regulatory Commission dated November 6, 2006, Transmittal of Approved Topical Report DOM-NAF-3 NP-A, “GOTHIC Methodology for Analyzing the Response to Postulated Pipe Ruptures inside Containment.” ADAMS Accession No. ML063190467.
2. R. C. Howard and L. E. Hochreiter, “PWR FLECHT SEASET Steam Generator Separate Effects Task Data Analysis and Evaluation Report”, NRC/EPRI/Westinghouse-9, June 1981

Table 11-b-1 GOTHIC Options Used for US-APWR Mass and Energy Release Evaluation, Long Term of Loss-of-Coolant Accident (1 Sheet of 2)

Rev. 2

Table 11-b-1 GOTHIC Options Used for US-APWR Mass and Energy Release Evaluation, Long Term of Loss-of-Coolant Accident (2 Sheet of 2)

Rev. 2

Rev. 2

Figure 11-b-1 Noding Diagram of US-APWR Containment Integrity Analysis for Loss-of-Coolant Accident

Item 11-c

On page 3-14 it is stated that the fuel rods are modeled as a single WALL type conductor with a thickness specified to include the total mass of the fuel. Please describe how the fuel rods, including the cladding, are represented in the GOTHIC model in greater detail. Justify that it is conservative to model the cylindrical fuel rods with slab geometry and that the sensible heat in the fuel rods is released to the containment in a conservative manner.

RESPONSE

The following figure of the cross section of the fuel illustrates how a fuel rod, including the cladding, is represented in the GOTHIC model. The slab conductor is defined such that the surface area exposed to the fluid and the mass of each material are preserved. Compared to the cylindrical rod geometry, the slab geometry has a shorter effective conduction length which results in a faster (conservative) release of the stored energy in the fuel.

Since the core has quenched and is covered, the energy to be released is from the decay power generation and a small amount of stored energy as the pressure slowly changes. Therefore, the exact core geometry is less important.

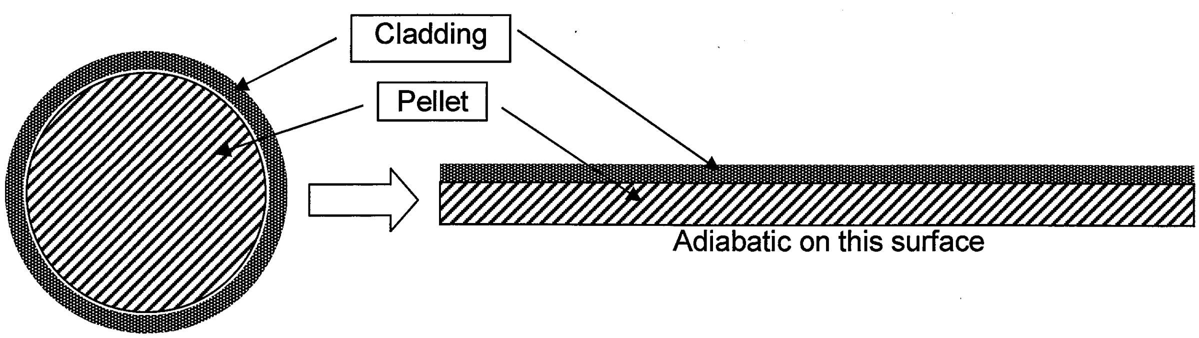

Cylindrical Fuel rod GOTHIC Slab Conductor

Rev. 2

Item 11-d

The FILM heat transfer option is stated to be used on all sides of the primary and secondary system conductors in contact with the fluid. Please describe this option in greater detail. What heat transfer correlations are used to calculate heat flow to liquid, steam and two-phase mixtures? Justify that these values are conservatively high for calculating the energy release.

RESPONSE

The FILM option is used for heat transfer for all conductors in the primary and secondary systems. This option includes convective and boiling heat transfer modes to the vapor and liquid. The heat transfer will be to the liquid phase unless there is insufficient water to support a liquid film on the surfaces. Convective heat transfer is the maximum of standard correlations for natural and forced convection. For boiling heat transfer, both nucleate and bulk boiling correlations are included. Film boiling is conservatively not considered.

The correlations are all based on best estimates. However, the following modeling conservatisms assure that the overall heat transfer rate is conservatively high:

1. All the vessel metal conductors are assigned to the core region to assure that they are in contact with the liquid to maximize the heat release.
2. The lumped modeling approach for the uphill SG tubes and the SG secondary side assures that both sides of the tubes are fully in contact with the water to maximize the heat transfer rate and the heat release from the steam generators.
3. For the downhill SG tubes, the outside of the tubes are in full contact with the SG water to maximize the heat transfer to the steam. The heat transfer to the steam on the inside of the tubes is the maximum of forced and natural convection.
4. All of the metal on the secondary side of the SG is in full contact with the liquid to maximize the heat release rate.

Using the FILM option, the logic for selecting the heat transfer coefficients for heat transfer between the conductor surface and the fluid is shown in Figure 11-d-1. Heat transfer coefficients are calculated for both the liquid and vapor phases, even though all heat transfer is generally to only one phase as determined by the logic shown in Figure 11-d-1. The phase heat transfer coefficients are multiplied by ramp functions that force the heat transfer to zero as the phase is depleted. The ramp functions are

Rev. 2

and

The ramp functions are applied as modifiers on the heat transfer coefficients, described below.

Single Phase Vapor

The single-phase vapor heat transfer coefficient (Hspv) is given by

$$H_{spv} = Max\begin{bmatrix} \dfrac{8k_v}{D_h} \\ \dfrac{k_v}{D_h}0.023Re_v^{0.8}Pr_v^{0.4} \\ \dfrac{k_v}{D_h}Max\left(0.13\left[Gr_vPr_v\right]^{1/3}, 0.59\left[Gr_vPr_v\right]^{0.25}\right) \end{bmatrix}$$

The first formula is a minimum value based on conduction through the vapor. The second formula is the Dittus-Boelter correlation for turbulent forced convection (Ref. 1). The third formula is for turbulent natural convection. The temperature difference in the Grashof number is given by

$$\Delta T = T_v - Max[T_w, T_{sat}(P_{vs})]$$

The wall source term for single-phase vapor heat transfer is

$$Q_{w_v} = \lambda_{w_v}H_{spv}A_{cn}(T_w - T_v)$$

Single-Phase Liquid

The single-phase liquid heat transfer coefficient is given by

$$H_{spl} = Max\begin{bmatrix} \dfrac{2k_l}{\delta} \\ \dfrac{k_l}{D_h}0.023Re_l^{0.8}Pr_l^{0.4} \\ \dfrac{k_l}{D_h}Max\left(0.13\left[Gr_lPr_l\right]^{1/3}, 0.59\left[Gr_lPr_l\right]^{0.25}\right) \end{bmatrix}$$

Rev. 2

These formulas are essentially identical to those used for single phase vapor. The primary difference is that the formulas are based on liquid properties. The first formula gives the heat transfer coefficient for conduction through a liquid film of thickness

[ ]

where the parameter f_{wa} is an adjustment factor for wetted areas. If there is sufficient liquid in the volume to cover all the wettable walls with a film that is at least 0.0001 ft thick, then all the wettable walls will be wet. If there is insufficient liquid to cover all the wettable walls, then a fraction of each wettable wall will be dry. A wall is wettable if the surface temperature is below the saturation temperature at the total fluid pressure.

The third formula is for turbulent natural convection. The temperature difference in the Grashof number is given by

$$\Delta T = T_l - Min[T_w, T_{sat}]$$

The wall source term for single-phase liquid heat transfer is

$$Q_{w_l} = \lambda_{w_l}H_{spl}A_{cn}(T_w - T_l)$$

Boiling

If the wall temperature is greater than the saturation temperature at the total pressure, then the liquid is in a boiling heat transfer regime. In the nucleate boiling regime, the Chen (Ref. 2) correlation is used. If the liquid is subcooled, subcooled boiling occurs that allows the generation of steam without bringing the bulk liquid temperature up to the saturation temperature. The Chen correlation is extended to cover subcooled nucleate boiling.

Condensation

Although condensation heat transfer correlations are incorporated into GOTHIC, they do not come into play for the reactor coolant system model.

References

1. Dittus, F.W., and L.M.K. Boelter, University of California, Publ. Eng., 2, 443, 1930.

2. Chen, J.C., A Correlation for Boiling Heat Transfer to Saturated Fluids in ConvectiveFlow, ASME 63-HT-34, American Society of Mechanical Engineers, 1963.

Rev. 2

Figure 11-d-1 Heat Transfer Selection Logic

Item 11-e

Core decay heat is stated to be calculated using the 1979 ANS model with two standard deviations of uncertainty added. NRC Information Notice 96-39 describes how users obtained differing results from the ANS standard depending on the input options selected. Please provide the assumptions selected for actinide contribution, actinide production, neutron capture effect, fissions per initial fissile atom and power history that will be input into the standard for US-APWR containment analysis and justify that conservative values have been selected.

RESPONSE

A decay heat curve based on ANSI/ANS-5.1-1979 (ANS-1979) model, which had been incorporated into the original SATAN and WREFLOOD codes, is used for the containment analyses for the US-APWR. The decay heat curve is shown in Figure 11-e-1 and the assumptions for input selection for this decay heat curve are described in the WCAP-10325-P-A "Westinghouse LOCA Mass and Energy Release Model for Containment Design March 1979 Version" as follows:

1.	Actinide contribution	: ^{239}U and ^{239}Np
2.	Actinide production (R-factor)	: 0.70
3.	Neutron capture effect	: Gmax
4.	Power history	: 10^8 seconds
5.	Fissile element	: 92% ^{235}U, 8% ^{238}U

These assumptions are considered applicable for the US-APWR since:

1. Actinide decay heat: the contribution of both ^{239}U and ^{239}Np decay heat was included considering an infinite operating time. Explicit analysis of the US-APWR core show that the most limiting R-factor is about [ ]. Rev. 2
2. Fission products (FPs) decay heat: the decay heat multiplier to account for the effect for neutron capture (G-factor) is assumed to be the maximum table value (G-max). The length of full power operation of 10^8 seconds before shutdown covers up to US-APWR 24-month operation conditions. Finally, the assumption that fission products are attributed to an 8% of ^{238}U and 92% ^{235}U with the conservative assumption that the fission energy release is 200MeV/fission covers US-APWR core conditions.

Therefore, the decay heat originally incorporated into SATAN and WREFLOOD code, which input selection assumptions are described in the WCAP-10325-P-A for generic use, can be apply for the US-APWR mass and energy analysis.

Rev. 2

Figure 11-e-1 Core Decay Heat Curve

Item 11-f

The GOTHIC model is stated to use two conductors to model the reactor system metal. Describe the components which are included within each to the conductors and justify that this treatment is conservative.

RESPONSE

Rev. 2

Item 11-g

Describe and justify the treatment of the sensible heat within the primary system piping.

RESPONSE

Item 11-h

Treatment of the “primary loop metal located on the secondary side of the steam generators” is discussed. Please identify the components referred to. The initial temperature of this metal is said to be set equal to the secondary side fluid temperature. Justify that this assumption is conservative.

RESPONSE

Rev. 2

Item 11-i

Please identify all code modifications made to GOTHIC for mass and energy release calculations.

RESPONSE

GOTHIC version 7.2a-patch5, revised from version 7.2a, is used for the US-APWR analyses.

This patch to GOTHIC version 7.2a was created to correct errors in the implementation of the Yeh correlation. The Yeh correlation is used to predict the two-phase mixture level and the vapor volume fraction within subdivided volume cells that are connected to a Flow Path or Network Link. These values are then used to determine the outflow conditions for the connected Flow Path or Network Link.

Two errors were identified in the original implementation: 1) the phase velocities were used to calculate the mixture level rather than the superficial velocities, 2) the Yeh correlation was only applied if the liquid volume fraction in the cell was above 0.5. Item 1 tended to cause the mixture level to be overestimated, while item 2 tended to cause the mixture level to be underestimated. Because of these counteracting effects, it is difficult to predetermine the impact of the problem on a particular model and to determine conservative input adjustments to counteract the errors. The patch was implemented for use in modeling situations that require the Yeh correlation on an interim basis until the next full release of GOTHIC becomes available. The patch is released under NAI's QA program for GOTHIC, which satisfies the requirements of 10CFR50 Appendix B with error reporting in accordance with 10CFR21.

The modifications to the Yeh correlation described above are the only differences between GOTHIC 7.2a and GOTHIC 7.2a-patch 5. No modifications were made to the GOTHIC version 7.2a-patch5.

Item 11-j

On page 3-15 the discussion of the treatment of two-phase level by GOTHIC is not clear. Please describe this modeling in greater detail and justify that the treatment of the two-phase mixture leaving the core and calculated to enter the steam generators is conservative. Describe the assumptions made for relative velocity between steam and the liquid and justify that these assumptions are conservative. For the sample calculation in MUAP-07012-P, provide plots of the void fractions and mass flow rates of the fluid leaving the core and entering the steam generators as a function of time. It would be helpful if a comparison could be made of the steaming rate for the post-reflood period between the methodology of WCAP-10325-P-A and that of the US-APWR topical. Rev. 2

RESPONSE

Plots of the void fractions and integrated mass flow rates of the fluid leaving the core and entering the steam generators as a function of time are provided with Figures 11-j-2 through 11-j-6.

A comparison is shown in Table 11-j-1 of the models affecting steaming rate for the post- reflood period between the methodology of WCAP-10325-P-A and that of the US-APWR topical report.

Rev. 2

Table 11-j-1 Comparison of GOTHIC US-APWR model with FROTH (1/3)

Item	FROTH	GOTHIC	Comment
1. Steam generation rate in core	FROTH calculates steam generation rate in core accounting for decay heat and heat from metal. Water is assumed always saturated.	GOTHIC calculates steam generation rate by energy balance in core accounting for inlet flow, outlet flow, decay heat and heat from metal. Inlet flow and outlet flow are calculated by momentum equation. Subcooled inlet water is allowable.	FROTH calculation model is too conservative. GOTHIC is realistic.
2. Core void fraction	Calculated by Yeh correlation with steam velocity of half of total core generated steam flow. The calculated void fraction is corresponding to core average.	All steam generated in the core is used for void fraction calculation. Ishii's drag coefficient is applied for interfacial force calculation. Calculated void fraction is corresponding to core exit void fraction.	Generally GOTHIC gives higher void fraction in the core because of higher steam velocity. Higher void fraction gives smaller water head in core and results in larger available water head for SG froth and larger available pressure drop for steam flow in loop. These result in conservative result.
3. Downcomer level	Assumed always full	GOTHIC calculates water level with mass and energy balance considering water flow from intact loop, injected water flow, water flow to core and spilt water flow.	No artificial modeling is applied in GOTHIC.GOTHIC model is realistic.
4. Flow split of steam flow from core		Loop momentum balance decides flow split internally.	GOTHIC calculates more flow to intact loop than FROTH. This results in more rapid heat release from intact loop SG secondary side than FROTH.

Rev. 2

Table 11-j-1 Comparison of GOTHIC US-APWR model with FROTH (2/3)

Item	FROTH	GOTHIC	Comment
5. Steam generator inlet water flow calculation		GOTHIC calculates droplet and water flow into SG U-tube from dynamic momentum equation for each phase. Water head and pressure drop due to flow are considered in momentum equation. If water enters hot side, entire heat transfer area in U-tube hot side is available for steam generation.	Global primary system momentum balance in GOTHIC is almost the same as in FROTH.

Rev. 2

Table 11-j-1 Comparison of GOTHIC US-APWR model with FROTH (3/3)

Item	FROTH	GOTHIC	Comment
6. Steam-water mixing	Assumed complete mixing in both intact loop and broken loop cold legs	Assumed almost complete mixing in only intact cold leg	GOTHIC model is conservative.
7. SG heat transfer model	McAdams correlation for secondary side is applied. Heat transfer resistance of tube and primary side is neglected.	GOTHIC FILM option heat transfer model is applied to both secondary side and primary side of U-tubes. Tubes are modeled by conductors. Heat transfer correlation of SG U-tube secondary side is by McAdams.	No substantial difference between FROTH and GOTHIC.
8. The steam condition at the outlet of steam generator	Saturated steam is assumed.	Steam condition is calculated by heat transfer model in SG tubes.	No artificial assumption is applied to GOTHIC. Actually no substantial effects on containment pressure.
9. The containment back pressure	The containment design pressure is used and constant during transient. This pressure is equal to primary system pressure in FROTH.	GOTHIC calculates both the primary system and the containment transients simultaneously. Transient containment pressure is used. GOTHIC treatment is realistic.	In US-APWR the advanced accumulator still works during post-reflood phase. Realistic primary system pressure transient is desirable for the advanced accumulator flow calculation.

Rev. 2

Rev. 2

Figure 11-j-1 Concept of two-phase level of the vessel by GOTHIC

Rev. 2

Figure 11-j-2 Transient of Total Vapor Volume Fraction in Hot Leg Inlet

Note: Both Void in the Pool and Separated Vapor Region are Considered, see Figure 11-j-1

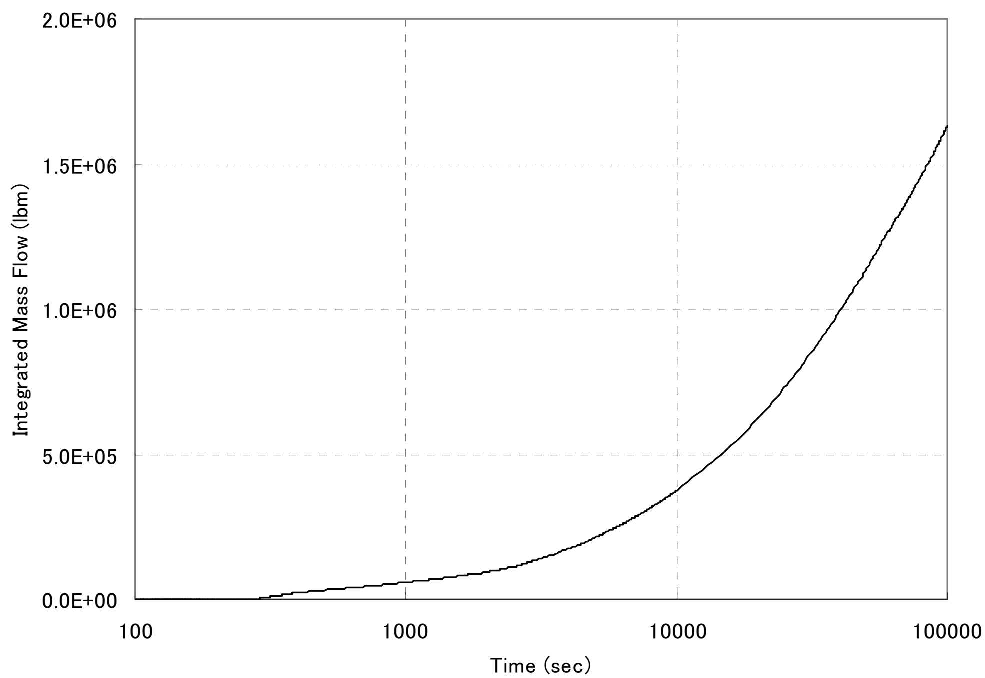

Rev. 2

Figure 11-j-3 Integrated Vapor Mass Flow Rate into SG (Intact Loop)

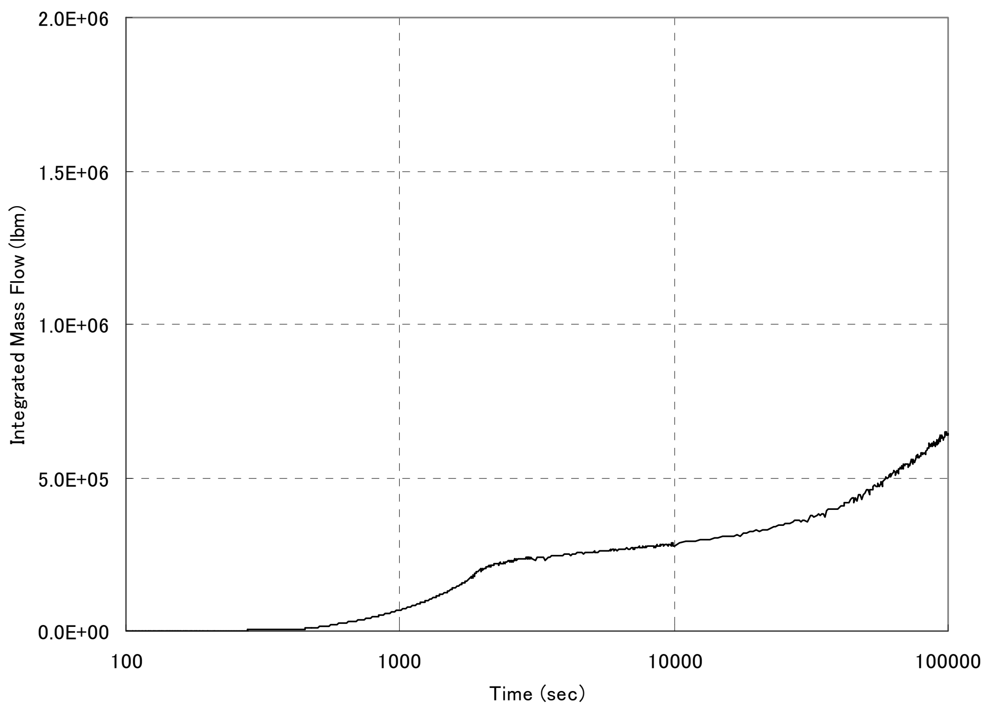

Rev. 2

Figure 11-j-4 Integrated Liquid Mass Flow Rate into SG (Intact Loop)

Notes: Drop Including

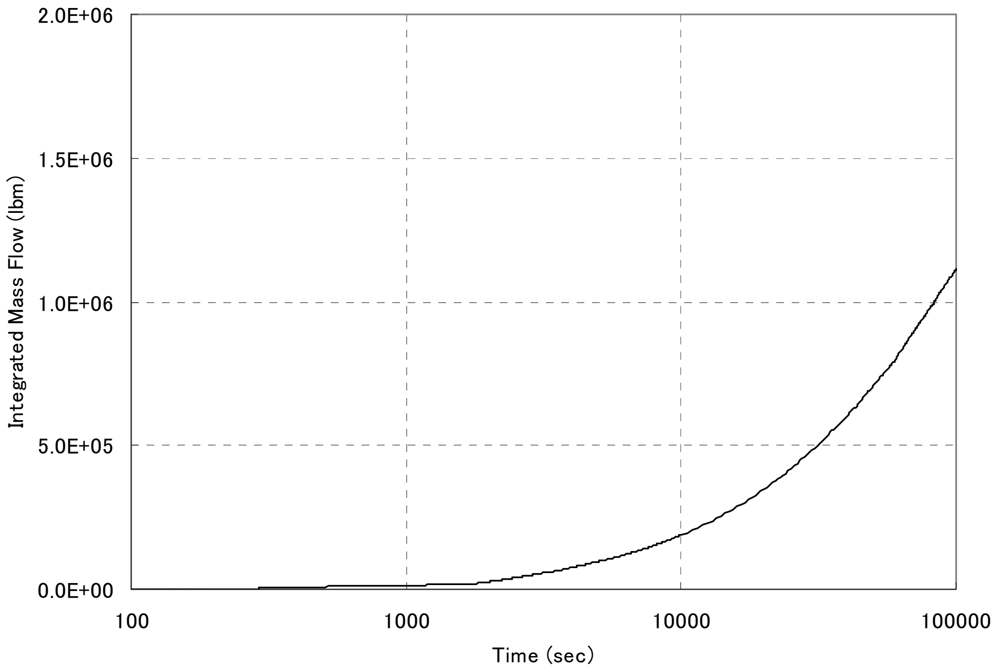

Rev. 2

Figure 11-j-5 Integrated Vapor Mass Flow Rate into SG (Broken Loop)

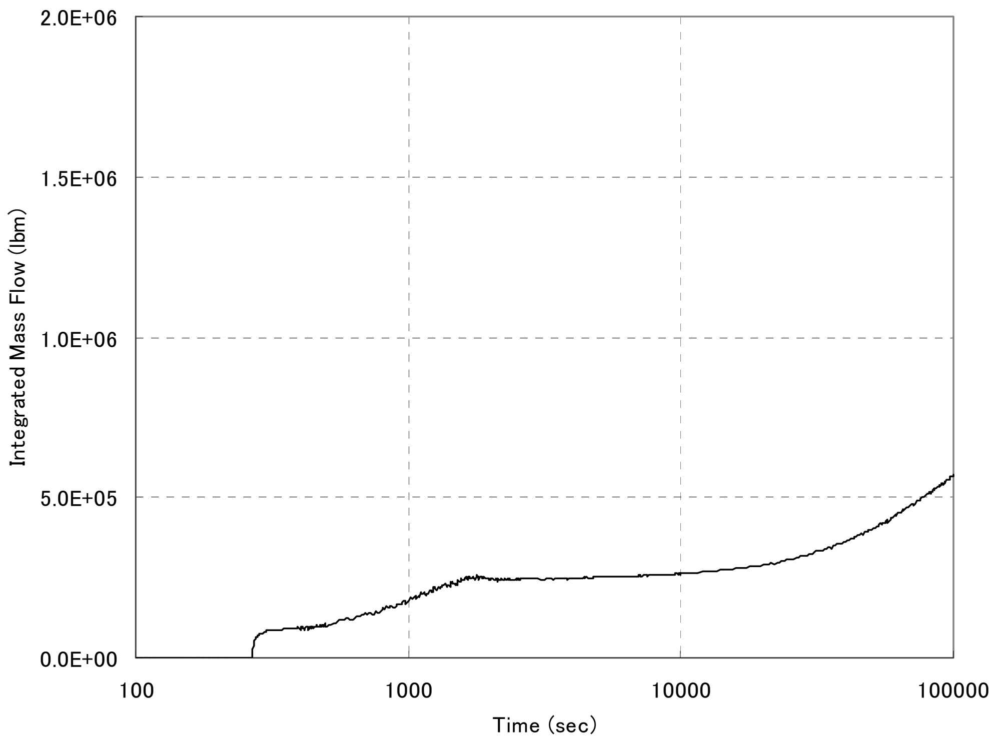

Figure 11-j-6 Integrated Liquid Mass Flow Rate into SG (Broken Loop)

Notes: Drop Including

Rev. 2

Item 11-k

In long term cooling analyses using RELAP5, the staff has found that the loop seals at the reactor coolant pump suctions close by being refilled with water. This water comes either from liquid carryover out of the core or from backflow of ECCS in the cold legs. During the blowdown period all the loop seals are calculated to open but during the post-reflood period the loop seals begin to close until only one loop seal is left open. Flow through a single loop is adequate to remove the steam produced by the core and provide for core cooling. The staff's concern is that if following a double ended pump suction break, if all the steam flow is through the broken loop, the steam will not pass through any ECCS injection points and will enter the containment through the break without any steam quenching occurring. As a sensitivity study, please provide an analysis of the containment pressure if three coolant loops were blocked during the post-reflood period and only the broken loop were open to pass steam.

RESPONSE

A sensitivity study was performed to address the concern raised by the NRC that the loop seal formation in the intact loop pump suction leg during post-reflood phase may occur and will block steam flow to the injection point of the intact loop cold leg with no steam condensation. This causes steam flow to increase in the broken loop and may raise containment pressure.

In the sensitivity study, steam flow to the intact loop cold leg is completely blocked by removing flow path from the pump suction leg to the cold leg as shown in Figure 11-k-1 to simulate the loop seal formation in the intact loop pump suction leg. Rev. 2

The following parameters from calculated results are shown in Figure 11-k-2 to Figure 11-k-7 in comparison to the base case.

Break steam flow from broken loop SG side (Figure 11-k-2)
Break steam flow from broken loop RCP side (Figure 11-k-3)
Integral of total steam flow to the containment (Figure 11-k-4)
Broken loop SG secondary side temperature (Figure 11-k-5)
Intact loop SG secondary side temperature (Figure 11-k-6)
Containment pressure (Figure 11-k-7)

For the sensitivity case, almost all steam generated in the core flows into the broken loop and the net steam release from the RCP side break is almost zero, as shown in Figures 11-k-2 and 11-k-3. On the other hand, the steam release from the RCP side for the base case is quite large because of the generated steam in the intact-loop SG tubes, as described below. As a result, total steam flow to the containment for the sensitivity case is much smaller than the base case as shown in Figure 11-k-4.

The secondary side temperature of the broken loop SG and intact loop SG are shown in Figure 11-k-5 and Figure 11-k-6, respectively. Cooldown of the broken loop SG secondary side is faster than the base case, but the intact loop SG secondary side, which has much more energy than broken loop SG, is only slightly cooled due to the oscillatory flow through the intact hot leg. The net result is much slower energy release to the containment and the containment pressure during post-reflood phase is much lower than the base case as shown in Figure 11-k-7.

Rev. 2

Figure 11-k-1 Noding Diagram of GOTHIC for Simulation of Loop Seal Formation in Intact Loop

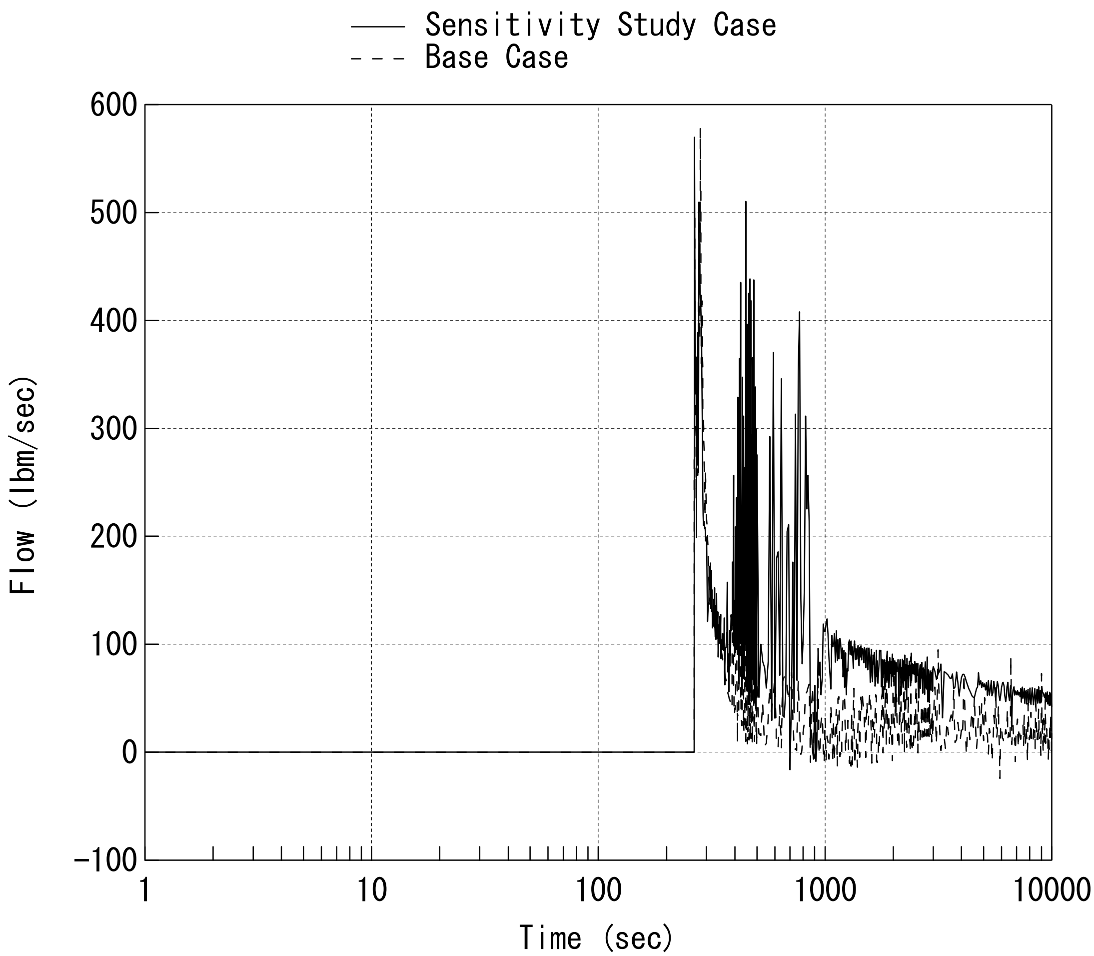

Figure 11-k-2 Break Steam Flow from Broken Loop SG Side

Rev. 2

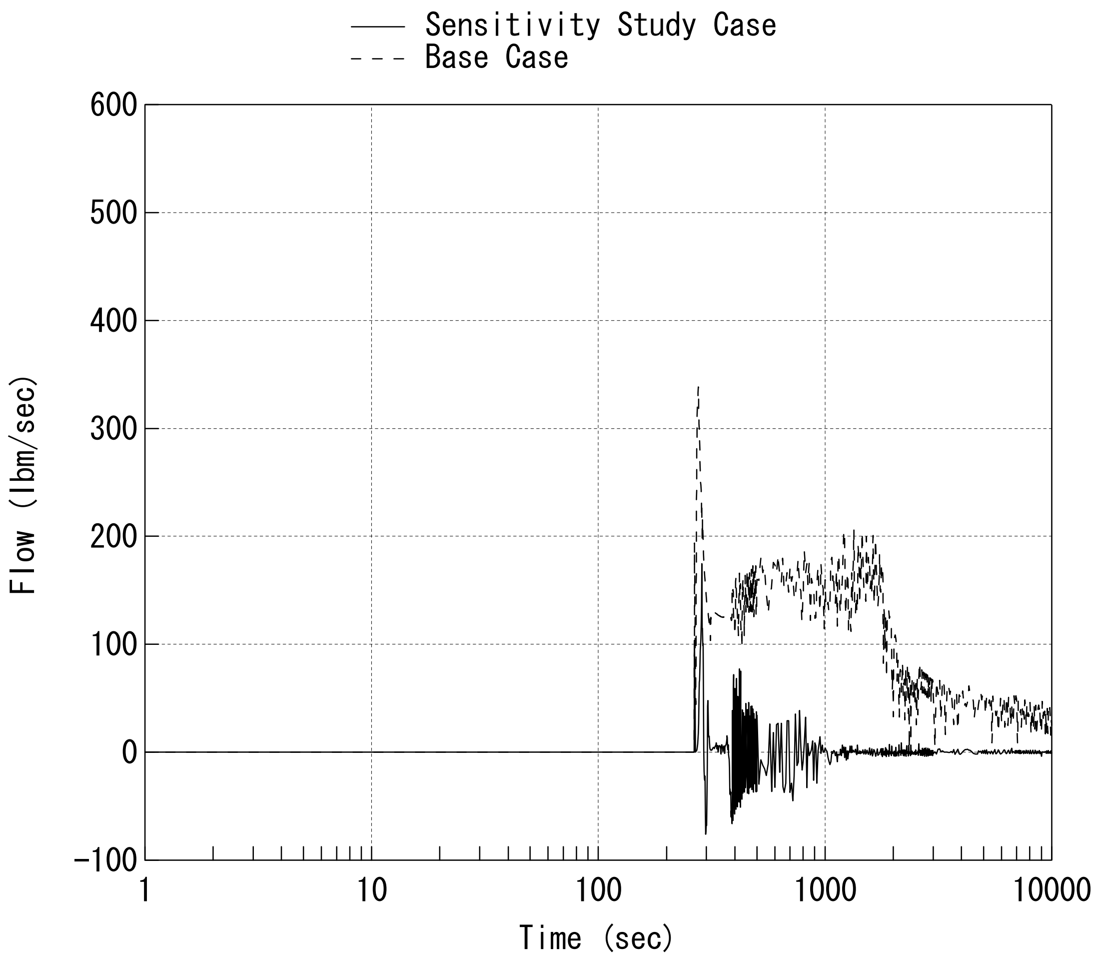

Figure 11-k-3 Break Steam Flow from Broken Loop RCP Side

Rev. 2

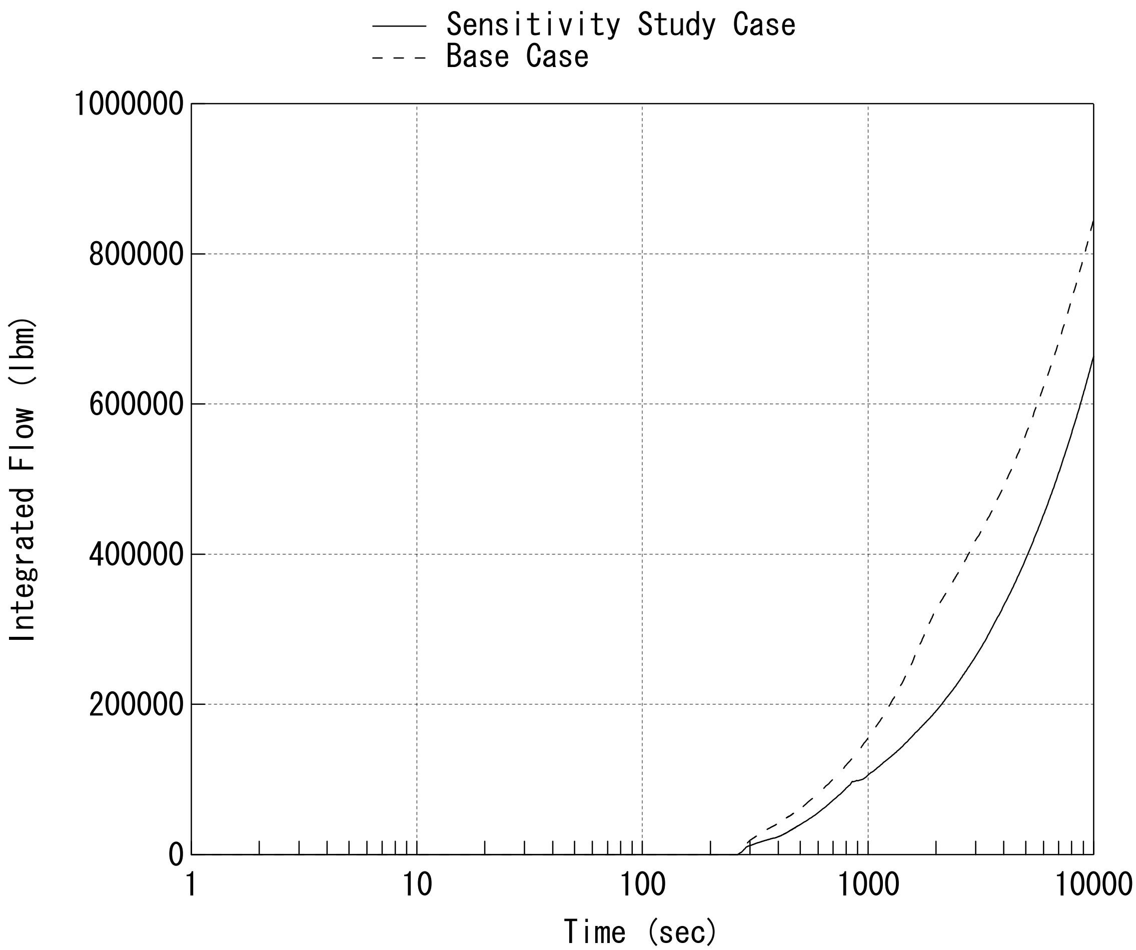

Figure 11-k-4 Integral of Total Steam Flow to the Containment

Rev. 2

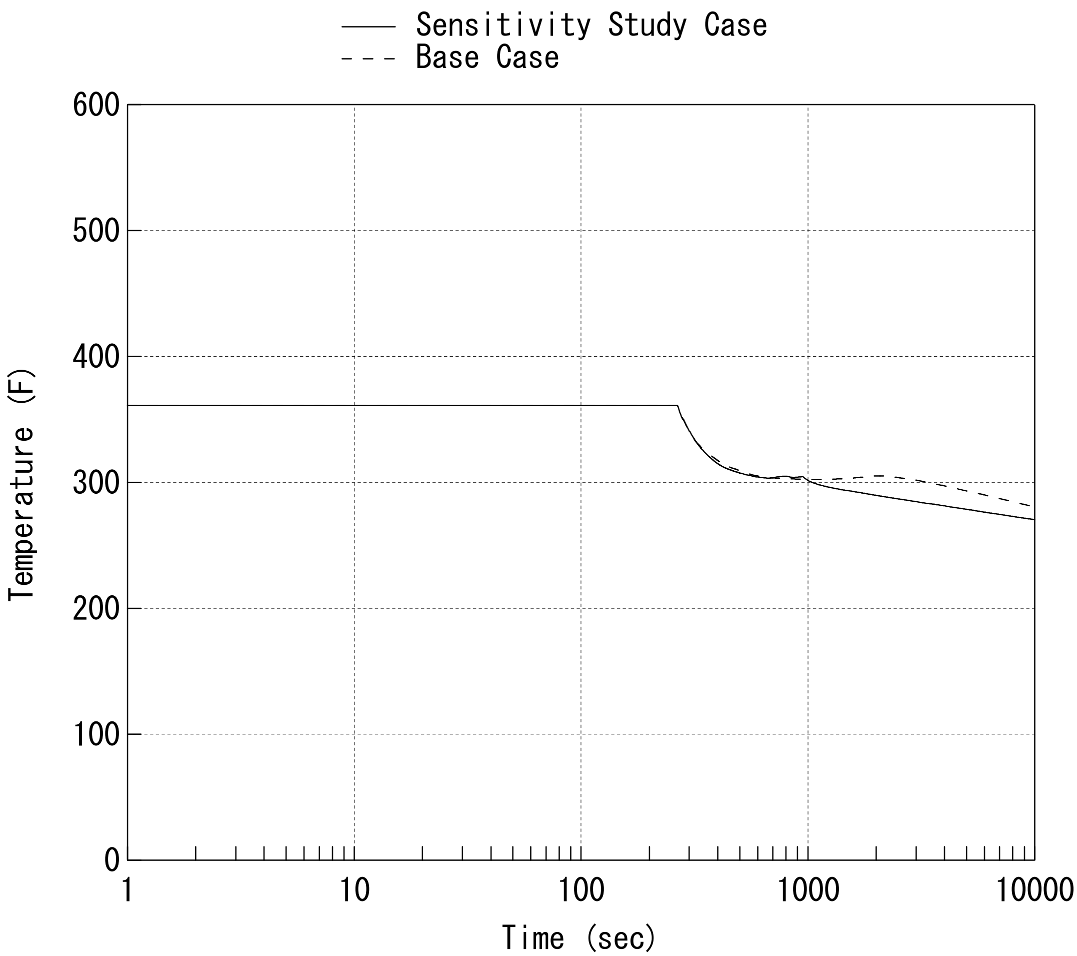

Figure 11-k-5 Broken Loop SG Secondary Side Temperature

Rev. 2

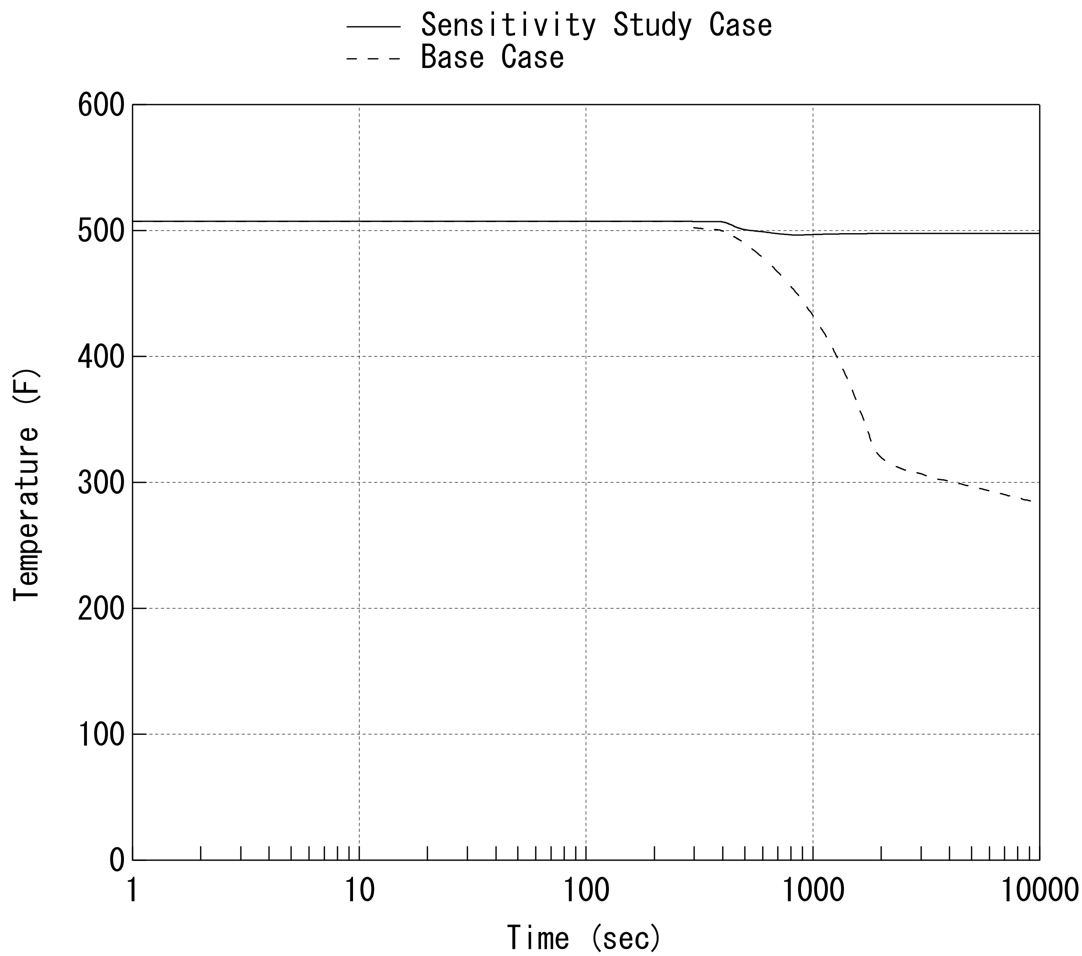

Figure 11-k-6 Intact Loop SG Secondary Side Temperature

Rev. 2

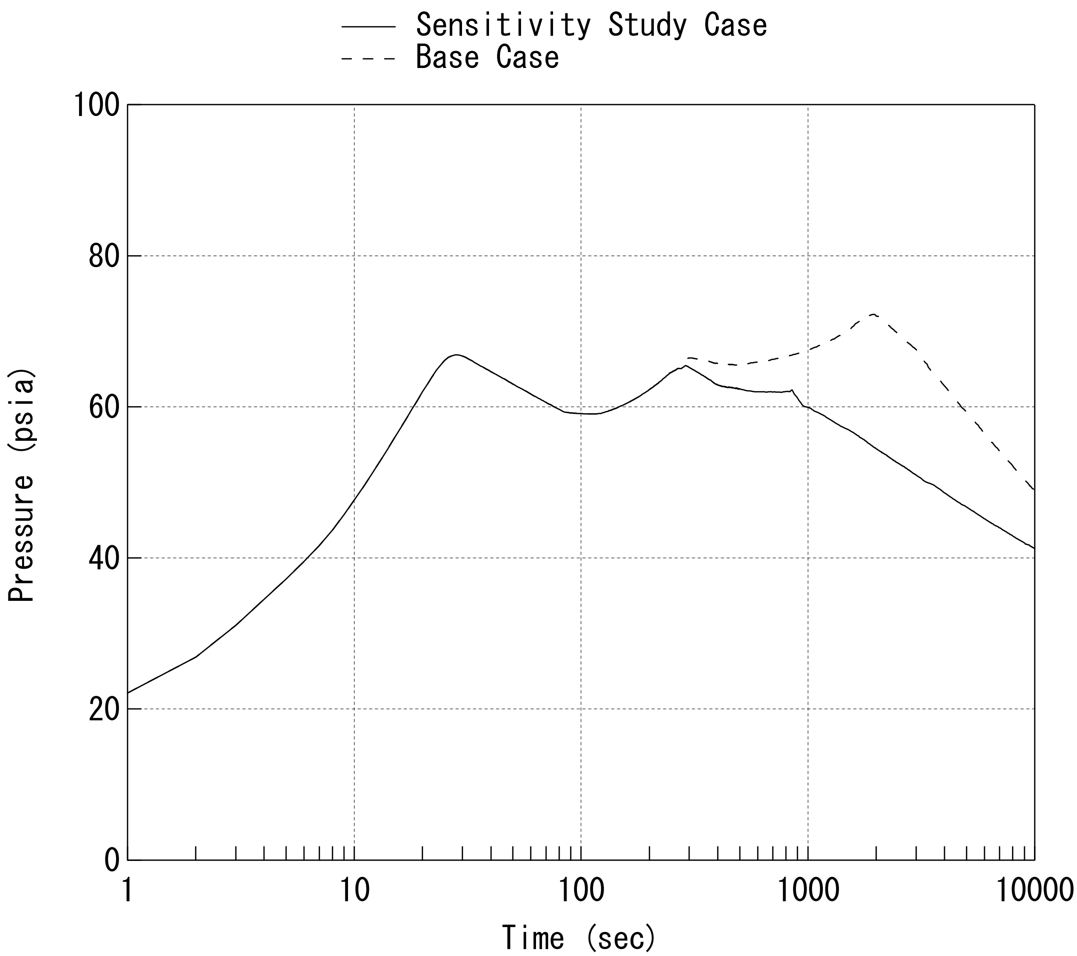

Figure 11-k-7 Containment Pressure

Rev. 2

Item 12

Section 5.1 of WCAP-10325-P-A describes model conservatisms which primarily involve code inputs. Please provide a comparison of the assumptions to be made for analysis of US-APWR with those of Section 5.1 of WCAP-10325-P-A and justify any differences.

RESPONSE

The assumptions for the US-APWR analysis are compared with those of Section 5.1 of WCAP-10325-P-A in Table 12-1. The comparison shows that the assumptions are essentially the same except for the SG secondary side mass and the post-reflood model, which is based on the GOTHIC code in the US-APWR compared to the FROTH code in WCAP-10325-P-A. In the FROTH analysis for post-reflood period, the steam exiting from the SG is artificially assumed to be saturated. In the GOTHIC analysis, the steam exit condition depends on the calculated heat transfer across the SG tubes and the steam may exit in a superheated condition. This is consistent with the observations from the FLECHT-SEASET Steam Generator Separate Effects tests. The influence of the steam condition on the containment peak pressure is slight.

Rev. 2

Table 12-1 A comparison of the assumptions to be made for analysis of US-APWR with those of Section 5.1 of WCAP-10325-P-A

	WCAP-10325-P-A Section 5.1	US-APWR
Initial system conditions		
Power level	102 %	same
Fluid temperature	+4 F	same
System volume	+3 %	same
Steam generator parameter, Secondary mass	Based on 100% power, +10%	Based on 100 % power, B.E. + 3 % (consistent with primary system mass.)
Metal stored energy	maximized	same
Decay heat	maximized	same
Core stored energy	maximized	same
Blowdown modeling		
Break size	A full double ended area	same
Core heat transfer coefficient	Best judgment for maximizing to heat release from the core	same
Reflood modeling		
Carryover fraction correlation	ECCS type application	same
Steam water mixing pressure drop	excluded	same
Exit steam generator fluid conditions	saturated	same
Post-reflood modeling		
Exit steam generator fluid conditions	saturated	GOTHIC calculated value

Item 13

Tables 6A and 7A of WCAP10325-P-A provide mass and energy balances for the sample case of a postulated double ended pump suction break. Please provide similar tables for the sample case in MUAP-07012-P and indicate the reference temperature upon which the energy balance is based.

RESPONSE

Mass and energy balance tables for the limiting case in the US-APWR DCD are provided as Tables 13-1 and 13-2.

Table 13-1 Mass Distribution Transient

Phase		Prior to LOCA	End of Blowdown	End of Core Reflood	At Peak Pressure	1 Day into Recirc.
Time (seconds)		0.00	31.60	265.54	1963.7	86400
Initial Mass	RCS and ACC	1278.06	1278.06	1278.06	1278.06	1278.06
Added Mass	Pumped Injection	0.00	0.00	49.70	613.90	28362.65
	Total Added	0.00	0.00	49.70	613.90	28362.65
Total Available (Initial Mass +Total added)		**1278.06**	**1278.06**	**1327.76**	**1891.96**	**29640.71**
RCS Mass Distribution	Reactor Coolant	752.18	68.17	207.23	189.83	206.26
	Accumulator	525.89	460.87	92.06	9.21	0.00
	RCS Total Contents	1278.06	529.05	299.28	199.04	206.26
Effluent	Break Flow	0.00	748.99	1028.49	1698.94	29439.66
	ECCS Spill	0.00	0.00	0.00	0.00	0.00
	Total Effluent	0.00	748.99	1028.49	1698.94	29439.66
Total Accountable		**1278.06**	**1278.04**	**1327.77**	**1897.98**	**29645.92**

Unit: Thousand lbm

Rev. 2

Table 13-2 Energy Distribution Transient

	Phase	Prior to LOCA	End of Blowdown	End of Core Reflood	At Peak Pressure	1 Day into Recirc.
	Time (seconds)	0.00	31.60	265.54	1963.7	86400
Initial Energy		1287.49	1287.49	1287.49	1287.49	1287.49
Added Energy	Pumped Injection	0.00	0.00	5.67	90.83	5021.69
	Energy Generated during Shutdown from Decay Heat	0.00	15.58	49.83	224.04	3254.97
	Heat from Secondary	0.00	26.04	26.04	26.04	26.04
	Total Added	0.00	41.62	81.54	340.91	8302.70
Total Available	**(Initial Energy + Added)**	**1287.49**	**1329.11**	**1369.03**	**1628.40**	**9590.19**
RCS Energy Distribution	Reactor Coolant Internal Energy	441.38	17.09	58.37	80.46	70.92
	Accumulator Internal Energy	47.09	41.27	8.24	0.81	0.00
	Energy Stored in Core	43.40	23.08	7.58	5.56	3.77
	Energy Stored in RCS Structure	267.87	255.87	183.82	104.11	63.84
	Steam Generator Coolant Internal Energy	349.58	379.25	318.99	197.89	141.91
	Energy Stored in Steam Generator Metal	138.16	136.48	117.14	77.51	65.60
	RCS Total Contents	1287.49	853.03	694.16	466.34	346.04
Effluent	Break Flow	0.00	476.08	652.54	1132.84	9231.34
	ECCS Spill	0.00	0.00	0.00	0.00	0.00
	Total Effluent	0.00	476.08	652.54	1132.84	9231.34
Total Accountable		**1287.49**	**1329.11**	**1346.70**	**1599.18**	**9577.38**

Unit: Million Btu
Reference Temperature: 32 degF

Rev. 2

Item 14

Tables 13A, 14A, 14B, 15A and 15B of WCAP10325-P-A provide tabulations of the mass and energy release of steam and water from the reactor including ECCS spillage as a function of time for containment analysis. Please provide similar tables for the sample case of MUAP-07012-P.

RESPONSE

Tables 13A, 14A, 14B, 15A and 15B of WCAP-10325-P-A are based on the old mass and energy release model that does not consider steam condensation on the injected water. MHI does not use this methodology. MHI's methodology corresponds to the revised mass and energy release model discussed in the same WCAP, and the results are listed Tables 8A, 9A and 10A.

Those tables show mass and energy releases as a function of time not for steam and water, but for Break Path No.1 (SG side) and Break Path No.2 (Reactor Vessel side), instead. Tables 14-1 through 14-3 provide tabulations of the mass and energy release for the postulated double ended pump suction break described in the US-APWR DCD, which correspond to the Tables 8A through 10A of WCAP 10325-P-A, respectively.

Table 14-3, the post-reflood mass and energy table for the limiting pump-suction break case, lists the mass and energy release rates for the reactor vessel side and the steam generator side of the break. Since steam and water are treated separately using non-equilibrium features in the GOTHIC, each enthalpy value in Table 14-3 is obtained by averaging the conditions either for saturated or superheated steam and that of subcooled water using GOTHIC output. Each set of time dependent mass and energy data in Table 14-3 is picked up from plotting data at regular intervals. The data in Table 14-3 are presented as Table 6.2.1-21 in the US-APWR DCD. Rev. 2

Table 14-4 gives the post-reflood mass and energy for the same case with the separated steam and liquid. Since mass and energy data in Table 14-4 are calculated ones so as to conserve integral values, they are not necessarily identical to values at the same time in Table 14-3. The data in Table 14-4 are included in the GOTHIC input data provided as the response to Item 19.

Table 14-1 Break Mass and Energy Flow for the Blowdown Phase of the DEPSG Break (Sheet 1 of 3)

Time (sec)	Break Flow (Reactor Vessel Side)			Break Flow (Steam Generator Side)		
	Mass (lbm/sec)	Enthalpy (Btu/lbm)	Energy (Thousand Btu/sec)	Mass (lbm/sec)	Enthalpy (Btu/lbm)	Energy (Thousand Btu/sec)
0.0	0.0	0.0	0.0	0.0	0.0	0.0
0.00037	39367.7	551.1	21695.5	47451.3	553.0	26240.6
0.00102	39475.9	548.5	21652.5	101757.9	550.6	56027.9
0.0112	39130.1	548.1	21447.2	42091.4	548.5	23087.1
0.0211	36128.7	547.7	19787.7	41741.5	548.6	22899.4
0.0515	23343.8	545.7	12738.7	41730.0	548.8	22901.4
0.0611	21272.1	546.1	11616.7	41772.5	549.0	22933.1
0.0711	20482.9	546.9	11202.1	49613.7	549.3	27252.8
0.0912	20875.8	547.9	11437.9	49573.9	549.5	27240.9
0.111	21872.9	548.2	11990.7	52298.0	549.9	28758.7
0.161	23599.5	548.5	12944.3	53529.7	550.8	29484.2
0.222	24642.8	548.5	13516.6	53292.9	552.1	29423.0
0.301	25143.0	548.8	13798.5	52771.2	554.1	29240.5
0.351	25174.2	549.0	13820.6	52247.1	555.6	29028.5
0.451	24831.4	549.4	13642.4	51440.1	558.8	28744.7
0.611	23851.7	549.8	13113.7	49667.7	564.7	28047.4
0.701	23376.9	550.0	12857.3	48773.6	568.3	27718.0
0.801	22955.5	550.1	12627.8	47097.0	572.2	26948.9
0.892	22593.8	550.2	12431.1	45168.5	575.4	25990.0
1.00	22156.2	550.2	12190.3	45392.0	579.0	26282.0
1.09	21789.4	550.3	11990.7	45312.7	581.6	26353.9
1.27	21309.6	550.4	11728.8	44761.2	586.5	26252.4
1.75	20552.4	550.6	11316.2	42786.2	600.7	25701.7
2.20	20134.6	550.7	11088.1	40939.5	616.1	25222.8
2.32	20005.2	550.7	11016.9	40291.3	620.9	25016.9
2.61	19758.0	550.8	10882.7	38300.3	634.5	24301.5
2.82	19471.7	550.9	10727.0	36444.7	646.1	23546.9
3.30	18855.6	551.2	10393.2	31566.7	676.2	21345.4
3.37	18744.9	551.2	10332.2	30574.1	680.5	20805.7
3.51	18535.4	551.3	10218.6	27856.7	689.3	19201.6
3.59	18426.4	551.4	10160.3	26605.1	694.5	18477.2
3.78	18178.5	551.6	10027.3	24039.6	705.4	16957.5
3.98	17916.9	551.8	9886.5	21866.8	714.3	15619.5
4.16	17712.0	552.0	9777.0	20321.5	721.2	14655.9
4.32	17550.1	552.2	9691.2	19287.2	726.8	14017.9
4.56	17298.1	552.5	9557.2	18071.0	733.8	13260.5
4.86	17033.0	552.9	9417.5	16955.9	740.8	12560.9

Rev. 2

Table 14-1 Break Mass and Energy Flow for the Blowdown Phase of the DEPSG Break (Sheet 2 of 3)

Time (sec)	Break Flow (Reactor Vessel Side)			Break Flow (Steam Generator Side)		
	Mass (lbm/sec)	Enthalpy (Btu/lbm)	Energy (Thousand Btu/sec)	Mass (lbm/sec)	Enthalpy (Btu/lbm)	Energy (Thousand Btu/sec)
5.12	16808.2	553.3	9300.0	16226.0	745.1	12090.0
5.60	16450.3	554.1	9115.1	15301.9	749.0	11461.1
5.92	16242.6	554.7	9009.8	14891.4	749.1	11155.1
6.14	16098.5	555.1	8936.3	14686.4	748.0	10985.4
6.68	15794.6	556.1	8783.4	14368.9	743.1	10677.5
7.22	15531.3	557.1	8652.5	14258.5	735.7	10490.0
7.62	15350.4	557.9	8564.0	14294.0	729.0	10420.3
7.98	15206.5	558.6	8494.4	14488.9	722.0	10461.0
8.02	15196.1	558.7	8490.1	14723.8	721.5	10623.2
8.26	15128.7	559.1	8458.5	15040.2	716.4	10774.8
8.34	15756.0	559.7	8818.6	15093.6	718.5	10844.8
8.40	16029.0	559.7	8971.4	15026.1	722.8	10860.9
8.52	16090.0	559.8	9007.2	14553.7	739.5	10762.5
8.78	16004.4	560.2	8965.7	12886.7	789.0	10167.6
8.90	15895.1	560.4	8907.6	12425.1	801.9	9963.7
9.08	15710.5	560.6	8807.3	12142.2	807.6	9806.0
9.86	14727.4	561.8	8273.9	11967.7	802.2	9600.5
10.1	14508.6	562.2	8156.7	11851.1	802.3	9508.1
10.5	14119.1	562.5	7942.0	11638.6	804.5	9363.3
11.2	13710.6	562.7	7715.0	11289.3	808.4	9126.3
11.6	13507.9	562.5	7598.2	11339.8	795.6	9021.9
11.9	13352.6	562.3	7508.2	11560.2	778.4	8998.5
12.5	13080.4	562.0	7351.2	12052.3	747.6	9010.3
13.1	12837.1	561.8	7211.9	12244.3	729.1	8927.3
13.6	12635.0	561.6	7095.8	12079.1	722.0	8721.1
14.5	12335.9	561.6	6927.8	11422.7	725.2	8283.7
15.1	12101.4	561.7	6797.4	10849.1	734.6	7969.7
16.1	11666.0	561.9	6555.1	10022.9	753.8	7555.3
16.8	11348.1	562.2	6379.9	9476.6	769.2	7289.4
17.7	10874.8	562.8	6120.3	8789.5	787.7	6923.5
18.4	10529.9	563.4	5932.5	8373.0	794.6	6653.2
19.0	10210.8	564.1	5759.9	8052.5	797.2	6419.5
20.0	9673.4	566.4	5479.0	7519.7	802.2	6032.3
20.6	9374.9	568.2	5326.8	7234.7	804.5	5820.3
21.8	8726.0	573.3	5002.6	6752.6	812.2	5484.5
22.0	8449.6	575.0	4858.5	6591.6	817.4	5388.0
22.1	8455.7	575.8	4868.8	6529.7	820.1	5355.0

Rev. 2

Table 14-1 Break Mass and Energy Flow for the Blowdown Phase of the DEPSG Break (Sheet 3 of 3)

Time (sec)	Break Flow (Reactor Vessel Side)			Break Flow (Steam Generator Side)		
	Mass (lbm/sec)	Enthalpy (Btu/lbm)	Energy (Thousand Btu/sec)	Mass (lbm/sec)	Enthalpy (Btu/lbm)	Energy (Thousand Btu/sec)
22.4	8174.3	575.8	4706.8	6346.2	827.6	5252.1
22.5	8121.9	576.2	4679.8	6197.9	834.7	5173.4
23.2	7506.8	565.4	4244.3	5537.6	857.3	4747.4
23.5	7418.9	546.8	4056.7	5363.3	856.3	4592.6
23.9	7051.1	525.4	3704.6	5304.6	868.6	4607.6
24.1	6856.5	513.9	3523.6	5096.0	903.6	4604.7
24.3	6495.3	498.7	3239.2	4570.4	988.9	4519.7
24.6	6032.6	482.1	2908.3	3837.4	1123.2	4310.2
24.9	5684.8	470.7	2675.8	3371.5	1203.1	4056.3
25.2	5326.6	456.8	2433.2	2966.9	1233.0	3658.2
25.6	4825.7	439.8	2122.3	2576.6	1242.3	3200.9
26.0	4511.2	428.2	1931.7	2360.9	1246.8	2943.6
26.3	4022.2	420.6	1691.7	2222.3	1249.5	2776.8
26.6	3691.6	407.9	1505.8	2051.7	1252.1	2568.9
26.7	3693.4	402.7	1487.3	1970.7	1253.3	2469.9
27.1	3875.1	388.7	1506.3	1753.1	1256.9	2203.5
27.3	3818.1	383.4	1463.9	1620.9	1258.7	2040.2
28.1	3258.2	364.5	1187.6	1223.5	1265.0	1547.7
28.3	3013.6	356.1	1073.1	1089.7	1266.4	1380.0
28.7	2733.2	342.7	936.7	863.0	1268.5	1094.7
29.0	2602.6	334.0	869.3	746.2	1269.7	947.5
29.2	2413.3	327.3	789.9	678.6	1270.3	862.0
29.6	1782.4	315.2	561.8	578.3	1271.8	735.5
29.9	1036.9	308.6	320.0	502.1	1272.6	639.0
30.2	0.0	0.0	0.0	408.8	1273.5	520.6
31.6	0.0	0.0	0.0	0.0	0.0	0.0

Rev. 2

Table 14-2 Break Mass and Energy Flow for the Reflood Phase of the DEPSG Break (Sheet 1 of 3)

Time (sec)	Break Flow (Reactor Vessel Side)			Break Flow (Steam Generator Side)		
	Mass (lbm/sec)	Enthalpy (Btu/lbm)	Energy (Thousand Btu/sec)	Mass (lbm/sec)	Enthalpy (Btu/lbm)	Energy (Thousand Btu/sec)
31.6	0.0	0.0	0.0	0.0	0.0	0.0
32.9	0.0	0.0	0.0	0.0	0.0	0.0
33.0	0.0	0.0	0.0	49.1	1179.3	57.9
33.1	0.0	0.0	0.0	17.1	1179.3	20.2
33.2	0.0	0.0	0.0	2.8	1179.3	3.3
33.4	0.0	0.0	0.0	0.0	0.0	0.0
33.5	0.0	0.0	0.0	21.6	1179.3	25.5
33.6	0.0	0.0	0.0	31.5	1179.3	37.1
33.7	0.0	0.0	0.0	35.3	1179.3	41.6
33.8	0.0	0.0	0.0	46.0	1179.3	54.2
33.9	0.0	0.0	0.0	52.2	1179.3	61.6
35.7	0.0	0.0	0.0	115.4	1179.6	136.1
36.7	0.0	0.0	0.0	140.3	1179.7	165.5
37.7	0.0	0.0	0.0	161.5	1179.9	190.6
38.7	0.0	0.0	0.0	180.2	1180.0	212.6
39.7	0.0	0.0	0.0	197.1	1180.2	232.6
40.7	0.0	0.0	0.0	212.4	1180.3	250.7
41.8	3737.2	158.2	591.2	444.4	1183.5	525.9
42.8	4175.0	166.3	694.3	495.5	1184.7	587.0
43.8	4145.4	167.3	693.5	491.6	1184.7	582.4
44.8	4094.6	167.9	687.5	485.3	1184.5	574.8
45.8	4041.6	168.5	681.0	478.8	1184.4	567.1
46.0	4030.9	168.7	680.0	477.5	1184.3	565.5
46.8	3988.3	169.2	674.8	472.4	1184.2	559.4
47.8	3935.2	169.7	667.8	466.0	1184.1	551.8
48.8	3882.9	170.3	661.3	459.8	1184.0	544.4
49.8	3831.4	170.9	654.8	453.8	1183.8	537.2
50.8	3781.0	171.5	648.4	447.9	1183.7	530.2
51.8	3731.6	172.1	642.2	442.2	1183.6	523.4
52.8	3683.4	172.6	635.8	436.6	1183.4	516.7
53.1	3669.1	172.8	634.0	435.0	1183.4	514.8
53.8	3636.3	173.2	629.8	431.3	1183.3	510.4
54.8	3590.3	173.7	623.6	426.1	1183.2	504.2
55.8	3545.5	174.3	618.0	421.0	1183.1	498.1
56.8	3501.8	174.8	612.1	416.1	1183.0	492.2
57.8	3459.1	175.4	606.7	411.4	1182.9	486.6
58.8	3417.4	175.9	601.1	406.8	1182.7	481.1
59.8	3376.7	176.5	596.0	402.3	1182.6	475.8

Rev. 2

Table 14-2 Break Mass and Energy Flow for the Reflood Phase of the DEPSG Break (Sheet 2 of 3)

Time (sec)	Break Flow (Reactor Vessel Side)			Break Flow (Steam Generator Side)		
	Mass (lbm/sec)	Enthalpy (Btu/lbm)	Energy (Thousand Btu/sec)	Mass (lbm/sec)	Enthalpy (Btu/lbm)	Energy (Thousand Btu/sec)
60.8	3337.0	177.0	590.6	398.0	1182.5	470.6
61.2	3321.4	177.2	588.6	396.2	1182.5	468.5
61.8	3298.2	177.5	585.4	393.7	1182.4	465.5
62.8	3260.4	178.1	580.7	389.6	1182.3	460.6
63.8	3223.3	178.6	575.7	385.7	1182.2	456.0
64.8	3187.2	179.1	570.8	381.8	1182.2	451.4
65.8	3151.8	179.6	566.1	378.0	1182.1	446.8
66.8	3117.2	180.2	561.7	374.4	1182.0	442.5
67.8	3083.3	180.7	557.2	370.8	1181.9	438.2
68.8	3050.2	181.2	552.7	367.3	1181.8	434.1
69.8	3017.7	181.7	548.3	363.9	1181.7	430.0
70.2	3004.9	181.9	546.6	362.6	1181.7	428.5
70.8	2985.9	182.2	544.0	360.6	1181.6	426.1
71.8	2954.8	182.8	540.1	357.4	1181.6	422.3
72.8	2924.3	183.3	536.0	354.3	1181.5	418.6
73.8	2894.3	183.8	532.0	351.2	1181.4	414.9
74.8	2865.0	184.3	528.0	348.2	1181.3	411.3
75.8	2836.2	184.8	524.1	345.3	1181.3	407.9
76.8	2808.0	185.3	520.3	342.4	1181.2	404.4
77.8	2780.2	185.8	516.6	339.6	1181.1	401.1
78.8	2753.0	186.3	512.9	336.9	1181.1	397.9
79.8	2726.3	186.8	509.3	334.2	1181.0	394.7
80.8	2700.0	187.4	506.0	331.6	1180.9	391.6
81.8	2674.2	187.9	502.5	329.0	1180.9	388.5
82.8	2648.8	188.4	499.0	326.5	1180.8	385.5
83.8	2623.9	188.9	495.7	324.1	1180.8	382.7
84.8	182.6	1140.4	208.2	410.6	1182.1	485.4
85.8	191.9	1039.8	199.5	404.4	1182.2	478.1
87.8	190.7	1042.8	198.9	403.0	1182.2	476.4
91.8	188.4	1049.3	197.7	400.2	1182.1	473.1
92.8	187.8	1051.0	197.4	399.5	1182.1	472.2
100.8	183.4	1064.4	195.2	394.2	1182.0	465.9
108.8	179.3	1076.7	193.1	389.2	1181.9	460.0
116.8	175.5	1087.6	190.9	384.2	1181.8	454.0
120.8	173.7	1092.5	189.8	381.6	1181.7	450.9
122.8	257.2	934.6	240.4	481.6	1183.7	570.1
124.8	256.2	936.2	239.9	480.5	1183.7	568.8
128.8	254.4	938.6	238.8	478.4	1183.7	566.3

Rev. 2

Table 14-2 Break Mass and Energy Flow for the Reflood Phase of the DEPSG Break (Sheet 3 of 3)

Time (sec)	Break Flow (Reactor Vessel Side)			Break Flow (Steam Generator Side)		
	Mass (lbm/sec)	Enthalpy (Btu/lbm)	Energy (Thousand Btu/sec)	Mass (lbm/sec)	Enthalpy (Btu/lbm)	Energy (Thousand Btu/sec)
132.8	252.7	940.1	237.6	476.0	1183.7	563.4
136.8	251.3	940.6	236.4	473.6	1183.6	560.6
140.8	249.9	940.2	235.0	471.1	1183.6	557.6
148.8	247.7	937.4	232.2	465.9	1183.5	551.4
150.8	247.2	936.3	231.5	464.6	1183.5	549.9
154.8	246.4	933.7	230.1	461.8	1183.5	546.5
162.8	244.8	927.5	227.1	456.2	1183.4	539.9
170.8	243.3	920.5	224.0	450.5	1183.4	533.1
174.8	242.7	916.9	222.5	447.6	1183.4	529.7
190.8	239.9	902.8	216.6	436.2	1183.3	516.2
198.8	238.3	896.6	213.7	430.6	1183.2	509.5
206.8	236.7	890.9	210.9	425.0	1183.2	502.9
214.8	234.8	886.2	208.1	419.4	1183.2	496.2
222.8	232.8	882.5	205.4	413.9	1183.1	489.7
230.8	230.5	880.0	202.8	408.4	1183.1	483.2
238.8	227.9	878.8	200.3	402.9	1183.1	476.7
246.8	225.2	878.3	197.8	397.4	1183.0	470.1
254.8	223.8	872.3	195.2	392.4	1183.0	464.2
262.8	222.1	867.5	192.7	387.4	1183.0	458.3
265.5	221.5	866.2	191.9	385.7	1182.9	456.2
265.6	92.6	114.1	10.6	119.9	1179.4	141.4

Rev. 2

Table 14-3 Break Mass and Energy Flow for the Long-term Cooling Phase of the DEPSG Break (Sheet 1 of 6)

Time (sec)	Break Flow (Reactor Vessel Side)			Break Flow (Steam Generator Side)		
	Mass (lbm/sec)	Enthalpy (Btu/lbm)	Energy (Thousand Btu/sec)	Mass (lbm/sec)	Enthalpy (Btu/lbm)	Energy (Thousand Btu/sec)
266.0	453.7	663.8	301.2	542.7	1207.8	655.5
270.0	2012.4	333.0	670.1	4548.9	321.9	1464.3
274.0	721.1	733.2	528.7	3042.4	347.9	1058.5
278.0	460.8	935.5	431.1	2599.8	416.8	1083.6
282.0	658.4	649.4	427.6	1056.3	775.8	819.5
286.0	303.0	1019.0	308.8	1014.9	649.0	658.7
290.0	305.0	844.4	257.5	840.9	591.8	497.6
294.0	357.9	666.6	238.6	543.7	705.7	383.7
298.1	414.3	564.2	233.7	258.3	1173.8	303.2
302.1	428.5	520.7	223.1	210.6	1174.2	247.3
306.1	424.4	496.6	210.8	175.1	1179.2	206.5
310.1	417.2	476.5	198.8	223.9	857.1	191.9
314.1	418.1	495.2	207.0	179.4	967.0	173.5
318.1	418.5	512.4	214.4	225.3	853.9	192.4
322.1	418.6	514.0	215.2	248.3	779.9	193.6
326.1	419.3	511.5	214.5	228.0	799.6	182.3
330.1	418.8	509.4	213.3	215.1	803.5	172.8
334.1	415.5	510.0	211.9	202.9	808.4	164.0
338.1	411.7	510.7	210.3	179.7	843.8	151.6
342.1	408.5	511.5	208.9	156.1	892.2	139.3
346.1	405.4	512.2	207.6	136.6	937.2	128.0
350.1	402.6	513.3	206.7	118.1	987.4	116.6
354.1	399.7	514.7	205.7	101.9	1041.7	106.1
358.1	397.4	516.9	205.4	88.7	1075.9	95.4
362.1	394.9	519.9	205.3	78.8	1117.7	88.1
366.1	392.5	522.6	205.1	68.2	1155.3	78.8
370.1	390.2	525.5	205.1	59.9	1184.1	70.9
374.1	388.2	528.6	205.2	53.5	1190.3	63.7
378.1	385.5	531.4	204.9	49.2	1189.8	58.5
382.1	381.7	532.9	203.4	45.4	1189.8	54.0
386.1	371.1	531.3	197.2	41.9	1189.8	49.9
390.1	416.0	577.5	240.2	142.3	985.9	140.3
394.1	355.2	592.8	210.6	252.8	671.2	169.7
398.1	356.1	558.1	198.7	35.3	1187.9	41.9
402.1	399.2	532.9	212.7	60.1	1188.5	71.4
406.1	355.0	619.2	219.8	400.9	545.4	218.7
410.2	316.0	580.3	183.4	9.1	1157.6	10.5

Rev. 2

Table 14-3 Break Mass and Energy Flow for the Long-term Cooling Phase of the DEPSG Break (Sheet 2 of 6)

Time (sec)	Break Flow (Reactor Vessel Side)			Break Flow (Steam Generator Side)		
	Mass (lbm/sec)	Enthalpy (Btu/lbm)	Energy (Thousand Btu/sec)	Mass (lbm/sec)	Enthalpy (Btu/lbm)	Energy (Thousand Btu/sec)
414.2	320.0	537.6	172.0	33.7	1187.6	40.0
418.2	414.1	591.8	245.1	113.9	1186.0	135.1
422.2	366.8	635.0	232.9	177.5	743.4	132.0
426.2	300.8	591.7	178.0	32.7	1175.5	38.4
430.2	324.9	536.2	174.2	24.6	1186.6	29.2
434.2	388.0	627.8	243.6	154.3	919.2	141.8
438.2	313.5	639.7	200.5	19.9	1172.0	23.3
442.2	356.8	595.1	212.3	33.3	1186.3	39.5
446.2	282.7	687.6	194.4	17.3	809.3	14.0
450.3	317.7	649.0	206.2	21.2	1185.5	25.1
454.3	273.9	709.0	194.2	10.8	930.9	10.1
458.3	338.0	685.2	231.6	77.8	1173.5	91.3
462.3	255.9	728.0	186.3	20.6	1143.1	23.5
466.3	255.8	731.9	187.2	10.0	1166.5	11.7
470.3	310.8	715.3	222.3	83.6	1095.6	91.6
474.4	333.2	716.7	238.8	59.6	1185.3	70.6
478.4	292.7	730.3	213.8	18.2	1184.6	21.6
482.4	275.9	760.8	209.9	53.0	1181.5	62.6
486.4	229.9	782.4	179.9	23.2	1104.2	25.6
490.4	305.0	775.5	236.5	70.3	1155.6	81.2
494.4	284.7	833.8	237.4	86.4	1026.3	88.7
498.4	243.6	774.8	188.7	14.2	1155.6	16.4
520.4	267.9	889.0	238.2	29.2	754.8	22.0
560.5	162.4	1028.7	167.1	234.8	393.5	92.4
600.5	229.7	1020.2	234.3	105.4	935.5	98.6
640.5	189.5	1031.6	195.5	21.3	449.8	9.6
680.5	189.8	1138.1	216.0	69.4	1076.7	74.7
720.5	164.9	1250.0	206.1	1664.7	288.1	479.6
760.5	184.6	1229.0	226.9	137.2	710.8	97.5
800.6	190.7	999.5	190.6	64.5	527.4	34.0
840.6	190.1	1073.2	204.0	60.8	1162.3	70.7
880.6	192.0	1064.3	204.3	95.6	848.0	81.1
920.6	219.3	959.3	210.4	37.7	1168.4	44.0
960.7	194.5	1145.2	222.7	1853.8	284.4	527.2
1000.7	199.1	1051.5	209.4	31.2	1180.8	36.8
1040.7	157.9	1055.4	166.6	91.9	270.3	24.8
1080.7	208.2	962.2	200.3	0.0	0.0	0.0

Rev. 2

Table 14-3 Break Mass and Energy Flow for the Long-term Cooling Phase of the DEPSG Break (Sheet 3 of 6)

Time (sec)	Break Flow (Reactor Vessel Side)			Break Flow (Steam Generator Side)		
	Mass (lbm/sec)	Enthalpy (Btu/lbm)	Energy (Thousand Btu/sec)	Mass (lbm/sec)	Enthalpy (Btu/lbm)	Energy (Thousand Btu/sec)
1120.7	184.4	1159.8	213.9	39.5	1179.4	46.6
1160.8	176.6	982.8	173.6	29.0	270.7	7.9
1200.8	236.0	1026.2	242.2	60.0	1038.2	62.3
1240.8	167.9	1075.9	180.6	290.0	337.9	98.0
1280.8	163.2	1029.3	168.0	125.9	271.6	34.2
1320.8	211.6	885.2	187.3	194.1	271.7	52.7
1360.8	193.7	889.7	172.3	69.7	305.1	21.3
1400.8	287.3	903.6	259.6	32.6	1180.6	38.5
1440.9	256.3	849.6	217.8	51.2	1180.5	60.4
1480.9	220.7	913.5	201.6	42.6	1146.0	48.8
1520.9	330.1	829.3	273.8	668.8	307.8	205.9
1560.9	295.8	799.8	236.6	387.0	368.2	142.5
1600.9	217.7	968.5	210.8	66.0	294.1	19.4
1641.0	215.4	913.6	196.8	27.9	1180.5	32.9
1681.0	258.7	865.0	223.8	52.0	1180.3	61.4
1721.0	232.5	837.3	194.7	12.7	1180.8	15.0
1761.0	219.7	890.0	195.5	25.4	1168.6	29.7
1801.0	215.3	921.5	198.4	0.2	269.9	0.1
1841.1	517.6	418.6	216.7	53.8	897.6	48.3
1881.1	212.3	823.0	174.7	56.1	1172.1	65.8
1921.1	178.0	907.3	161.5	8.5	1173.6	10.0
1961.1	151.5	974.9	147.7	34.9	1175.6	41.0
2001.1	943.9	275.0	259.6	93.3	1120.4	104.5
2041.2	125.8	1061.7	133.6	39.5	1175.4	46.4
2081.2	219.6	507.0	111.3	19.7	1181.2	23.3
2121.2	236.4	385.9	91.2	2.0	1179.1	2.4
2161.2	135.6	737.2	100.0	82.1	1141.7	93.7
2201.2	222.1	593.2	131.7	28.2	1181.2	33.3
2241.2	128.5	737.2	94.7	0.0	0.0	0.0
2281.3	403.6	345.1	139.3	24.2	1173.4	28.4
2321.3	387.3	359.3	139.2	27.2	1174.4	31.9
2361.3	188.5	588.3	110.9	10.6	1180.9	12.5
2401.3	162.8	596.0	97.0	1.8	1159.7	2.1
2441.3	143.6	584.1	83.9	2.9	1179.3	3.4
2481.3	133.8	685.6	91.7	25.7	1180.9	30.3
2521.4	127.5	708.1	90.3	78.1	1133.8	88.5
2561.4	234.3	436.5	102.3	22.5	1180.8	26.6

Rev. 2

Table 14-3 Break Mass and Energy Flow for the Long-term Cooling Phase of the DEPSG Break (Sheet 4 of 6)

Time (sec)	Break Flow (Reactor Vessel Side)			Break Flow (Steam Generator Side)		
	Mass (lbm/sec)	Enthalpy (Btu/lbm)	Energy (Thousand Btu/sec)	Mass (lbm/sec)	Enthalpy (Btu/lbm)	Energy (Thousand Btu/sec)
2601.4	122.7	876.1	107.5	19.3	1180.9	22.8
2641.4	329.9	376.5	124.2	26.3	1180.8	31.1
2681.4	204.7	550.3	112.6	14.1	1180.7	16.6
2721.4	201.5	552.5	111.3	14.3	1180.6	16.9
2761.4	204.5	541.2	110.7	14.8	1180.6	17.5
2801.4	201.5	541.8	109.2	14.9	1180.5	17.6
2841.4	205.6	527.7	108.5	15.0	1180.5	17.7
2881.4	203.5	528.3	107.5	14.6	1180.4	17.2
2921.5	197.6	536.8	106.1	13.7	1180.4	16.2
2961.5	304.1	373.6	113.6	24.7	1180.4	29.2
3001.6	368.9	339.3	125.2	28.2	1180.5	33.3
3201.6	152.9	648.0	99.1	22.4	1176.9	26.4
3401.9	463.1	272.3	126.1	3.5	1179.3	4.1
3602.0	294.1	408.0	120.0	34.4	1179.5	40.6
3802.1	276.8	408.2	113.0	11.6	1179.2	13.7
4002.2	208.4	441.0	91.9	20.5	1178.7	24.2
4202.4	193.7	438.0	84.8	0.0	0.0	0.0
4402.5	386.4	356.3	137.7	29.9	1178.4	35.2
4602.8	322.9	348.5	112.5	28.5	1178.3	33.6
4803.0	454.7	323.9	147.3	42.4	1177.9	49.9
5003.1	179.1	501.9	89.9	10.7	1177.5	12.6
5203.3	190.1	476.7	90.6	15.7	1177.5	18.5
5403.4	191.5	467.8	89.6	14.0	1176.4	16.5
5603.5	237.8	390.3	92.8	23.9	1175.6	28.1
5803.6	297.6	284.3	84.6	47.2	1107.3	52.3
6003.8	171.1	370.4	63.4	25.1	1176.0	29.5
6203.9	274.9	306.2	84.2	12.8	1174.6	15.0
6404.1	366.0	290.0	106.1	13.1	1176.1	15.4
6604.2	266.3	313.7	83.5	103.4	1048.9	108.5
6804.4	183.9	496.2	91.3	8.7	1176.0	10.2
7004.5	220.9	438.3	96.8	21.9	1175.9	25.8
7204.6	73.2	785.9	57.5	19.6	1175.8	23.0
7404.8	275.1	369.5	101.6	26.4	965.2	25.5
7605.0	182.9	479.9	87.8	7.7	1166.9	9.0
7805.2	211.2	370.4	78.2	0.0	0.0	0.0
8005.3	149.1	522.2	77.9	15.4	1175.2	18.1
8205.5	156.0	470.6	73.4	7.1	1174.9	8.3

Rev. 2

Table 14-3 Break Mass and Energy Flow for the Long-term Cooling Phase of the DEPSG Break (Sheet 5 of 6)

Time (sec)	Break Flow (Reactor Vessel Side)			Break Flow (Steam Generator Side)		
	Mass (lbm/sec)	Enthalpy (Btu/lbm)	Energy (Thousand Btu/sec)	Mass (lbm/sec)	Enthalpy (Btu/lbm)	Energy (Thousand Btu/sec)
8405.7	156.3	361.4	56.5	20.3	1174.9	23.9
8605.8	331.2	304.2	100.8	9.7	1174.0	11.4
8806.0	230.1	389.3	89.6	12.1	1110.4	13.4
9006.1	647.5	258.8	167.6	72.8	1173.9	85.5
9206.3	304.5	361.4	110.0	30.9	1173.8	36.3
9406.5	121.4	507.9	61.7	8.4	1165.8	9.8
9606.7	112.3	372.9	41.9	13.4	1173.9	15.7
9806.7	440.2	315.9	139.1	27.5	1173.9	32.3
10006.9	267.1	308.4	82.4	20.2	1165.8	23.5
12007.1	378.1	308.9	116.8	22.3	1172.6	26.1
14007.2	188.4	392.9	74.0	14.7	1105.2	16.2
16007.3	179.1	339.2	60.8	9.0	1159.5	10.4
18007.5	530.7	259.7	137.8	17.9	1170.1	20.9
20007.7	394.4	277.2	109.3	27.3	1164.9	31.8
22007.8	398.4	250.6	99.8	11.2	1168.0	13.1
24008.0	301.4	271.9	82.0	11.9	1068.0	12.7
26008.2	310.7	304.5	94.6	24.0	1165.8	28.0
28008.4	304.2	289.6	88.1	28.3	1139.7	32.3
30008.4	272.1	247.6	67.4	1.5	317.2	0.5
32008.6	200.9	301.6	60.6	14.2	1029.4	14.6
34008.7	40.7	580.2	23.6	0.1	218.1	0.0
36008.9	1096.6	210.1	230.4	5.6	1164.5	6.5
38009.1	76.0	581.2	44.2	8.6	1130.2	9.7
40009.3	434.7	207.5	90.2	11.3	1152.9	13.0
42009.4	128.3	366.3	47.0	4.1	1129.4	4.6
44009.6	933.0	210.4	196.3	1.7	1163.5	2.0
46009.7	0.0	0.0	0.0	26.5	894.8	23.7
48009.8	509.0	210.5	107.1	18.3	1105.4	20.2
50010.0	62.7	544.9	34.2	3.9	1162.5	4.5
52010.2	1164.9	202.6	236.0	6.9	1162.2	8.0
54010.3	394.7	206.1	81.3	24.4	1160.1	28.3
56010.5	181.1	319.0	57.8	10.1	1161.3	11.7
58010.6	259.6	205.5	53.3	12.3	1114.4	13.7
60010.9	78.5	368.4	28.9	1.8	1143.2	2.1
62011.0	297.4	204.5	60.8	7.9	1151.7	9.1
64011.2	0.0	0.0	0.0	76.2	906.3	69.1
66011.4	433.7	194.3	84.3	1.2	1160.9	1.4

Rev. 2

Table 14-3 Break Mass and Energy Flow for the Long-term Cooling Phase of the DEPSG Break (Sheet 6 of 6)

Time (sec)	Break Flow (Reactor Vessel Side)			Break Flow (Steam Generator Side)		
	Mass (lbm/sec)	Enthalpy (Btu/lbm)	Energy (Thousand Btu/sec)	Mass (lbm/sec)	Enthalpy (Btu/lbm)	Energy (Thousand Btu/sec)
68011.4	404.2	204.3	82.6	5.5	1160.9	6.4
70011.6	608.6	183.8	111.9	1.5	1160.5	1.7
72011.8	190.9	206.1	39.3	2.5	1140.8	2.9
74011.9	101.0	295.1	29.8	0.1	1140.3	0.1
76012.0	1078.9	188.1	202.9	4.8	1160.1	5.6
78012.1	475.9	185.4	88.2	1.2	1159.8	1.4
80012.2	0.0	0.0	0.0	91.0	881.2	80.2
82012.3	517.3	189.6	98.1	21.6	1159.6	25.0
84012.5	470.0	185.8	87.3	6.0	1158.6	7.0
86012.6	168.4	183.8	31.0	3.8	1159.7	4.4
88012.8	197.0	225.8	44.5	4.1	1158.5	4.7
90013.1	83.7	332.5	27.8	3.0	1156.5	3.5
92013.3	545.3	192.9	105.2	9.8	1093.7	10.7
94013.4	94.1	386.1	36.3	6.2	1158.6	7.2
96013.6	157.3	229.6	36.1	0.1	200.9	0.0
98013.8	114.7	178.1	20.4	27.6	1145.6	31.6
100000.0	410.8	182.6	75.0	3.0	949.8	2.8

Rev. 2

Table 14-4 Break Mass and Energy Flow for the Long-term Cooling Phase of the Limiting DEPSG Break (Sheet 1 of 23)

Time (sec)	Break Flow (Reactor Vessel Side)				Break Flow (Steam Generator Side)			
	Steam		Liquid		Steam		Liquid	
	Mass (lbm/sec)	Enthalpy (Btu/lbm)	Mass (lbm/sec)	Enthalpy (Btu/lbm)	Mass (lbm/sec)	Enthalpy (Btu/lbm)	Mass (lbm/sec)	Enthalpy (Btu/lbm)
266.0	81.8	1184.6	41.3	270.4	185.6	1199.1	0.6	267.6
267.0	114.2	1192.6	1263.7	277.8	465.1	1205.9	12.3	269.3
268.0	68.1	1208.8	5362.7	278.3	376.2	1204.0	183.5	269.4
269.0	52.2	1206.2	3192.5	278.5	368.1	1203.3	435.3	269.4
270.0	82.3	1232.4	2074.6	278.4	359.8	1202.8	922.2	271.7
271.0	165.4	1239.4	1581.6	279.5	248.3	1193.4	6194.5	276.5
272.0	240.4	1268.3	972.3	281.2	295.8	1187.8	6842.2	273.9
273.0	288.4	1275.1	618.9	283.8	277.2	1188.1	5117.8	271.8
274.0	318.2	1274.3	446.1	287.0	257.6	1189.3	3677.4	270.7
275.0	329.6	1272.5	340.6	290.2	299.6	1191.2	2432.6	270.7
276.0	334.6	1271.0	254.2	294.0	372.8	1191.3	2645.3	271.9
277.0	330.5	1267.4	194.0	297.2	420.6	1190.2	2980.2	272.6
278.0	312.5	1266.1	150.4	297.7	417.2	1191.0	2323.9	271.8
279.0	301.2	1269.3	206.0	280.4	399.7	1191.4	2233.7	271.7
280.0	294.4	1272.4	299.0	268.4	386.4	1191.4	2361.2	271.8
281.0	281.4	1272.6	394.0	259.9	379.8	1191.3	2313.3	271.7
282.0	264.0	1271.0	427.1	255.3	407.8	1191.7	1800.5	271.6
283.0	249.8	1269.7	334.7	255.6	556.8	1195.1	52.2	271.2
284.0	245.4	1271.2	198.4	257.0	416.6	1195.5	1066.3	272.4
285.0	237.0	1272.3	127.3	257.1	366.8	1192.6	2103.5	271.9
286.0	225.2	1273.1	87.7	256.6	353.3	1192.5	1396.3	271.1
287.0	210.9	1271.4	63.5	253.3	403.7	1194.2	614.6	270.9
288.0	211.7	1236.6	63.0	218.1	408.6	1195.8	35.8	270.1
289.0	210.3	1210.6	79.2	203.8	358.4	1196.0	413.0	271.0
290.0	199.6	1203.9	98.2	199.9	325.4	1195.5	524.4	270.4
291.0	191.2	1200.4	118.7	200.0	320.7	1195.8	398.0	270.3
292.0	179.4	1198.8	136.8	201.0	299.3	1196.0	318.5	270.1
293.0	172.9	1197.5	157.4	201.7	284.4	1196.3	259.0	270.0
294.0	168.1	1196.0	178.4	202.2	266.0	1196.7	221.3	269.9
295.0	164.9	1195.0	200.7	202.7	245.7	1196.7	289.8	269.8
296.0	160.9	1195.4	221.6	203.0	225.8	1196.7	332.8	269.8
297.0	157.2	1195.7	241.3	203.5	238.8	1196.0	370.5	269.9
298.1	153.1	1195.7	257.7	204.1	254.2	1195.7	170.2	269.9
299.1	149.0	1195.2	270.5	204.6	243.4	1196.7	5.6	269.7
300.1	145.1	1194.6	279.7	205.0	230.9	1196.7	5.5	269.6

Rev. 2

Table 14-4 Break Mass and Energy Flow for the Long-term Cooling Phase of the Limiting DEPSG Break (Sheet 2 of 23)

Time (sec)	Break Flow (Reactor Vessel Side)				Break Flow (Steam Generator Side)			
	Steam		Liquid		Steam		Liquid	
	Mass (lbm/sec)	Enthalpy (Btu/lbm)	Mass (lbm/sec)	Enthalpy (Btu/lbm)	Mass (lbm/sec)	Enthalpy (Btu/lbm)	Mass (lbm/sec)	Enthalpy (Btu/lbm)
301.1	141.6	1194.5	286.2	205.3	219.8	1196.7	5.4	269.7
302.1	138.1	1194.5	290.3	205.5	210.1	1196.7	5.2	269.6
303.1	134.8	1194.5	292.8	205.6	201.2	1196.6	4.9	269.6
304.1	131.9	1194.5	295.1	205.7	193.0	1196.5	4.6	269.6
305.1	128.9	1194.5	296.9	205.7	184.7	1196.4	4.2	269.6
306.1	126.1	1194.4	298.5	205.7	176.2	1196.4	3.6	269.7
307.1	123.4	1194.3	300.2	205.7	166.1	1196.3	24.0	269.5
308.1	121.1	1194.3	301.9	205.5	157.3	1194.5	134.3	269.5
309.1	118.2	1194.2	302.1	205.3	145.5	1194.3	103.5	269.4
310.1	116.0	1194.0	303.0	204.9	141.4	1194.4	85.3	269.4
311.1	114.9	1193.8	303.8	204.3	139.2	1194.4	69.0	269.4
312.1	114.2	1192.9	306.2	203.8	135.7	1194.5	58.6	269.3
313.1	118.6	1195.1	311.3	202.8	128.1	1194.6	42.7	269.3
314.1	120.1	1192.0	306.1	202.5	137.4	1194.4	57.0	269.3
315.1	127.0	1193.0	309.3	202.1	133.7	1194.4	50.4	269.3
316.1	129.7	1191.2	301.8	202.0	139.4	1194.2	65.1	269.4
317.1	131.2	1190.9	294.5	202.1	142.8	1194.0	68.0	269.3
318.1	131.3	1190.9	289.0	202.3	143.1	1193.8	81.5	269.3
319.1	131.2	1191.0	286.6	202.7	141.4	1193.7	76.5	269.4
320.1	131.4	1190.9	286.6	203.2	139.0	1193.6	71.9	269.3
321.1	131.6	1190.9	287.1	203.7	137.9	1193.4	89.0	269.3
322.1	131.5	1190.9	287.3	204.3	137.4	1193.2	105.3	269.3
323.1	131.1	1191.0	287.3	204.8	136.7	1193.0	110.6	269.3
324.1	130.6	1190.9	287.6	205.2	135.0	1193.0	103.7	269.3
325.1	130.3	1190.9	288.2	205.6	132.9	1192.9	94.0	269.3
326.1	130.1	1190.8	289.0	206.0	131.4	1192.8	93.8	269.3
327.1	129.8	1190.8	289.5	206.3	130.4	1192.7	100.8	269.3
328.1	129.4	1190.8	289.8	206.7	129.2	1192.5	102.2	269.3
329.1	129.0	1190.8	289.9	206.9	127.3	1192.4	97.1	269.3
330.1	128.8	1190.8	290.1	207.1	125.4	1192.4	91.9	269.2
331.1	128.6	1190.7	290.0	207.2	123.9	1192.3	90.9	269.2
332.1	128.4	1190.7	289.5	207.3	122.6	1192.1	92.6	269.2
333.1	128.2	1190.7	288.7	207.4	121.2	1192.0	92.0	269.2
334.1	127.9	1190.7	288.0	207.4	119.5	1192.0	87.3	269.2
335.1	127.7	1190.7	287.3	207.4	117.7	1191.9	81.5	269.2

Rev. 2

Table 14-4 Break Mass and Energy Flow for the Long-term Cooling Phase of the Limiting DEPSG Break (Sheet 3 of 23)

Time (sec)	Break Flow (Reactor Vessel Side)				Break Flow (Steam Generator Side)			
	Steam		Liquid		Steam		Liquid	
	Mass (lbm/sec)	Enthalpy (Btu/lbm)	Mass (lbm/sec)	Enthalpy (Btu/lbm)	Mass (lbm/sec)	Enthalpy (Btu/lbm)	Mass (lbm/sec)	Enthalpy (Btu/lbm)
336.1	127.6	1190.6	286.7	207.4	116.0	1191.8	77.1	269.2
337.1	127.4	1190.6	285.9	207.3	114.5	1191.7	74.1	269.2
338.1	127.2	1190.6	285.1	207.3	112.9	1191.7	70.3	269.1
339.1	127.0	1190.6	284.4	207.3	111.1	1191.6	65.2	269.1
340.1	126.8	1190.6	283.7	207.2	109.3	1191.5	59.8	269.1
341.1	126.6	1190.6	283.1	207.2	107.6	1191.4	55.3	269.1
342.1	126.5	1190.6	282.5	207.2	106.1	1191.3	52.2	269.1
343.1	126.3	1190.6	281.8	207.1	104.6	1191.3	48.9	269.1
344.1	126.1	1190.5	281.1	207.1	103.1	1191.2	45.4	269.1
345.1	126.0	1190.5	280.5	207.1	101.3	1191.1	41.9	269.0
346.1	125.8	1190.5	279.9	207.1	99.7	1191.0	38.9	269.0
347.1	125.7	1190.5	279.3	207.0	98.1	1191.0	36.1	269.0
348.1	125.6	1190.5	278.7	207.0	96.4	1190.9	33.3	269.0
349.1	125.5	1190.5	278.0	207.0	94.7	1190.9	30.2	269.0
350.1	125.4	1190.5	277.5	207.0	92.9	1190.8	27.4	269.0
351.1	125.3	1190.5	276.9	207.0	91.2	1190.7	24.8	269.0
352.1	125.2	1190.5	276.3	207.0	89.6	1190.7	22.4	268.9
353.1	125.2	1190.5	275.6	207.0	87.9	1190.5	20.1	269.0
354.1	125.1	1190.5	275.0	207.0	86.2	1190.5	17.8	269.0
355.1	125.1	1190.5	274.4	207.0	84.1	1190.4	15.2	268.9
356.1	125.2	1190.5	273.9	207.0	82.3	1190.4	13.7	268.9
357.1	125.2	1190.5	273.2	207.0	80.7	1190.3	12.7	268.9
358.1	125.2	1190.6	272.5	207.1	78.7	1190.2	11.6	268.9
359.1	125.3	1190.6	272.0	207.1	77.0	1190.2	10.2	268.7
360.1	125.5	1190.6	271.6	207.2	75.9	1190.1	8.9	268.9
361.1	125.6	1190.6	270.8	207.2	74.8	1190.1	7.8	269.0
362.1	125.6	1190.6	269.8	207.3	73.5	1190.0	6.8	268.7
363.1	125.5	1190.7	269.0	207.3	71.3	1189.9	5.6	268.8
364.1	125.6	1190.7	268.6	207.4	69.1	1189.8	4.4	268.9
365.1	125.8	1190.7	268.1	207.4	67.7	1189.9	3.5	268.6
366.1	125.8	1190.7	267.2	207.5	66.5	1189.8	2.9	268.9
367.1	125.7	1190.7	266.2	207.5	64.8	1189.7	2.1	268.8
368.1	125.8	1190.7	265.6	207.6	62.4	1189.7	1.2	268.0
369.1	126.0	1190.8	265.3	207.6	60.7	1189.9	0.7	269.9
370.1	126.1	1190.8	264.6	207.7	59.9	1190.1	0.5	266.5

Rev. 2

Table 14-4 Break Mass and Energy Flow for the Long-term Cooling Phase of the Limiting DEPSG Break (Sheet 4 of 23)

Time (sec)	Break Flow (Reactor Vessel Side)				Break Flow (Steam Generator Side)			
	Steam		Liquid		Steam		Liquid	
	Mass (lbm/sec)	Enthalpy (Btu/lbm)	Mass (lbm/sec)	Enthalpy (Btu/lbm)	Mass (lbm/sec)	Enthalpy (Btu/lbm)	Mass (lbm/sec)	Enthalpy (Btu/lbm)
371.1	126.0	1190.8	263.5	207.7	58.7	1190.3	0.3	274.4
372.1	125.9	1190.8	262.7	207.8	57.0	1190.4	0.0	0.0
373.1	126.2	1190.8	262.4	207.8	55.2	1190.5	0.0	0.0
374.1	126.6	1190.9	262.0	207.9	53.9	1190.5	0.0	0.0
375.1	126.5	1190.9	260.9	208.0	53.2	1190.4	0.0	0.0
376.1	126.3	1190.9	259.7	208.0	52.3	1190.4	0.0	0.0
377.1	126.3	1190.9	259.1	208.1	50.3	1190.4	0.0	0.0
378.1	126.6	1190.9	258.9	208.1	49.2	1190.3	0.0	0.0
379.1	126.8	1190.9	258.2	208.2	49.1	1190.2	0.0	0.0
380.1	126.3	1190.9	256.6	208.2	48.8	1190.2	0.0	0.0
381.1	125.8	1190.9	255.4	208.2	47.5	1190.1	0.0	0.0
382.1	125.8	1190.8	255.2	208.1	45.7	1190.0	0.0	0.0
383.1	126.7	1190.9	255.9	208.1	45.8	1190.0	0.0	0.0
384.1	127.0	1191.0	255.3	208.2	46.6	1189.9	0.0	0.0
385.1	124.7	1190.8	251.5	208.3	46.6	1189.9	0.0	0.0
386.1	122.1	1190.6	248.2	208.0	42.6	1189.8	0.0	0.0
387.1	122.6	1190.4	250.4	207.7	42.2	1189.8	0.0	0.0
388.1	124.6	1190.6	253.1	207.4	42.1	1189.7	0.0	0.0
389.1	144.0	1193.7	277.2	208.3	58.9	1189.7	0.1	273.4
390.1	155.0	1196.0	272.8	211.3	99.6	1189.2	4.3	268.6
391.1	152.6	1196.5	252.0	214.4	125.8	1187.6	94.2	268.8
392.1	152.3	1195.9	242.0	216.3	137.9	1186.2	217.1	268.8
393.1	150.6	1195.3	234.3	217.5	128.5	1185.4	347.0	268.8
394.1	143.5	1194.3	225.0	217.7	117.8	1185.3	332.5	268.7
395.1	126.8	1191.8	208.2	216.3	95.3	1186.3	51.7	268.5
396.1	125.1	1190.9	212.5	213.3	43.7	1186.7	3.2	268.4
397.1	126.8	1190.5	222.6	211.2	36.3	1187.2	0.1	280.4
398.1	127.1	1190.7	228.0	209.8	35.5	1187.7	0.0	0.0
399.1	123.2	1190.6	227.2	208.7	36.2	1188.0	0.0	0.0
400.1	112.4	1189.6	216.4	207.2	38.8	1188.3	0.0	0.0
401.1	114.7	1189.6	224.7	205.4	40.9	1188.3	0.0	0.0
402.1	132.3	1191.2	256.2	204.9	43.3	1188.5	0.0	0.0
403.1	148.3	1194.3	269.7	206.9	82.3	1188.2	1.4	267.8
404.1	159.8	1197.6	261.6	210.8	110.8	1187.8	9.1	268.6
405.1	162.6	1200.3	243.3	215.8	126.1	1186.5	112.0	268.7

Rev. 2

Table 14-4 Break Mass and Energy Flow for the Long-term Cooling Phase of the Limiting DEPSG Break (Sheet 5 of 23)

Time (sec)	Break Flow (Reactor Vessel Side) Steam Mass (lbm/sec)	Steam Enthalpy (Btu/lbm)	Liquid Mass (lbm/sec)	Liquid Enthalpy (Btu/lbm)	Break Flow (Steam Generator Side) Steam Mass (lbm/sec)	Steam Enthalpy (Btu/lbm)	Liquid Mass (lbm/sec)	Liquid Enthalpy (Btu/lbm)
406.1	149.7	1199.4	216.9	218.8	128.3	1184.9	277.4	268.7
407.1	143.8	1195.8	209.4	218.8	105.4	1185.3	191.4	268.5
408.1	140.9	1193.7	209.8	218.0	85.0	1185.9	73.0	268.5
409.2	136.7	1192.9	209.9	217.0	68.9	1186.2	21.5	268.4
410.2	125.5	1191.7	203.0	215.3	18.3	1186.5	1.9	269.0
411.2	116.4	1190.3	198.4	212.4	24.8	1186.5	0.2	262.6
412.2	119.1	1189.7	211.7	209.9	36.2	1187.1	0.0	0.0
413.2	116.8	1189.1	214.9	207.9	33.0	1187.3	0.0	0.0
414.2	112.8	1189.0	215.7	206.1	32.6	1187.6	0.0	0.0
415.2	105.9	1188.6	209.8	204.3	32.7	1187.6	0.0	0.0
416.2	121.3	1190.6	241.7	203.2	31.8	1187.7	0.0	0.0
417.2	142.0	1193.0	267.8	204.6	68.1	1187.7	0.2	265.5
418.2	156.1	1196.0	263.0	208.4	103.9	1187.1	2.9	268.7
419.2	165.1	1200.8	246.5	214.0	114.3	1186.8	25.0	268.5
420.2	155.1	1204.9	216.1	219.3	110.8	1185.5	98.2	268.6
421.2	140.7	1200.3	193.8	219.9	103.4	1184.9	110.6	268.5
422.2	151.4	1195.8	206.2	219.3	94.1	1185.1	81.5	268.5
423.2	155.7	1196.8	209.3	220.3	101.5	1184.9	111.1	268.6
424.2	141.5	1196.5	192.3	220.9	80.1	1184.6	94.2	268.4
425.2	116.6	1192.0	168.7	217.6	50.4	1185.2	15.0	268.3
426.2	117.8	1189.7	178.5	213.0	37.8	1185.5	2.0	268.6
427.2	115.2	1188.5	186.0	209.7	31.4	1185.7	0.1	272.5
428.2	112.6	1188.7	192.1	207.0	28.9	1186.2	0.0	0.0
429.2	102.8	1188.1	188.2	204.7	27.7	1186.4	0.0	0.0
430.2	105.9	1188.9	200.7	202.3	25.7	1186.6	0.0	0.0
431.2	128.1	1191.1	240.1	201.9	33.8	1186.7	0.0	0.0
432.2	142.8	1193.4	256.9	204.0	78.1	1186.7	1.0	269.7
433.2	153.2	1196.2	250.0	208.1	103.7	1186.2	3.1	268.1
434.2	164.5	1201.3	235.9	214.1	111.5	1186.0	21.7	268.5
435.2	161.1	1211.6	210.5	220.7	103.7	1185.2	66.9	268.5
436.2	139.7	1216.2	177.7	223.1	52.8	1184.7	38.6	268.1
437.2	138.3	1199.3	173.0	220.6	31.2	1185.1	5.4	268.2
438.2	136.5	1193.0	175.3	218.2	22.2	1185.2	0.9	268.0
439.2	133.3	1192.6	179.2	216.3	21.8	1185.6	0.1	263.5
440.2	113.0	1190.8	165.9	213.7	29.6	1185.9	0.0	0.0

Rev. 2

Table 14-4 Break Mass and Energy Flow for the Long-term Cooling Phase of the Limiting DEPSG Break (Sheet 6 of 23)

Time (sec)	Break Flow (Reactor Vessel Side)				Break Flow (Steam Generator Side)			
	Steam		Liquid		Steam		Liquid	
	Mass (lbm/sec)	Enthalpy (Btu/lbm)	Mass (lbm/sec)	Enthalpy (Btu/lbm)	Mass (lbm/sec)	Enthalpy (Btu/lbm)	Mass (lbm/sec)	Enthalpy (Btu/lbm)
441.2	117.9	1191.1	179.4	210.1	29.3	1186.0	0.0	0.0
442.2	136.3	1192.0	213.2	209.3	25.3	1186.3	0.0	0.0
443.2	149.7	1195.1	227.6	211.1	60.1	1186.3	0.0	0.0
444.2	162.1	1199.5	228.2	215.2	94.2	1186.2	4.0	268.3
445.2	164.9	1211.3	205.8	221.3	99.3	1185.3	35.3	268.4
446.2	142.8	1233.4	169.1	225.7	51.2	1184.7	26.8	268.2
447.2	134.3	1212.3	152.2	222.3	14.7	1185.1	2.9	268.4
448.2	134.1	1194.1	153.3	218.2	20.5	1185.1	0.5	266.0
449.3	129.6	1191.8	156.5	214.9	26.2	1185.3	0.1	266.2
450.3	130.9	1192.6	166.4	212.4	22.7	1185.7	0.0	0.0
451.3	145.9	1194.6	189.2	212.0	27.6	1185.8	0.0	0.0
452.3	159.5	1197.6	201.6	214.7	67.5	1186.0	0.0	0.0
453.3	168.3	1206.8	195.5	220.1	92.2	1185.5	16.0	268.4
454.3	143.9	1230.2	157.3	226.1	44.7	1184.8	14.2	268.3
455.3	133.8	1215.4	141.1	222.9	16.3	1185.0	1.2	267.9
456.3	136.4	1196.0	145.5	218.9	18.6	1184.9	0.2	272.0
457.3	142.1	1195.4	157.8	216.3	21.9	1185.3	0.0	0.0
458.3	159.1	1200.3	177.8	217.5	56.3	1185.6	0.1	269.5
459.3	164.7	1212.9	175.6	221.5	86.0	1185.3	13.6	268.4
460.3	160.7	1242.4	157.1	228.2	88.4	1184.4	49.1	268.3
461.3	130.3	1251.0	122.3	230.9	26.7	1184.2	13.6	268.3
462.3	134.9	1209.3	120.6	223.0	16.6	1184.5	2.2	268.4
463.3	138.1	1195.7	129.5	217.6	21.2	1184.7	0.5	266.0
464.3	160.8	1197.8	154.7	217.5	29.0	1185.0	0.1	273.1
465.3	164.8	1207.1	160.1	223.4	71.4	1185.1	2.7	268.4
466.3	138.1	1225.9	133.8	225.6	23.4	1184.8	1.7	267.7
467.3	132.6	1205.6	125.0	219.3	16.1	1185.0	0.1	267.1
468.3	134.4	1195.5	131.1	214.0	20.9	1185.1	0.0	0.0
469.3	157.7	1197.0	157.3	214.2	30.4	1185.4	0.0	0.0
470.3	166.7	1205.2	165.8	220.7	73.0	1185.3	2.2	268.5
471.3	140.9	1227.8	138.3	225.5	33.7	1184.8	2.7	267.7
472.3	132.2	1212.4	124.8	220.4	19.8	1185.0	0.1	275.0
473.3	135.4	1196.8	129.9	215.1	15.1	1185.1	0.0	0.0
474.4	160.0	1197.7	154.6	215.3	31.7	1185.3	0.0	0.0
475.4	167.6	1208.3	161.3	222.4	72.0	1185.2	2.2	267.6

Rev. 2

Table 14-4 Break Mass and Energy Flow for the Long-term Cooling Phase of the Limiting DEPSG Break (Sheet 7 of 23)

Time (sec)	Break Flow (Reactor Vessel Side)				Break Flow (Steam Generator Side)			
	Steam		Liquid		Steam		Liquid	
	Mass (lbm/sec)	Enthalpy (Btu/lbm)	Mass (lbm/sec)	Enthalpy (Btu/lbm)	Mass (lbm/sec)	Enthalpy (Btu/lbm)	Mass (lbm/sec)	Enthalpy (Btu/lbm)
476.4	140.4	1233.8	132.0	228.1	31.6	1184.6	2.6	268.4
477.4	132.1	1215.7	118.8	222.6	13.0	1185.0	0.1	276.5
478.4	137.9	1197.4	124.9	216.6	19.4	1184.9	0.0	0.0
479.4	160.0	1197.8	148.3	217.0	26.2	1185.2	0.0	0.0
480.4	165.2	1208.6	152.8	223.7	68.6	1185.2	1.1	268.4
481.4	140.8	1234.1	126.6	228.6	69.9	1184.7	8.1	268.3
482.4	139.1	1215.8	117.5	223.0	57.4	1184.5	2.3	268.6
483.4	155.1	1202.0	129.5	220.2	59.0	1184.8	0.4	268.7
484.4	171.0	1209.5	138.1	225.1	73.3	1184.6	9.5	268.1
485.4	151.2	1235.5	118.3	232.5	65.3	1184.0	24.0	268.2
486.4	127.3	1228.0	98.3	228.4	13.8	1184.0	5.5	268.1
487.4	129.4	1199.1	101.6	218.8	23.2	1184.1	1.1	268.6
488.4	144.0	1195.6	121.2	213.7	15.6	1184.1	0.2	260.5
489.4	160.1	1197.9	141.3	216.4	17.1	1184.5	0.0	0.0
490.4	163.2	1210.2	142.5	223.2	63.1	1184.7	0.6	268.3
491.4	152.8	1241.5	126.7	229.7	69.2	1184.4	6.4	268.2
492.4	140.8	1246.7	108.7	231.1	70.8	1184.1	10.9	268.2
493.4	155.3	1212.4	110.5	227.7	68.7	1184.1	7.8	268.4
494.4	170.0	1214.0	114.9	230.1	69.6	1184.1	9.6	268.3
495.4	161.8	1239.2	103.4	237.1	66.5	1183.8	16.9	268.3
496.4	131.7	1250.8	82.3	237.8	22.6	1183.6	6.2	268.1
497.4	130.1	1212.2	80.8	224.3	22.4	1183.6	1.3	268.7
498.4	134.4	1195.6	90.2	214.0	16.9	1183.5	0.6	266.6
499.4	152.4	1195.5	112.1	212.1	9.7	1183.4	0.4	269.9
500.4	166.9	1202.2	126.2	217.7	35.6	1183.6	0.7	267.4
510.4	151.0	1241.4	86.1	230.7	54.1	1182.8	225.1	268.5
520.4	158.7	1241.8	81.2	230.5	55.1	1182.5	64.1	268.4
530.4	159.0	1240.1	63.6	231.9	50.3	1182.2	80.4	268.4
540.4	152.2	1248.9	53.4	233.2	47.6	1182.2	131.0	268.5
550.4	155.3	1250.4	57.0	236.9	52.5	1181.9	196.3	268.7
560.5	155.8	1246.6	61.5	233.4	49.5	1181.9	61.4	268.6
570.5	153.4	1239.7	63.3	229.7	42.5	1181.9	51.6	268.5
580.5	153.1	1238.8	63.9	229.1	42.6	1181.6	91.2	268.5
590.5	159.3	1252.8	37.1	248.8	36.5	1181.6	67.7	268.6
600.5	155.5	1240.3	39.6	215.4	38.4	1181.1	331.2	269.1

Rev. 2

Table 14-4 Break Mass and Energy Flow for the Long-term Cooling Phase of the Limiting DEPSG Break (Sheet 8 of 23)

Time (sec)	Break Flow (Reactor Vessel Side)				Break Flow (Steam Generator Side)			
	Steam		Liquid		Steam		Liquid	
	Mass (lbm/sec)	Enthalpy (Btu/lbm)	Mass (lbm/sec)	Enthalpy (Btu/lbm)	Mass (lbm/sec)	Enthalpy (Btu/lbm)	Mass (lbm/sec)	Enthalpy (Btu/lbm)
610.5	154.3	1248.1	38.8	248.1	25.8	1181.7	5.6	268.6
620.5	163.3	1249.0	17.3	231.4	37.5	1181.4	179.0	268.8
630.5	151.3	1237.7	30.9	222.6	26.8	1181.4	6.2	268.7
640.5	157.7	1258.3	30.4	247.3	42.3	1181.3	270.7	269.0
650.5	161.7	1250.9	30.0	241.0	33.4	1181.3	9.8	268.7
660.5	154.8	1242.3	26.3	220.0	33.0	1180.9	214.3	269.0
670.5	151.6	1237.5	40.1	222.9	32.8	1180.9	119.7	268.8
680.5	160.5	1251.7	40.8	251.8	41.9	1181.0	17.0	268.9
690.5	166.0	1262.7	6.3	263.9	34.6	1180.9	316.3	269.6
700.5	155.6	1255.6	4.3	248.0	28.6	1180.9	50.3	269.0
710.5	152.3	1237.2	31.4	210.2	32.0	1180.5	126.9	269.0
720.5	163.6	1260.0	24.2	261.8	35.4	1181.0	135.1	269.4
730.5	152.4	1245.5	10.1	243.1	25.4	1180.6	159.9	269.5
740.5	160.0	1248.0	9.5	218.0	32.3	1180.8	230.5	269.4
750.5	155.0	1234.5	39.6	235.0	25.9	1180.6	3.0	269.0
760.6	161.3	1251.2	20.6	258.3	34.0	1181.1	2.8	268.9
770.6	155.4	1237.6	16.8	194.3	24.6	1180.6	474.7	269.9
780.6	145.7	1243.3	37.0	240.2	30.8	1180.8	1.4	269.3
790.6	150.6	1240.6	52.5	245.4	34.2	1180.9	2.7	269.3
800.6	153.4	1236.8	55.2	245.1	30.4	1180.9	8.9	269.4
810.6	161.7	1246.1	30.4	256.3	29.7	1180.7	142.1	269.7
820.6	154.2	1236.4	16.4	209.7	24.5	1180.4	552.3	270.0
830.6	159.9	1255.0	23.8	259.6	37.0	1180.8	13.6	269.4
840.6	145.0	1233.5	26.2	224.5	21.7	1180.4	123.5	269.5
850.6	149.6	1235.4	31.9	240.2	24.9	1180.6	0.4	270.1
860.6	158.8	1249.7	21.0	253.9	39.8	1180.8	387.9	270.0
870.6	149.4	1235.1	39.5	235.7	27.4	1180.5	0.7	269.0
880.6	150.2	1235.0	23.3	234.6	21.0	1180.6	68.4	269.6
890.6	153.1	1237.0	33.5	250.2	30.1	1180.6	214.8	269.8
900.6	151.6	1243.2	39.3	255.9	34.0	1180.4	37.6	269.6
910.6	155.5	1237.9	49.0	248.4	31.8	1180.4	52.3	269.8
920.6	148.7	1235.3	45.3	248.5	22.3	1180.3	29.2	269.7
930.6	143.4	1232.0	44.7	243.2	20.4	1180.4	0.1	271.9
940.6	160.3	1246.3	31.6	260.4	28.5	1180.8	467.6	270.5
950.7	158.1	1247.1	12.8	275.2	32.4	1180.4	44.0	270.0

Rev. 2

Table 14-4 Break Mass and Energy Flow for the Long-term Cooling Phase of the Limiting DEPSG Break (Sheet 9 of 23)

Time (sec)	Break Flow (Reactor Vessel Side)				Break Flow (Steam Generator Side)			
	Steam		Liquid		Steam		Liquid	
	Mass (lbm/sec)	Enthalpy (Btu/lbm)	Mass (lbm/sec)	Enthalpy (Btu/lbm)	Mass (lbm/sec)	Enthalpy (Btu/lbm)	Mass (lbm/sec)	Enthalpy (Btu/lbm)
960.7	161.9	1241.5	10.5	276.7	31.0	1180.4	213.6	270.3
970.7	148.0	1236.1	10.6	272.3	19.1	1180.1	209.3	270.6
980.7	150.0	1233.5	13.7	230.9	16.6	1180.9	66.5	270.1
990.7	147.8	1241.8	30.0	263.1	28.4	1180.2	12.2	269.8
1000.7	150.9	1232.7	35.5	251.3	26.4	1180.3	0.2	264.0
1010.7	157.5	1240.0	23.8	265.5	21.9	1180.7	432.1	270.6
1020.7	161.3	1236.2	29.3	256.7	36.0	1180.3	145.9	270.4
1030.7	148.8	1233.6	18.4	259.1	20.6	1180.1	66.4	270.3
1040.7	155.3	1240.8	32.2	243.9	18.2	1180.6	76.0	270.4
1050.7	159.8	1239.6	22.3	258.7	33.8	1180.2	132.2	270.5
1060.7	156.9	1241.5	3.3	264.6	27.5	1180.1	103.0	270.4
1070.7	153.9	1230.6	7.0	257.5	15.2	1180.6	525.8	271.1
1080.7	143.0	1231.8	35.5	248.9	27.2	1180.2	0.5	270.0
1090.7	147.9	1227.6	48.0	249.7	26.6	1180.2	0.1	267.3
1100.7	154.8	1236.0	13.4	266.1	20.8	1180.8	200.9	270.7
1110.7	164.0	1233.5	20.3	268.7	35.9	1180.2	119.9	270.9
1120.7	146.5	1229.1	16.9	268.8	21.3	1180.1	103.2	270.8
1130.7	158.9	1235.7	4.6	258.9	24.9	1180.6	374.1	271.1
1140.7	147.4	1221.2	35.7	245.2	30.1	1180.2	2.1	270.0
1150.7	141.5	1221.8	34.2	255.8	11.8	1179.8	26.5	270.8
1160.8	147.8	1226.4	42.3	249.0	21.0	1180.8	36.4	270.9
1170.8	144.9	1232.6	40.4	256.1	20.5	1179.9	9.6	270.4
1180.8	150.5	1233.1	54.9	246.0	23.4	1180.4	20.6	270.9
1190.8	161.3	1234.0	45.5	247.2	35.1	1180.2	83.5	271.1
1200.8	147.4	1233.0	42.2	243.6	21.0	1180.0	125.9	271.1
1210.8	163.4	1231.9	45.4	251.7	21.8	1180.3	314.2	271.5
1220.8	150.7	1231.2	43.8	242.2	18.2	1180.2	45.1	271.2
1230.8	155.7	1231.1	37.1	250.1	24.6	1180.5	82.4	271.3
1240.8	168.3	1230.9	39.3	263.8	39.2	1180.2	377.0	271.8
1250.8	151.5	1229.7	24.9	257.4	24.6	1180.2	12.8	271.4
1260.8	144.7	1226.3	30.2	256.6	16.7	1180.0	2.0	269.7
1270.8	149.9	1222.9	44.6	246.6	17.5	1180.9	131.4	271.6
1280.8	157.6	1226.2	42.3	258.7	32.6	1180.1	47.4	271.5
1290.8	149.5	1227.1	49.1	245.1	20.1	1179.9	43.4	271.5
1300.8	138.5	1217.9	55.5	249.9	14.8	1179.9	0.1	267.3

Rev. 2

Table 14-4 Break Mass and Energy Flow for the Long-term Cooling Phase of the Limiting DEPSG Break (Sheet 10 of 23)

Time (sec)	Break Flow (Reactor Vessel Side)				Break Flow (Steam Generator Side)			
	Steam		Liquid		Steam		Liquid	
	Mass (lbm/sec)	Enthalpy (Btu/lbm)	Mass (lbm/sec)	Enthalpy (Btu/lbm)	Mass (lbm/sec)	Enthalpy (Btu/lbm)	Mass (lbm/sec)	Enthalpy (Btu/lbm)
1310.8	147.2	1220.7	51.0	259.6	24.4	1180.2	0.0	0.0
1320.8	166.4	1224.4	82.1	241.2	17.2	1180.6	195.8	271.8
1330.8	161.5	1224.8	86.4	240.2	26.7	1180.2	70.4	271.8
1340.8	149.5	1223.7	57.5	241.8	20.1	1180.1	234.9	272.1
1350.8	165.1	1222.6	60.2	243.7	20.7	1180.5	116.9	272.0
1360.8	158.8	1223.1	65.6	245.6	24.4	1180.1	57.2	271.9
1370.8	154.1	1221.9	65.8	247.5	22.0	1180.1	24.9	271.9
1380.8	156.0	1220.8	66.2	241.2	7.4	1180.0	0.5	272.1
1390.9	151.1	1220.0	80.4	238.7	21.0	1180.1	0.0	0.0
1400.9	149.9	1219.9	81.7	244.1	20.9	1180.1	0.0	0.0
1410.9	149.2	1219.3	91.2	241.3	14.7	1180.1	7.3	271.6
1420.9	155.6	1218.1	95.5	239.6	18.0	1180.7	62.8	272.2
1430.9	164.9	1218.9	94.2	241.5	28.8	1180.1	70.9	272.3
1440.9	157.8	1217.2	84.6	239.5	19.7	1180.2	252.3	272.7
1450.9	161.0	1216.7	79.5	242.4	18.9	1180.2	0.0	0.0
1460.9	154.7	1216.0	80.5	241.1	19.0	1180.2	35.6	272.4
1470.9	158.8	1215.4	81.3	241.2	16.1	1180.1	1.4	271.4
1480.9	154.7	1214.6	85.9	242.1	13.1	1180.1	0.9	270.2
1490.9	150.4	1213.9	91.8	241.4	14.9	1180.4	0.1	269.0
1500.9	157.5	1213.9	98.4	242.8	19.7	1180.1	0.0	0.0
1510.9	157.0	1212.3	108.7	239.9	17.9	1180.5	45.4	272.8
1520.9	165.8	1212.8	112.0	241.4	28.8	1180.3	89.8	272.9
1530.9	162.8	1210.9	96.9	239.8	18.3	1180.5	376.9	273.3
1540.9	163.2	1210.5	78.6	243.9	16.6	1180.5	99.8	273.0
1550.9	159.0	1210.0	76.5	246.3	18.7	1180.4	20.3	272.8
1560.9	170.7	1209.8	86.8	247.1	27.1	1180.5	30.3	273.1
1570.9	160.3	1208.4	79.1	244.1	19.5	1180.4	180.1	273.2
1580.9	165.4	1208.0	77.6	245.9	18.6	1180.4	57.8	273.2
1590.9	166.6	1207.1	72.9	245.5	17.8	1180.6	172.8	273.4
1600.9	168.0	1206.2	62.3	249.5	21.4	1180.8	143.7	273.5
1611.0	168.4	1206.1	63.4	246.1	22.3	1180.4	46.4	273.4
1621.0	171.2	1205.8	62.9	248.3	26.7	1180.6	85.3	273.6
1631.0	163.2	1204.0	53.8	247.6	10.0	1180.2	106.9	273.7
1641.0	162.3	1204.3	70.0	242.3	15.3	1180.3	1.0	272.8
1651.0	157.7	1203.0	68.8	242.8	8.2	1180.8	1.0	273.7

Rev. 2

Table 14-4 Break Mass and Energy Flow for the Long-term Cooling Phase of the Limiting DEPSG Break (Sheet 11 of 23)

Time (sec)	Break Flow (Reactor Vessel Side)				Break Flow (Steam Generator Side)			
	Steam		Liquid		Steam		Liquid	
	Mass (lbm/sec)	Enthalpy (Btu/lbm)	Mass (lbm/sec)	Enthalpy (Btu/lbm)	Mass (lbm/sec)	Enthalpy (Btu/lbm)	Mass (lbm/sec)	Enthalpy (Btu/lbm)
1661.0	168.8	1203.5	77.2	244.7	29.9	1180.5	11.4	273.4
1671.0	158.5	1202.0	72.1	243.6	13.1	1180.3	64.0	273.8
1681.0	158.9	1201.5	74.6	243.7	14.7	1180.3	1.1	273.3
1691.0	162.6	1199.9	85.3	243.1	16.7	1180.9	38.5	274.0
1701.0	159.4	1200.4	82.3	243.3	18.6	1180.3	20.6	273.8
1711.0	160.6	1199.5	93.7	241.8	14.1	1180.4	0.2	275.0
1721.0	153.6	1199.2	90.3	244.5	16.3	1180.3	0.0	0.0
1731.0	155.3	1197.8	80.1	249.0	3.9	1180.6	0.0	0.0
1741.0	154.2	1198.1	78.9	251.9	10.9	1180.0	0.0	0.0
1751.0	151.6	1197.1	72.7	253.5	10.8	1180.5	0.1	275.1
1761.0	152.9	1196.6	78.7	250.5	13.3	1180.6	0.1	282.1
1771.0	160.7	1196.3	76.0	251.6	21.4	1180.4	0.1	269.1
1781.0	176.0	1195.1	60.5	246.5	35.6	1181.0	242.4	274.6
1791.0	162.8	1194.0	50.1	248.7	28.9	1180.9	30.5	274.6
1801.0	155.6	1192.7	33.8	242.4	33.1	1181.3	77.9	274.8
1811.1	134.2	1194.0	242.6	225.8	50.8	1180.9	14.9	274.8
1821.1	100.9	1189.9	278.4	230.4	28.5	1181.4	20.3	274.9
1831.1	133.0	1191.8	95.8	249.2	24.9	1180.6	0.2	266.7
1841.1	75.0	1192.8	913.1	239.9	62.0	1181.2	22.6	274.8
1851.1	130.4	1191.0	160.0	250.9	16.9	1180.8	0.7	274.5
1861.1	85.0	1189.7	397.5	252.3	48.6	1181.2	15.7	274.9
1871.1	111.0	1190.6	117.2	257.8	52.0	1181.1	8.3	274.9
1881.1	103.5	1190.2	230.8	259.7	28.4	1181.0	3.5	274.8
1891.1	126.5	1190.0	62.2	269.2	38.9	1181.1	3.0	274.8
1901.1	130.0	1189.4	55.4	267.0	24.4	1181.1	0.2	276.8
1911.1	129.3	1188.9	54.4	262.3	22.8	1181.1	0.1	274.5
1921.1	127.7	1188.6	53.2	259.5	20.7	1181.1	0.1	272.3
1931.1	125.2	1188.3	51.3	256.5	19.1	1181.1	0.1	279.2
1941.1	124.2	1188.3	45.1	254.9	20.7	1181.1	0.1	270.5
1951.1	121.9	1188.2	28.3	255.3	19.2	1181.1	0.1	280.7
1961.1	116.5	1188.0	27.7	245.0	18.9	1181.1	0.1	270.4
1971.1	105.8	1187.6	58.9	233.1	21.9	1181.1	1.1	275.0
1981.1	52.8	1188.7	595.3	224.5	66.6	1181.3	7.8	275.0
1991.1	70.5	1183.2	179.6	226.7	9.7	1180.4	0.0	0.0
2001.1	33.6	1187.1	1126.6	240.1	55.2	1181.3	6.9	274.8

Rev. 2

Table 14-4 Break Mass and Energy Flow for the Long-term Cooling Phase of the Limiting DEPSG Break (Sheet 12 of 23)

Time (sec)	Break Flow (Reactor Vessel Side)				Break Flow (Steam Generator Side)			
	Steam		Liquid		Steam		Liquid	
	Mass (lbm/sec)	Enthalpy (Btu/lbm)	Mass (lbm/sec)	Enthalpy (Btu/lbm)	Mass (lbm/sec)	Enthalpy (Btu/lbm)	Mass (lbm/sec)	Enthalpy (Btu/lbm)
2011.2	80.1	1186.9	353.8	243.8	50.6	1181.3	1.5	274.8
2021.2	105.3	1187.2	64.2	257.1	22.5	1181.2	0.2	274.2
2031.2	106.2	1187.0	41.1	263.6	20.0	1181.2	0.0	0.0
2041.2	105.5	1186.9	25.3	265.4	22.3	1181.2	0.0	0.0
2051.2	103.3	1186.8	18.2	264.7	22.9	1181.2	0.1	273.2
2061.2	94.7	1184.7	23.2	254.7	21.0	1181.2	0.2	274.3
2071.2	84.2	1184.0	79.7	232.5	20.0	1181.3	0.4	275.1
2081.2	58.7	1184.2	232.5	221.2	42.2	1181.2	1.9	274.5
2091.2	74.8	1183.2	102.9	217.7	30.8	1181.2	0.2	273.2
2101.2	85.3	1186.3	63.9	231.4	22.9	1181.2	0.0	0.0
2111.2	75.2	1184.1	127.2	230.6	18.5	1181.0	0.2	275.6
2121.2	48.7	1183.0	393.0	225.3	37.9	1181.2	2.7	274.5
2131.2	33.2	1183.0	745.7	232.7	46.2	1181.1	3.7	274.3
2141.2	64.4	1184.9	308.8	237.6	30.6	1181.3	0.0	0.0
2151.2	77.5	1183.7	126.7	243.3	18.6	1181.2	0.0	0.0
2161.2	74.3	1183.0	101.5	235.3	38.2	1181.2	1.1	274.4
2171.2	63.2	1181.9	175.4	223.6	31.4	1181.1	0.7	273.8
2181.2	58.3	1182.7	256.5	224.0	34.2	1181.2	0.9	274.2
2191.2	65.1	1182.9	182.2	232.6	27.3	1181.1	0.4	274.5
2201.2	64.6	1183.3	263.3	235.4	31.2	1181.2	0.4	274.2
2211.2	69.0	1183.7	157.1	235.3	29.4	1181.2	0.6	273.9
2221.2	67.7	1183.2	228.5	231.0	38.1	1181.1	0.9	273.5
2231.2	63.2	1185.0	251.1	230.5	32.9	1181.2	1.1	273.9
2241.2	69.0	1185.0	167.6	229.7	45.3	1181.1	2.2	273.9
2251.3	50.6	1185.2	292.6	227.8	44.1	1181.1	1.7	273.6
2261.3	50.7	1185.9	366.7	230.3	30.0	1181.1	0.1	276.3
2271.3	72.9	1184.7	113.6	238.8	25.2	1181.1	0.1	273.0
2281.3	65.5	1183.8	121.1	235.6	20.2	1181.1	0.5	273.9
2291.3	37.9	1185.3	670.5	230.1	52.4	1181.0	2.2	273.4
2301.3	61.3	1184.1	200.7	234.1	27.8	1181.2	0.1	271.9
2311.3	72.9	1184.6	64.8	243.4	26.0	1181.1	0.0	0.0
2321.3	63.1	1183.2	69.4	240.2	19.6	1181.0	0.8	273.1
2331.3	27.7	1185.7	878.0	233.0	55.3	1181.0	2.2	273.3
2341.3	64.2	1184.2	269.3	235.8	27.6	1181.1	0.0	0.0
2351.3	75.8	1184.2	57.7	246.2	27.7	1181.1	0.2	272.1

Rev. 2

Table 14-4 Break Mass and Energy Flow for the Long-term Cooling Phase of the Limiting DEPSG Break (Sheet 13 of 23)

Time (sec)	Break Flow (Reactor Vessel Side)				Break Flow (Steam Generator Side)			
	Steam		Liquid		Steam		Liquid	
	Mass (lbm/sec)	Enthalpy (Btu/lbm)	Mass (lbm/sec)	Enthalpy (Btu/lbm)	Mass (lbm/sec)	Enthalpy (Btu/lbm)	Mass (lbm/sec)	Enthalpy (Btu/lbm)
2361.3	72.1	1184.2	119.8	236.4	26.8	1181.0	0.1	271.2
2371.3	67.1	1184.4	140.3	232.9	27.6	1181.1	0.1	275.9
2381.3	67.4	1184.2	102.6	234.3	29.8	1181.0	0.5	273.0
2391.3	48.3	1184.2	266.2	229.6	46.8	1181.0	1.4	273.0
2401.3	46.6	1184.5	270.5	230.8	36.8	1181.0	0.7	273.0
2411.3	59.1	1184.3	208.6	232.9	31.8	1181.0	0.5	272.7
2421.3	61.9	1184.2	229.2	231.6	32.4	1181.0	0.5	273.0
2431.3	62.3	1183.9	220.4	229.0	30.0	1181.0	0.4	273.1
2441.3	61.3	1183.8	134.5	229.5	30.0	1181.0	0.5	272.0
2451.3	50.1	1184.4	299.8	228.1	45.2	1180.9	1.2	272.8
2461.3	53.2	1184.0	174.3	229.1	32.6	1181.0	0.5	272.6
2471.3	57.7	1184.0	232.7	228.8	30.9	1180.9	0.3	272.7
2481.3	60.9	1184.1	215.5	227.5	33.6	1181.0	0.1	271.2
2491.4	54.1	1182.9	165.7	229.8	20.4	1180.8	0.0	0.0
2501.4	30.0	1183.6	610.5	228.2	46.6	1180.9	1.7	272.3
2511.4	52.3	1183.5	216.2	232.3	33.0	1180.9	0.1	276.0
2521.4	68.5	1183.4	77.1	238.0	30.0	1181.0	0.3	272.3
2531.4	47.1	1182.6	292.7	232.9	16.4	1180.4	0.1	273.0
2541.4	29.5	1183.4	590.9	232.6	48.3	1180.9	1.6	272.2
2551.4	63.9	1183.0	118.8	237.5	19.7	1180.9	0.0	0.0
2561.4	63.4	1183.2	166.3	236.1	28.0	1180.9	0.1	270.6
2571.4	35.0	1183.9	278.8	233.5	42.9	1180.8	1.1	272.4
2581.4	43.8	1183.9	341.1	238.0	38.3	1180.8	2.2	272.0
2591.4	57.2	1183.9	76.0	238.0	33.0	1180.8	0.0	0.0
2601.4	74.7	1183.5	42.8	235.3	20.4	1180.9	0.0	0.0
2611.4	81.7	1182.9	32.9	233.1	19.3	1180.8	0.0	0.0
2621.4	79.3	1183.1	17.5	232.3	20.6	1180.9	0.0	0.0
2631.4	75.1	1183.2	51.7	208.7	22.0	1180.8	0.0	0.0
2641.4	66.1	1183.3	208.2	205.1	24.8	1180.8	0.0	0.0
2651.4	67.2	1183.3	206.0	204.1	26.1	1180.7	0.0	0.0
2661.4	64.5	1183.3	222.6	202.3	27.1	1180.8	0.0	0.0
2671.4	69.1	1183.0	268.6	201.1	24.4	1180.7	0.0	0.0
2681.4	70.7	1182.8	220.0	200.4	22.1	1180.8	0.0	0.0
2691.4	67.5	1182.9	238.1	199.8	24.5	1180.7	0.0	0.0
2701.4	67.5	1183.1	249.3	199.3	27.9	1180.7	0.0	0.0

Rev. 2

Table 14-4 Break Mass and Energy Flow for the Long-term Cooling Phase of the Limiting DEPSG Break (Sheet 14 of 23)

Time (sec)	Break Flow (Reactor Vessel Side)				Break Flow (Steam Generator Side)			
	Steam		Liquid		Steam		Liquid	
	Mass (lbm/sec)	Enthalpy (Btu/lbm)	Mass (lbm/sec)	Enthalpy (Btu/lbm)	Mass (lbm/sec)	Enthalpy (Btu/lbm)	Mass (lbm/sec)	Enthalpy (Btu/lbm)
2711.4	68.8	1182.8	232.9	198.8	25.0	1180.7	0.0	0.0
2721.4	69.4	1182.8	213.3	198.3	22.4	1180.6	0.0	0.0
2731.4	67.0	1182.8	228.6	197.7	24.3	1180.7	0.0	0.0
2741.4	67.0	1183.0	249.6	197.4	28.0	1180.6	0.0	0.0
2751.4	67.9	1182.8	234.8	197.1	24.8	1180.6	0.0	0.0
2761.4	68.2	1182.8	212.8	197.0	22.6	1180.6	0.0	0.0
2771.4	65.8	1182.7	229.2	196.7	24.5	1180.6	0.0	0.0
2781.4	65.9	1182.9	248.7	196.5	27.9	1180.6	0.0	0.0
2791.4	67.0	1182.7	237.8	196.3	24.6	1180.6	0.0	0.0
2801.4	67.2	1182.7	216.9	196.2	22.5	1180.5	0.0	0.0
2811.4	64.6	1182.6	233.2	196.1	24.7	1180.6	0.0	0.0
2821.4	64.6	1182.9	251.7	196.1	28.1	1180.5	0.0	0.0
2831.4	65.9	1182.7	239.3	196.0	24.6	1180.6	0.0	0.0
2841.4	66.4	1182.5	218.5	195.9	22.3	1180.5	0.0	0.0
2851.4	63.7	1182.6	236.5	195.9	24.6	1180.5	0.0	0.0
2861.4	63.7	1182.8	252.2	195.9	28.2	1180.5	0.0	0.0
2871.4	64.8	1182.6	239.2	195.9	24.8	1180.5	0.0	0.0
2881.4	65.2	1182.5	217.7	195.9	22.5	1180.5	0.0	0.0
2891.5	63.0	1182.5	234.0	195.9	24.4	1180.5	0.0	0.0
2901.5	62.6	1182.6	256.5	195.9	28.1	1180.5	0.0	0.0
2911.5	63.7	1182.5	244.0	195.9	24.9	1180.4	0.0	0.0
2921.5	64.2	1182.3	222.1	196.0	22.5	1180.5	0.0	0.0
2931.5	61.7	1182.4	237.5	196.0	24.7	1180.4	0.0	0.0
2941.5	62.5	1182.6	247.3	196.0	26.9	1180.4	0.0	0.0
2951.5	63.8	1182.3	235.4	196.0	23.9	1180.4	0.0	0.0
2961.5	62.3	1182.3	229.7	196.0	22.7	1180.4	0.0	0.0
2971.5	60.5	1182.5	243.2	196.1	25.7	1180.5	0.0	0.0
2981.5	62.3	1182.4	257.5	196.2	27.1	1180.5	0.0	0.0
2991.5	62.7	1182.3	226.4	196.2	21.7	1180.5	0.0	0.0
3001.6	61.3	1182.3	231.2	196.3	23.9	1180.6	0.0	0.0
3051.6	33.6	1182.6	441.1	211.2	29.7	1180.3	2.5	270.1
3101.6	26.4	1182.7	498.5	235.0	28.7	1180.3	0.7	269.7
3151.6	65.7	1181.8	21.8	245.2	19.1	1180.2	0.0	0.0
3201.7	45.3	1181.8	114.5	232.7	28.6	1180.1	0.2	270.0
3251.7	56.0	1181.4	210.1	220.4	23.7	1180.1	0.0	0.0

Rev. 2

Table 14-4 Break Mass and Energy Flow for the Long-term Cooling Phase of the Limiting DEPSG Break (Sheet 15 of 23)

Time (sec)	Break Flow (Reactor Vessel Side)				Break Flow (Steam Generator Side)			
	Steam		Liquid		Steam		Liquid	
	Mass (lbm/sec)	Enthalpy (Btu/lbm)	Mass (lbm/sec)	Enthalpy (Btu/lbm)	Mass (lbm/sec)	Enthalpy (Btu/lbm)	Mass (lbm/sec)	Enthalpy (Btu/lbm)
3301.7	52.9	1181.7	246.4	224.6	23.2	1180.0	0.1	269.0
3351.8	58.0	1181.3	219.7	210.8	23.8	1180.0	0.0	0.0
3401.9	38.6	1181.6	266.3	219.2	17.2	1179.8	0.6	268.0
3451.9	32.2	1181.7	510.7	241.1	33.7	1179.8	1.5	267.9
3502.0	35.8	1181.3	263.4	243.0	37.1	1179.7	0.9	267.4
3552.0	54.5	1181.0	87.1	241.1	22.0	1179.7	0.0	0.0
3602.0	56.1	1180.8	132.0	227.4	22.6	1179.6	0.0	0.0
3652.0	54.3	1180.6	235.6	212.5	23.1	1179.6	0.0	0.0
3702.1	40.4	1180.8	292.1	217.9	30.7	1179.4	0.6	266.7
3752.1	48.8	1180.5	259.6	222.0	25.4	1179.3	0.5	266.6
3802.1	53.8	1180.5	232.4	213.6	23.5	1179.4	0.0	0.0
3852.1	42.3	1180.3	317.9	213.8	27.3	1179.2	0.6	266.0
3902.1	38.4	1180.8	296.0	227.7	25.7	1179.2	0.4	266.1
3952.2	54.0	1180.4	177.6	218.6	21.9	1179.2	0.0	0.0
4002.3	49.1	1180.1	251.0	216.4	22.3	1179.0	0.1	268.6
4052.3	51.2	1180.2	234.9	214.6	21.8	1179.0	0.3	265.0
4102.3	39.3	1181.2	321.4	217.0	27.2	1178.9	2.1	264.8
4152.3	40.8	1180.8	277.4	226.0	26.2	1178.8	0.9	264.8
4202.4	39.0	1179.9	235.3	229.8	24.0	1178.7	0.3	264.6
4252.4	41.8	1179.8	246.5	229.3	26.3	1178.7	0.3	264.2
4302.5	44.6	1179.8	238.4	228.3	23.6	1178.7	0.1	264.8
4352.5	49.9	1179.7	246.2	221.1	22.1	1178.6	0.1	264.1
4402.5	49.8	1179.7	235.3	216.9	21.3	1178.5	0.0	0.0
4452.6	50.7	1179.6	262.1	215.1	21.4	1178.5	0.0	0.0
4502.6	47.2	1179.5	233.7	216.1	23.6	1178.4	0.5	263.3
4552.7	36.1	1179.9	295.3	222.1	26.1	1178.3	2.1	263.1
4602.8	42.5	1179.8	246.0	225.9	23.4	1178.3	0.4	263.3
4652.8	43.0	1179.9	260.2	221.0	22.3	1178.2	1.5	262.4
4702.8	39.5	1179.9	285.4	229.1	21.6	1178.1	0.3	262.7
4752.9	39.8	1180.1	252.0	230.4	27.7	1178.1	1.6	262.4
4803.0	47.6	1179.2	229.3	222.5	22.2	1178.1	0.1	262.3
4853.0	46.4	1179.1	232.8	219.6	21.2	1178.0	0.2	261.7
4903.0	46.2	1179.1	288.7	218.5	23.0	1178.0	0.2	262.1
4953.1	48.0	1178.9	254.0	217.0	22.2	1178.0	0.0	0.0
5003.1	49.8	1178.9	239.5	216.1	19.9	1177.8	0.0	0.0

Rev. 2

Table 14-4 Break Mass and Energy Flow for the Long-term Cooling Phase of the Limiting DEPSG Break (Sheet 16 of 23)

Time (sec)	Break Flow (Reactor Vessel Side)				Break Flow (Steam Generator Side)			
	Steam		Liquid		Steam		Liquid	
	Mass (lbm/sec)	Enthalpy (Btu/lbm)	Mass (lbm/sec)	Enthalpy (Btu/lbm)	Mass (lbm/sec)	Enthalpy (Btu/lbm)	Mass (lbm/sec)	Enthalpy (Btu/lbm)
5053.2	47.4	1179.0	240.6	215.6	21.1	1177.8	0.0	0.0
5103.2	43.2	1178.7	285.2	218.8	17.4	1177.6	0.3	261.8
5153.3	47.4	1178.8	242.8	222.0	18.4	1177.5	0.1	261.9
5203.3	46.2	1178.7	261.1	218.7	23.3	1177.6	0.7	261.0
5253.3	41.5	1178.8	257.7	219.1	22.1	1177.6	0.4	260.1
5303.3	34.0	1179.5	294.4	226.2	24.5	1177.5	1.7	260.6
5353.4	43.6	1178.5	251.2	228.0	19.8	1177.3	0.0	0.0
5403.4	47.9	1178.5	223.9	221.9	20.5	1177.5	0.0	0.0
5453.5	43.7	1178.5	262.4	219.4	20.9	1177.4	0.0	0.0
5503.5	43.4	1178.4	268.1	223.1	19.8	1177.3	0.2	259.4
5553.5	41.1	1178.4	276.7	221.1	22.9	1177.3	0.6	259.8
5603.5	46.6	1178.3	237.4	221.1	19.4	1177.2	0.0	0.0
5653.5	42.6	1178.3	263.9	220.1	20.6	1177.1	0.0	0.0
5703.5	33.8	1178.1	284.3	225.9	25.2	1177.0	1.5	259.2
5753.5	43.5	1178.1	215.1	225.2	20.0	1177.2	0.3	259.5
5803.6	36.5	1178.1	297.7	225.4	24.4	1177.0	1.7	258.7
5853.7	39.3	1178.0	250.4	228.8	20.0	1176.9	0.6	258.8
5903.7	36.6	1178.0	270.7	231.5	23.8	1177.0	1.1	258.6
5953.8	40.3	1178.0	252.1	227.8	21.6	1176.9	0.2	258.4
6003.8	46.6	1177.8	230.1	222.7	17.6	1176.8	0.0	0.0
6053.8	31.4	1178.2	364.6	224.9	23.9	1176.7	1.0	258.2
6103.9	44.2	1177.9	197.9	231.0	19.6	1176.8	0.0	0.0
6153.9	44.5	1177.8	232.2	223.9	19.8	1176.8	0.0	0.0
6203.9	39.5	1177.6	275.2	222.7	19.5	1176.7	0.2	257.7
6254.0	28.5	1177.5	316.7	230.8	25.2	1176.6	1.7	257.5
6304.1	36.2	1178.2	272.3	234.1	23.1	1176.6	0.5	257.1
6354.1	44.6	1177.5	219.2	228.2	19.0	1176.6	0.0	0.0
6404.1	41.3	1177.4	251.3	224.2	18.3	1176.5	0.0	0.0
6454.1	30.8	1177.9	352.8	231.4	25.6	1176.3	1.5	257.0
6504.1	45.8	1177.4	169.0	228.4	18.8	1176.5	0.0	0.0
6554.1	44.4	1177.3	218.4	223.8	17.8	1176.3	0.0	0.0
6604.2	36.2	1177.3	298.2	224.5	21.4	1176.3	1.0	256.6
6654.3	37.8	1177.3	278.4	228.4	21.6	1176.1	1.0	256.1
6704.3	41.3	1177.2	254.0	224.7	17.1	1176.2	0.0	0.0
6754.3	35.6	1177.3	291.2	225.6	23.9	1176.2	1.2	256.2

Rev. 2

Table 14-4 Break Mass and Energy Flow for the Long-term Cooling Phase of the Limiting DEPSG Break (Sheet 17 of 23)

Time (sec)	Break Flow (Reactor Vessel Side)				Break Flow (Steam Generator Side)			
	Steam		Liquid		Steam		Liquid	
	Mass (lbm/sec)	Enthalpy (Btu/lbm)	Mass (lbm/sec)	Enthalpy (Btu/lbm)	Mass (lbm/sec)	Enthalpy (Btu/lbm)	Mass (lbm/sec)	Enthalpy (Btu/lbm)
6804.4	42.4	1177.3	246.3	229.2	17.3	1176.1	0.1	255.7
6854.4	43.7	1177.1	237.4	224.6	18.4	1176.1	0.0	0.0
6904.4	38.5	1177.1	258.7	223.3	20.0	1176.1	0.7	255.9
6954.4	32.5	1177.5	343.3	229.4	22.1	1175.9	1.8	255.4
7004.5	43.9	1177.1	190.0	228.5	18.4	1176.0	0.0	0.0
7054.6	41.7	1176.9	225.0	224.7	18.1	1175.9	0.0	0.0
7104.6	32.4	1176.9	303.9	227.4	22.6	1175.8	0.9	255.3
7154.6	18.0	1177.2	564.5	235.4	25.8	1175.8	2.3	255.0
7204.7	45.4	1176.8	49.8	241.7	19.7	1175.7	0.2	254.7
7254.7	43.4	1176.8	157.7	228.7	17.5	1175.8	0.0	0.0
7304.7	41.6	1176.6	231.8	225.2	18.3	1175.8	0.0	0.0
7354.8	32.2	1176.6	302.3	226.9	20.2	1175.7	0.8	254.6
7404.8	35.3	1176.6	350.4	228.9	23.9	1175.6	1.8	254.4
7454.8	39.1	1176.6	224.5	227.9	19.7	1175.7	0.2	254.4
7504.8	41.1	1176.6	253.5	224.8	17.4	1175.5	0.0	0.0
7554.9	32.1	1176.6	362.0	226.4	20.3	1175.5	1.2	254.1
7605.0	39.2	1176.5	191.3	231.4	20.3	1175.6	0.6	254.0
7655.0	41.4	1176.4	235.9	226.1	17.0	1175.3	0.0	0.0
7705.1	36.8	1176.3	285.4	225.9	19.2	1175.3	0.8	253.7
7755.2	40.7	1176.4	261.9	226.7	18.4	1175.4	0.0	0.0
7805.2	39.9	1176.3	261.8	224.3	18.3	1175.4	0.0	0.0
7855.2	36.0	1176.3	272.9	225.7	21.3	1175.3	1.2	253.4
7905.2	32.1	1176.4	269.5	227.0	23.4	1175.2	3.1	253.1
7955.3	33.6	1176.4	250.2	229.0	21.1	1175.3	1.2	253.2
8005.3	34.8	1176.2	273.5	227.2	22.4	1175.2	1.0	253.0
8055.3	27.9	1176.6	292.1	230.4	22.5	1175.2	2.1	252.9
8105.4	33.0	1176.3	279.6	232.3	20.4	1175.1	1.4	252.8
8155.5	40.3	1176.4	210.9	232.3	17.5	1175.0	0.0	0.0
8205.5	39.9	1176.1	226.9	226.6	17.4	1175.0	0.0	0.0
8255.6	34.1	1175.9	291.0	227.2	16.9	1175.0	0.1	253.3
8305.6	29.1	1176.5	344.1	231.7	24.5	1175.0	3.9	252.3
8355.6	33.0	1176.4	263.2	233.3	21.3	1175.0	1.6	252.1
8405.7	32.5	1176.2	210.8	233.8	22.4	1175.0	1.8	252.1
8455.7	30.4	1176.0	292.5	232.7	21.9	1174.9	1.2	252.0
8505.7	25.7	1175.7	342.5	235.8	25.8	1174.9	1.6	251.8

Rev. 2

Table 14-4 Break Mass and Energy Flow for the Long-term Cooling Phase of the Limiting DEPSG Break (Sheet 18 of 23)

Time (sec)	Break Flow (Reactor Vessel Side)				Break Flow (Steam Generator Side)			
	Steam		Liquid		Steam		Liquid	
	Mass (lbm/sec)	Enthalpy (Btu/lbm)	Mass (lbm/sec)	Enthalpy (Btu/lbm)	Mass (lbm/sec)	Enthalpy (Btu/lbm)	Mass (lbm/sec)	Enthalpy (Btu/lbm)
8555.8	35.0	1175.8	210.5	233.3	21.2	1174.9	0.6	251.7
8605.9	28.0	1175.8	313.0	232.6	21.6	1174.8	1.4	251.6
8655.9	35.4	1175.8	214.5	235.9	20.3	1174.7	0.3	251.4
8706.0	39.4	1175.6	243.6	228.7	17.4	1174.8	0.0	0.0
8756.0	37.7	1175.6	262.5	226.2	16.3	1174.6	0.0	0.0
8806.0	38.1	1175.5	281.6	225.7	17.0	1174.7	0.1	251.6
8856.0	38.8	1175.5	269.9	225.1	16.6	1174.5	0.1	251.3
8906.1	34.6	1175.5	268.5	226.6	17.9	1174.4	0.8	250.9
8956.1	29.7	1175.5	280.2	231.4	22.4	1174.5	1.2	250.9
9006.1	32.6	1175.5	309.5	230.5	18.5	1174.5	0.6	250.8
9056.2	35.4	1175.7	222.8	232.6	21.7	1174.4	0.9	250.7
9106.2	38.8	1175.4	231.0	227.2	16.9	1174.5	0.0	0.0
9156.2	35.2	1175.4	271.3	225.5	17.3	1174.4	0.0	0.0
9206.3	28.2	1175.7	330.8	230.2	23.3	1174.5	2.1	250.4
9256.4	40.1	1175.3	212.3	227.8	16.0	1174.3	0.0	0.0
9306.4	37.8	1175.3	263.5	225.3	16.6	1174.3	0.0	0.0
9356.4	29.8	1175.2	313.4	227.1	23.2	1174.3	2.0	250.2
9406.5	30.0	1175.2	272.3	231.4	20.1	1174.3	0.8	249.9
9456.5	31.6	1175.2	264.8	229.3	20.9	1174.2	1.5	249.9
9506.5	27.8	1175.4	287.5	234.1	19.4	1174.2	1.0	249.6
9556.6	39.5	1175.1	217.9	230.2	17.3	1174.2	0.0	0.0
9606.7	36.1	1175.1	253.0	226.4	16.9	1174.1	0.0	0.0
9656.7	29.3	1175.1	307.2	228.7	20.5	1174.1	1.6	249.6
9706.7	33.6	1175.0	228.5	230.7	18.4	1174.0	0.6	249.1
9756.7	27.5	1175.5	299.2	230.7	23.2	1174.0	1.5	248.9
9806.7	37.5	1175.0	259.2	229.2	16.7	1174.0	0.2	249.1
9856.8	38.4	1174.8	236.0	225.8	17.0	1174.0	0.0	0.0
9906.8	32.2	1174.9	316.7	225.6	18.3	1173.9	1.3	249.2
9956.9	27.1	1174.9	302.6	230.9	20.7	1174.0	0.7	248.8
10006.9	23.7	1175.3	349.8	235.4	23.1	1173.9	2.7	248.7
10507.0	32.5	1174.8	260.3	229.6	19.0	1173.7	0.7	248.2
11007.0	32.3	1174.5	270.3	227.5	18.2	1173.5	1.0	247.3
11507.1	32.3	1174.2	270.3	226.8	17.7	1173.2	0.7	246.5
12007.1	30.6	1173.9	272.2	227.3	18.7	1172.9	1.1	245.8
12507.1	29.4	1173.8	277.1	228.1	18.3	1172.7	1.1	244.9

Rev. 2

Table 14-4 Break Mass and Energy Flow for the Long-term Cooling Phase of the Limiting DEPSG Break (Sheet 19 of 23)

Time (sec)	Break Flow (Reactor Vessel Side)				Break Flow (Steam Generator Side)			
	Steam		Liquid		Steam		Liquid	
	Mass (lbm/sec)	Enthalpy (Btu/lbm)	Mass (lbm/sec)	Enthalpy (Btu/lbm)	Mass (lbm/sec)	Enthalpy (Btu/lbm)	Mass (lbm/sec)	Enthalpy (Btu/lbm)
13007.1	31.0	1173.5	271.5	224.8	17.5	1172.4	0.8	244.0
13507.1	28.2	1173.3	282.6	226.4	18.1	1172.2	1.4	243.3
14007.2	28.6	1173.0	274.9	225.4	17.9	1172.0	1.1	242.6
14507.2	27.0	1172.9	278.1	226.8	18.1	1171.7	1.4	241.8
15007.2	26.5	1172.6	273.9	227.3	18.0	1171.5	1.3	241.0
15507.3	27.2	1172.3	280.0	223.5	17.4	1171.3	1.2	240.3
16007.3	27.5	1172.1	271.5	223.2	17.1	1171.1	1.0	239.7
16507.4	25.2	1171.9	290.1	222.9	17.5	1170.9	1.4	239.1
17007.4	26.9	1171.7	272.3	220.2	16.8	1170.7	1.1	238.4
17507.4	26.7	1171.5	273.7	220.2	16.2	1170.4	1.0	237.8
18007.5	23.5	1171.4	288.5	223.0	17.4	1170.3	1.8	237.2
18507.6	24.2	1171.1	279.4	222.1	17.3	1170.1	1.4	236.4
19007.6	25.5	1170.9	282.8	217.1	16.3	1169.8	1.5	235.9
19507.7	23.4	1170.8	289.7	220.1	16.4	1169.6	1.3	235.3
20007.7	25.0	1170.4	263.0	219.9	16.1	1169.5	1.2	234.7
20507.7	23.9	1170.4	302.8	214.5	16.0	1169.3	1.5	234.1
21007.8	21.9	1170.2	279.3	218.6	17.2	1169.2	1.8	233.6
21507.8	22.9	1170.0	285.0	216.1	16.0	1168.9	1.3	233.0
22007.8	21.5	1169.9	300.2	216.6	16.9	1168.8	2.2	232.4
22507.9	24.4	1169.6	273.7	215.1	14.4	1168.6	1.0	231.9
23008.0	22.0	1169.5	291.1	214.4	16.0	1168.5	2.0	231.5
23508.0	23.6	1169.3	263.6	216.0	14.5	1168.3	1.2	230.8
24008.0	22.6	1169.1	284.3	210.5	15.7	1168.1	2.0	230.6
24508.1	22.4	1169.0	294.3	215.4	13.8	1167.9	1.6	230.1
25008.1	21.8	1168.9	291.7	210.5	15.2	1167.8	2.0	229.6
25508.1	20.8	1168.8	292.7	210.7	15.9	1167.7	2.3	229.2
26008.2	20.3	1168.6	286.6	214.4	15.4	1167.6	2.0	228.6
26508.3	19.6	1168.5	291.7	210.8	16.3	1167.4	2.6	228.3
27008.4	20.3	1168.3	270.9	210.0	16.1	1167.3	2.0	227.9
27508.4	20.6	1168.1	297.0	206.6	15.1	1167.1	2.1	227.6
28008.4	20.8	1168.1	285.6	205.5	15.4	1167.0	2.0	227.2
28508.4	22.0	1167.9	281.7	205.0	13.7	1166.9	2.1	226.8
29008.4	20.8	1167.9	299.8	203.8	13.9	1166.7	2.2	226.5
29508.4	20.1	1167.7	304.9	203.1	15.3	1166.7	2.6	226.1
30008.4	21.8	1167.5	264.2	200.8	13.9	1166.6	2.1	225.8

Rev. 2

Table 14-4 Break Mass and Energy Flow for the Long-term Cooling Phase of the Limiting DEPSG Break (Sheet 20 of 23)

Time (sec)	Break Flow (Reactor Vessel Side)				Break Flow (Steam Generator Side)			
	Steam		Liquid		Steam		Liquid	
	Mass (lbm/sec)	Enthalpy (Btu/lbm)	Mass (lbm/sec)	Enthalpy (Btu/lbm)	Mass (lbm/sec)	Enthalpy (Btu/lbm)	Mass (lbm/sec)	Enthalpy (Btu/lbm)
30508.5	20.3	1167.5	311.2	202.2	13.8	1166.4	2.0	225.4
31008.5	20.4	1167.3	271.7	204.6	14.1	1166.3	2.1	225.0
31508.5	18.4	1167.2	299.5	203.2	15.3	1166.2	2.4	224.8
32008.6	18.0	1167.0	289.0	202.7	15.2	1166.1	2.5	224.4
32508.6	20.4	1166.9	281.8	199.6	13.6	1166.0	2.2	224.0
33008.6	17.9	1167.0	328.9	203.7	13.4	1165.8	2.0	223.5
33508.6	18.1	1166.8	280.8	200.6	14.7	1165.7	2.2	223.2
34008.7	18.4	1166.7	297.7	201.7	14.0	1165.6	2.5	222.8
34508.7	18.4	1166.5	283.2	199.5	13.7	1165.5	2.0	222.5
35008.7	17.4	1166.4	300.2	200.4	14.4	1165.4	2.5	222.2
35508.8	15.3	1166.3	297.1	206.1	14.4	1165.3	2.6	221.8
36008.9	17.9	1166.0	299.3	200.7	12.6	1165.1	1.7	221.4
36508.9	19.1	1166.0	277.3	195.8	13.8	1165.1	2.2	221.2
37009.0	17.8	1166.0	297.6	198.7	12.8	1165.0	2.0	220.9
37509.0	16.6	1165.8	287.1	199.7	14.0	1164.9	2.4	220.5
38009.1	16.0	1165.7	315.8	199.1	12.8	1164.8	2.0	220.2
38509.1	15.5	1165.7	317.9	201.5	13.2	1164.6	1.9	219.8
39009.2	15.8	1165.5	300.8	198.6	13.2	1164.5	2.0	219.3
39509.3	17.1	1165.5	285.0	197.7	11.1	1164.4	1.3	219.1
40009.3	16.3	1165.3	284.5	199.5	13.5	1164.3	1.9	218.9
40509.3	16.6	1165.3	279.7	198.4	12.3	1164.1	2.0	218.5
41009.3	14.4	1165.1	325.8	197.2	12.9	1164.1	2.1	218.4
41509.3	15.9	1165.0	291.0	193.9	12.8	1164.0	2.3	218.1
42009.4	16.3	1164.9	289.5	198.7	11.3	1163.9	1.6	217.7
42509.4	14.3	1164.9	333.4	196.1	12.1	1163.8	2.2	217.5
43009.5	14.6	1164.7	287.5	195.5	13.2	1163.8	2.6	217.3
43509.5	13.7	1164.6	336.2	201.2	11.6	1163.7	1.8	217.1
44009.6	14.3	1164.4	270.7	199.3	11.4	1163.6	1.7	216.6
44509.6	15.2	1164.3	271.8	202.6	12.2	1163.4	1.9	216.2
45009.6	13.3	1164.4	307.7	194.7	13.1	1163.4	2.3	216.0
45509.7	12.1	1164.4	327.7	194.1	13.5	1163.4	3.1	216.0
46009.7	14.3	1164.3	292.2	194.0	12.2	1163.2	1.8	215.7
46509.7	13.8	1164.2	292.2	193.0	12.8	1163.2	2.5	215.5
47009.8	10.2	1163.9	307.0	201.0	14.5	1163.2	3.3	215.3
47509.8	13.1	1163.8	294.2	198.5	12.0	1163.0	1.7	214.9

Rev. 2

Table 14-4 Break Mass and Energy Flow for the Long-term Cooling Phase of the Limiting DEPSG Break (Sheet 21 of 23)

Time (sec)	Break Flow (Reactor Vessel Side)				Break Flow (Steam Generator Side)			
	Steam		Liquid		Steam		Liquid	
	Mass (lbm/sec)	Enthalpy (Btu/lbm)	Mass (lbm/sec)	Enthalpy (Btu/lbm)	Mass (lbm/sec)	Enthalpy (Btu/lbm)	Mass (lbm/sec)	Enthalpy (Btu/lbm)
48009.8	10.2	1163.8	318.8	196.1	13.2	1163.0	2.3	214.7
48509.9	13.3	1163.6	297.1	197.7	11.0	1162.8	1.8	214.4
49009.9	14.5	1163.7	284.8	190.4	11.0	1162.6	1.9	214.2
49509.9	12.2	1163.7	323.8	199.0	11.6	1162.6	1.7	214.0
50010.0	12.4	1163.7	317.1	190.7	12.2	1162.6	2.4	214.0
50510.0	12.6	1163.5	278.3	193.6	12.6	1162.7	2.3	213.8
51010.1	11.2	1163.4	318.2	197.0	11.3	1162.5	1.6	213.4
51510.2	10.9	1163.3	333.9	198.6	10.8	1162.3	1.5	213.1
52010.2	13.4	1163.3	284.7	192.1	10.9	1162.3	1.9	213.0
52510.2	12.7	1163.3	276.2	195.1	11.4	1162.3	2.1	212.8
53010.2	9.9	1162.9	339.7	199.5	10.5	1162.2	1.8	212.5
53510.3	10.3	1162.8	306.5	200.0	11.2	1162.2	1.8	212.2
54010.3	11.0	1162.7	277.5	198.4	11.8	1162.0	2.0	212.0
54510.4	10.4	1162.9	336.1	193.1	10.5	1162.0	2.1	211.8
55010.4	11.4	1162.8	309.6	196.0	10.6	1161.8	1.3	211.6
55510.4	12.1	1162.9	289.1	193.1	9.7	1161.8	1.3	211.5
56010.5	11.9	1162.8	316.6	192.0	10.0	1161.7	2.1	211.5
56510.5	11.6	1162.5	280.2	195.9	11.3	1161.8	2.2	211.3
57010.5	8.6	1162.6	324.8	190.5	12.9	1161.8	2.6	211.3
57510.6	11.8	1162.7	310.2	192.1	9.2	1161.6	1.0	211.0
58010.6	11.1	1162.5	288.1	194.3	10.8	1161.6	1.7	210.8
58510.7	10.8	1162.3	325.8	196.2	8.6	1161.4	1.2	210.5
59010.8	9.8	1162.3	304.9	191.2	11.8	1161.5	2.1	210.6
59510.8	9.2	1162.4	319.2	193.5	10.3	1161.4	2.0	210.2
60010.9	10.3	1162.4	298.0	187.5	12.1	1161.4	2.9	210.3
60510.9	8.9	1162.5	304.4	189.7	12.4	1161.5	2.4	210.2
61011.0	9.1	1162.3	314.8	186.6	12.1	1161.4	2.5	210.3
61511.0	9.0	1162.2	290.3	187.4	11.8	1161.4	2.4	210.2
62011.0	8.5	1162.1	310.4	188.5	13.2	1161.4	2.9	210.0
62511.1	8.3	1162.1	309.0	189.4	12.2	1161.3	2.7	209.8
63011.1	11.4	1162.2	298.3	185.6	9.8	1161.2	1.3	209.7
63511.2	9.7	1162.2	315.2	185.2	11.6	1161.2	2.5	209.6
64011.2	8.2	1162.1	330.6	187.5	11.3	1161.2	2.7	209.6
64511.2	9.4	1162.0	297.7	187.6	11.3	1161.2	1.7	209.4
65011.3	9.7	1162.0	293.1	187.3	10.7	1161.0	2.1	209.1

Rev. 2

Table 14-4 Break Mass and Energy Flow for the Long-term Cooling Phase of the Limiting DEPSG Break (Sheet 22 of 23)

Time (sec)	Break Flow (Reactor Vessel Side)				Break Flow (Steam Generator Side)			
	Steam		Liquid		Steam		Liquid	
	Mass (lbm/sec)	Enthalpy (Btu/lbm)	Mass (lbm/sec)	Enthalpy (Btu/lbm)	Mass (lbm/sec)	Enthalpy (Btu/lbm)	Mass (lbm/sec)	Enthalpy (Btu/lbm)
65511.3	7.3	1161.9	322.3	187.9	12.4	1161.1	2.7	209.1
66011.4	10.4	1161.8	310.7	187.1	9.2	1160.9	1.1	208.9
66511.4	7.5	1161.6	313.4	187.3	12.3	1161.0	2.6	208.9
67011.4	10.6	1161.6	288.4	188.6	9.1	1160.9	1.3	208.6
67511.4	7.0	1161.9	328.5	188.5	11.2	1160.9	2.2	208.5
68011.4	7.3	1161.6	312.6	187.6	12.4	1160.9	2.3	208.4
68511.5	7.2	1161.7	305.5	187.7	12.0	1160.8	2.1	208.2
69011.5	8.9	1161.7	298.7	185.4	11.5	1160.8	2.2	208.3
69511.5	7.9	1161.6	339.8	189.7	8.0	1160.5	0.9	207.8
70011.6	10.7	1161.3	294.3	189.5	8.5	1160.5	1.2	207.7
70511.6	7.8	1161.6	335.0	184.5	10.5	1160.5	2.0	207.8
71011.6	8.9	1161.6	297.6	184.0	10.8	1160.6	2.2	207.7
71511.7	7.2	1161.5	328.0	187.1	10.5	1160.6	1.8	207.7
72011.8	7.8	1161.6	302.6	187.9	10.7	1160.5	2.0	207.4
72511.8	6.3	1161.3	315.1	187.0	11.7	1160.6	2.5	207.4
73011.8	8.8	1161.0	296.3	184.2	10.2	1160.5	1.6	207.3
73511.9	8.1	1161.2	296.0	184.3	11.2	1160.5	1.7	207.4
74011.9	8.2	1161.5	327.8	183.3	8.4	1160.3	1.4	207.2
74511.9	9.1	1161.3	294.9	185.9	10.5	1160.3	2.2	207.1
75012.0	8.7	1161.4	334.9	184.5	8.3	1160.2	1.3	206.9
75512.0	8.0	1161.3	319.4	183.1	9.8	1160.3	1.9	206.9
76012.0	9.0	1161.2	302.6	182.3	9.1	1160.2	1.5	206.8
76512.1	7.8	1161.2	303.2	184.3	11.2	1160.3	2.4	206.8
77012.1	7.2	1160.9	321.4	184.5	9.9	1160.2	1.7	206.7
77512.1	8.0	1161.5	303.2	184.6	8.8	1160.1	1.5	206.4
78012.1	9.2	1161.2	311.1	181.5	8.7	1160.0	1.4	206.3
78512.2	7.0	1161.2	321.7	181.8	10.9	1160.1	1.9	206.5
79012.2	7.2	1161.2	317.8	183.0	11.0	1160.2	2.0	206.5
79512.2	8.5	1161.3	306.4	179.5	8.4	1160.0	1.3	206.3
80012.2	8.7	1161.3	326.5	180.9	9.4	1159.9	2.2	206.2
80512.2	8.2	1160.8	295.9	181.3	10.3	1160.0	1.7	206.2
81012.3	7.5	1161.0	319.6	179.9	9.1	1160.0	1.5	206.2
81512.3	7.0	1161.3	324.8	184.1	9.5	1159.9	1.2	205.8
82012.3	9.4	1161.0	303.3	182.4	7.8	1159.7	0.7	205.7
82512.3	8.5	1161.0	325.2	180.3	8.2	1159.7	1.4	205.8

Rev. 2

Table 14-4 Break Mass and Energy Flow for the Long-term Cooling Phase of the Limiting DEPSG Break (Sheet 23 of 23)

Time (sec)	Break Flow (Reactor Vessel Side)				Break Flow (Steam Generator Side)			
	Steam		Liquid		Steam		Liquid	
	Mass (lbm/sec)	Enthalpy (Btu/lbm)	Mass (lbm/sec)	Enthalpy (Btu/lbm)	Mass (lbm/sec)	Enthalpy (Btu/lbm)	Mass (lbm/sec)	Enthalpy (Btu/lbm)
83012.4	7.6	1160.8	323.0	185.6	8.3	1159.8	1.1	205.6
83512.4	6.1	1160.7	312.6	186.5	10.0	1159.8	1.8	205.4
84012.5	8.1	1160.6	284.1	179.7	9.7	1159.8	1.8	205.6
84512.5	6.8	1160.8	330.2	177.7	10.2	1159.9	2.2	205.6
85012.5	8.1	1160.8	295.6	177.8	10.0	1159.8	1.9	205.6
85512.5	7.4	1160.6	323.0	180.0	9.7	1159.9	1.9	205.7
86012.6	6.4	1160.7	325.6	177.8	9.5	1159.8	1.6	205.5
86512.6	8.5	1160.7	290.3	178.2	9.1	1159.7	1.5	205.4
87012.7	6.2	1160.7	318.7	177.6	10.8	1159.8	2.1	205.4
87512.8	8.7	1160.6	311.1	174.2	8.7	1159.7	1.4	205.3
88012.8	7.7	1161.0	334.9	179.9	8.6	1159.6	1.5	205.3
88512.9	8.5	1160.8	311.5	179.9	6.9	1159.4	0.8	205.0
89013.0	8.3	1160.7	323.9	180.3	8.2	1159.5	1.2	205.0
89513.0	8.3	1160.7	311.3	179.4	7.5	1159.5	0.9	205.1
90013.1	6.8	1160.8	312.5	183.4	8.9	1159.5	1.3	204.7
90513.1	7.4	1160.6	309.4	177.1	9.2	1159.5	1.5	204.7
91013.2	6.0	1160.8	326.2	181.6	8.5	1159.5	1.7	204.7
91513.2	7.8	1160.5	318.1	178.2	8.4	1159.4	1.3	204.6
92013.3	8.0	1160.6	308.9	181.9	6.7	1159.1	0.5	204.1
92513.3	7.1	1160.6	323.1	180.4	8.6	1159.4	2.0	204.4
93013.4	6.9	1160.4	304.0	180.4	8.7	1159.3	1.2	204.4
93513.4	5.9	1160.2	323.9	179.0	9.8	1159.4	1.6	204.3
94013.4	8.3	1160.2	301.5	176.4	7.3	1159.3	1.2	204.4
94513.5	7.1	1160.4	328.1	175.9	8.5	1159.2	1.3	204.4
95013.5	8.3	1160.5	309.5	178.8	7.1	1159.1	0.6	204.2
95513.5	9.2	1160.6	318.1	175.0	6.7	1158.9	0.7	204.0
96013.6	8.6	1160.7	322.2	177.6	6.6	1159.0	0.7	204.2
96513.7	9.3	1160.7	311.3	174.4	6.8	1159.0	1.1	204.0
97013.7	7.8	1160.7	328.0	181.0	6.9	1159.1	0.8	204.0
97513.8	9.0	1160.3	294.4	174.3	7.9	1159.1	1.5	204.1
98013.8	6.4	1160.2	336.5	174.8	9.4	1159.4	2.2	204.3
98513.8	6.0	1160.1	312.2	174.9	9.4	1159.3	1.6	204.2
99013.9	8.3	1160.3	302.2	175.1	8.0	1159.2	1.0	204.0
99514.0	6.9	1160.4	320.9	174.8	7.7	1159.1	1.0	203.9
100000.0	7.6	1160.4	324.2	178.1	6.7	1158.9	0.6	203.6

Rev. 2

Item 15

On page 3-15 it is stated that steam condensation in the downcomer and the broken loop cold leg volume is prevented in the GOTHIC analysis of the post-reflood period by setting the liquid/vapor interface areas in those regions to zero. Page 3-5 states that no mixing of steam and safety injection water in the downcomer is assumed for the reflood analysis. Please describe how this type of condensation is prevented during the reflood period when mass and energy release is being calculated by WREFLOOD.

RESPONSE

As described in the response to Item 6, the following modification is made to WREFLOOD:

DVI flow is directly accounted for in the mass and energy balances for the accumulated water in the downcomer. Complete mixing of DVI flow and water flow from the intact loop is assumed before they enter the downcomer. All flow from DVI and the intact loop is added to the downcomer water when the downcomer is not full. When the downcomer is full, the combined DVI and intact loop flow that is in excess of the core inlet flow is spilled to the containment. The enthalpy of this spillage is the mixture enthalpy of the combined DVI and intact loop water flow. Steam flow from the intact loop passes the downcomer with no interaction with DVI flow. Condensation due to direct contact of DVI water flow with steam flow from the intact loop in the downcomer is disregarded.

Rev. 2

Item 16

The treatment of spilled accumulator water from the broken cold leg is not discussed for the blowdown period. Please provide the assumptions for containment analysis and justify that they are conservative.

Item 17

The treatment of the spilled accumulator water from the broken cold leg is not discussed for the reflood calculation. Please provide these assumptions and justify that they are conservative. If the accumulators will still be discharging during the post-reflood period please describe and justify the assumptions for treatment of this water that will affect the containment analysis.

RESPONSE to Item 16 and 17

The LOCA mass and energy topical report is focused on the limiting pump suction break, where accumulator water injected into the pump-discharge side does not spill directly from the break. In case of a cold leg (pump-discharge) break, spillage of the broken loop accumulator is possible. The cold-leg break is much less limiting in terms of the overall containment peak pressure than the pump suction break and is not evaluated for peak containment pressure analysis.

The relation between the pump-suction break and the cold-leg break for the blowdown and reflood phases has been demonstrated for current 4-loop plants with the approved methodology described in WCAP-10325-P-A. This relation should be the same for the US-APWR due to almost the same plant configuration and the analytical methodology. Rev. 2

Therefore, in order to demonstrate the conservativeness of the GOTHIC model and the actual relation between both break cases, additional calculations for both break cases have been performed using a more realistic GOTHIC model within the expected parameter ranges.

1. Realistic GOTHIC Model

Rev. 2

Rev. 2

Rev. 2

2. Analyses

The containment analyses for the limiting pump-suction break and the cold leg (pump discharge) break have been performed using above mentioned GOTHIC realistic model. The relevant modeling assumptions for each model are summarized in Table 16-1. Figures 16-4 and 16-5 illustrate GOTHIC noding diagrams for the more realistic analyses for the pump suction break and the cold leg (pump discharge), respectively. The methodology for the blowdown and reflood phase is the same as the evaluation model.

Initial containment conditions, chosen conservatively for the evaluations, are listed in Table 16-2. Assumptions for the containment heat removal and the SI system operability are shown in Table 16-3.

Summary results for each LOCA analyzed are presented in Table 16-4 and compared with the limiting pump suction break case with the evaluation model. The containment pressures and vapor temperatures are compared in Figures 16-6 and 16-7, respectively.
Comparison of results for the limiting pump suction break using the evaluation model and the realistic model demonstrates large conservatism in the evaluation model. Also, comparison of results for the pump suction break and the cold leg (pump discharge) break using the more realistic model demonstrates that the pump suction is the limiting break location.

During the post-reflood period, the cold leg break is found to give higher containment pressure rise than the pump suction break because of earlier heat release from the secondary side of the intact loop SG. However, since the increase of the containment pressure is small enough, the peak pressure for the cold leg break is still less than the peak pressure at the end of reflood for the pump suction break.

3. Conclusion

For the limiting pump suction break, accumulator water injected into the pump-discharge side does not spill directly from the break. It has been demonstrated with the analyses simulating realistic phenomena that the cold leg (pump-discharge) break, where spillage of the broken loop accumulator is possible, is much less limiting in terms of the overall containment peak pressure than the pump suction break. Rev. 2

4. References

(1) H. C. Yeh, "Modification of Void Fraction Correlation", Proceedings of 4th International Topical Meeting on Nuclear Thermal Hydraulics, Operations and Safety, Volume 1, Taipei, Taiwan, April 5-9, 1994.ANS Transactions, Vol. 17, 1973, p369-370.

Table 16-1 Comparison between Evaluation Model and Realistic Model with GOTHIC

Rev. 2

Table 16-2 Initial Conditions for Containment Pressure Analytical Model

Parameters	Value	Setting for Conservatism
A. Reactor Coolant System		
1. Reactor Power Level, MWt	4,451×1.02	Max (102%)
2. Average Coolant Temperature, °F	587.8	Max
3. Mass of Reactor Coolant System Liquid, lbm	7.42×10^{5}	Max
4. Mass of Reactor Coolant System Steam, lbm	1.02×10^{4}	
5. Liquid Plus Steam Energy,* Btu	4.41×10^{8}	Max
B. Containment		
1. Pressure, psig	2	Max
2. Temperature, °F	120	Max
3. Relative Humidity, %	0	Min
4. Service Water Temperature, °F	95	Max
5. Refueling Water Temperature, °F	120	Max
6. Outside Temperature, °F	Not Considered	Thermal Insulation is Assumed.
C. Stored Water (as applicable)		
1. RWSP water volume, ft^3** (gallon)	44,000 (329,000)	Min
2. Accumulators water volume, ft^3	1.03×10^{4}	Min

Notes:
* All energies are relative to 32°F [0°C].
** This includes RWSP minimum inventory and return water, plus a safety margin, but does not include the ineffective pool volume.

Rev. 2

Table 16-3 Engineered Safety Feature Systems Information

US APWR Specification	Value	
	Full Capacity	Value Used for Containment Design Evaluation
I. Passive Safety Injection System		
A. Number of Accumulators	4	4
B. Pressure, psig	695	586
II. Active Safety Injection Systems		
A. High Head Injection System (HHIS)		
1. Number of Lines	4	2
2. Number of Pumps	4	2
3. Flow Rate, gpm/train *	1,540	1,259
4. Response Time, sec (after analytical limit of SI signal reached)	3 (Offsite Power Available)	118
III. Containment Spray System (CSS)		
A. Number of Lines	4	2
B. Number of Pumps	4	2
C. Number of Headers	1	1
D. Flow Rate, gpm	9,800 (4 pumps)	5,290 (2 pumps)
E. Response Time, sec (after analytical limit of SI signal reached)	5 (Offsite Power Available)	243
IV. Refueling Water Storage Pit (RWSP)		
A. Liquid volume. Gallons	651,000	329,000
B. Liquid surface area ,ft^2	4,985	Interface Area is Ignored
V. Containment		
A. Free Volume (Air Volume), ft^3	2,800,000	2,743,000

Notes:
* HHIS flow rate is the value when RCS pressure is at 0psig.
Hot leg switch-over is conservatively not assumed, which leads to ignoring steam condensation with the hot leg injection.

Rev. 2

Table 16-4 Summary of Analysis Results

Rev. 2

Rev. 2

Figure 16-1 Concept of Two-phase Level of the Vessel by GOTHIC

Figure 16-2 Core Power Shape for the Realistic Analysis

Rev. 2

Figure 16-3 Core Void Profile

Figure 16-4 Noding Diagram of GOTHIC for Realistic Analysis Pump Suction Break Case

Rev. 2

Rev. 2

**Figure 16-5 Noding Diagram of GOTHIC for Realistic Analysis
Cold Leg (Pump Discharge) Break Case**

Rev. 2

Figure 16-6 Comparison of Containment Pressure vs. Time

Rev. 2

Figure 16-7 Comparison of Containment Atmospheric Temperature vs. Time

Item 18

The equation for carryout rate fraction on page 3-8 contains a quench front level term Zq. Based on FLECHT data, the correlation was found to be valid until the quench front level neared but did not reach the top of the core. At that elevation the core was found to be quenched from the top so that water was no longer carried out the top of the core. The FLECHT data was obtained from a facility simulating a 12 foot reactor core. Please describe the assumptions used in modeling the 14 foot fuel of US-APWR with regard to termination of liquid carryout as the quench front level reaches the top of the core. Justify that this assumption is conservative for containment analysis.

RESPONSE

Liquid entrainment is assumed to continue until the water level in the core is 2 feet from the top of the core in modeling the 14-foot fuel of US-APWR, in conformance with Acceptance Criterion 1.C.iii. of SRP 6.2.1.3. The same approach is being used for the 14-foot core as was used previously for the 12-foot core. The description of this assumption will be included in the revised topical report.

Rev. 2

2.0 Response to Follow-up Request dated January 30, 2008

Item 19

Please provide the NRC staff with an electronic file of the US-APWR GOTHIC input for the double ended pump suction break. The staff would like to use this input to develop a description of the US-APWR containment using the MELCOR computer code for the purpose of performing confirmatory analysis. We also would like to share it with NRC research staff as they are developing a MELCOR containment model for the Chapter 6.2 evaluation.

RESPONSE

The GOTHIC containment model is combined with the GOTHIC reactor cooling system (RCS) model for long-term cooling phase. It is also coupled with WREFLOOD (M1.0) for reflood phase. Therefore the US-APWR GOTHIC input does not include mass and energy tables for the reflood phase and the long-term cooling phase.

In order to provide a complete GOTHIC containment model for the confirmatory analysis, the GOTHIC input has been changed from that for the double ended pump suction break case as follows:

- The RCS model is removed.
- Mass and Energy table for the reflood phase is added. The table is the same as one provided as Table 14-2 for the response to Item 14. Rev. 2
- Mass and Energy table for the long-term cooling phase is added.

The mass and energy table for the long-term cooling phase has been made so as to conserve integral values for the mass and energy release since the data transference from the RCS to the containment in the combined GOTHIC calculation is done on every time step and the interval is too short.

As shown in Figure 19-1 the containment pressure with the provided data here is almost the same as that for the US-APWR double ended pump suction break case.

Electronic files for the US-APWR GOTHIC input and the input listing are provided as the following files.

Electronic file :
Input Listing :

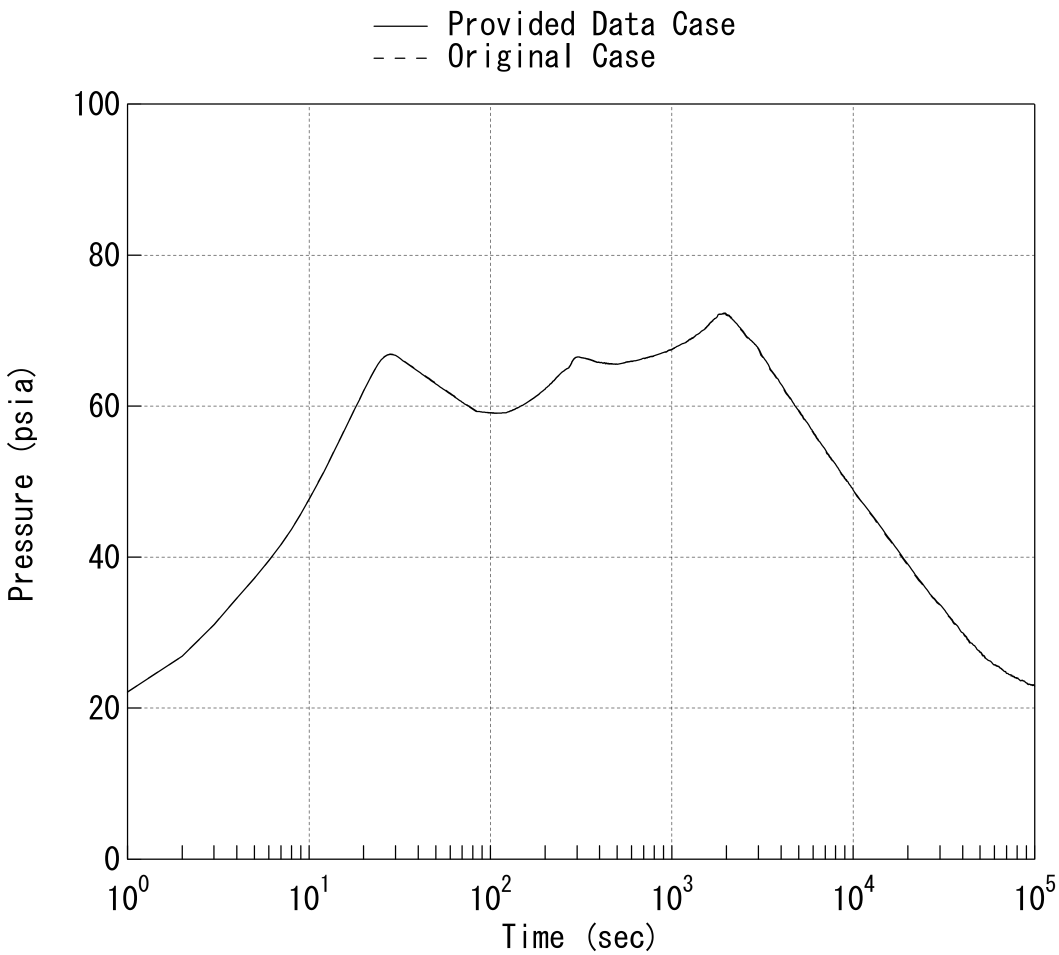

Figure 19-1 Containment Pressure

Rev. 2

3.0 Response to Request in March 2008

Item 20

Based on the response to Item 14 (Tables 14-1,14-2 and 14-3 in the January responses), it is noted that the post-reflood steam release to the containment as calculated by the GOTHIC reactor system simulation is oscillatory as compared with the previously approved methodology in WCAP-10325 which MHI references. In addition, after approximately 30,000 seconds, the steam release to the containment is less than that which one would expect from continued core boil-off. The staff is concerned that the oscillations may be an artifact of the GOTHIC code and may cause unrealistic steam condensation to be calculated within the core and lower plenum of the reactor vessel. The staff does not understand why the long term steam release rate predicted by GOTHIC would be less than that resulting from decay heat boiling.

We note that Standard Review Plan 6.2.1.3 recommends the following:
“Steam from decay heat boiling in the core should be assumed to flow to the containment by the path which produces the minimum amount of mixing with the ECCS injection water.” For a postulated break at the reactor system pump suction, compliance with this recommendation would mean that steam from the core is assumed to flow directly to the break without passing any of the ECCS injection locations.

RESPONSE

Rev. 2

(1) Long-term Steam Release Rate

In the GOTHIC primary system model, steam-water interfacial areas at the cold leg and the downcomer are set to zero to avoid mixing of the steam from decay heat boiling in the core and the SI water in accordance with SRP 6.2.1.3.

Figure 20-1 compares the integral of the steam release rate calculated by GOTHIC with steaming rate due to decay heat calculated using the following expression.

(2) Effects of Oscillation

Rev. 2

(3) Evaluation Model

The GOTHIC evaluation model that eliminates the effects of the flow oscillation will be described in the revised version of the topical report.

Rev. 2

Rev. 2

Figure 20-1 Integral of Steam Release Rate after Peak Pressure

Rev. 2

Figure 20-2 Integral of Mass Flow Rate between Downcomer and Lower Plenum

Rev. 2

Figure 20-3 Containment Pressure

Rev. 2

Figure 20-4 Temperature of Injected Water and Lower Plenum Water

Item 21

Describe the treatment of N_2 gas of the accumulator.

RESPONSE

For the US-APWR, N_2 gas of the accumulator is released to the containment via reactor coolant loops after the low flow injection mode is terminated during post-reflood phase. The release of the N_2 gas is accounted in the GOTHIC evaluation model using boundary conditions that inject the N_2 gas directly into the containment. Parameters related to the gas injection are given conservatively as follows:

Rev. 2